DISSERTATION

MICROBES IN THE MUCOSA: IMPACTS OF THE MUCOSAL IMMUNE SYSTEM AND ORAL VACCINATION WITH *LACTOBACILLUS ACIDOPHILUS* ON THE GUT MICROBIOME

Submitted by

Bridget E. Fox

Department of Microbiology, Immunology, and Pathology

In partial fulfillment of the requirements

For the Degree of Doctor of Philosophy

Colorado State University

Fort Collins, Colorado

Fall 2021

Doctoral Committee:

Advisor: Gregg Dean
Co-Advisor: Zaid Abdo

Stuart Tobet
Elizabeth Ryan

ABSTRACT

MICROBES IN THE MUCOSA: IMPACTS OF THE MUCOSAL IMMUNE SYSTEM AND ORAL VACCINATION WITH *LACTOBACILLUS ACIDOPHILUS* ON THE GUT MICROBIOME

The mucosal immune system is constantly balancing between the clearance of pathogens, tolerance of self-antigen and food, and maintenance of homeostasis within the microbiota. Vaccination via mucosal routes is advantageous because it provides protection at local mucosal sites and systemically. However, induction of efficacious responses are often difficult due to the inherent barriers of the mucosal tissues. We have developed a probiotic-based mucosal vaccination platform that utilizes recombinant *Lactobacillus acidophilus* (rLA) to overcome these obstacles presented in oral vaccination.

Here, we sought to determine whether repeated administration of rLA alters the intestinal microbiome as a result of *L. acidophilus* probiotic activity (direct competition and selective exclusion) or from the host's mucosal immune response against the rLA vaccine. To address the latter, IgA-seq was employed to characterize shifts in IgA-bound bacterial populations. Additionally, we determined whether using rice bran as a prebiotic would influence the immunogenicity of the vaccine and/or IgA bound bacterial populations. Our results show that the prebiotic influenced the kinetics of rLA antibody induction, and that the rLA platform does not cause lasting disturbances to the microbiome.

Nucleotide-binding oligomerization domain containing 2 (NOD2) has presented itself as an essential regulator of immune responses within the gastrointestinal tract. This innate immune receptor is expressed by several cell types, including both hematopoietic and nonhematopoietic cells within the gastrointestinal tract. Mice harboring knockouts of NOD2 only in CD11c+ cells were used to better characterize NOD2 signaling during mucosal vaccination with rLA. We show that NOD2 signaling in CD11c+ cells is critical for mounting a humoral immune response against rLA. Additionally, disruption of NOD2 signaling in CD11c+ cells results in an altered bacterial microbiome profile in both vaccinated and unvaccinated mice.

ACKNOWLEDGMENTS

The work presented here would not have been possible without the support and encouragement from many individuals. First, I would like to thank Dr. Nathan Fisher for welcoming me into his lab as a freshman at NDSU. This journey would not have started without your invaluable training, encouragement in my future career goals, and inspiring psychological views about science. I would not be where I am today without your commitment to mentoring.

I would like to thank my advisors, Dr. Zaid Abdo and Dr. Gregg Dean. Zaid has spent countless hours training me to be a better scientist and think independently. I am thankful for our weekly meetings full of discussion of research progress, problem solving, and constant encouragement. Gregg's understanding unwavering support, and exceptional mentorship has made this journey into a rewarding and fulfilling experience. I could not have asked for better role models for how to be a great scientist and leader.

This research would also not have been possible without the outstanding labs Zaid and Gregg have established. I would like to recognize the work of current and former lab members and collaborators: Dr. Allison Vilander, Alora LaVoy, Dr. Ben Curtis, Darby Gilfillan, Kimberly Shelton, Brianna Ramirez Rubio, McKenzie Smith, Dr. Jonathan LeCureux, Morgan Pearson, Max Drummond, Matt Hopken, Chris Dean, Steven Lakin, and Reed Woyda. Specifically, I would like to express my endless gratitude to Dr. Allison Vilander for her inspirational work ethic and being an incredible mentor. Thank you for all your help during the early mornings and late nights throughout so many necropsy days. I am also so grateful for the friendship that sprouted from the many hours in the Flow Core with Darby. I would also like to thank my committee members Dr. Elizabeth Ryan and Dr. Stuart Tobet for their time and guidance.

I am very fortune to have gained so many friendships throughout my time at CSU. I would like to thank my cohort for being such a critical support system; the regular check-ins aided in both mental and academic stability. Especially thanks to Shaun for teaming up for so many outreach activities. The GAUSSI program introduced me to so many peers in different departments and encouraged me to think

outside the niche of my specific research projects. I gained so much knowledge in bioinformatics and connected with many outreach opportunities, which I am so grateful for. I would be remiss if I didn't thank our softball team that started as a group of graduate students and developed into many life-long friends.

Lastly, I would like to thank my family. I am so grateful for the encouragement from my parents, and their contributions to fostering an interest in science at a young age. Your support has been felt and appreciated across the country by Sam, Luke, and I. We are all so thankful for supporting our continued education. I am grateful for the benevolent competition of my brothers, and always pushing me to 'do better'. Thank you to Freddie, my dog, for keeping my feet warm during the many late-night writing sessions. A huge thank you to my husband, Bill Fox, for your patience after listening to countless presentations and checking many color-blind friendly figures. Thank you for keeping me grounded and always being down for the next adventure, wherever that may take us.

TABLE OF CONTENTS

LIST OF TABLES

LIST OF FIGURES

CHAPTER 1: Overview of the Literature

1.1: Introduction

Pathogens commonly enter the body through mucosal tissues, yet the vast majority of vaccines against these mucosal pathogens are delivered parenterally. These vaccines therefore only target the systemic immune system instead of local mucosal immune responses. Mucosal vaccination presents several obstacles, but lactic acid bacteria, such as *Lactobacillus acidophilus*, have shown great promise as a platform for delivering antigens to mucosal tissues. An additional safety concern unique to orally delivered mucosal vaccines is the possible risk to the resident microbiome. Here, we review the current literature regarding the bacterial microbiome, the mucosal immune system, and mucosal vaccination. In the following chapters, we also present our findings from studies that utilize *L. acidophilus* as a vaccine platform, with results that describe impacts on the microbiome and critical mechanisms of immune induction.

1.2: The Bacterial Microbiome

In 2007, the National Institutes of Health (NIH) launched the Human Microbiome Project (HMP), one of the first large-scale initiatives to characterize the role of the human microbiome in health and disease [1]. The term "human microbiome" refers to the collective genomic community of bacteria, archaea, fungi, and viruses living within our intestinal tract, on our skin, and on other mucosal surfaces [2]. In the first phase of this project, a reference set of over three-thousand microbial genomes were sequenced, the complexity of the microbiome was evaluated for several body sites, and new tools for analysis were developed. The second phase, the Integrative Human Microbiome Project, focused on impacts from three specific conditions: pregnancy, inflammatory bowel diseases (IBD), and stressors that affect those with prediabetes [3]. The impact of this initiative opened doors for multiple avenues of microbiome research. Driven by the optimization of Next Generation Sequencing (NGS) technology, there has been an exponential increase of microbiome research in the past decade. This also resulted in an appreciation of the complexity of the microbiome and its role in numerous aspects of human health and disease. For example,

the gut microbiome was found to be a critical stimulator of the immune system, participates in host metabolism, protects against invasive pathogens, and has recently been linked to neurodevelopmental, cognitive, and emotional health outcomes [4].

Today, it is known that the microbiota profiles change over time as they are exposed to different external factors, including antibiotics and an array of dietary components. In a healthy adult human on a typical western diet, the microbiome is dominated by the Firmicutes and Bacteroidetes phyla, followed by members of Actinobacteria, Proteobacteria, Fusobacteria, and Verrucomicrobia [5]. Efforts focusing on how exposures early in life can have long-term impacts on health and disease are beginning to reveal how impressionable the developing microbiome is during the first several years of life [6, 7]. In adulthood, the microbiome stabilizes, but is still prone to alterations in diversity caused by changes in diet, lifestyle, antibiotics, gastrointestinal infections and others [4]. In what follows we introduce sequencing methods used to evaluate changes in the microbiome, followed with further explanation to how diet and antibiotics impact the gut microbiome and associated health outcomes.

1.2.1: Methods of Microbiome Sequencing

The use of 16S ribosomal RNA (rRNA) to classify bacteria started in the 1970's, when Carl Woese characterized the 16S rRNA of 10 methanogenic bacteria, and thereupon established the field of molecular phylogenetics [8]. In the early 2000's, high-throughput NGS methods were developed and led to an increase in microbiome research. These new NGS techniques allowed for by the higher sensitivity of detection of microbes compared to culture-based methods. This was driven by the fact that >90% of the microbiota could not be cultured [9]. 16S rRNA amplicon sequencing approaches have been very popular for investigating the bacterial microbiome due to their ability to simultaneously sequence multiple samples at once with sufficient depth to answer relevant biological questions [10]. Although very useful, variations in protocols may lead to dramatic differences in results [11]. For example, primers targeting different variable regions, thermocycler settings, choice of sequencing platform, alignment to reference databases, and filtering and clustering parameters can all influence outcomes [12–16]. However, the inclusion of synthetic

mock communities allows for the determination of optimal parameters for filtering, assessing contamination, and evaluating biases between sequencing runs [17]. Furthermore, inclusion of both cellular and extracted DNA mock communities can provide insight into the efficiency of DNA extractions. Another drawback to 16S rRNA amplicon sequencing is the low resolution between closely related species and biases related to primer selection [17]. Shotgun sequencing approaches and new long read third generation (i.e. Nanopore and PacBIO sequencing) have aimed to overcome these limitations. As these technologies improve, their application in the clinical field may increase as well.

Currently, there are many logistical hurdles to permit the use of sequencing technologies in clinical setting. The high costs, intensive bioinformatics processing and analysis, high levels of human contamination, and suboptimal differentiation between pathogens and commensals make it difficult for the regular use of 16S rRNA sequencing, for example, in clinical and diagnostic applications [18]. On the other hand, long read and shotgun metagenomic approaches can characterize both microbial and host transcriptional changes without having to PCR amplification of specific genomic regions [19]. While it's application in complex microbiome studies may be years off, the capability to sequence RNA directly provides a platform for highly accurate microbiome and metatranscriptome analysis in the clinical setting [19, 20]. These meta-omics approaches would open the doors for personalized treatments and microbe-targeted therapies.

1.2.2: Alterations to the Gastrointestinal Microbiome

The composition of the gut microbiome can be influenced by a range of factors, including change in diet, exposure to antibiotics, and onset of immune mediated diseases, among others [21–25]. These factors can ultimately induce dysbiosis of the microbiome, which can be classified into three types: (1) loss of beneficial microorganisms, (2) expansion of pathobionts, and (3) loss of microbial diversity [26]. If prolonged, dysbiosis can result in a myriad of diseases, including IBD, obesity, diabetes, colorectal cancer, and even neurological diseases [26–29]. Often, changes in the microbiota are reported in terms of differences in abundances of the major phyla. Recent efforts have focused on using multi-omics approaches

to characterize relationships between microbial metabolites, functional capabilities of the microbiome, and immune profile for a deeper understanding of how the activity, rather than species abundances, of the microbiome is correlated with health and disease [30, 31]. Although the gastrointestinal microbiome is constantly influence by environmental and genetic factors, diet and antibiotic usage remain as some of the most powerful drivers of microbiota diversity and function [32, 33]. Below, we describe how diet and antibiotics influences the composition of the microbiome and the associated impacts to human health.

1.2.2.1 Diet

Diet has a substantial influence on the function and composition of the gut microbiome. Diets that are high in fats have been linked to a decrease in Bacteroidetes and an increase in Firmicutes and Proteobacteria [34–36]. Importantly, this change in microbiota composition has been identified as a causative agent in the development of obesity. One hypothesis is that high-fat diets leads to the establishment of a microbiome with a higher abundance of Firmicutes, and hence an increased ability to break down otherwise indigestible food into short chain fatty acids (SCFAs) [37, 38]. Although SCFA provide benefits to the host through inhibition of histone deacetylases and activation of G-coupled protein receptors to regulate metabolism and inflammation, an overabundance of SCFA production in the gut leads to increased energy extraction from a given diet [39, 40]. The elevated levels of free SCFAs are absorbed and metabolized into lipids by the liver, and then stored in adipose tissue. This was shown by an increase in gene expression of pathways involving metabolism of non-absorbed carbohydrates in mice fed a high-fat diet [37]. A study in humans also found elevated levels of SCFAs in overweight or obese participants compared to lean participants, as well as a negative correlation between SCFA and *Bacteroides/Prevotella* abundances [37]. The increase in gram-negative bacteria, especially within the gamma-Proteobacteria class, following consumption of a high fat diet leads to an increase in LPS, which ultimately impairs barrier function, increases permeability, and decreases the thickness of the mucus layer [41]. The resulting increased intestinal inflammation has been associated with obesity-induced cancers, cardiovascular disease,

and diabetes, all accompanying disorders stemming from metabolic endotoxemia due to circulating LPS [29, 42–44]. Importantly, LPS concentrations were found to be elevated after a single high-fat meal [45].

In addition to being high in fats, the western diet is also hallmarked by an elevated level of sugar intake. Do *et al*. (2018) explored alterations in the gut microbiota associated with high glucose or fructose intake [46]. A marked decrease in Bacteroidetes and increase in Proteobacteria abundances were found following high-sugar diets in mice [46]. Protobacteria are equipped to utilize simple carbohydrates and can proliferate rapidly with the excess of simple monosaccharides compared to other commensals designed to degrade complex carbohydrates [47]. Although data are conflicting regarding associations between abundances of specific taxa and sugar intake, there is a common trend of decreased abundances of Bacteroidetes following high sugar intake [48–50]. Investigations into different prediabetic fat-to-sugar ratio diets revealed distinct microbial compositions between the diets, but further analyses revealed similarities in metabolite and metagenomic profiles [51]. These results suggest there may be redundancy between the altered microbial communities found in high-fat and high-sugar diets. The metabolites produced from these diets often resemble pre-diabetic profiles, providing further evidence for the microbiota's role in the onset of diabetes [51].

The rate at which the microbiome is affected by a change in diet has also become a recent concern, especially as we begin to question whether the high-sugar and high-fat Western diets may have irreversible implications. While murine models have shown a shift in the microbiota profile within a day of switching from a low-fat plant-rich diet to a Western diet (high-fat, high-sugar) [35, 52], results from human cohorts are inconsistent in the duration needed to observe changes [53–56]. However, strategic swapping of diets between high-fat, low-fiber and low-fat, high-fiber within individuals in the same geographical region in Africa showed that changes in the microbiome and metabolome can be seen within two weeks [57]. Notably, the low-fat, high-fiber diet resulted in decreased biomarkers of intestinal inflammation and epithelial proliferation that are correlated with increased colon cancer risk [57].

Together with a high-fat and high-sugar intake, the Western diet is also associated with a deficiency in fiber. Fiber can be broadly defined as plant-based carbohydrates that cannot be digested by human-

encoded enzymes [58]. Fibers are also classified based on their solubility, viscosity, and degree of fermentability [59]. Most soluble fibers can be fermented by the gut microbiome to produce SCFAs, mainly butyric, acetic, and propionic acids, which in turn positively regulate lipid and glucose metabolism [40]. Higher levels of SCFA-producing bacteria (*Actinobatceria*, *Bacteroidetes*, and *Prevotella*) were found in children in Burkina Faso compared to children in Italy, where abundances of protein and lipid metabolizers (Firmicutes and Proteobacteria) were dominant [60]. A follow up study attributed the different microbiota profiles to the decreased consumption of fiber in European children [61]. Numerous studies have come to similar conclusions when comparing cultures who have incorporated a Western diet and industrialized lifestyles to those of non-industrialized populations [61–63]. Additionally, microbiome profiles of vegans and vegetarians in Western cultures are found to be similar to those in non-industrialized countries that consume similar plant-rich diets [56]. Studies involving high-fiber diet consistently present *Prevotella* as a key member of the microbiome associated with high-fiber intake (vegan, vegetarian, and low-animal product diets) [35, 60–65]. Health effects observed by *Prevotella* are likely strain dependent, as there are studies showing both beneficial and adverse health outcomes linked with the presence of *Prevotella.* *Prevotella* has been associated with an increase glucose metabolism, SCFA production, and overall anti-inflammatory responses in the gut [66–69]. Conversely, *Prevotella* classification as a pathobiont has emerged through association with rheumatoid arthritis, low-grade systemic inflammation, insulin resistance, and glucose intolerance [70, 66, 71]. Multi-omics approaches may aid in understanding the functional capabilities of *Prevotella* and other microbes with conflicting health outcomes [30].

Given the appreciation for the microbiome's essential role in health, diet-based strategies to modulate its metabolic function have emerged [46, 72, 73]. Prebiotics are non-digestible food ingredients or substances that increase the growth and activity of certain beneficial microbes [74]. Common prebiotics include oligosaccharide fructans (fructooligosaccharides and insulin) and galactans, that often enrich *Lactobacillus* and *Bifidobacterium* sp. in the gut [75]. In 2016, the International Scientific Association for Probiotics and Prebiotics (ISAPP) officially broadened the definition of prebiotics to include "non-carbohydrate substances, applications to body sites other than the gastrointestinal tract, and diverse

categories other than food" [75]. However, the hallmark characteristic that prebiotics cannot be digested by host enzymes but instead selectively utilized by host microorganisms remains a key factor. In mice, intake of prebiotics has been linked to a decrease in Firmicutes and increase in Bacteroidetes [76]. Importantly, the increased growth of Bacteroidetes, especially *Bifidobacterium,* restricts the activity of proinflammatory microbes such as *Escherichia coli* and *Clostridium* sp. [77]. Evidence shows that prebiotics prompt a functional change of the microbiome resulting in a profound effect on human health. Respondek *et al*. (2013) described how intake of prebiotic short-chain fructo-oligosaccharides resulted in decreased levels of plasma leptin and insulin [78]. Prebiotic treatment has also been linked to a decrease in the severity of inflammatory bowel disease symptoms, decreased concentrations of circulating C-reactive protein, increase in serum levels of the anti-inflammatory cytokine IL-10, and increased blood-brain barrier integrity [72, 73, 79].

Fermented foods, such as yogurt, kefir, kimchi, sauerkraut, and kombucha, have long been consumed by populations around the world, and on average make up one-third of food intake [80]. The majority of dairy products are fermented by lactic acid bacteria (*Lactobacilllus* sp. and *Streptococcus thermophilus*), and *Bifidobacteria* sp. and *Saccharomyces* yeasts contributing to fermentation of beverages and cereals [80]. Human studies analyzing how consumption of fermented food alters the gut microbiome indicates their potential role in alleviating dysbiosis (systematically reviewed in [81]). Wastyk *et al*. (2021) recently reported their findings from a longitudinal randomized human study comparing high-fiber and high-fermented food diets based on the microbial diversity, human and microbe metabolomes, and immune profiling [82]. Results showed the high-fiber diet did not influence diversity of the microbiome, but it did lead to an increase in abundance of microbial proteins per gram of stool and increased relative abundances of carbohydrate-active enzymes. The high fermented foods diet did show an increase in alpha-diversity and abundances of the Firmicutes phylum (nearly half of which were members of the Lachnospiraceae family) [82]. These results show that while fiber may increase overall bacterial concentration, fermented foods achieved increased diversity through shifts in abundances of the resident microbial community. Another multi-omics study comparing consumers and nonconsumers of fermented foods (self-reported) found

significant differences in their gut communities [83]. Specific microbiomes that were associated with consumption of fermented foods included *Bacteroides*, *Pseudomonas*, *Lachnospiraceae*, *Prevotella*, *Oscillospira*, *Enterobacteriaceae*, *Fusobacterium*, *Alistipes putredinis, Lactobacillus acidophilus*, *Lactobacillus brevis, Lactobacillus kefiranofaciens, Lactobacillus parabuchneri, Lactobacillus helveticus*, and *Lactobacillus sakei* [83].

Together, studies presented above provide evidence for the profound impact diet has on the microbiome, which subsequently impacts overall health. Decreases in high-fat and high-sugar diets, as well as consumption of fermented foods may be key to reducing non-communicable diseases associated with decreased bacterial diversity and alterations to the metabolome.

1.2.2.2 Antibiotics

Exposure to antibiotics can have profound implications on both short- and long-term function of the gastrointestinal microbiome. Aside from reduced species diversity, antibiotics can alter the metabolic activity of microorganisms and lead to increased presence of antibiotic-resistant bacteria [22]. One well documented result of antibiotic exposure is recurrent *Clostridium difficile* infection. Many antibiotics have been associated with the onset of *C. difficile* infection, including clindamycin, lincomycin, ampicillin, and cephalosporins (including cefoperazone) [84]. Even a single dose of clindamycin increases the susceptibility to *C. difficile* associated diarrhea and colitis and reduces bacterial diversity by 90% [85]. The broad-spectrum antibiotic tigecycline has also been associated with reduced levels of *Bacteroidetes* drastic increases in *Proteobacteria* directly after tigecycline exposure in mice [86]. A subsequent challenge with *C. difficile* spores left animals susceptible to colonization and displayed clinical signs of infection [86].

Antibiotic exposure can have long term impacts when taken during the critical window of microbiota development and immune system maturation in a child's infancy [33]. Premature infants are often prescribed empirical antibiotic treatment within the first few days of life based on perceived risk of infection, even though broad-spectrum antibiotic use has been linked to drug-resistant sepsis, invasive fungal infections, significant alterations to the intestinal microbiome, necrotizing enterocolitis, and overall

mortality [87]. Antibiotic exposure early in life has also been shown as an independent risk factor for increased childhood obesity and body weight through a dose-dependent relationship [6]. In mice, early-life exposure to antibiotics exhibited an increased risk to pathogen challenge 80-days after exposure [88]. Additionally, the antibiotic-perturbed microbiome was transferred into germ-free mice and resulted in worsened colitis and susceptibility compared to transfer of a healthy microbiome during challenge [88]. Recent results for studying early life exposure to penicillin in a murine model linked low-dose exposure to substantial effects on the frontal cortex of the brain, providing evidence that the gut-brain axis can be affected by exposures to antibiotics starting at birth [89]. Other outcomes associated with early antibiotic exposure includes asthma, allergic rhinitis, atopic dermatitis, celiac disease, attention deficit hyperactivity disorder, and development of inflammatory bowel diseases [90–92].

In adults, past exposure to certain antibiotics, including penicillin, cephalosporins, macrolides, and quinolones correlated with an increased risk of developing type 1 and type 2 diabetes [23, 93]. In type 2 diabetes, an increased use of antibiotics up to 15 years prior to diagnosis was found [93]. Similar to exposures in children, antibiotic treatment can lead to weight gain in adults [94, 95]. This could be a result of decreased populations of SCFA producing bacteria, especially Firmicutes, after antibiotic exposure. Zaura *et al*. (2015) reported how a single dose of clindamycin and ciprofloxacin resulted in decreased abundances of butyrate-producing bacteria for several months after treatment [96]. Additionally, exposure to antibiotics can lead to lasting shifts in the microbiota, where *Bacteroides* communities especially never recover to their original composition [97].

In addition to the decreased diversity in the microbiome and long-term persistence of resistant species, antibiotics can also have profound effects on the gut metabolome. Disruption of the competitive ecosystem caused by antibiotics results in increased levels of carbohydrates available in the gut [98, 99]. The free carbohydrates, specifically sialic acids and fucose, allow for pathogens like *Salmonella* sp. and *C. difficile* to rapidly colonize the gut [98]. Furthermore, bacterial metabolism of bile acid, hormones, and cholesterol and synthesis of key vitamins is impaired during antibiotic therapy [31].

Efforts in active reconstitution of the microbiome following antibiotic administration have emerged. Analogous fecal microbiome transplantation and even spontaneous microbiota reconstitution are more effective than probiotic administration, where a delayed repopulation of the microbiome was observed [100]. Suez *et al*. (2018) suggested the inhibition of microbiome recovery following probiotic administration in humans and mice was due to soluble factors secreted by *Lactobacillus* and blooming abundances of *Lactobacillus*, *Bifidobacterium*, and *Streptococcus* [100].

Collectively, these studies provide ample evidence that antibiotics have a profound effect on the resident microbiome and include long-term consequences. Further investigation into the advantages and limitations of probiotics in therapeutic approaches are required before making accurate recommendation to patients after antibiotic exposures.

1.3: Mucosal Immune System

The mucosal immune system is comprised of various mucosa-associated lymphoid tissues (MALTs) and represents one of the largest mammalian organs. Examples of these tissues in mammals include the gut-associated lymphoid tissue (GALT), nasopharynx-associated lymphoid tissue (NALT), and inducible bronchus-associated lymphoid tissue (iBALT) [101]. Although MALT sites are anatomically distant, activated B cells from one tissue can migrate to other mucosal effector sites as part of the "common mucosal immune system" [102]. These systems are designed to protect the mucosal tissues from colonization and damage from pathogens while activating tolerance mechanisms to prevent pro-inflammatory immune responses against food and commensal antigens [103]. Secretory IgA is the predominate immunoglobin in the GALT, and its complex role in maintenance of the microbiota is still being discovered [104]. In the next sections, we will further describe the characteristics of induction and homing unique to the musical immune system, and the critical roles of IgA in maintenance of the gut microbiota.

1.3.1: Induction and Homing of the GALT

Induction of the mucosal humoral immune response is a central tenant in the development of efficacious vaccines. Oral vaccines are designed to specifically target the inductive sites within the GALT. These include Peyer's patches (PP), cecal patches, colonic patches, isolated lymphoid follicles (ILF), and gut-draining mesenteric lymph nodes (MLNs) [101]. PPs are composed of B cell follicles surrounded by interfollicular region rich with T cells [105]. Mice have eight to ten PPs, while humans have upwards of 300 that are overlayed by follicle-associated epithelium and Microfold cells (M cells) [105]. M cells specialize in transferring antigens from intestinal lumen to PPs, and the high abundance of DCs in PPs allows for immediate presentation of processed antigens to T cells [103]. Antigen-primed T follicular helper cells then support IgA-class switching and somatic hypermutation through CD40/CD40 ligand integrations and cytokine expression of TGF-β, IL-4, and IL-2, resulting in high-affinity IgA secreting plasma cells [106]. In contrast, T cell-independent pathways of B cell activation do not induce somatic hypermutation for affinity maturation, thus leading to secretion of low-affinity polyreactive IgA, further described in 1.3.2.

Migratory DCs are commonly found in MLN, which form a chain-like structure of draining lymph nodes from the gastrointestinal tract [107]. The continuous migration from intestinal tissues to MLNs allows for DCs to present antigen to T cells. Previously, it was thought that lymphatics from both the small intestine and colon drain as a continuous flow to all nodes of the MLN. However, it is now understood that lymphatics of the different regions of the intestine drain into distinct MLN nodes, and the activity of DCs within these nodes vary. Importantly, small intestine MLNs harbor DCs with higher retinal dehydrogenase activity that is required for upregulation of homing receptors on T and B cells [107].

One characteristic of the mucosal immune system is the high degree of compartmentalization of different anatomical mucosal sites. Efforts to understand how antibody secreting cells (ASCs) migrate between MALTs have revealed specific chemokines and receptors are needed for efficient migration [108]. Expression of the integrin α4β7 on B cells, that binds to the MAdCAM-1 receptor on intestinal epithelial cells, is required for homing to the intestinal mucosa [109]. General trafficking of IgA-ASCs to most mucosal tissues is dependent on expression of CCR10 by IgA-secreting cells and secretion of the chemokine

CCL28/MEC by epithelial cells in salivary glands, stomach, and colon [110]. Furthermore, specific migration to the small intestine is mediated secretion of CCL25 by epithelial cells and the expression of the chemokine receptor CCR9 by ASCs [111].

Expression of these chemokine receptors, especially α4β7 and CCR9, on T and B cells have been shown to be induced by DCs from PPs and MLN [112]. The increase in α4β7 and CCR9 expression has been attributed to retinoic acid (RA) produced by DCs via retinaldehyde dehydrogenases (RALDH: aladh1a1 and aladh1a2) from vitamin A [108]. This role of RA from GALT-DCs has further been shown through studies with vitamin A deficiencies, where animals showed significant decreases in ASCs and T-cells in the gut [113]. The TLR2 ligand has also been proven to be a significant inducer of CCR9 and CCR10 on circulating B cells [114]. Studies further identifying adjuvants that lead to activation of these induction and homing pathways will be crucial for engineering vaccines that elicit specific immune responses.

1.3.2: Function of IgA

IgA plays a complex role in host health by simultaneously excluding harmful microorganisms and maintaining the presence of symbiotic bacteria. IgA is most abundant at mucosal surfaces, where most adults secrete several grams per day into the lumen [115]. IgA is found in its monomeric form in the serum of humans, and is produced by plasma cells in the bone marrow and marginal zone B cells [116]. Serum IgA has been shown to have both proinflammatory and anti-inflammatory properties, and intestinal dimeric IgA plays a definitive role in selection and maintenance of the gut microbiome [117, 118].

Humans, along with chimpanzees, gorillas, and gibbons, have two subtypes of IgA, IgA1 and IgA2, which differ by the number of glycosylation sites and length of their hinge region [119]. IgA1 has more of a “T” shape compared to the conventional “Y” shape of immunoglobins [119]. The greater separation between the Fab regions is advantageous for binding two antigen fragments, and allows for the increased avidity of immunoglobins that recognize repeated structures on the surface of microorganisms [120]. IgA1 is the predominant subtype found in the serum and comprises 90% of circulating IgA molecules. IgA1 is

also more heavily glycosylated compared to IgA2 [121]. Recent studies have reported that IgA1 may be important for immune homeostasis, where IgA2 often aids in inflammatory responses [121]. IgA2, with its shorter hinge region, is more resistant to the protease activity of bacterial pathogens and may be the evolutionary reason for its high prevalence in mucosal secretions [119].

Although IgA is the second highest immunoglobin in the serum, behind IgG, its participation in systemic immune responses is limited, especially compared to its definitive role at mucosal sites. Under homeostatic conditions, anti-inflammatory effects can be regulated through covalent bonding between the C-terminal of IgA and serum proteins, including albumin, α1-antitrypsin, HC-protein, and fibronectin, to reduce chemotaxis of neutrophils and leukocytes [122, 123]. IgA can also down-regulate IgG-mediated phagocytosis, bactericidal activity, chemotaxis, and pro-inflammatory cytokines in the serum by polymorphonuclear leukocytes (PMNs) and peripheral blood monocular cells (PBMCs) [117, 124]. However, IgA also drives proinflammatory responses. Cross-linking of the Fc alpha receptor (FcαRI, or CD89) on neutrophils by IgA complexes in both serum and the mucosa can lead to an increased release of the neutrophil chemoattractant leukotriene B4, which induces migration of monocyte derived DCs [125, 126]. The FcαRI is also expressed on monocytes, eosinophils, and some macrophages and dendritic cells. Binding FcαRI on these cells to the interdomain of the Fc region of IgA can also cause long distance conformational changes along IgA, possibly from the hinge up to the Fab region [127, 128]. These changes may act as an anti-inflammatory mechanism by impairing IgA's ability to bind antigen.

In both humans and murine models, IgA producing PCs are created via T cell-dependent (TD) and T cell-independent (TI) mechanisms. TD maturation of IgA-secreting B cells requires CD40-CD40L interactions with follicular helper T cells (T_{FH}) within Peyer's patches, which promotes class-switch recombination and eventual proliferation [129]. Conversely, TI-IgA is generated when the transmembrane activator and CAML (calcium modulator and cyclophilin ligand) interactor (TACI) receptor on B cells bind DC-secreted factors, including B cell activating factor (BAFF), a proliferation inducing ligand (APRIL), retinoic acid (RA), and TGF-β [106, 130]. It is believed that TI-B cell maturation results in a pool of

polyreactive IgA that often recognize broader range species within the microbiota, and TD-IgA has high-affinity for specific antigens since B cells undergo somatic hypermutation for affinity maturation [130]. Studies in mice with a genetic loss of T cells has proved inconsistent, due to varying findings in the reduction or even increase of IgA-coated bacteria relying on TI-pathways of IgA induction (reviewed in Huus *et al.,* 2021) [130]. IgA-seq methods, where bacteria are sorted by bound IgA and then sequenced by 16S rRNA, could reveal biological differences in the bacteria coated by TI and TD IgA.

Since IgA can be translocated across the epithelial layer into mucosal compartments, it plays a principal role in defense against pathogens and foreign antigens along the gastrointestinal tract. Plasma cells in the lamina propria produce dimeric IgA, which are then taken up by the polymeric Ig receptor (pIgR) on epithelial cells and excreted into the lumen. This process of transcytosis through epithelial cells results in secretory IgA (SIgA), due to the secretory component of pIgR remaining covalently linked to IgA [131]. SIgA primarily prevents colonization of microorganisms through immune exclusion by preventing attachment to epithelial cell receptors (Figure 1.1) [104]. Toxins are similarly neutralized by IgA and facilitates their excretion (Figure 1.1) [104]. One example of IgA's prevention of epithelial attachment is its activity against cholera toxin (CT). Protection was markedly decreased in mice with a J-chain deficiency, which restricted transport of IgA into the lumen and prevented IgA's ability to block epithelial binding [132]. Another method of protection utilized by IgA is agglutination and entrapment within the mucus to prevent interaction between the epithelium and microbial pathogens or toxins (Figure 1.1). The resulting macroscopic clumps are cleared via peristalsis or uptake via M cells and DCs (Figure 1.1) [133].

SIgA also plays a distinct role in maintaining intestinal homeostasis, as demonstrated with activation-induced cytidine deaminase deficient mice [134]. These mice lack the ability to class switch from IgM to IgA, and have significant increases in the number of non-pathogenic commensals and enlargement of isolated lymphoid follicles [134]. In humans, IgA-deficiencies are often asymptomatic, but lead to dysbiosis marked by increased abundances of pathobionts and decreased abundances of SIgA-targeted commensals (specifically the Lachnospiraceae family) [130]. IgA-deficiencies in humans are also associated with enhanced susceptibility to celiac disease, autoimmunity, and respiratory infections [135].

It is believed that some commensal bacteria utilize IgA to enhance colonization [130]. Slow growing commensal bacteria can exploit SIgA to form small aggregates that are less susceptible to clearance by peristaltic flow and immune exclusion (Figure 1.1). This has been demonstrated with *Bacteroides fragilis*, where IgA binding was required for colonization due to the ability to form dense aggregates of *B. fragilis* [136]. Similar colonization was found *in vitro* with *Bifidobacterium lactis, Lactobacillus ramnosus,* and non-pathogenic *E. coli* [136]. Fast growing pathogenic bacteria form larger more dense aggregates that are more susceptible to clearance [130].

Binding of IgA on bacterial surfaces can also have direct impact on their transcriptional profiles [133]. Early studies involving *Shigella flexneri* revealed IgA entrapped the bacterium in a thin mucosal layer as a method of immune exclusion [137]. Current sequencing technologies have also revealed the additional activity of IgA on changes to gene expression [138]. Binding of murine monoclonal IgA specific for the O-antigen of *S. flexneri* results in suppressed activity of the type 3 secretion system, thus decreasing its virulence [138]. IgA binding to flagella can also limit motility and decrease the expression of flagellar genes (Figure 1.1) [138, 139]. When SIgA binds to the flagella and O-antigen of *S.* Typhimurium, a confirmational change in the surface of the bacterium impairs motility within 15 minutes of binding [140]. Similar outcomes of decreased motility and flagellar expression were observed in commensal Proteobacteria and Firmicutes following TLR5 signaling and anti-flagellar SIgA [139]. Monocolonization of *Bacteroides thetaiotaomicron* in mice resulted in decreased bacterial and expression of specific IgA-binding epitopes following IgA binding [141].

In summary, IgA has a complicated purpose within the intestinal system, as demonstrated by its ability to clear pathogens, modulate microbial activity, and encourage commensal colonization. While important progress regarding understanding of IgA and microbe interactions has been made, many aspects of how IgA shapes the microbiota remain poorly understood.

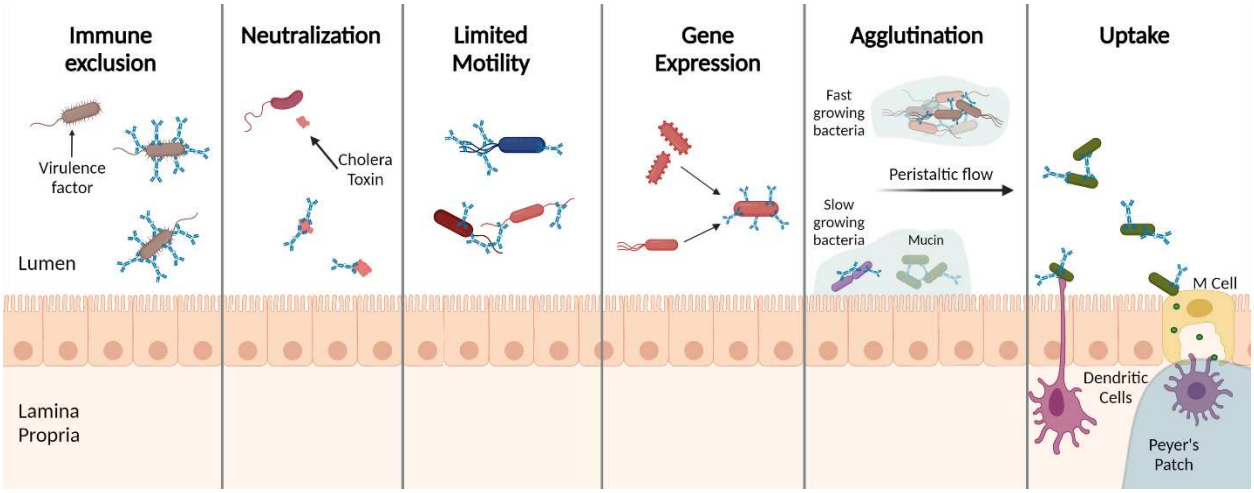

Figure 1.1. Functions of IgA in response to microbiota. Potential functions of IgA in response to the microbiota and exogenous antigens, inuding immune exclusion, neutralization of toxins, decrease motility, alterations in gene expression (specifically surface epitopes and flagellin), agglutination for clearance and biofilm-like colonization, and improved uptake. These functions are further described in 1.3.2. Created with BioRender.com.

1.4: Mucosal Vaccination

As described above, the mucosal immune system and related tissues collectively represent the largest mammalian immune organ. The majority of pathogens enter the body through mucosal tissues, including the gastrointestinal, intranasal, respiratory, and urogenital tracts. However, the vast majority of current approved vaccines are delivered systemically (parenteral injection), and may not be optimal for eliciting local immune responses at mucosal tissues [142]. Currently, only nine mucosal vaccines are approved for human use, which target *Salmonella typhimurium*, *Vibrio cholerae,* Influenza, Poliovirus, and Rotavirus [143]. Of these, eight are delivered orally and one (targeting Influenza) is delivered nasally [143]. Notably, all approved vaccines constructs are either live-attenuated or live-reassorted (*Vibrio cholerae*: Vaxchora, *Salmonella typhimurium*: Vivotif*,* Poliovirus: Biopolio and mOPV/tOPV, Rotavirus: Rotateq and Rotarix, and Influenza: FluMist/Fluenz) or whole-cell inactivated (*Vibrio cholerae*: Dukoral, Euvichol, and ShanChol) [143, 144].

There are many advantages associated with mucosal vaccination. For example, needleless administration eliminates need for specialized personnel, and noninvasive administration often improves

patient compliance. In addition, oral vaccination is ideal for achieving mass immunizations quickly, distribution to rural areas without need for cold-chain, and they are often inexpensive to manufacture [142, 143, 145]. Aside from these advantages in human populations, oral administration is highly favorable for vaccination of agricultural animals and baiting in wildlife vaccination [144]. In addition, mucosally delivered vaccines elicit both IgA and IgG antigen-specific responses to provide protection at local and distal mucosal sites as well as systemically [145–149].

Mucosal vaccine efficacy and immunogenicity is greatly influenced by the route of vaccination, selected adjuvants or modulators, and immunization schedule [150–153]. Additionally, targeting of the mucosal immune system presents a myriad of challenges for vaccine development, as further described below. We also review strategies used to overcome these obstacles, current findings about the microbiome's influence on vaccine efficacy, and inversely, the potential influences of mucosal vaccination on the composition of the microbiome.

1.4.1: Challenges

A principal challenge to eliciting a strong efficacious immune response with orally administrated mucosal vaccination is overcoming biological barriers in the mucosa [151]. Vaccine antigens must be able to traverse the epithelial layer into immune-inductive lymphoid structures to stimulate an adaptive immune response [154]. Activity of nucleases and proteases, removal through mucosal secretions, highly acidic conditions of the stomach and GI tract, and bile salts all act to digest food material, invading pathogens, and vaccine antigens alike [155]. Therefore, soluble protein or synthetic peptide vaccines that are highly immunogenic when delivered parenterally often do not elicit the mucosal immune response before being denatured or degraded [156]. Additionally, the thick mucosal layer, ranging from 100-800μM, is difficult to penetrate and designed to trap foreign antigens and particles to quickly clear them [155]. To combat these chemical barriers and penetrate through the mucosal barrier, oral vaccines need to be administered at much higher concentrations compared to parenteral vaccines [156]. The increased concentration of antigen

needed in orally delivered vaccines also increases the risk of developing tolerance instead of inducing protective immunity [154].

Evading mechanisms of immune tolerance remains a major concern while designing novel mucosal vaccines. Oral tolerance actively suppresses inflammatory responses against antigens encountered in the gastrointestinal tract, and is primarily initiated by a subset of $CD103^+$ DCs [157]. These DCs deliver antigen to the MLN to prime naïve T cells into $Foxp3^+$ regulatory T cells [157, 158]. Impaired oral tolerance to food or microbes results in allergies or inflammatory bowel diseases [157], while development of oral tolerance against vaccine antigens leads to dampened immune response [159]. To combat the induction of tolerance, the addition of adjuvants to oral vaccines have shown great promise. Historically, the cholera toxin was the first adjuvant shown to not only prevent oral tolerance, but also reverse oral tolerance induced by the keyhole limpet hemocyanin antigen in a murine model [160]. Currently, cholera toxin B subunit is the only licensed subunit adjuvant being used in oral vaccinations [144]. Further investigations into mechanisms of adjuvanticity is required to circumvent the tolerogenic responses against subunit vaccines.

Development of oral vaccines that achieve high efficacy globally has also proved to be problematic. Given that enteric pathogens cause approximately 800,000 deaths annually, with the vast majority of mortalities occurring in low-income countries, the need for efficacious vaccines against these pathogens cannot be denied [161]. Of these enteric pathogens, Rotavirus was the leading cause of death resulting from diarrheal associated deaths in children [162]. While there are currently two vaccines approved for Rotavirus, there are major discrepancies between efficacy rates in European children (>95%) and children in low-income countries (50% in Malawi, 40% in Sub-Sahara Africa, and 50% in developing countries in Asia) [162]. Average titers of IgA produced from oral poliovirus vaccinations were four-fold lower in infants from lower-middle income countries compared to infants in high-income countries [163]. These differences in efficacy of oral vaccines are attributed to malnutrition, pro-inflammatory skewed gut microbiome, high rates of enteric infections, genetic factors, and pre-vaccination exposures [164]. Therefore, strategies to produce efficacious mucosal vaccines globally may require additional interventions, such as prebiotic, probiotic, or antibiotic treatment.

1.4.2: Strategies

Approaches to overcome the challenges facing mucosal vaccines and improve immune responses include choice of administration route, platform, and addition of adjuvants [165]. Mucosal vaccines can be administered by several routes, which result in varying immune responses [150, 166]. Oral and nasal routes are used most frequently for mucosal vaccination, followed by ocular, sublingual, vaginal, and rectal routes [144]. Consideration for the pathogen type and target mucosal tissue is critical for the rational design of novel vaccines. For example, systemic immunization is sufficient for neutralizing influenza since serum IgG antigen-specific antibodies can penetrate into nasopharyungeal secretions more efficiently than the gastrointestinal tract, and parenteral vaccination still induces a strong protective T cell response [167, 168]. However, systemic administration of the vaccine does not protect against influenza infection itself, just lessens associated symptoms [168]. Route of mucosal vaccination impacting vaccine efficacy has also been shown in chickens given live-attenuated *Mycoplasma gallisepitcum* vaccines via ocular, nasal, and oral routes [169]. Results indicated that eye drop vaccination lead to significantly higher protection against respiratory infection from *M. gallisepitcum* [169]. A study in rhesus macaques revealed a marked difference in antigen-specific antibodies between intramuscular or aerosol immunization against SIV [170]. While both routes provided some level of protection, a combination strategy may further protect the host against initial infection at mucosal sites and systemic distribution of the pathogen.

Recent advances in oral delivery mechanisms have provided strategies to overcome the harsh conditions of the gastrointestinal tract. Nanoparticles coated in pH-sensitive polymers, such as alginate, cellulose derivatives, or polyethylene glycol are able to resist degradation by enzymes and low pH to eventually penetrate the mucosa and release antigenic cargo to M cells or other target cells [165, 171]. For synthetic particles to reach the epithelial layer, they must have a neutral charge and be small enough to pass through the cross-linked negatively charged structure created by mucins [172]. For example, mice orally administered 100 nm thiolorganosilica particles had significantly higher levels of IgA+ cells in Peyer's Patches compared to larger sized particles [173].

On the other hand, utilizing live lactic acid bacteria (LAB) that are inherently equipped to persist in the gastrointestinal tract has shown great potential [174]. Most commonly, species in the *Lactococcus, Lactobacillus,* and *Streptococcus* genera have been used as vaccine platforms [175]. Compared to efforts using attenuated pathogenic bacteria as vaccine platforms, the lack of LPS on LAB removes the risk for developing endotoxic shock, and there is no possibility of reverting back to a virulent status [174]. Instead, LAB are Gram-positive bacteria that are generally recognized as safe (GRAS). The cell wall components of LABs (peptidoglycan, lipoproteins, and lipoteichoic acids) are capable of activating pattern recognition receptors, including Toll-like receptor 2 (TLR2), nucleotide-binding oligomerization domain (NOD)-like receptors (NLR, especially NOD2), and C-type lectins [175]. Evidence for strain-dependent activation of TLR3, TLR6, TLR9, and interferon production has also been demonstrated [176]. Strain-variability has also been demonstrated in DC activation, where IL-12 and TNF-α cytokine production was highly variable depending on the LAB strain and DC phenotype [177].

Genetic modification of LAB allows for expression of antigen either on the cell surface, anchored to the cell wall, or in the cytoplasm [178]. Display methods largely depend on properties of the antigen (size, net charge, importance of confirmational modifications, etc.) and concentration of expression needed [178]. In *Lactobacillus* species, expression of antigen can be modulated through either constitutive (surface layer protein A [slpA], phosphoglycerate mutase, or the lactate dehydrogenase) or inducible (α-amylase, sakacin-P, and p-coumaric acid decarboxylase, among others) [175, 179, 180]. The understanding of how selected promoters alter antigen expression is critical when designing efficacious LAB vaccines.

One method to increase immunogenicity of LAB platforms and other mucosal vaccines has been the addition of adjuvants [176]. However, most adjuvants have been studied in the context of parenteral immunization, and their activity in mucosal vaccines are not fully defined. The influenza vaccine Nasalflu incorporating the heat-labile toxin (LT) from *E. coli* was the only licensed mucosal vaccine with a mucosal adjuvant, but it is no longer on the market due to unintended side-affects [181]. Cholera toxin (CT) subunits have also been incorporated into mucosal vaccines, and resulted in Th1 polarized immune responses [182]. Other adjuvant strategies include LAB secreting cytokines to attract immune cells or achieve a desired

immune response. IL-1β, IL-2, and IL-12 have all been evaluated in murine studies for their ability to enhance oral and intranasal vaccines [176, 183]. Expression of DC-peptides or anti-CD205 has been used to specifically target DC uptake and activation [176]. Strategies employing surface expression or co-administration of bacterial derived adjuvants with LAB have shown promise in animal models but have yet to be studied in humans. These adjuvants include Salmonella flagellin, PorA from *Neisseria meningitidis*, Internalin A from *Listeria monocytogenes,* Fibronectic-Binding Protein A from *Staphylococcus aureus*, among others [176].

These advances in mucosal vaccine delivery and immunogenicity have moved mucosal vaccine platforms closer to being commercially available. However, their use in human models and biological protection during natural infections remains to be investigated. Moreover, potential off-target impacts on the commensal microbiome form bacterial derived adjuvants need to be characterized.

1.4.3: Modulation of the microbiome to increase efficacy

There is increasing support from both animal studies and human cohorts that indicate the gut microbiome is a major modulator of immune responses against vaccination [184]. Results from germ-free mice provide compelling evidence, where vaccine-specific antibodies are significantly reduced in germ-free mice compared to specific-pathogen-free mice following systemic influenza vaccination [185]. Pregnant mice administered a combination of broad-spectrum antibiotics gave birth to infant mice with an altered microbiota resembling that of the mother, and the infant mice were vaccinated with ovalbumin and complete Freund's adjuvant at 7 days old [186]. Importantly, antibiotic exposed mice had significantly decreased titers of ovalbumin specific IgG compared to control mice. The same study also compared germ-free mice vaccinated between 3-12 weeks of age, and again found significantly decreased levels of ovalbumin-specific IgG compared to control mice [186]. Lynn *et al*. (2018) demonstrated the long-term impairment of vaccine responses in mice with early exposure to antibiotics [187]. Pregnant mice were also administered antibiotics, and antibiotics were continuously given via drinking water post-weaning until 1 week prior to vaccination. Six vaccines that are commonly administered to infants were tested (Bacillus

Calmette-Guerin (BCG), Pneumococcal Conjugate Vaccine, Meningococcal serogroup B vaccine, Meningococcal serogroup C vaccine, INFANRIX hexa combination vaccine, and the seasonal influenza vaccine), and only the seasonal influenza vaccine showed no difference of antigen-specific IgG titers between antibiotic treated and control mice. All other vaccines had significantly decreased titers of IgG in antibiotic exposed mice throughout the 12-weeks mice were followed post-immunization and booster [187]. A different approach was used by Oh *et al*. (2014) to demonstrate the adjuvant activity of the resident microbiota: adult *Tlr5–/–*, germ-free, and antibiotic-treated mice were all had significantly impaired antibody responses against the seasonal influenza vaccine compared with littermate controls [185].

Several human cohort studies have provided evidence for the microbiota's role in vaccine efficacy. In human cohort and randomized control studies, oral rotavirus vaccines have shown significant associations between the microbiome of infants in low-income countries that respond to the vaccine and the microbiome composition of age-matched infants in Norther European countries compared to non-responders [188, 189]. A study in China showed high titers of poliovirus-specific IgA were positively correlated with abundances of *Bifidobacterium* [190]. In adults, administration of broad-spectrum, narrow-spectrum, or no antibiotics before rotavirus vaccination all resulted in different levels of anti-rotavirus IgA boosting and rotavirus shedding [191]. While both broad spectrum and narrow-spectrum antibiotic administration resulted in higher levels of fecal shedding, administration of Vancomycin alone led to a significant increase of anti-rotavirus IgA [191]. Adults with low levels of pre-existing immunity against influenza also showed markedly decreased influenza-specific IgG and IgA following antibiotic treatment and influenza vaccination [192]. These results indicate that the microbiome can be manipulated with narrow-spectrum antibiotics to selectively decrease the abundance of certain species as a means to achieve higher vaccine efficacy.

As noted above, diet can have an immense impact on the composition of the microbiome as well, and therefore can provide an avenue for enhancing vaccine efficacy. A gnotobiotic pig model was used to show that protein deficiency may be impairing rotavirus vaccine responses in infants with protein malnutrition [193]. Gnotobiotic pigs were inoculated with infant fecal microbiota and fed a protein-

deficient or protein-sufficient bovine milk diets prior to oral vaccination with attenuated human rotavirus vaccine. Subsequent challenge with rotavirus revealed that protein malnutrition leads to higher titers of fecal viral shedding and lower protection rates against diarrheal symptoms [193]. The authors hypothesized that this outcome was due to the dual impacts of the altered gut microbiota and impaired innate, T cell, and cytokine responses [193, 194]. Alternatively, including certain dietary compounds may increase vaccine efficacy. Administration of a prebiotic mixture of fructooligosaccharides was shown to increase *Salmonella* vaccine efficacy in mice by providing greater protection following challenge with virulent *S. typhimurium* [195]. The enumeration methods used in this study severely limited observations to changes in the microbiota. Current high throughput, culture independent methods in microbiome analysis and transcriptomics could reveal a more precise reciprocal effect of diet on the microbiome and subsequent the enhanced immune responses.

Collectively, the above provides evidence that the microbiota plays a critical role in vaccine responses through adjuvant activity. The above also indicates that modulation of the gut microbiota via diet and select antibiotics is a practicable approach to achieve greater efficacy for mucosal vaccines globally.

1.4.4: Impact of vaccination on the microbiome

While there have been great advances in research identifying how the microbiome influences vaccine efficacy, minimal efforts have focused on how vaccination might impact the composition and function of the microbiome. Evidence so far presents conflicting results, likely due to the various vaccine delivery methods and targets which result in multifarious effects on the resident microbiome. Recently, Leite *et al*. (2018 and 2021) investigated how an oral live vaccine and challenge with *Lawsonia intracellularis* changes the microbiome composition at several anatomical locations along the gastrointestinal tract in pigs [196, 197]. Originally, they concluded vaccination with a single dose of a live attenuated vaccine against *L. intracellularis* resulted in altered microbiota only after co-challenge with *Salmonella enterica serovar Typhimurium* and *L. intracellularis.* Their results also showed that co-infection without vaccination had a greater impact on beta-diversity compared to animals receiving vaccination with

or without challenge [196]. Specifically, vaccinated pigs had decreased abundances of *Collinsella* and *Prevotella* during co-infection compared to unvaccinated co-infected animals. However, direct changes to the microbiome from vaccination without challenge were not shown. In a follow up study, oral vaccination and challenge with *L. intracellularis* were again evaluated, but focused on microbiome changes in select locations of the intestinal tract (ileal mucosa, ileal digesta, cecal digesta, and feces) [197]. Vaccination alone (prior to any challenge) was shown to have a significant effect on the community structure within the intestines. In fecal samples, 73 genera had significantly different abundances between vaccinated and unvaccinated pigs. During *L. intracellularis* infection, non-vaccinated animals had a marked increase of several pathobionts (*Campylobacter*, *Chlamydia*, *Fusobacterium*, and *Collinsella*) within the small and large intestine [197].

In humans, oral vaccination using live-attenuated typhoid Ty21 had no significant impact on the gut microbiome, but differences in the microbiome of individuals who displayed multiphasic cell-mediated immunological responses compared to later responders were observed. Given the small sample size, these findings weakly showed an increase in diversity for multiphasic responders, but no temporal differences in the microbiome were observed between vaccinated and unvaccinated individuals [198]. In infants, it is important to identify alterations to the microbiome due to vaccination since disturbances to the developing microbiome may result in complications later in life [7]. While this is important for all vaccines, it is especially crucial for vaccines with the potential for off-target effects on species related to the vaccine target. As described above, the mucosal immune system delicately balances between clearance of pathogens and maintenance of commensal microbes, and we cannot yet predict how administration of specific vaccines may impact this balance.

Studies that looked at temporal changes to the microbiome during mucosal vaccination have found various degrees of impact to the microbiome, from none at all to vast changes in diversity [152, 199–202]. Salgado *et al*. (2020) provided evidence that the pneumococcal conjugate vaccine (PCV10) that targets 10 different serovars of *Streptococcus pneumoniae* did not lead to significant alterations to the nasopharyngeal microbiome of children [199]. However, correlation network analysis revealed that vaccinated children had

a higher degree of microbial community (or network) complexity compared to the unvaccinated group, indicating that the increased complexity of the upper respiratory tract after vaccination could be a result of increased commensals that provide resistance against pathogen colonization. For the mucosal pathogen human immunodeficiency virus (HIV), vaccine efforts have primarily targeted systemic immunization even though HIV infections primarily occur at the rectal/genital mucosa. Vaccine approaches that target the mucosal immune system have shown promise for increased vaccine-mediated protection [200]. However, targeting the mucosal immune system also possess a great risk for altering the microbiome. Recently, a combined mucosal and systemic approach using Ad5hr-SIV recombinant immunizations resulted in distinct shifts in bacterial profiles within the rectal microbiota of female and male Rhesus macaques [152]. In females, four out of the five predominant phyla exhibited significant changes after two priming mucosal immunizations, with *Bacteroidetes* and *Cyanobacteria* dropping significantly and *Proteobacteria* and *Spirochaetae* increasing compared to the preimmunization timepoint. However, males only showed a slight increase in *Proteobacteria* and a modest decrease in *Cyanobacteria* [152]. The intramuscular systemic boost using either recombinant protein or DNA from SIV/HIV envelope proteins also resulted in distinct shifts in beta-diversity compared to pre-vaccination microbiome and post-mucosal priming in both males and females [152]. Investigations into the immunological response also provided evidence for mechanisms into the sex-difference that was seen between viral loads after SIV-vaccination, mainly attributing to the pre-vaccination difference of the rectal microbiome between males and females. Again, this provides further evidence that the microbiome influences vaccine efficacy.

Harnessing the inherent properties of probiotics as a vaccine platform also possess a greater risk to altering homeostasis within the gut microbiome. The bacterium *Lactobacillus acidophilus* was engineered to express the membrane proximal external region (MPER) epitope of HIV-1, along with the adjuvants FliC or murine IL-1β. While mice were administered live doses of recombinant *L. acidophilus* over twelve weeks, changes to the microbiome were also monitored [201]. The impact to the microbiome, shown through reduced richness and shifts in beta diversity, was dependent on the adjuvants expressed by *L. acidophilus*: FliC had a minimal impact while major shifts were seen with expression of IL-1β and MPER

alone [201]. Redweik *et al*. (2020) revealed that chickens orally administered commercial probiotics and/or the recombinant attenuated Salmonella vaccine (RASV) χ9373 resulted in significant shifts in beta diversity in fecal and cecal samples [202]. RASV administration, either alone or with prior probiotic treatment, resulted in a decrease of SCFA producing bacteria (*Clostridium* and *Weisella*). Probiotic administration resulted in an increase in Proteobacteria, and RASV vaccination without probiotics saw an increase in Verrucomicrobia. A broader investigation into off-target effects to the resident taxa following oral administration of probiotics as a platform or co-administered with other oral vaccines, and the addition of adjuvant, is still required.

These studies provide evidence that various mucosal vaccines result in varying influences on the composition of the microbiome. However, these studies are limited to analysis utilizing 16S rRNA amplicon sequencing, often using different sequencing platforms and methods of analysis. Therefore, findings so far are limited to analyzing the presence, absences, and abundances of bacteria and not differentiating between active and inactive bacteria. There is evidence of prominent transcriptional changes of the commensal microbiota following acute immune responses to administration of flagellin and the anti-CD3 antibody [203]. These changes were detected six hours following administration without any significant changes in abundances of bacterial taxa, suggesting different bacterial species may react similarly to changes in host responses. Therefore, how the immediate and long-term functional diversity in the microbiome may be impacted by vaccination remains to be elucidated.

CHAPTER 2: Influence of Oral Immunization with *Lactobacillus acidophilus* and Modulation of Diet on the Bacterial Microbiome

2.1: Introduction

There is an ongoing need for the development of oral vaccine platforms that can be used to immunize under-served populations against mucosally transmitted pathogens. It is well known that the route of vaccination determines the nature and distribution of the immune response [150]. Vaccination via mucosal routes is attractive because it provides both mucosal and systemic immunity, whereas parenterally delivered vaccines often do not provide protection at mucosal surfaces [204]. An important feature of the mucosal immune system is that lymphocytes exposed to antigen at one mucosal site can migrate to other mucosal sites, thus providing widespread protection against a pathogen [145]. However, the advantages of mucosal vaccines also come with a set of challenges. The inherent physical defense mechanisms of the gastrointestinal tract, such as the low pH of gastric acid, digestive enzymes, and the antimicrobial peptide rich mucus, prevent many antigens from reaching immune inductive sites [205]. Vaccine strategies to overcome these obstacles harness either natural or artificial delivery vehicles, including nanocarriers such as liposomes, virus-like particles, plant-based expression systems, and probiotics [175, 206, 207].

We have developed a probiotic-based mucosal vaccination platform that utilizes the bacterium *Lactobacillus acidophilus*. *Lactobacillus* species express several microbe-associated molecular patterns that are recognized by host pattern recognition receptors [208, 209]. *L. acidophilus* expresses natural ligands for toll-like receptor 2 (TLR2: peptidoglycans, lipoteichoic acid), nucleotide-binding oligomerization domain 2 (NOD2: muramyl dipeptide), and C-type lectin receptors (surface layer proteins) [210–212]. Furthermore, *L. acidophilus* is bile-acid tolerant, allowing the bacterium to survive throughout the gastrointestinal tract [213, 214]. Oral vaccination via *L. acidophilus* provides an attractive and easy delivery system with several logistic benefits: cold-chain is not required for distribution or storage, medical training is not required for the needleless administration, and large-scale production is inexpensive [207, 215]. These characteristics are particularly critical in low- and middle-income countries. Using *L. acidophilus* as a vaccine platform is also appealing due to the availability of genetic manipulation methods [216, 217].

Previously, we have reported on the construction of several recombinant rLA vaccine strains and characterized their immunogenic properties [214, 217, 218]. Recombinant *L. acidophilus* (rLA) strains can achieve massive surface expression of selected antigens when embedded in the surface layer protein A (slpA) [217]. Furthermore, adjuvants can be added to these rLA constructs, enhancing the immune responses and to avoid the induction of tolerance [151]. Thus, the rLA vaccine platform could be useful against a variety of important pathogens of humans and animals including rotavirus, coronaviruses, influenza, and HIV-1.

An important consideration unique to mucosal vaccination compared to parenteral vaccination is the reciprocal influence of the microbiome and mucosal immune responses. The immune system is constantly balancing between the clearance of pathogens and the tolerance of self-antigen, food, and the microbiota [219, 220]. The mucosal immune system has evolved not only to defend against pathogens through physical barriers and immune responses, but also to tolerate and possibly promote colonization of the microbiome in the gastrointestinal tract [104, 131, 221–223]. Indeed, the mucosal immune system directs the immunoselection of a "healthy" microbiome through the production of a diverse repertoire of IgA [222, 224–226]. There is additional evidence that the host microbiome plays an essential role during both oral and parenteral vaccination, as bacterial cells provide natural adjuvants necessary for promoting vaccine-induced immunity [185, 227]. For example, the variable flagellin structures in Proteobacteria, muramyl dipeptides found in bacterial cell walls, and short chain fatty acids produced by many bacterial species all aid in stimulating the mucosal immune response during vaccination [153, 228–230]. To date, research has primarily focused on the differences in the pre-vaccination composition of the microbiome and vaccine efficacy [153, 164, 227, 229, 231, 232], but has rarely addressed potential safety concerns related to lasting effects of vaccination on the resident microbiome [152, 202, 233].

We previously reported that co-expression of a model peptide antigen with different adjuvants by rLA resulted in strain-dependent shifts of the microbiome [201]. Three strains were tested that expressed the membrane proximal external region (MPER) from human immunodeficiency virus type 1 (HIV-1) and either no exogenous adjuvant, the Toll like receptor 5 ligand flagellar filament structural protein (FliC), or

soluble mouse interleukin-1β (IL-1β). The MPER peptide is a very weak antigen that allows comparison of different adjuvant effects. Our results showed that MPER alone and MPER + IL-1β (strain GAD19) resulted in microbiome shifts while no such shift was observed with the MPER + FliC strain. Furthermore, no clear associations were observed between total or MPER-specific IgA and the microbiome suggesting a role for other immune mechanisms including alterations in IgA-bound, resident microbiota.

It is known that secretory IgA plays a major role in maintaining the homeostasis of a healthy gut microbiome [131, 225, 226]. Several studies have revealed that natural polyreactive IgA often coats members of the commensal microbiome population to aid in their colonization, while high-affinity specific IgA binds to pathogens resulting in their clearance [104, 118, 234]. The rLA platform poses the potential to influence this balance in IgA coating through its combined function as a probiotic and activation of high-affinity antibodies against the vaccine antigen through a T-cell dependent response. Therefore, identifying changes in bacterial communities bound and not bound by IgA after repeated vaccination might reveal whether stimulating the mucosal immune system by oral vaccination with a probiotic vaccine platform might shift the IgA-bound microbiome in either a beneficial or detrimental way.

Another important contributor to gut microbiome composition is diet [235–237]. Singh *et al.* (2017) has demonstrated that consumption of particular foods leads to predictable changes in the abundance of specific bacterial genera [21]. Of interest, is how diet may lead to a favorable environment for the rLA vaccine. It has previously been demonstrated that the incorporation of the prebiotic rice bran into the diet of both animals and humans leads to increased abundances of *Lactobacillus* and increased titers of secretory IgA in fecal samples [238, 239]. Our preliminary studies showed that adding rice bran to the standard mouse chow diet did result in a significant change in intestinal microbial community structure but did not increase the immunogenicity of rLA expressing MPER [201]. To further investigate the potential of rice bran as a prebiotic, rice bran was incorporated into the diet in this study to assess the possible increase in MPER-specific antibody titers from oral vaccination with GAD19 that includes both antigen and exogenous adjuvant.

In this study, we sought to determine whether repeated administration of rLA alters the host intestinal microbial community as a result of the probiotic, due to direct competition and selective exclusion, or as a result of the host mucosal immune response against the rLA vaccine. To address the latter, IgA-seq was employed to characterize shifts in IgA-bound bacterial populations. Additionally, we determined whether using rice bran as a prebiotic would influence the immunogenicity of the GAD19 vaccine and/or IgA bound bacterial populations. Our results show that diet influenced the kinetics of rLA antibody induction, and that the rLA platform does not cause lasting disturbances to the microbiome (whole, IgA-bound or unbound). Diet played a primary role in modifications to the microbiome, while the *L. acidophilus* vector had a greater intermediate impact on the IgA-bound microbiome.

2.2: Materials and Method

2.2.1: Ethics Statement

This study was carried out with strict accordance to relevant guidelines and regulations, including ARRIVE guidelines (https://arriveguidelines.org), the Guide for the Care and Use of Laboratory Animals of the National Institutes of Health, and the Association for the Assessment of Laboratory Animal Care standard with approval from the Institutional Animal Care and Use Committee of Colorado State University (protocol number 14-5332A). Animals were monitored daily for clinical signs of illness or stress, and humanely euthanized at the study endpoint via carbon dioxide inhalation and thoracotomy.

2.2.2: Experimental Design

The experimental unit was classified as each individual animal throughout the study. Sample size was n=8, except for the Buffer_SC (Buffer Standard Chow) group, where one animal was not included in data analysis due to the development of splenomegaly. This number was determined based on power calculation in R using ELISA results from previous studies, and no other animals or data points were excluded from analysis except for the one mentioned. Experimental groups with respective diet and vaccine

treatment are shown in Table 2.1. Throughout analysis, the dosing buffer groups were used as the negative control to compare the GAD19 and NCK1895 results, and randomization for sample processing are described in microbiome methods below.

Table 2.1 Experimental groups with assigned vaccine treatment and diet. N=8 mice for each group, except Buffer_SC where 7 mice were used. All mice received the same number of treatment doses.

Group	N	Treatment	Diet
Buffer_SC	7	Carrier Buffer only	Standard chow
NCK1895_SC	8	NCK1895	Standard chow
GAD19_SC	8	GAD19	Standard chow
Buffer_RB	8	Carrier Buffer only	10% Rice Bran
NCK1895_RB	8	NCK1895	10% Rice Bran
GAD19_RB	8	GAD19	10% Rice Bran

2.2.3: Bacterial Strains and Culture Conditions

Wild-type *Lactobacillus acidophilus* strain NCK1895 [240] (harboring plasmid pTRK882) and GAD19 [214] (*L. acidophilus* strain NCK2208 with plasmid pGAD17) were grown in MRS broth (BD Diagnostics, Sparks, MD) with 5 μg/ml of erythromycin (Em). Cultures were incubated overnight at 37°C under static conditions. Expression of the membrane proximal external region (MPER) derived from human immunodeficiency virus type 1 (HIV-1) in the surface layer of our GAD19 strain was confirmed using flow cytometry. Bacterial cells were first incubated with the anti-Human Immunodeficiency Virus (HIV)-1 gp41 Monoclonal Antibody (2F5) in a 1% BSA PBS buffer, and then incubated with goat anti-human IgG conjugated with Alexa Fluor 488 (Biolegend, San Diego, CA). NCK1895 showed minimal background fluorescence, while GAD19 had high (>90%) fluorescence. Data was analyzed in FlowJo version 10.4 and gated on forward scatter (FSC), side scatter (SSC) to eliminate doublets and debris, and then FL1 to identify

FITC positive events to indicate MPER-positive cells. Secretion of mouse IL-1β in GAD19 was confirmed using an ELISA-based detection kit.

2.2.4: Mouse Immunization and Housing

Female Balb/c mice from the Jackson Laboratory (Bar Harbor, Maine) were used, and all mice had ad libitum water and standard chow (Envigo, Teklad Rodent Diet) for two weeks at CSU's Lab Animal Resources (LAR). After this two-week acclimatization period, mice were 8-weeks of age at the start of the study, and half of the mice were switched to a Teklad custom 10% rice bran diet (Envigo, Madison, WI). Mice were housed in specific pathogen free conditions, with n=4 per cage and a continuous 12h light/12h dark cycle. Live-bacterial vaccines were prepared using freshly grown overnight bacterial cultures. NCK1895 and GAD19 bacterial cells were washed twice in PBS (Corning, Corning, NY) and resuspended in a dosing buffer containing soybean trypsin inhibitor (STI, Sigma) and sodium bicarbonate ($NaHCO_3$). Mice were given $5x10^9$ CFU of either NCK1895 or GAD19 in 200ul of dosing buffer, or dosing buffer alone. Vaccines were delivered intragastrically three days in a row during weeks 0, 2, 4, 6, 8, and 10. Mice were housed in groups of four and provided ad lib water and food throughout the study. Two weeks after the last dosing timepoint, mice were euthanized, and tissues were processed to obtain single-cell suspensions.

2.2.5: Sample Collection and Processing

Blood, fecal, and vaginal samples were collected from each animal prior to administration of vaccination for investigation of antibody titers. Fecal samples were collected and homogenized with PBS supplemented with ProteaseArrest at a 10x weight to volume ratio. Homogenates were spun at 9,390 Relative Centrifugal Force (RCF), for 10 minutes to pellet particulates and bacteria. Clear supernatants were aliquoted and stored at -80°C for long term storage. Fecal samples for microbiome analysis were collected directly from the anus of the animal into a sterile PCR tube and placed immediately on ice and

transferred to -80°C freezer for long term storage. Serum samples were collected via tail bleeds. Blood was collected with a microvette (Sarstedt, Nümbrecht, Germany) and processed according to manufacturer's protocols for serum isolation. Serum was aliquoted and stored at -80°C. Vaginal lavage samples were collected by gently washing the vagina of mice with 100ul of PBS. The collected sample was immediately placed on ice, spun at 9,000 RCF to pellet any debris, and then aliquoted and stored at -80°C.

2.2.6: Preparation of Single Cell Suspensions

Two weeks after the last immunization, mice were euthanized via carbon dioxide inhalation and thoracotomy. Tissues collected included the spleen (Sp), mesenteric lymph nodes (MLN), Peyer's patches (PP), large intestine (LI), and female reproductive tract (FRT), as previously described [241]. Briefly, Sp and PP were prepared using a GentleMACS dissociator. Sp red blood cells were lysed with ACK (ammonium chloride potassium) lysis buffer and washed with complete media. The Sp and PP suspensions were filtered through cell strainers to obtain single cell suspensions. Mucus and epithelium were removed from LI and FRT in PBS containing 1 mM dithiothreitol and 5 mM EDTA. LI and FRT tissues were cut into smaller sections and placed in digestion media, containing Liberase TM and DNAse I (Roche, Basel, Switzerland), with agitation for 30 minutes at 37°C. LI and FRT lymphocytes were isolated using a Percol (GE Healthcare) underlay step. LI and FRT cells were washed and filtered once more to obtain single cells. The MLNs were isolated via physical dissociation, washed, and filtered for a single cell suspension. Viability and concentration of cells was determined using cell staining with the Cellometer Auto 2000 Cell Viability Counter (Nexcelom Biosciences). Purity of B cells was determined using flow cytometry. Cells were stained with anti-mouse CD45-FITC, CD19-Pacific Blue, and 7-ADD, and gated based on single cells, live cells, CD45+, and CD19+.

2.2.7: MPER-Specific ELISA and ELISpot Assays

An enzyme-linked immunosorbent assay (ELISA) was developed for the detection of MPER-specific and SlpA-specific murine antibodies from serum, fecal, and vaginal samples. Plates (Maxisorp; Nunc, Rochester, NY) were coated with either MPER peptide (Bio-Synthesis Inc, Lewisville, TX) at 1 μg/ml or SlpA protein (isolated from NCK1895) in carbonate coating buffer and incubated overnight at 4°C. Plates were washed five times with PBS containing 0.05% Tween-20 (PBST) and blocked with 1% bovine serum albumin (BSA) in PBS for one hour at room temperature (RT). Plates were washed five times again with PBST. Samples were serially diluted in 1% BSA, 0.1% Kathon in PBS and incubated for 2 hours RT. Plates were washed five times with PBST and incubated with either anti-mouse IgG (Cell Signaling Technology, 20ng/mL) for serum samples, or IgA (Bethyl Laboratories, 40ng/mL) for vaginal wash and fecal samples. Both anti-mouse IgG and IgA antibody were conjugated with horseradish peroxidase (HRP) and incubated for 1 hour at RT. Plates were washed six times with PBST. 3,3',5,5'-Tetramethylbenzidine (TMB) peroxidase (SeraCar, Milford, MA) was filtered with a 40uM syringe-filter and acclimated to RT before adding to each well. The reaction was stopped with an equal volume of 1N HCl. The absorbance was read with a plate reader (BioTek, Winooski, VT), with both 450nm and 570nm recorded (to remove any background noise with 570nm reading). The week -2 and 0 time points were used in calculations for the mean baseline value for each group. This mean was then added to the standard deviation for each group times the standard deviation cutoff multiplier based on n=8 and 95% confidence level [242]. This value was used as the cutoff value to determine the reported endpoint titers used in statistical analysis.

IgA secreting cells and MPER-specific IgA secreting cells were quantified using the enzyme-linked immunosorbent spot (ELISpot) assay, similar to what has been described previously. Ninety-six-well MultiScreenHTS IP filter plates (Millipore Sigma) were treated with 35% ethanol and washed with sterile distilled water. Plates were coated with 15 μg/ml anti-mouse IgA (Mabtech) in PBS and incubated overnight at 4°C. Plates were washed five times with PBS and blocked with CTL medium for 1 hour at 37°C. Cells from single cell suspensions were added in duplicate at a concentration of 2.5 X 105 for MPER-specific

detection and 1 X 104 for total IgA. Plates were incubated for 20 hours at 37°C. Plates were then washed with PBST six times to remove cells. For total IgA, 1 μg/ml of biotinylated polyclonal goat anti-mouse IgA (Mabtech) in PBS with 1% FBS was added to each well. For MPER-specific IgA, 1 μg/ml of biotinylated MPER peptide was used in the same buffer. Plates were incubated for 2 hours at RT and washed six times. Streptavidin conjugated with horseradish peroxidase (HRP) was added to wells in PBS with 1% FBS and incubated for 1-hour RT. Plates were washed three times with PBST, and three times with PBS. TMB was filtered with 0.44μM filter and added to wells for either two minutes for total IgA or 10 minutes for MPER-specific IgA. Plates were washed with distilled water ten times and air dried. Spots were counted with an ImmunoSpot analyzer (Cellular Technology Limited).

2.2.8: Statistical Methods for ELISA and ELISpot Data

Statistical analyses were performed in R version 3.6.1. A Kruskal-Wallis test of analysis of variance was used with a Dunn's multiple comparison post-hoc test for each timepoint in ELISA analysis, as data was not normally distributed. Multiple testing was corrected using the Benjamini-Hochberg method to obtain adjusted p-values and are listed in Table 2.2. Endpoint titer means and standard error for each timepoint were plotted, with asterisks (*) representing significance ($P < 0.05$). ELISpot data was analyzed in a similar manor since data were also not normally distributed. The Kruskal-Wallis test of analysis of variance with Dunn's multiple comparison post-hoc test and P-values were corrected using the Benjamini-Hochberg method for each spot (MPER-specific or total IgA) and tissue type. Resulting P-values are listed in Table 2.3, with ($P < 0.05$) highlighted in green, correlating to significance (*) plotted in Figure 2.4.

Table 2.2. Adjusted P-values from pairwise comparisons of ELISA endpoint titers. To determine significance of ELISA endpoint titers between experimental groups for each timepoint, the Kruskal-Wallis test of analysis of variance was followed by Dunn's multiple comparison post-hoc test, since data was not normally distributed. The Benjamini-Hochberg method was used for multiple testing adjustment.

Source	Comparison-1	Comparison-2	Week_2	Week_4	Week_6	Week_8	Week_10	Week_12
Fecal	Buffer_RB	Buffer_SC	0.3001	0.3650	0.5000	0.3938	0.4316	0.3928
Fecal	Buffer_RB	Gad19_RB	0.1057	0.0017	0.0004	0.0023	0.0003	0.0003

Fecal	Buffer_SC	Gad19_RB	0.0184	0.0002	0.0005	0.0008	0.0004	0.0008
Fecal	Buffer_RB	Gad19_SC	0.3143	0.5702	0.0489	0.0015	0.0003	0.0004
Fecal	Buffer_SC	Gad19_SC	0.1600	0.4362	0.0559	0.0008	0.0007	0.0015
Fecal	Gad19_RB	Gad19_SC	0.2022	0.0020	0.0619	0.4643	0.4906	0.4440
Fecal	Buffer_RB	NCK1895_RB	0.3301	0.4015	0.5357	0.4091	0.4709	0.3347
Fecal	Buffer_SC	NCK1895_RB	0.5000	0.5000	0.5769	0.2630	0.5000	0.4506
Fecal	Gad19_RB	NCK1895_RB	0.0276	0.0003	0.0007	0.0090	0.0005	0.0016
Fecal	Gad19_SC	NCK1895_RB	0.1866	0.4986	0.0652	0.0062	0.0008	0.0029
Fecal	Buffer_RB	NCK1895_SC	0.3668	0.4461	0.6250	0.4266	0.5357	0.5000
Fecal	Buffer_SC	NCK1895_SC	0.5357	0.5357	0.6818	0.5000	0.5179	0.4286
Fecal	Gad19_RB	NCK1895_SC	0.0552	0.0006	0.0015	0.0011	0.0005	0.0006
Fecal	Gad19_SC	NCK1895_SC	0.2240	0.5817	0.0782	0.0017	0.0004	0.0005
Fecal	NCK1895_RB	NCK1895_SC	0.5769	0.5769	0.7500	0.2922	0.5755	0.3719
Serum	Buffer_RB	Buffer_SC	0.1249	0.2790	0.5000	0.3306	0.5000	0.3851
Serum	Buffer_RB	Gad19_RB	0.1561	0.1759	0.0920	0.0286	0.0104	0.0009
Serum	Buffer_SC	Gad19_RB	0.5000	0.0419	0.1226	0.0056	0.0119	0.0029
Serum	Buffer_RB	Gad19_SC	0.2082	0.5000	0.1321	0.1656	0.0008	0.0019
Serum	Buffer_SC	Gad19_SC	0.5357	0.3069	0.2641	0.0510	0.0011	0.0057
Serum	Gad19_RB	Gad19_SC	0.5769	0.2199	0.5138	0.2351	0.2720	0.3998
Serum	Buffer_RB	NCK1895_RB	0.3122	0.3410	0.3405	0.3606	0.3778	0.3124
Serum	Buffer_SC	NCK1895_RB	0.6250	0.5357	0.3714	0.5000	0.4093	0.2012
Serum	Gad19_RB	NCK1895_RB	0.6818	0.0629	0.1622	0.0084	0.0035	0.0002
Serum	Gad19_SC	NCK1895_RB	0.7500	0.3836	0.1669	0.0595	0.0003	0.0003
Serum	Buffer_RB	NCK1895_SC	0.6245	0.4385	0.4086	0.3967	0.4465	0.4172
Serum	Buffer_SC	NCK1895_SC	0.8333	0.5769	0.4540	0.5357	0.4911	0.2928
Serum	Gad19_RB	NCK1895_SC	0.9375	0.1258	0.1854	0.0168	0.0042	0.0003
Serum	Gad19_SC	NCK1895_SC	1.0000	0.5115	0.2003	0.0714	0.0005	0.0006
Serum	NCK1895_RB	NCK1895_SC	1.0000	0.6250	0.5357	0.5769	0.5357	0.4043
Vaginal	Buffer_RB	Buffer_SC	0.2022	0.2920	0.3445	0.5000	0.4096	0.3785
Vaginal	Buffer_RB	Gad19_RB	0.5000	0.4080	0.1719	0.2248	0.0467	0.0068
Vaginal	Buffer_SC	Gad19_RB	0.2311	0.2380	0.0826	0.2698	0.0172	0.0028
Vaginal	Buffer_RB	Gad19_SC	0.2697	0.3212	0.0992	0.0753	0.0010	0.0010
Vaginal	Buffer_SC	Gad19_SC	0.5357	0.5000	0.0674	0.1506	0.0002	0.0007
Vaginal	Gad19_RB	Gad19_SC	0.3236	0.3570	0.3881	0.3486	0.1106	0.3455
Vaginal	Buffer_RB	NCK1895_RB	0.4045	0.3569	0.3732	0.3639	0.4468	0.5000
Vaginal	Buffer_SC	NCK1895_RB	0.5769	0.5357	0.5000	0.3942	0.5000	0.4076
Vaginal	Gad19_RB	NCK1895_RB	0.5393	0.7139	0.1101	0.3245	0.0200	0.0079
Vaginal	Gad19_SC	NCK1895_RB	0.6250	0.5769	0.1348	0.1222	0.0003	0.0015
Vaginal	Buffer_RB	NCK1895_SC	0.8090	0.4015	0.3721	0.4301	0.4915	0.4416
Vaginal	Buffer_SC	NCK1895_SC	0.6818	0.1414	0.2144	0.4731	0.5357	0.3386
Vaginal	Gad19_RB	NCK1895_SC	1.0000	0.5830	0.2837	0.3651	0.0241	0.0175
Vaginal	Gad19_SC	NCK1895_SC	0.7500	0.1697	0.2329	0.1629	0.0007	0.0029
Vaginal	NCK1895_RB	NCK1895_SC	0.8333	0.2121	0.2412	0.5357	0.5769	0.4817

Table 2.3. Adjusted P-values for multiple comparisons of ELISpot data. The Kruskal-Wallis test of analysis of variance was followed by Dunn's multiple comparison post-hoc test with Benjamini-Hochberg adjusted p-values for multiple testing was used for significance of ELISpot counts between experimental groups for each tissue type in the study. Analysis was conducted independently for each spot type too. Green shading indicates ($P < 0.05$), and correlates to significance represented by (*) in Figure 2.4. FRT: female reproductive tract, LI: large intestine, MLN: mesenteric lymph nodes, PP: Peyer's patches, Sp: spleen.

Spot-Type	Comparison_1	Comparison_2	FRT	LI	MLN	PP	Sp
MPER-Specific	Buffer_RB	Buffer_SC	0.5000	0.5000	0.2161	0.5000	0.5000
MPER-Specific	Buffer_RB	GAD19_RB	0.1202	0.1616	0.5000	0.1249	0.2741
MPER-Specific	Buffer_SC	GAD19_RB	0.1402	0.2424	0.2470	0.1561	0.3015
MPER-Specific	Buffer_RB	GAD19_SC	0.0259	0.3199	0.3135	0.5357	0.3388
MPER-Specific	Buffer_SC	GAD19_SC	0.0389	0.3733	0.6863	0.5769	0.3873
MPER-Specific	GAD19_RB	GAD19_SC	0.2747	0.2856	0.4179	0.2082	0.5879
MPER-Specific	Buffer_RB	NCK1895_RB	0.5357	0.3141	0.5357	0.6250	0.5357
MPER-Specific	Buffer_SC	NCK1895_RB	0.5769	0.3490	0.2882	0.6818	0.5769
MPER-Specific	GAD19_RB	NCK1895_RB	0.1683	0.4479	0.5769	0.3122	0.3350
MPER-Specific	GAD19_SC	NCK1895_RB	0.0778	0.5108	0.6269	0.7500	0.4518
MPER-Specific	Buffer_RB	NCK1895_SC	0.6250	0.5357	0.6250	0.8333	0.1699
MPER-Specific	Buffer_SC	NCK1895_SC	0.6818	0.5769	0.3458	0.9375	0.2549
MPER-Specific	GAD19_RB	NCK1895_SC	0.1326	0.4847	0.6818	0.6245	0.6067
MPER-Specific	GAD19_SC	NCK1895_SC	0.0689	0.5599	1.0000	1.0000	0.5422
MPER-Specific	NCK1895_RB	NCK1895_SC	0.7500	0.3927	0.7500	1.0000	0.5097
Total_IgA	Buffer_RB	Buffer_SC	0.1502	0.2085	0.4809	0.0017	0.3473
Total_IgA	Buffer_RB	GAD19_RB	0.4404	0.0804	0.4598	0.1421	0.4353
Total_IgA	Buffer_SC	GAD19_RB	0.1436	0.0202	0.5186	0.0004	0.4075
Total_IgA	Buffer_RB	GAD19_SC	0.1514	0.1253	0.4632	0.0066	0.3548
Total_IgA	Buffer_SC	GAD19_SC	0.4508	0.0201	0.6196	0.3622	0.3268
Total_IgA	GAD19_RB	GAD19_SC	0.1337	0.4190	0.4581	0.0002	0.2011
Total_IgA	Buffer_RB	NCK1895_RB	0.2544	0.2333	0.4581	0.3645	0.3883
Total_IgA	Buffer_SC	NCK1895_RB	0.3868	0.4508	0.5149	0.0044	0.4315
Total_IgA	GAD19_RB	NCK1895_RB	0.2264	0.0192	0.5466	0.0815	0.3816
Total_IgA	GAD19_SC	NCK1895_RB	0.4079	0.0268	0.4551	0.0152	0.3007
Total_IgA	Buffer_RB	NCK1895_SC	0.1514	0.4801	0.5007	0.0175	0.4145
Total_IgA	Buffer_SC	NCK1895_SC	0.4409	0.2035	0.7530	0.2087	0.4644
Total_IgA	GAD19_RB	NCK1895_SC	0.2086	0.0861	0.4362	0.0008	0.3487
Total_IgA	GAD19_SC	NCK1895_SC	0.4207	0.1298	0.4716	0.3496	0.3494
Total_IgA	NCK1895_RB	NCK1895_SC	0.2851	0.2301	0.5227	0.0374	0.4374

2.2.9: IgA-Bound Bacterial Sorting

Fecal pellets collected from animals from each timepoint were processed at the same time. Block randomization was used so that weekly timepoints and animal groups were evenly distributed between plates to avoid batch bias in extraction, library generation, and sequencing. Additionally, samples were labeled with an assigned randomized number for all downstream work to blind investigators of sample origin during library preparation and initial data processing. Fecal samples were first homogenized with PBS containing ProteaseArrest. Homogenates containing bacteria were placed on ice for 10 minutes to allow large particulates to fall out of suspension. The remaining suspension was washed twice with PBS. One third of the suspension was saved for direct microbiome processing (whole microbiome), while the remaining two-thirds were further processed for IgA-sorting. Samples were stained with an IgG rat anti-mouse IgA antibody conjugated with FITC (Clone C10-3, BD Biosciences San Jose, CA) in a PBS staining buffer containing 0.01% bovine serum albumin (Sigma-Aldrich) and 1mM EDTA. Samples were washed with staining buffer and filtered using 40uM filter cap Falcon tubes before sorting with a fluorescence activated cell sorter (FACS) Aria III at the CSU Flow Cytometry Facility. Sorting gates were set using both unstained samples and an isotype control with FACSDiva version 6.1.3 and FlowJo version 10.4. Side scatter (SSC) threshold was set to 250 to account for the small bacterial cells, and a 100μM nozzle was used. Fresh CS&T beads (BD Biosciences) were run each day to ensure the machine was consistent in sensitivity detection throughout the sorting process. The gating strategy for sorting included selecting for intact cells based on FCS and SSC, then single cells to avoid clumps of heterogenous bacterial cells, then gated on fluorescens in the FL-1 FITC channel to sort IgA-positive and IgA-negative cells (Fig. 2.1). Samples from droplet stream were collected before and after sorting for negative controls. Several sorted samples were resorted to assess the accuracy of IgA-positive and IgA-negative streams, with purity ranging from 95-100%. Both IgA-positive and IgA-negative fractions were collected into sterile tubes and saved for 16S-library preparation. Sorting parameters were set to collect at least 100,000 cells in each fraction and stopped after 1million cells were collected in either fraction so collection tubes would not overflow.

Samples were stored on ice throughout the sorting process until they were pelleted and frozen at -80°C for later DNA extraction.

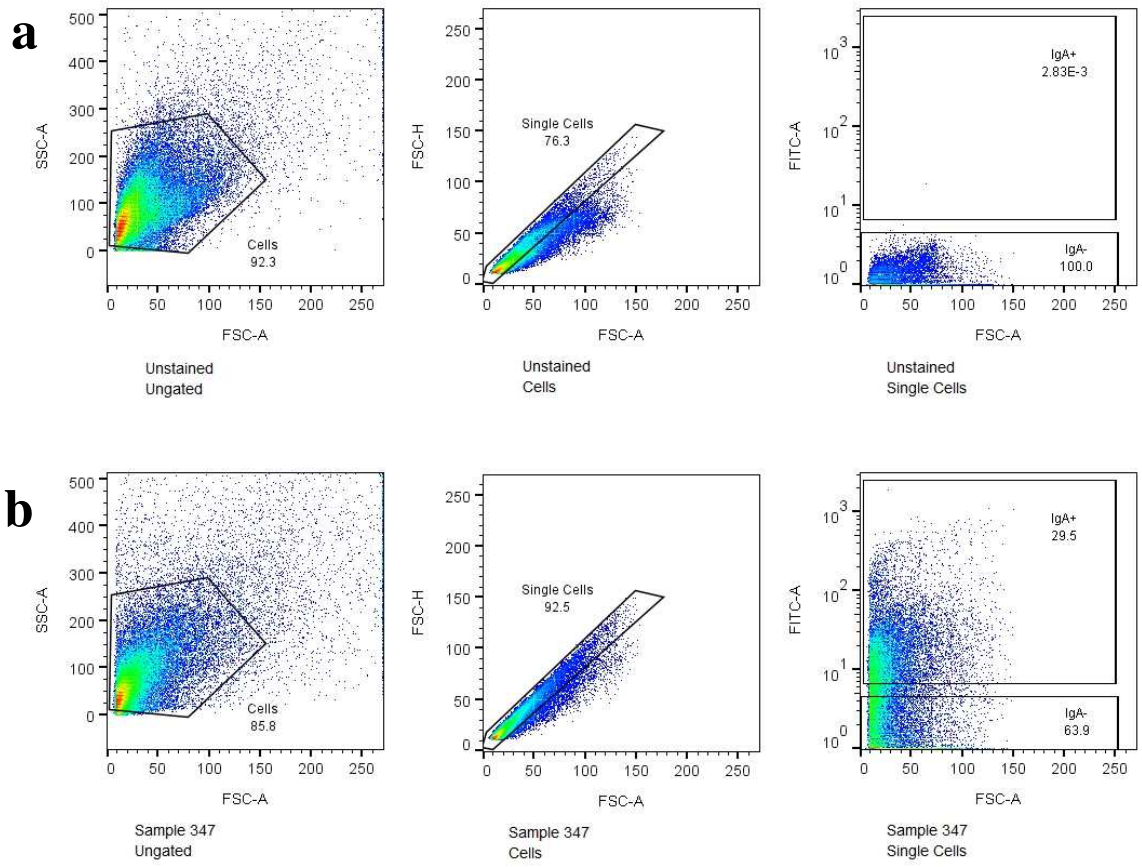

Figure 2.1 Gating of fecal samples to obtain IgA-positive and IgA-negative fractions. First, cells were gated based on SSC and FSC, the FSC-H and FSC-A to gate for single cells. IgA-negative and IgA-positive populations were selected based on intensity of FITC fluorescence and collected into sterile tubes. FITC and PE graphs were analyzed to observe spill over into the PE channel. Panel A shows unstained cells, and panel B shows cells stained with anti-mouse IgA with a FITC tag from the randomized sample 347.

2.2.10: Microbiome Library Preparation

Each of the three fractions (whole microbiome, IgA-positive, and IgA-negative) were randomized into a 96-well plate format. Each plate received either three or six controls, which included no-template controls from either FACS sorting, extractions, PCR, or magnetic separation to track any contamination. Positive controls included ZymoBIOMICS Microbial Community Standards in the extraction (bacterial

cells D6300), and in PCR (DNA D3605). DNA was extracted using the MagAttract PowerSoil DNA KF Kit (Qiagen) in conjugation with the KingFisher Flex (ThermoFisher Scientific). Extracted DNA was used to create Illumina library molecules from the hyper variable region 4 (V4) of the 16S rDNA gene as described previously [201]. Briefly, primers with multiplexed barcodes were used, and also included an Illumina adapter, pad and linker, and V4-16S primer sequence. Dual indexed libraries were purified using magnetic Mag-Bind TotalPure NGS beads (Omega Bio-Tek) to select for DNA fragments greater than 300 bp to remove primers and any other unwanted PCR products. Library molecules in each sample were estimated using the AccuBlue dsDNA Quantitation Kit (Biotim). An equimolar amount of each sample was added to one of four pools. Each of the four pools were quality controlled and sequenced on an Illumina MiSeq at Colorado State University's Next Generation Sequencing Core Facility (Fort Collins, CO). Illumina MiSeq v2 500-cycle kits were used to sequence the 2 x 250 paired end reads. Raw data are available on National Center for Biotechnology Information's (NCBI) Sequence Read Archive (SRA) under BioProject PRJNA723356, https://www.ncbi.nlm.nih.gov/bioproject/PRJNA723356.

2.2.11: Microbiome Data Processing

We used the software fastqc [243] (version v0.11.5) to evaluate the quality of demultiplexed fastq reads obtained from the MiSeq runs, totaling 56,460,071 reads. The software trimmomatic [244] (version 0.39) was used to filter and trim data using a sliding window of four and a cutoff quality of PHRED 25 in order to select for high quality reads for downstream analysis. Only reads 150 base-pairs or longer were used to ensure overlap between forward and reverse reads for assembling contigs in downstream processing, resulting in 25,387,655 reads. Filtered data were processed using mothur [245] (version 1.44.2), using the developers' standard operating procedure to further clean and process files, resulting in 24,748,343 sequences with 848,893 being unique. The output of this pipeline included an operational taxonomic unit (OTU)-based data-table and taxonomic classification. The SILVA database [246] version 132 was used for alignment and classification. The microbial community standards (mock community) from ZymoBIOMICS were used to assess both sequencing error rate and DNA extraction efficiency from different microbial taxa

between extraction plates and sequencing batches. Negative controls were used to gauge the potential contamination introduced throughout library preparation. These controls were also used to establish the cutoff for removing OTUs. Here, we removed OTUs with less than seven reads. Samples with lower than 5000 reads were also removed. This cutoff also allowed for the convergence of non-metric multidimensional scaling plots (NMDS). This process of data cleaning from the original mothur OTU table reduced the number from 4567 to 417 OTUs. Rarefaction curves were generated with the package vegan in R (version 3.6.1) to check that the depth of coverage for each sample allowed for adequate discovery of OTUs (Fig. 2.2).

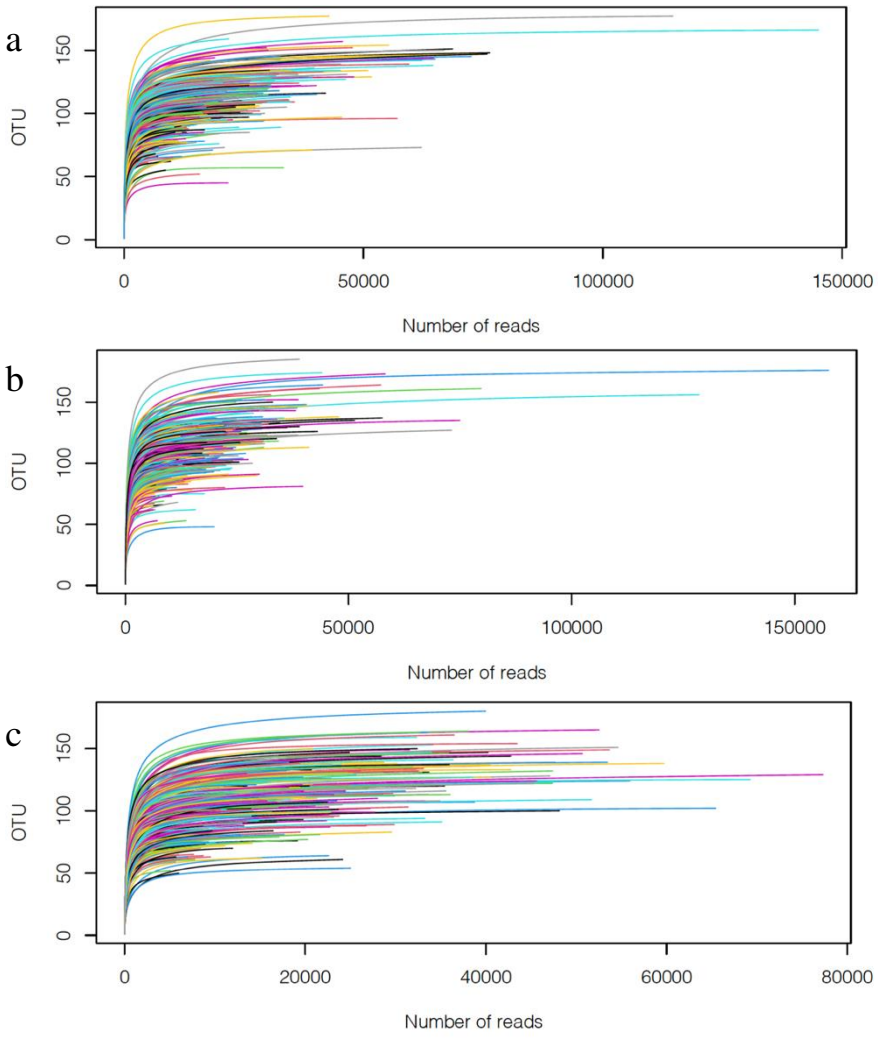

Figure 2.2 Rarefaction curves of each sample. Samples divided by (a) whole microbiome, (b) IgA-positive, and (c) IgA-negative fractions. Samples are each represented by a colored line, with OTU counts per sample on the X-axis and number of reads per sample on the y-axis. Horizontal lines indicate a low chance for the discovery of more OTUs based on the number of reads.

2.2.12: Diversity and Correlation Analysis

Alpha diversity was assessed using the Shannon diversity index and rarified richness. Shannon diversity was estimated with the phyloseq package [247] on non-normalized data. Richness was calculated based on the rarified data through the package vegan [248]. The R package lme4 was used to create a linear mixed effects model in order to account for random effects from sampling the same mice over time. This model specified individual mice as subject-specific random effects, and experimental group as fixed variables. Autocorrelation was not used as the AIC values between models with autocorrelation component and those without were comparable (within 2 for all models). Predicted values were plotted as means with standard error using ggplot2 and the sjPlot package.

Beta-diversity was analyzed via Nonmetric Multidimensional Scaling (NMDS) at the OTU level after normalization using Cumulative Sum Scaling [249]. The full dataset was used for ordination through the vegan package and applying Bray-Curtis dissimilarity. 95% confidence ellipsoids were plotted for each timepoint, group, and microbiome fractions, depending on the graph. Plotting was also conducted for each sequencing pool to identify possible batch bias. Venn Diagrams were constructed using the VennDiagram package in R based on both OTU and genus level taxa counts. Data was separated either by IgA-fraction, or IgA-fraction and treatment group to show similarities and differences between the various groupings.

Spearman's correlation coefficient was used to assess the association between the microbiome and MPER-specific IgA. The top 20 taxa identified as the most important for classification into treatment groups in Random Forests (described below) were used in this correlation analysis.

2.2.13: Random Forest

To create a list of taxa that had the most influence on the prediction of the treatment-groups (Table 2.1) associated with vaccination and diet from the study, we used Random Forests (RF) [250], which was calculated by the R package randomForest (version 4.6-14) [251]. IgA-fractions were analyzed independently to find the most important taxa from each fraction. The optimal number of features was identified with an iterative approach and used in constructing trees. We used the tuneRF function to iterate over 100 random forests with different mtry values, and ntreeTry was set to 200. The mtry value, representing the number of features to use in sampling when creating regression trees in the RF model, with the lowest median out-of-bag (OOB) error was selected (whole microbiome =46, IgA-positive microbiome = 98, IgA-negative microbiome = 60, Fig. S2.1). The confusion matrices showing group and class errors and overall error rate for each of the microbiome fractions is shown in Table 2.4. We used ntree = 1000 and importance = TRUE to create the RF model to identify features that were most important in classification to the experimental groups. All OTUs, sample collection time points (week), and sequencing pool were included in this analysis. Sequencing pool was included as a feature to assess any bias based on sequencing batch, and no bias was detected. Additional RF models classified samples based on vaccine treatment and diet were created, and confusion matrix for each model are shown in tables S2.1 and S2.2. The features and their importance are represented by mean decrease in Gini [252], using a cutoff of 0.2 when plotting.

Table 2.4 Confusion matrices for Random Forest models. The classification and associated error for each experimental group are shown for each model that was created for the three microbiome fractions. The overall error rate for each model is also shown by "OOB estimate of error rate".

Whole Microbiome

Type of Random Forest: classification
Number of trees: 1000
Number of variables tried a teach split: 46
OOB estimate of error rate: 28.09%

	Buffer RB	**NCK1895 RB**	**Gad19 RB**	**Buffer SC**	**NCK1895 SC**	**Gad19 SC**	**Class error**
Buffer RB	37	1	2	12	3	0	0.327272
NCK1895 RB	1	56	2	1	2	1	0.111111

Gad19 RB	2	4	43	0	1	12	0.306451
Buffer SC	4	2	0	34	8	4	0.346153
NCK1895 SC	4	1	0	7	34	15	0.442623
Gad19 SC	0	4	5	0	2	52	0.174603

IgA-Positive Microbiome

Type of Random Forest: classification
Number of trees: 1000
Number of variables tried a teach split: 98
OOB estimate of error rate: 51.04%

	Buffer RB	**NCK1895 RB**	**Gad19 RB**	**Buffer SC**	**NCK1895 SC**	**Gad19 SC**	**Class error**
Buffer RB	26	2	5	7	6	6	0.500000
NCK1895 RB	5	34	8	4	2	6	0.423728
Gad19 RB	7	9	30	2	1	11	0.500000
Buffer SC	3	3	0	28	9	7	0.440000
NCK1895 SC	7	7	2	12	17	13	0.706896
Gad19 SC	3	6	6	5	8	30	0.482758

IgA-Negative Microbiome

Type of Random Forest: classification
Number of trees: 1000
Number of variables tried a teach split: 60
OOB estimate of error rate: 42.56%

	Buffer RB	**NCK1895 RB**	**Gad19 RB**	**Buffer SC**	**NCK1895 SC**	**Gad19 SC**	**Class error**
Buffer RB	20	3	5	6	8	6	0.583333
NCK1895 RB	2	32	12	7	3	2	0.448275
Gad19 RB	2	3	39	1	4	10	0.338983
Buffer SC	2	3	3	31	11	2	0.403846
NCK1895 SC	2	2	3	11	28	13	0.525423
Gad19 SC	3	5	4	2	3	43	0.283333

2.3: Results

2.3.1: Rice Bran Diet Enhancement of MPER-Specific Antibody Responses

To investigate the kinetics and magnitude of the antigen-specific immune response induced by the recombinant *L. acidophilus* vaccine platform, mice were orally dosed with *L. acidophilus* expressing MPER and secreting IL-1β (GAD19), control strain *L. acidophilus* (NCK1895), or the carrier buffer alone (Buffer). For each treatment type, mice were fed either standard chow diet (SC), or SC supplemented with 10% rice bran (RB) (Table 2.1). Fecal and vaginal wash MPER-specific IgA and serum IgG showed a pattern of

increasing titers with each vaccine boost, reaching a maximum titer after the 6th immunization with GAD19 (Fig. 2.3, adjusted P-values for pairwise comparisons shown in Table 2.2). Notably, mice fed the RB diet showed significantly higher antibody titers in feces and serum after two immunizations with GAD19 (week 4) as compared to all other treatment groups (Fig. 2.3A and 2.3C). This trend continued for the GAD19_RB group that had significantly higher titers of serum IgG after the 4th immunization as well (Fig. 2.3C). These results show GAD19 vaccinated groups produced significant levels of MPER-specific antibodies in all three sample types (fecal, vaginal and serum), but rice bran can improve the early mucosal and systemic humoral responses to rLA vaccination.

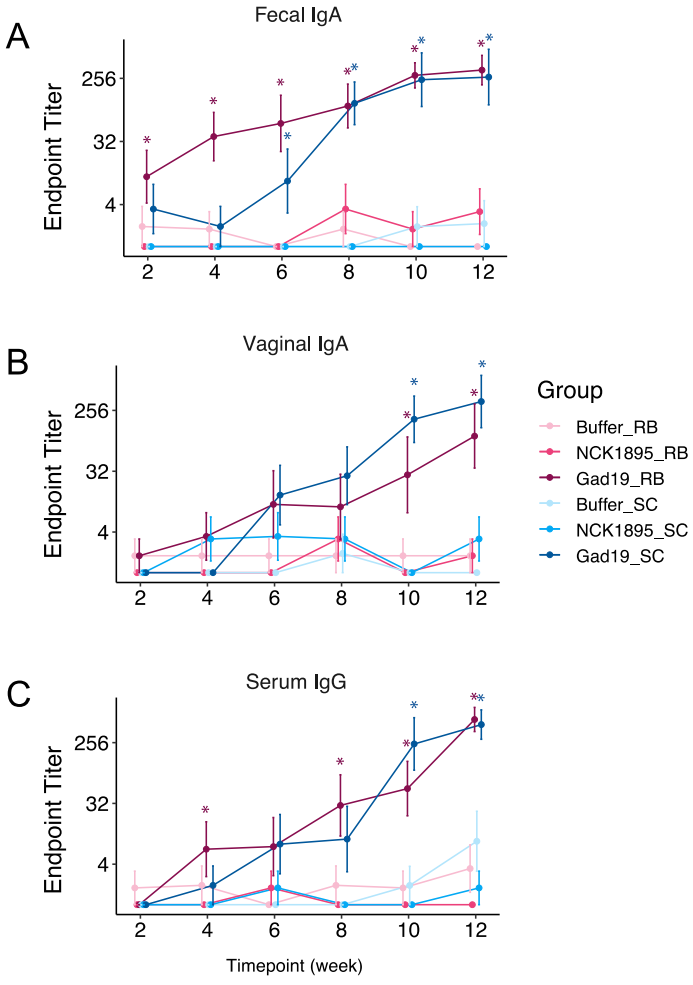

Figure 2.3 Diet improves antigen-specific antibody response to vaccination. Mice were fed either a standard chow (SC) or SC supplemented with 10% rice bran (RB) diet throughout the study and samples were taken every 2 weeks, prior to the next vaccine boost. MPER-specific antibodies were detected with

colorimetric ELISAs. (a) Fecal IgA, (b) vaginal IgA, and (c) serum IgG endpoint titers from ELISAs are reported for each group, with samples having no detection being assigned a value of 1. For all graphs, asterisks (*) indicated significance ($P < 0.05$) when compared to Buffer groups. Adjusted significant P-values are listed in Table 2.2 for all comparisons.

The immune response to GAD19 and the impact a rice bran diet has on the humoral immune response was also assessed via ELISpot. This method allowed for direct quantification of both MPER-specific antibody secreting cells (ASCs) and total non-specific IgA ASCs. Figure 2.4 shows the mean spot counts for each group with error bars representing the standard error for MPER-specific IgA (2.4A) and non-specific IgA (2.4B) ASCs. Although MPER-specific ASCs were detected in all tissue types from either GAD19_RB or GAD19_SC, only the female reproductive tract (FRT) in the GAD19_SC had significantly higher counts compared to the buffer groups (Fig 2.4A and Table 2.3).

Importantly, the RB diet had a significant increase in the number of IgA secreting cells in the Peyer's Patches (2.4B). All RB groups had significantly higher IgA ASCs counts compared to all other SC groups (Table 2.3) from pairwise comparisons. The large intestine (LI) also had significantly higher levels of IgA producing cells in both GAD19_RB and GAD19_SC compared to the Buffer_SC and NCK1895_RB groups (Fig. 2.4B and Table 2.3). These data indicate the RB diet can increase the overall production of IgA in the small intestine due to the increase IgA ASCs in Peyer's patches.

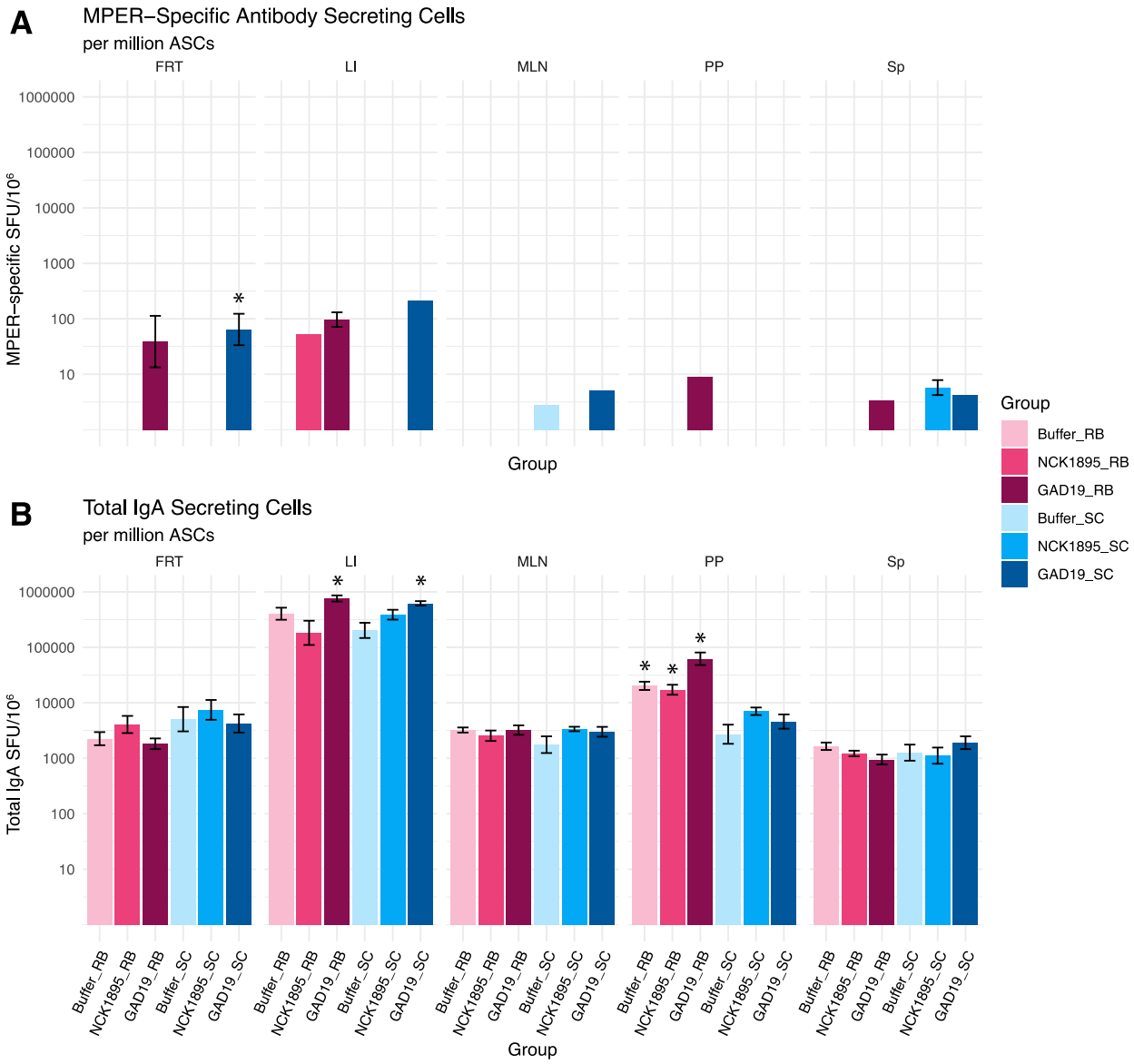

Figure 2.4 MPER-specific and total IgA producing cells. Cells producing either (A) MPER-specific IgA or (B) unspecific IgA was determined using ELISpot from single cell suspensions obtained from each designated tissue. Spot counts were normalized to 1 million antibody secreting cells (ASCs). ASCs were defined as live CD19+CD45+ cells via flow cytometry as cells were simultaneously plated. Bars represent mean MPER or IgA spots in each group, per million ASC, with error bars indicating standard error. Asterisk (*) indicates significance ($P < 0.05$) between treatment and buffer group and additional groups shown in Table 2.3. FRT: female reproductive tract, LI: large intestine, MLN: mesenteric lymph nodes, PP: Peyer's patches, Sp: spleen.

2.3.2: Vaccination and Diet Did Not Impact Alpha Diversity

We used linear mixed effects (LME) models to fit both the Shannon diversity index and expected richness. Each model was fitted separately for the different microbiome fractions (IgA-positive, IgA-negative, and whole). Figure 2.5 shows alpha diversity indices for each microbiome fraction. Although no significant differences were observed between any of the timepoints or groups in the whole microbiome (Fig. 2.5A), the trajectory of the means of Shannon diversity for most groups increased overtime. There was less variability in the confidence intervals for the whole microbiome compared to the IgA-positive and IgA-negative populations (Fig. 2.5B and 2.5C). The means and confidence intervals for both of these fractions did not follow a linear trend. Figure 2.5C also indicates that prior to vaccination (week 0), a significant impact on the Shannon diversity of the IgA-negative microbiome was associated with the RB treatment. However, these impacts recovered quickly after that time point.

The predicted values of expected richness also show a non-linear trend over time for each microbiome fraction (Fig 2.5D-F). No significant differences were found between treatment groups at any timepoint or between IgA-positive and IgA-negative fractions (Fig 2.5E and 2.5F). The sample collection timepoint, which occurred two-weeks post-vaccination, also provides time for recovery from a short-term perturbation caused by vaccination. Therefore, these results indicate that our live-bacterial vaccine platform does not lead to lasting effects on alpha diversity of the intestinal microbiome.

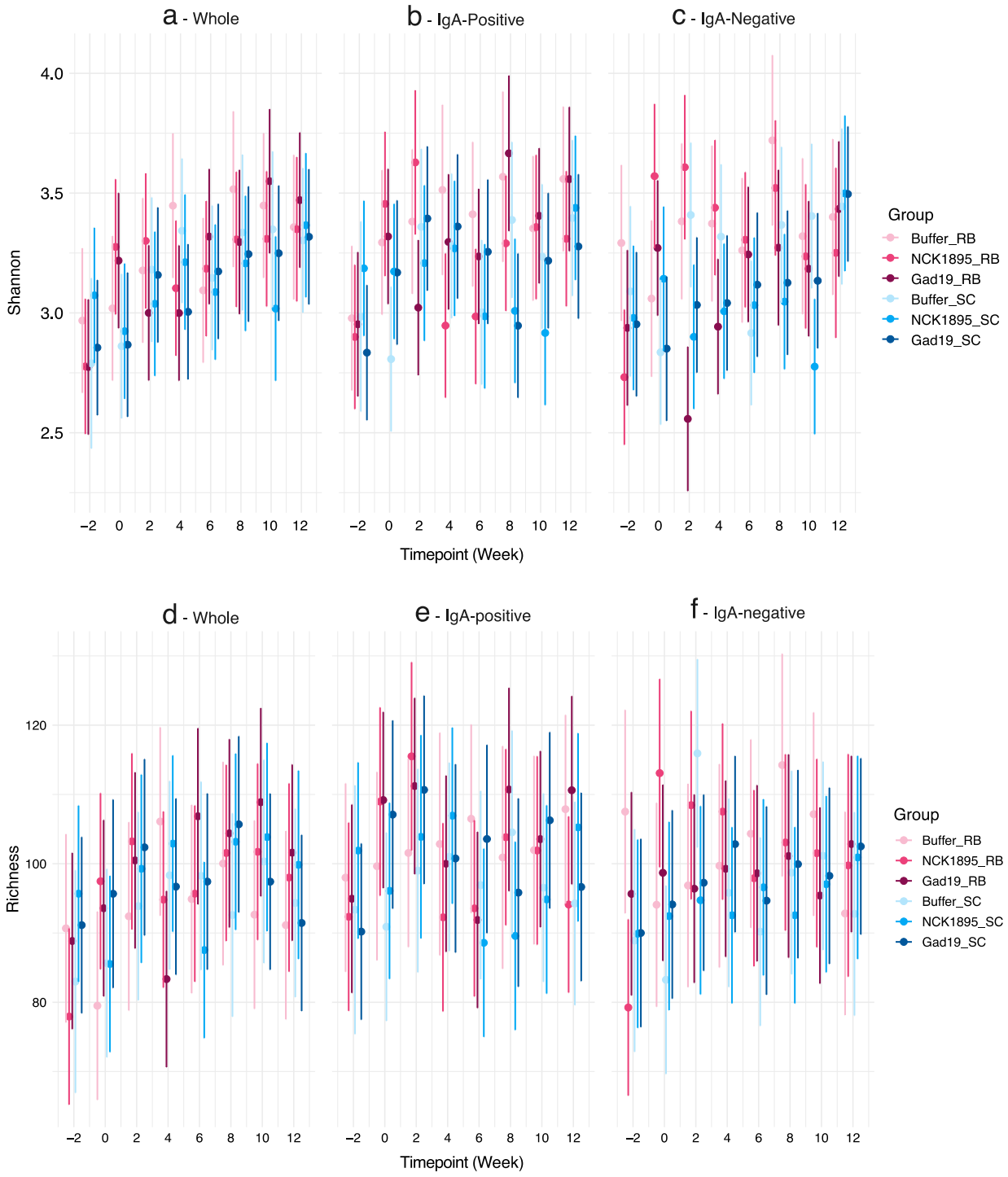

Figure 2.5 Alpha diversity is not affected by diet or vaccination. (a) Predicted values of Shannon diversity index for the whole microbiome from each timepoint (weeks -2, 0, 2, 4, 6, 8, 10, 12) taken from each group are represented by the 95% credibility intervals. (b) IgA-positive and (c) IgA-negative microbiome fractions are also represented by the 95% credibility intervals for Shannon. Richness predictions are shown for (d) whole microbiome, (e) IgA-positive, and (f) IgA-negative fractions. Linear mixed effects models were used to determine predicted values for each microbiome type (whole, IgA-positive, and IgA-negative) and diversity index (Shannon and observed richness).

2.3.3: Temporal Changes in Beta Diversity Influenced by Diet

A clear separation of whole microbial communities based on diet is demonstrated in Figures 2.6. Beta diversity is presented based on the nonmetric multidimensional scaling (NMDS) ordination using the Bray-Curtis distance matrix utilizing the full dataset. The 3-D representation of these data (Fig. 2.6A) highlights the separation of the microbial communities based on diet and partially on immunization type, where the 95% confidence ellipsoids represent the community structure for each group from all three microbiome fractions. The overlapping ellipsoids from GAD19_SC and NCK1895_SC indicates the microbiome communities of these two groups were not significantly different. These treatment groups were administered the same species but different strains of *L. acidophilus*, indicating shifts in the microbiome may be caused by the administration of the live *L. acidophilus* vector itself. The close proximity between GAD19_RB and NCK1895_RB also supports this possibility. In addition, the control buffer group is distant from the *L. acidophilus* groups for both diets (Fig. 2.6A). The 2D projections clearly show the separation of the groups based on diet along NMDS1 (Fig 2.6B and 2.6C).

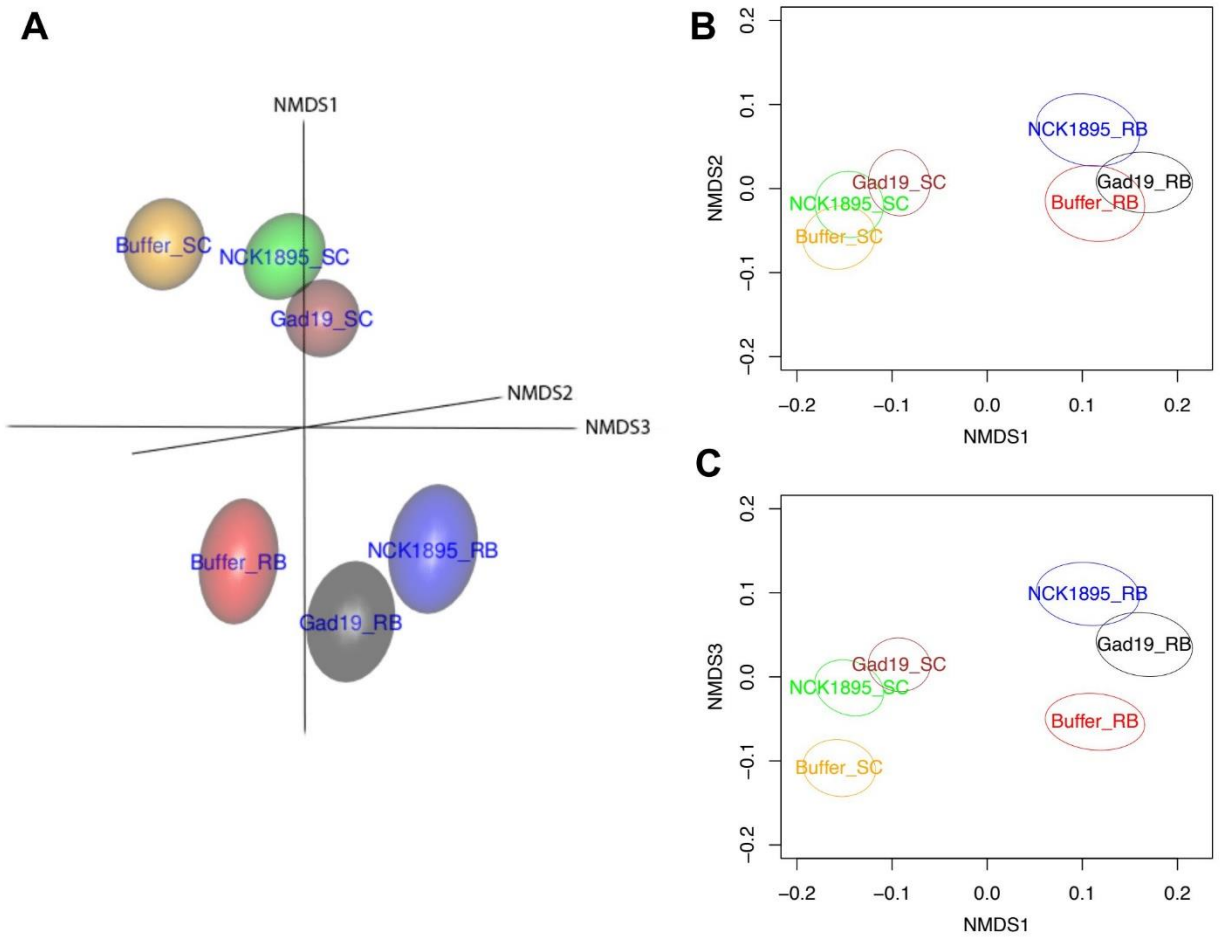

Figure 2.6 Separation of beta-diversity based on experimental groups. Nonmetric multidimensional scaling (NMDS) using the Bray-Curtis distance matrix was used to determine differences in microbiome community structure between groups. (a) the three-dimensional plot represents the three NMDS axes, while the two-dimensional projections NMDS1 and NMDS2 are shown in (b), and NMDS1 and NMDS3 are shown in (c). Data is represented by the 95% confidence ellipsoids and includes all samples from all timepoint from each experimental group.

Figure 2.7 reveals the temporal changes in the microbial community throughout the duration of the study. Differences in microbial communities caused by diet alone are highlighted in the control buffer group (Fig. 2.7A and 2.7B). The centroids for all IgA fractions in the Buffer_SC group shifted downwards overtime, with the microbiome seeming to stabilize between weeks 8-12. Conversely, the microbiome in the RB buffer group shifted from week -2 to 0 for all IgA fractions (Fig. 2.7A), again emphasizing diet as a primary driver of changes to the microbiome. The whole microbiome samples for this group had two main clusters, one with the -2, 2, 4, and 6-week timepoints and another cluster containing the 0, 8, 10, and 12-week time points. A similar clustering pattern was seen in the IgA-negative and IgA-positive communities, but the overlapping ellipsoids at many of the timepoints indicates the difference is not significant, whereas differences in the whole microbiome are.

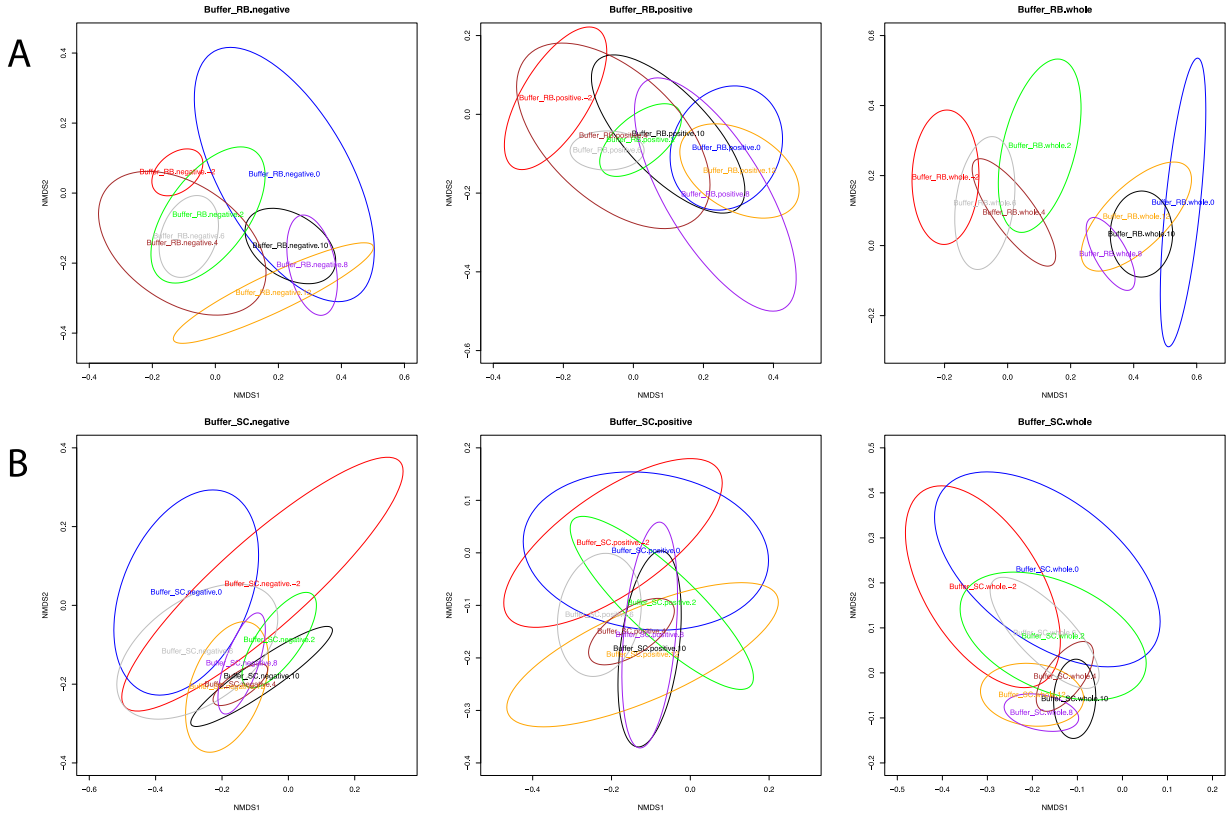

C

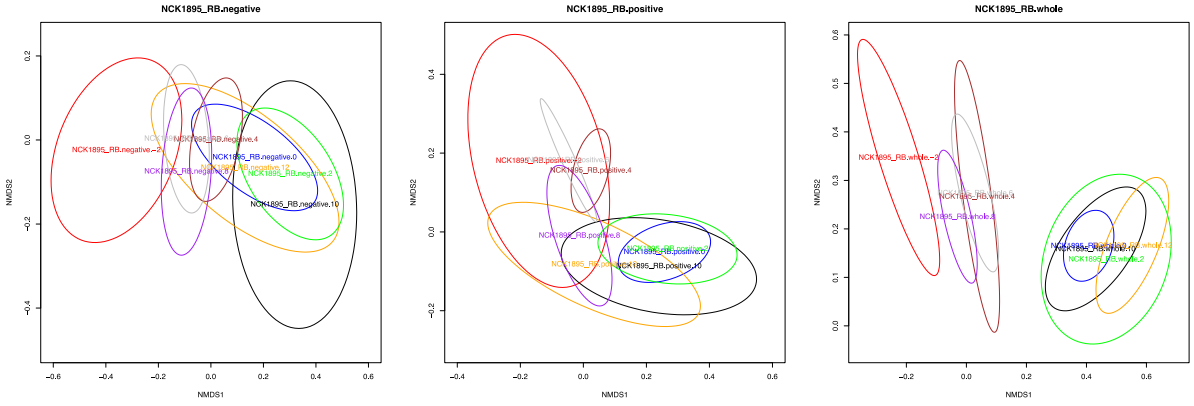
NCK1895_RB.negative
NCK1895_RB.positive
NCK1895_RB.whole
NMDS1
NMDS2

D

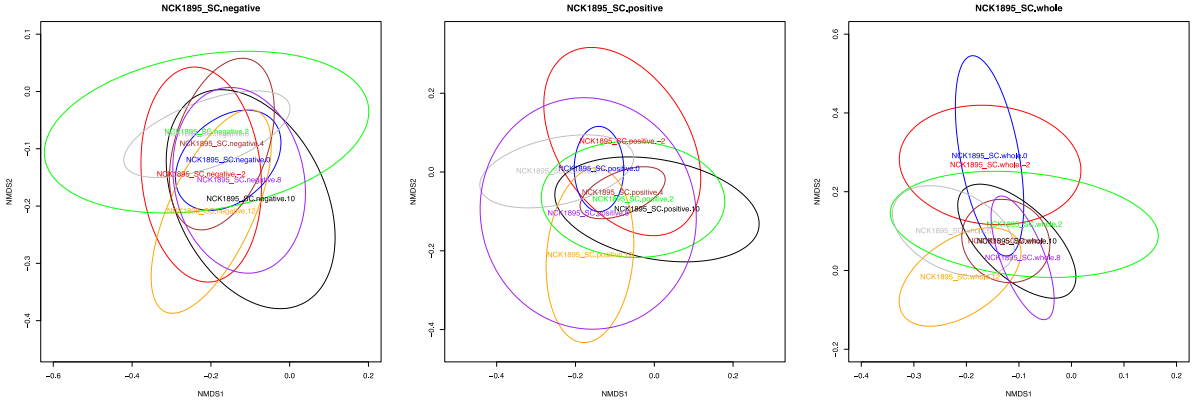
NCK1895_SC.negative
NCK1895_SC.positive
NCK1895_SC.whole
NMDS1
NMDS2

E

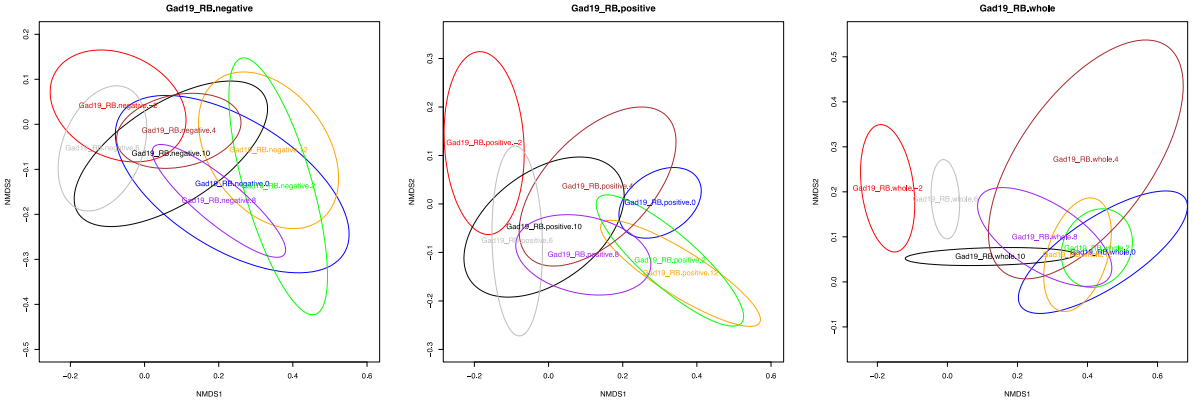
Gad19_RB.negative
Gad19_RB.positive
Gad19_RB.whole
NMDS1
NMDS2

F

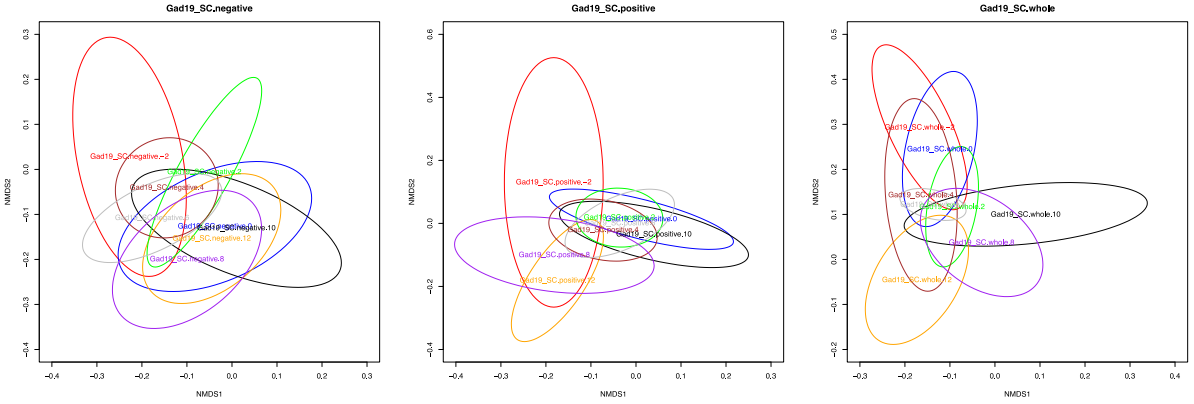
Gad19_SC.negative
Gad19_SC.positive
Gad19_SC.whole
NMDS1
NMDS2

Figure 2.7 Temporal changes in beta-diversity. NMDS ordinations for each experimental group is shown in sections a-f, with data separated into plots for IgA-negative, IgA-positive, and whole microbiome communities, respectively, as indicated by title above each plot. Each 95% confidence ellipsoid represents the samples taken at that timepoint, with number at the end of the label corresponding with the week of the sample collection.

A comparable pattern was seen in the NCK1895 groups, with the SC diet mice showing little change in community structure over time, while the RB diet group showed significant changes and similar clustering patterns (Fig. 2.7C and 2.7D). The IgA-negative and positive microbiome fractions for the NCK1895 group on the SC diet showed no significant changes over time, while the only significant differences in the whole microbiome appeared between week -2 and 12 (Fig. 2.7D). Animals on the RB diet in the NCK1895 group did show significant changes in the microbiome over time, but this is likely attributed to a change in diet (Fig. 2.7C). The whole microbiome community showed clusters between weeks 4, 6, and 8, and 0, 2, 10, and 12. Because the 0 time point overlaps with the 10 and 12-week timepoints, we conclude that the microbiome recovered to its pre-probiotic state. These results indicate that repeated dosing with the probiotic bacterium *L. acidophilus* does not significantly alter the microbiome as a whole or the subset of the microbiome that is recognized by the mucosal immune system.

Mice immunized with the GAD19 strain again showed differences during the switch from SC diet at week -2 to the RB diet at week 0 (Fig. 2.7F). This shift is clearly seen in both the whole microbiome and IgA-positive microbiome. The centroids for each timepoint also followed a similar trajectory between the two sample types (whole microbiome and IgA-positive) in the GAD19 RB group. Animals in the GAD19 and SC diet did not show a significant difference between the community structure at weeks 0 and 12 for any of the microbiome fractions (Fig. 2.7E). The IgA-negative microbiome fraction for the GAD19 animals on both diets showed a similar pattern, as seen by the overlapping ellipsoids for the majority of the timepoints. The shifts in community structure earlier in the study shows that the perturbations caused by vaccination were resolved and return to the starting homeostasis by the conclusion of the study, highlighted by the similarities in the week 0 and week 12 timepoints.

These data show the large role diet plays in inducing changes to the microbiome. However, the impact from diet is mainly observed in the whole microbiome samples and partially observed in the IgA-positive fractions. Additionally, the administration of our *L. acidophilus* strains did not induce long-lasting effects on the microbiome, as shown by the overlapping ellipsoids representing the community structure between early and late timepoints. The similarities across the IgA-negative fractions between treatment groups shows that neither the rLA vaccine nor RB diet cause a major disturbance in the IgA-negative bacterial community. The similar temporal clustering patterns of the GAD19 and NCK1895 IgA-positive and whole microbiome samples also indicates that the intermediate shifts seen in the whole microbiome samples are attributed to changes in the IgA-positive bacterial communities.

2.3.4: IgA Fractions Uncover Low Abundant Taxa

In order to quantify the shared and unique taxa between the different microbiome fractions, Venn diagrams were generated at both the OTU and genus levels (Fig. 2.8). 293 OTUs were shared between all microbiome fractions, and the whole microbiome community had 26 unique OTUs, IgA-positive had 38, and IgA-negative had 28, as shown in Figure 2.8A. Without sorting IgA-positive and IgA-negative fraction, 83 OTUs would not have been identified. At the genus level, there was only one unique taxon in the whole microbiome community, while the IgA-positive community had 24 unique taxa and IgA-negative had 15 (Fig. 2.8B). Although 73 genera were shared between all the microbiome fractions, 51 genera were found between the IgA-positive and IgA-negative fractions and not in the whole microbiome. These 51 genera found in IgA-fractions account for 40.5% of the total identified genera in the study, while the IgA-fractions discovered 19.9% of the total OTUs. The majority of OTUs found in the IgA-fractions that are absent in whole microbiome samples are represented by less than 50 reads. These taxa were often present in at least half of the experimental groups, and many OTUs were from the Proteobacteria phylum (Fig. 2.9). These lowly abundant bacteria may not have been detected in whole microbiome samples due to limitations in sequencing depth and the inherent nature of random sampling during library generation.

Venn diagrams for each experimental group show a similar pattern, with 60-68 genera shared between all microbiome fractions, and 5-13 unique genera in IgA-positive and IgA-negative fractions (Fig 2.10). Research shows that rare bacteria can account for up to 20% of the diversity within the bacterial microbiome and often remain undetected [253, 254], and it is necessary to investigate the impact that vaccination with rLA has on diversity of lowly abundant taxa.

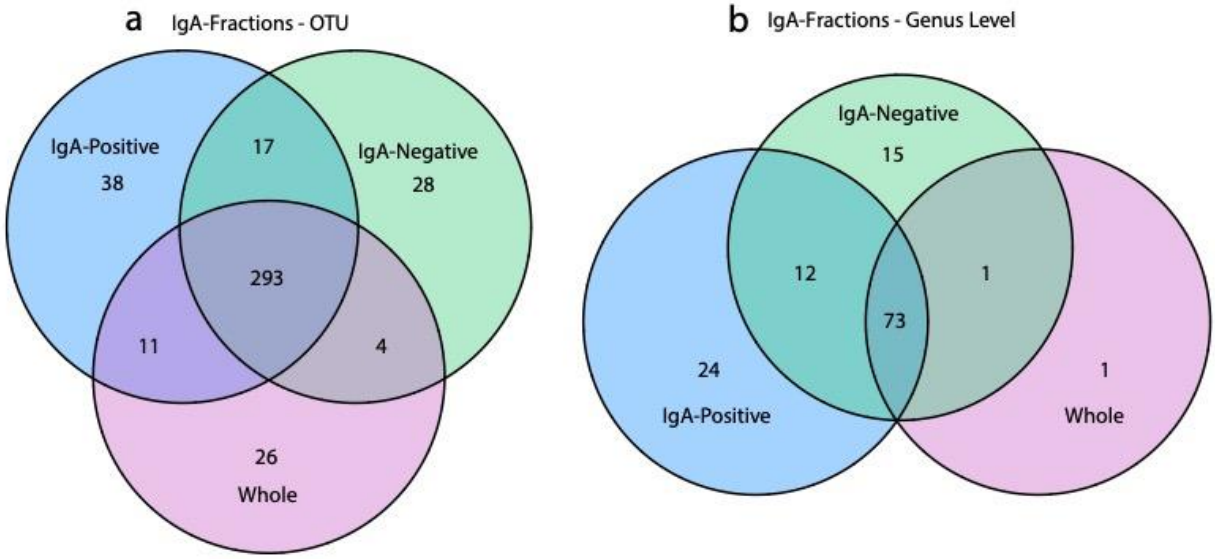

Figure 2.8 Shared and unique bacteria in different microbiome fractions. Venn diagrams represent the number of (a) OTUs or (b) genera found in the three microbiome types (whole, IgA-positive, and IgA-negative). Data is based on the Cumulative Sum Scaling normalized counts for each OTU.

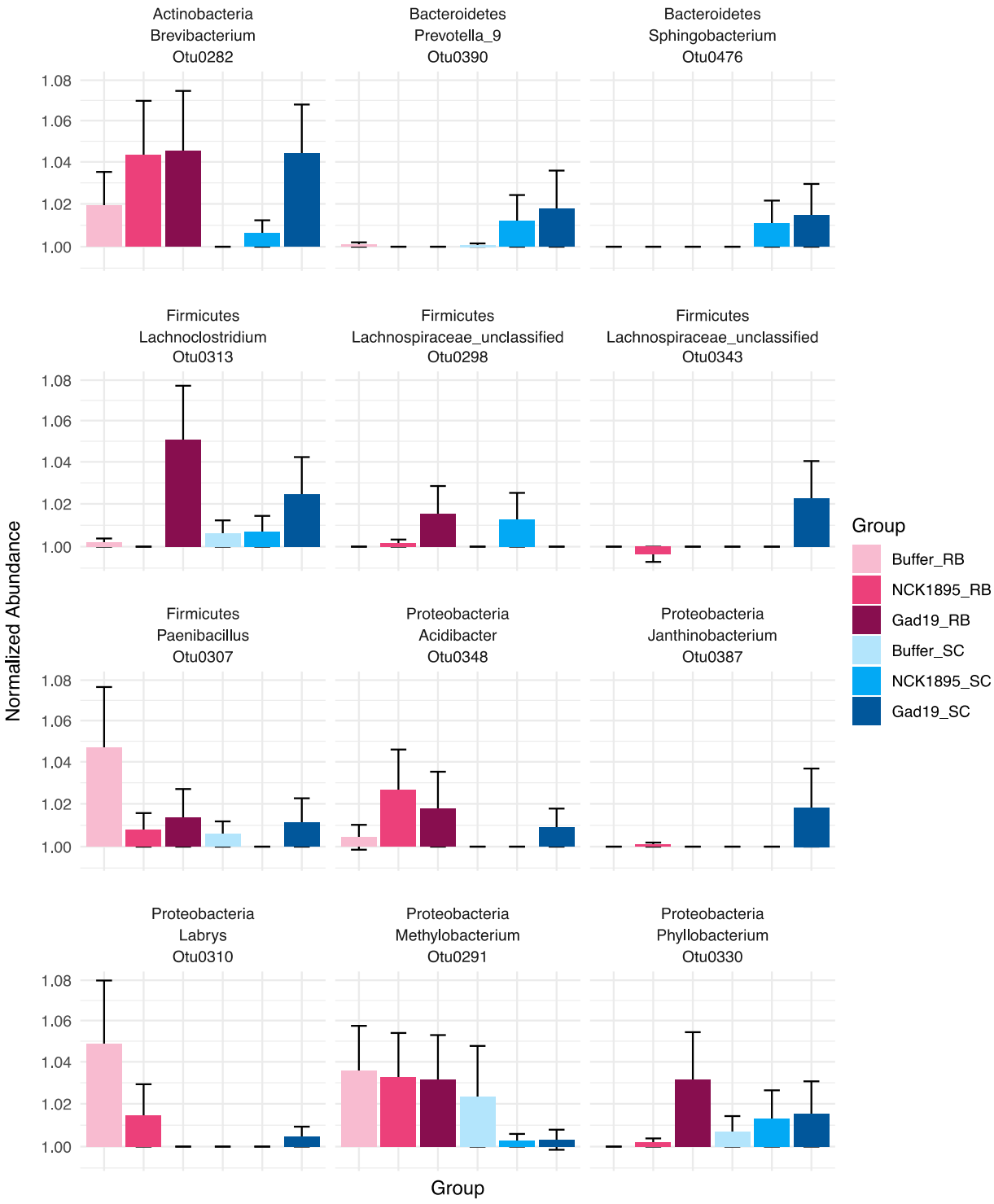

Figure 2.9 Normalized abundances of OTUs found only in IgA-positive or IgA-negative fractions. Each OTU is labeled with the phylum and genus it belongs to, and the relative abundance for each experimental group. Normalized abundances were calculated by Cumulative Sum Scaling as described in the Methods.

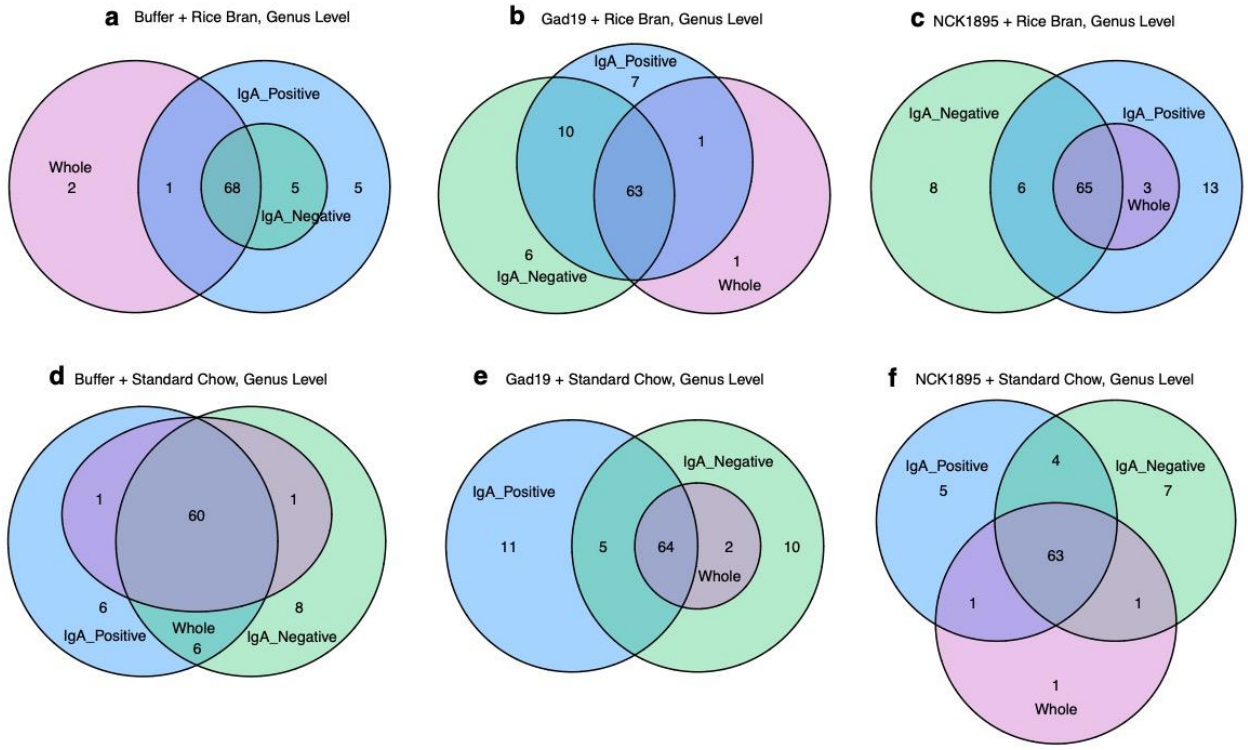

Figure 2.10 Unique and shared genera between microbiome fractions for each experimental group. Each Venn diagram represents genera found in each mouse group used in this study.

2.3.5: Random Forest Predictions of Important Taxa

The Random Forests (RF) [250] machine learning approach was used to classify samples into the designated treatment groups (Table 2.1) and important taxonomic drivers of differences between these treatment-groups were identified. Figure 2.11 shows the Mean Decreasing Gini (MDG) coefficients for the most important drivers in each microbiome fraction, calculated from OTU counts and identified by their genus classification. These MDG coefficients were calculated based on the original RF model which uses the treatment-group as the classifier, and OTUs with MDG greater than 0.2 were plotted. *Lachnospiraceae_UCG−001* was identified as the most important driver for classification within the whole microbiome samples, with uncultured bacteria and *Ruminococcaceae_UCG−005* also in the top three (Fig 2.11A). The top 77 OTUs all belong to the Firmicute phylum, except for OTU0073, which is an *Anaeroplasma* in the Tenericutes phylum. The majority of these Firmicutes are classified in either the

family *Ruminococcaceae* or *Lachnospiraceae*, both of which belong to the Clostridia family. Similar patterns were seen in both the IgA-positive and IgA-negative fractions (Fig. 2.11B and 2.11C, respectively). Similar to whole microbiome samples, members of the Firmicutes phylum made up the vast majority of the important taxa. OTU0023 and OTU00109 were the most important variables in both the whole microbiome and IgA-negative models, with OTU0023 (of the *Lachnospiraceae_UCG-001* genus) being the second important variable in the IgA-positive microbiome.

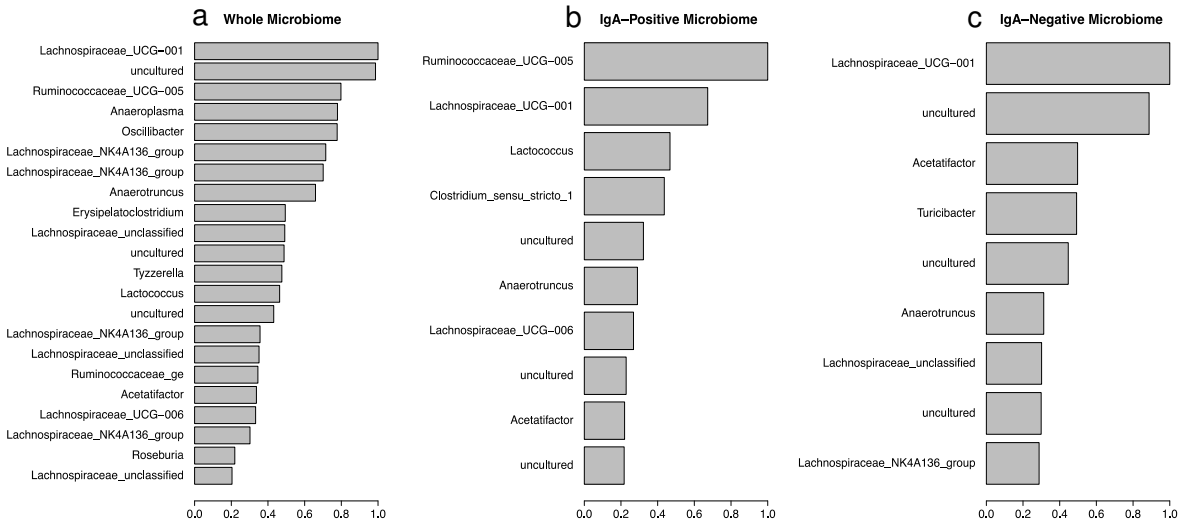

Figure 2.11 Mean Decreasing Gini (MDG) coefficients plot shows important OTUs. The MDG value represents the importance of the OTU, labeled by assigned genera, in Random Forest classification for each microbiome fraction. Cutoff was set to greater than 0.2.

The overall out-of-bag (OOB) misclassification error rates for whole microbiome, IgA-positive, and IgA-negative were 28.09%, 51.04%, and 42.56%, respectively (Table 2.4). The highest misclassification error rates were consistently found in NCK1895_SC diet classification (44.26% in whole, 70.69% in IgA-positive, and 52.54% in IgA-negative), with misclassification often occurring in the other SC groups. Treatment-group error rates for the whole microbiome ranged from 11.11% to 44.26%, with NCK1895_RB having the lowest error rate and NCK1895_SC having the highest. Within NCK1895_SC classification for whole microbiome, 34 samples were identified correctly, 7 were misclassified as

Buffer_SC, 15 were misclassified as GAD19_SC, and 5 samples were misclassified into the RB groups (4 as Buffer_RB and 1 as NCK1895_RB, Table 2.4). The error rates in the IgA-positive RF model were high for all treatment-groups, ranging from 42.37% to 70.69%. Because of these high error rates, RF models were also generated using vaccine type (buffer, NCK1895, or GAD19, Supplementary Table S2.1), or diet type (SC or RB, Supplementary Table S2.2). For these RF models, the whole microbiome again had the lowest misclassification error rates, with vaccine classification model showing a 16.6% error rate, and the diet classification model having 14.6% error rate. The IgA-positive models had 41.8% and 38.1% error rates for vaccine and diet models. The IgA-negative models showed 24.1% and 25.9% error rates also for vaccine and diet models. These results indicate that some of the treatments overlap, and error rates are improved when diet or vaccination is used separately in classification.

2.3.6: *Lactobacilli* Importance and Abundance Over Time

Since four out of our six animal groups received a strain of *Lactobacillus acidophilus* (NCK1985 or GAD19), we investigated the importance that the *Lactobacillus* genus had on RF classification and abundances throughout the study. Results from RF show that *Lactobacillus* was the 15th most impactful taxon in the IgA-positive model, 64th in whole microbiome, and 112th in IgA-negative (Supplementary Tables S2.3, S2.4, and S2.5, each showing the top 150 OTUs). The most important *Lactobacillus* OTUs observed in both the whole microbiome and IgA-positive tables were represented by OTU0017, while the *Lactobacillus* in the IgA-negative table was OTU0004. Due to the limitations of 16S-sequencing, we were unable to identify the species of the *Lactobacillus* OTU's that were observed. Importantly, timepoint and sequencing pool (to identify any batch bias) were both included as features in the RF, neither of which were highly important for classifying the microbiome samples into treatment group.

We also investigated changes in the normalized abundances of these *Lactobacillus* OTUs between the different microbiome fractions overtime (Fig. 2.12). The greatest changes between microbiome fractions can be observed in the GAD19_SC group. The abundance of *Lactobacillus* within this group was greatest in the IgA-negative fraction until week 10, where abundances of *Lactobacillus* were higher in the

IgA-positive fraction. This pattern was not observed in the GAD19_RB group, where *Lactobacillus* levels were consistently higher in either the IgA-positive group or whole microbiome. Alternatively, the NCK1895_RB group had high levels of *Lactobacillus* abundance in the IgA-positive and whole microbiome fractions. OTU0017 also appeared to be more prevalent in the IgA-positive and whole microbiome communities compared to the IgA-negative fraction, especially within RB groups, while OTU0004 accounted for the majority of the detected *Lactobacillus* in the IgA-negative samples. These data indicate that *Lactobacillus* was most impactful in the RF classification of experimental groups for IgA-positive samples, which could be attributed to the high abundance of OTU0017 in the IgA-positive fraction of NCK1895_RB samples.

Figure 2.12 Normalized abundances of *Lactobacillus* over time. The normalized abundances of the most abundant OTUs in the *Lactobacillus* genus are shown for the whole microbiome (top row), IgA-positive microbiome (middle row), and IgA-negative microbiome (bottom row). Values displayed are based on the normalized abundances calculated using Cumulative Sum Scaling as described in the methods. Bars represent the mean count for each group at each timepoint, with error bars showing the standard error.

2.3.7: Correlation Between Antigen-specific IgA and Microbial Taxa

Data from MPER-specific fecal ELISAs (Fig. 2.3) was used in Spearman's correlation to highlight associations between specific taxa and increased MPER-specific antibodies. Only GAD19 vaccinated groups were included in correlation to the 20 most important taxa from the whole microbiome at the OTU level, found using RF. Figure 2.13 shows significant positive (red) and negative (blue) correlations between MPER-specific IgA and OTUs, without correction for multiple testing. Antigen-specific IgA associated with the RB group displayed negative correlation with several *Lachnospiraceae* taxa in weeks 2 and 4, but no negative correlations with any other taxa were found after week 4 (Fig. 2.13A). Positive correlations associated with the RB group included *Acetatifactor* and *Lachnospiraceae_NK4A136_group* at week 2, *Anaerotruncus* at week 10, and *Lachnospiraceae_NK4A136_group* again at week 12.

Conversely, antigen-specific IgA within the SC diet group displayed both positive and negative correlations with several different taxa during weeks 10 and 12 (Fig. 2.13B). Significant negative correlations include *Acetifactor, Lachnospiraceae_UCG−001*, and an uncultured bacterium in the Lachnospiraceae family. Only *Lachnospiraceae_UCG−001* continued with a negative correlation during week 12. Week 10 had two taxa that were positively correlated with antigen-specific IgA in the GAD19_SC group: *Ruminococcaceae_ge* and *Lactococcus*. However, during week 12, there were four taxa with positive correlations, including *Lachnospiraceae_UCG−006, Erysipelatoclostridium, Anaeroplasma,* and *Anaerotruncus*. These results follow patterns with MPER-specific antibodies between the two diet groups, with more correlations found in earlier timepoints for RB groups and most correlations for SC groups found in weeks 10 and 12.

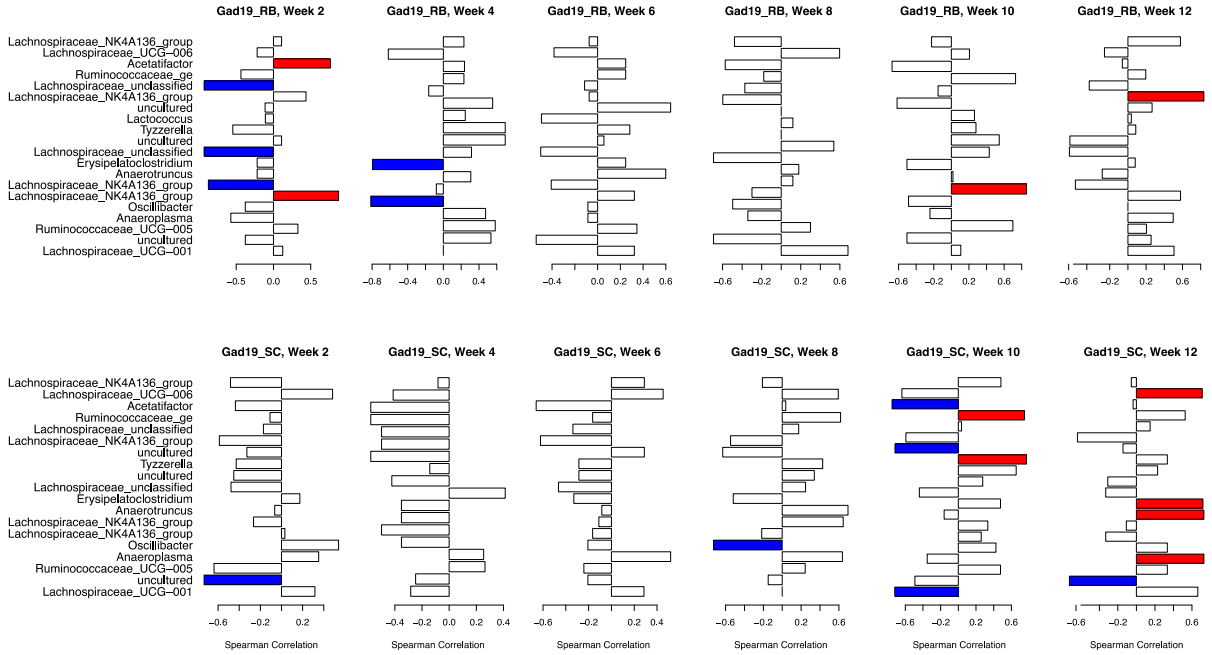

Figure 2.13 Spearman's correlation between important taxa and MPER-specific IgA. Plots show Spearman's correlation between the 20 most impactful taxa from the whole microbiome and MPER-specific IgA production in fecal samples. Positive correlations are represented in red, and negative correlations in blue. No correction for multiple testing was applied, and significance was set to $P < 0.1$.

2.4: Discussion

In this study, we addressed two key questions regarding the use of recombinant *Lactobacillus acidophilus* (rLA) as a vaccine platform. Firstly, we asked whether use of a prebiotic would enhance the immune response against antigens orally delivered utilizing rLA. We determined that using rice bran as a prebiotic resulted in a quicker induction of mucosal and systemic humoral responses and increased the number of IgA-secreting cells within Peyer's patches. Secondly, we evaluated the microbiome to determine whether repeated administration of rLA might alter the microbial community directly due to the presence and activity of the probiotic itself through competition and selective exclusion, or indirectly by inducing a host mucosal immune response against rLA. IgA-seq was used to further identify if the combined effects from rLA vaccination and the activated mucosal immune response impacted the IgA-bound bacterial population of the microbiome. Neither *L. acidophilus* itself (NCK1895) nor the rLA vaccine (GAD19) resulted in long-term alterations of the intestinal microbial community diversity. As would be expected,

differences in diet as a result of the prebiotic did alter the microbiome. It remains to be determined whether the observed more rapid immune response was due to shifts in the microbiome or to a direct influence of the rice bran on the performance of the rLA platform.

The rLA vaccine platform offers several logistical and immunological advantages over parenterally delivered vaccines. Immunological results from this study highlight the ability of orally delivered vaccines to induce both mucosal and systemic humoral immune responses. The presence of MPER-specific IgG indicates that a systemic immune response was mounted, while MPER-specific IgA detected in both fecal and vaginal samples highlight the ability of the GAD19 vaccine to stimulate the gut-associated lymphoid tissues leading to the migration of effector cells to distant mucosal tissues. This property of oral vaccination allows for both local control of mucosally-transmitted pathogens as well as surveillance of systemic spread [204, 255, 256].

L. acidophilus as a vaccine platform is advantageous due to the ease of genetic manipulation to achieve massive surface expression of desired antigens. The GAD19 strain co-expresses the 16-mer MPER peptide and mature mouse-IL-1β [214]. The MPER peptide, although weakly immunogenic, is highly conserved among HIV-1 and is a known target of broadly neutralizing antibodies [257]. Due to this low immunogenicity, GAD19 was engineered to secrete the adjuvant IL-1β to increase the humoral immune response. IL-1β is a pro-inflammatory cytokine and known mucosal adjuvant [183, 258, 259]. This combination of a poorly immunogenetic peptide and successful mucosal adjuvant resulted in the activation of the humoral immune response without inducing tolerance. The induction of mucosal tolerance instead of protective immunity is often attributed to direct administration of purified antigens or overdosage of the vaccine but can be avoided by inclusion of adjuvants in a carrier system to deliver antigens [260]. In this case, the strengthening of the inflammatory response with IL-1β in combination with innate LA adjuvants that stimulate TLR2, NOD2 and DC-SIGN, likely tip the balance toward an adaptive immune response. TLR2 activation, in particular, has also been associated with inhibition of regulatory T-cells [261]. The

results presented here show no signs of mucosal tolerance against the MPER peptide, but further studies are needed to confirm these findings through challenge with the vaccine target or re-exposure to the antigen.

The present study shows the possibility of improving the humoral immune response through the use of the prebiotic rice bran. Previous studies showed a 10% rice bran diet increased abundance of *Lactobacillus* populations and increased levels of secretory IgA in animals and humans [238, 239, 262]. The use of prebiotics, indigestible food components that promote the activity of probiotics in the host [239], is a practical opportunity to increase vaccine efficacy. Rice bran is especially attractive as it is globally accessible and an abundant grain byproduct [238]. The use of prebiotics could be a solution to the known variation in vaccine efficacy between high-income and low or middle income countries [162], where Rotavirus vaccines, for example, are 30-50% less efficacious, possibly due to poor sanitation, malnutrition of mothers and their children, and chronic intestinal inflammation [162, 164, 254, 263, 264]. Because this study did not recapitulate a state of malnutrition in mice, the full potential of rice bran as a prebiotic could not be assessed. Future studies using animal models of malnutrition and/or dysbiosis would better simulate conditions of populations in developing countries. The accelerated antibody induction and significant increase in IgA-secreting cells within the Peyer's patches of rice bran supplemented animals in this study justifies continued investigation of prebiotics as a means to enhance the immune response to rLA in individuals with compromised mucosal immunity.

The use of a commensal organism as a vaccine platform raises concerns of potential off-target effects of vaccine-induced IgA on the microbiome. Several recent theories on the role of secretory mucosal IgA include maintaining a core microbiome, both promotion and restriction of colonization, and regulating the function of the microbiome [265, 266, 104, 253, 225]. To address this concern, we used IgA-seq to further investigate potential disturbance of the microbiome fraction that is recognized by the mucosal immune system. We showed that the IgA-positive and IgA-negative fractions account for 40% of the diversity within identified genera and 20% of OTUs. This is in concordance with results using a similar technique of bacterial sorting reported by D'Auria *et al.* (2013) where 20% of total diversity was attributed to rare bacteria [253]. This occurrence is hypothesized to be due to traditional sequencing methods that may

not recover these rare taxa or data processing that filters out rare taxa. In agreement with the literature [253], we show that these lowly abundant bacteria have a greater likelihood of being sequenced as a result of IgA-sorting. Additionally, many of the taxa absent from the whole microbiome group but present in IgA-fractions are members of the Proteobacteria phylum, which has also been observed by others [253, 267]. Due to the pathogenic nature of many members of the Proteobacteria phylum, including *Escherichia*, *Shigella*, *Salmonella*, *Brucella*, and *Helicobacter*, high abundance of these species is often not found in healthy individuals . It has also been proposed that rare species provide a pool of genetic resources that are utilized when necessary [269, 270]. For example, a higher diversity of lowly-abundant bacteria was associated with reduced severity of bacterial infections in patients with cystic fibrosis [271]. Another proposed function of the lowly abundant taxa is the continuous competition with closely related species. Specifically, the presence of endogenous non-pathogenic *Enterobacterales* aid in the resistance of colonization from pathogenic *Salmonella* serovars in several animal models [272].

Significant changes in predicted alpha diversity were not found throughout the study, but beta-diversity was altered with diet as a primary driver and the *L. acidophilus* platform contributing to intermediate shifts. This pattern of a change in diet leading to alterations in beta diversity but not alpha diversity has been documented previously [273], but to date, the diversity of IgA-positive and negative fractions have not been evaluated. We show that IgA-positive communities had a closer resemblance to trends observed in beta-diversity of whole microbiome samples compared to IgA-negative communities, especially regarding longitudinal shifts from the initial change in diet. Previously, we have shown the impact of rLA on the whole microbiome, and found IL-1β secretion from rLA to have the greatest impact on variation in beta-diversity [201]. However, the results presented here demonstrate that rice bran leads to the greatest changes in beta-diversity. These results also indicate that separation between the negative control groups (Buffer) and *L. acidophilus* vaccinated groups (GAD19 and NCK1895) was likely due to the probiotic itself, and not a result from the rLA vaccine construct alone. The impacts on the resident microbiome from probiotics have been documented, with main conclusions being that alterations to community structure are short-lived, at least in the fecal microbiome [153, 274–277]. Further studies are

needed to investigate any possible alterations the rLA vaccine has on specific niches within the gastrointestinal tract, as fecal samples used in this study best represent microbial changes found in the lower colon.

The influence of *Lactobacillus* and *Lachnospiraceae* were also observed during Random Forests classification of experimental groups. While *Lactobacillus*, specifically OTU0004, was classified as the 15th most impactful taxon in the IgA-positive fractions based on the Gini coefficient, *Lactobacillus* was 64th in the whole microbiome and 112th in the IgA-negative fractions, both represented by OTU0017. These results suggest IgA-positive samples rely more on the presence of *Lactobacillus* to identify the experimental group to which they belong compared to IgA-negative and whole microbiome samples. OTU0017 had a higher abundance in the NCK1895_RB and GAD19_SC groups for both whole and IgA-positive microbiomes, while OTU0004 was often the most abundant *Lactobacillus* OTU in the other experimental groups. The Gini coefficient highlighted several *Lachnospiraceae* taxa as being highly important for classification, especially the genus *Lachnospiraceae_NK4A136_group*. Correlation analysis also shows the importance of *Lachnospiraceae* abundance with antigen-specific IgA production. The function of many of members of the *Lachnospiraceae* family and the *Erysipelatoclostridium* genus have an associated role in obesity, diabetes, or intestinal inflammation, although findings are often strain dependent [278, 279]. However, *Lachnospiraceae* are also among the main producers of short chain fatty acids in the gut. *Lachnospiraceae_NK4A136_group* and *Ruminococcaceae* are both known butyrate producers and are correlated with enhanced gut barrier function and lower long-term weight gain when a high fiber diet was consumed [64, 280]. Others have shown how a change in diet, including salt, walnuts, and processed foods can alter the abundances of members of the *Clostridia* class, specifically *Lachnospiraceae* and *Ruminococcaceae* [281–283]. Our results show an overall negative correlation between *Lachnospiraceae* and antigen-specific IgA production for mice on the RB diet early in the study, and both positive and negative correlations between several taxa in the *Lachnospiraceae* family in the SC diet at the end of the study. Together, these results suggest *Lachnospiraceae* may play a dual role, based on the strain and environment within the gut, in both instigating and resolving inflammation.

2.5: Conclusion

While we have shown the rLA vaccine platform does not lead to long-term shifts in the bacterial microbiome, the immediate impacts on diversity and transcriptional profile remains to be investigated. Becattini *et al*. (2021) has demonstrated a rapid shift in gene transcription and metabolite production from the microbiome within 6 hours of activation of the host's immune system [203]. These findings emphasize that activation of the mucosal immune response through the MPER antigen and other adjuvants associated with rLA may be altering the function of the bacterial community, but it may not be in the conventional idea of changes in abundance. Correlation results here provide evidence that members of the *Lachonspiraceae* family may play an important role in this rapid response to immune activation. Since *L. acidophilus* does not colonize the gut and only persist for two to three days [284], taking a series of samples between primary vaccination and booster immunizations would provide insight into how long it takes the microbiome to recover from the sudden high abundance of *L. acidophilus.*

CHAPTER 3: NOD2 Signaling in Antigen Presenting Cells During Oral Vaccination is Critical for Eliciting a Humoral Immune Response and Maintaining the Gut Microbiome

3.1: Introduction

Addressing the ongoing global threat of mucosally transmitted pathogens will require novel mucosal vaccine platforms to compliment or replace existing parenteral vaccines. Rational development of mucosal vaccines requires a comprehensive understanding of how, where, and through what cell types a candidate vaccine engages the host immune system. Lactic acid bacteria (LAB) such as *Lactobacillus acidophilus* provide an attractive platform to deliver selected antigens to mucosal immune inductive sites [174, 175]. *L. acidophilus* persists but does not colonize the digestive tract, is generally regarded as safe by the FDA, and offers practical and logistical benefits as a vaccine platform including inexpensive manufacturing, room temperature storage, and oral delivery [211, 216, 240]. *L. acidophilus* expresses microbial associated molecular patterns that are recognized by the innate immune system and serve as endogenous adjuvants. Importantly, *L. acidophilus* can also be readily engineered to express high levels of exogenous antigens and adjuvants [176, 285, 286]. We have previously reported on the immunogenicity of recombinant *Lactobacillus acidophilus* (rLA) expressing several antigens [149, 287]. However, a mechanistic understanding of mucosal immune activation by rLA, *in vivo*, is needed to further optimize this potentially powerful vaccine platform.

Nucleotide-binding oligomerization domain containing 2 (NOD2) is a cytoplasmic pattern recognition receptor in the NOD-like receptor (NLR) family that recognizes the peptidoglycan breakdown product, muramyl dipeptide (MDP), from many bacterial species including *L. acidophilus* [288]. Ligation of NOD2 results in a pro-inflammatory response mediated by NF-κB, caspase-1, and mitogen-activated protein kinase-signaling (MAPK) cascades [212]. NOD2 is expressed by a variety of cells in the intestinal tract, including hematopoietic (dendritic cells, macrophages, and T and B cells) and nonhematopoietic cells (Paneth cells, goblet cells, and enterocytes) [289]. It has previously been demonstrated that NOD2 signaling in antigen presenting cells (APCs), and specifically dendritic cells (DCs), is essential for initiating a T_H2-type and innate T_H17 immune responses, while NOD2-signaling in Paneth cells leads to the increased

production of antimicrobial peptides and a T_H1 driven response [288, 290–292]. Additionally, NOD2 Studies have shown that NOD2-signaling is required for the recognition and clearance of pathogens and toxins including *Streptococcus pneumoniae*, *Citrobacter rodentium*, *Salmonella typhimurium*, *Bacillus anthracis*, and cholera toxin (CT), among others [290, 293–296].

NOD2 signaling also provides an excellent opportunity for targeting the innate immune response to increase the adaptive immune response against rLA to achieve higher antigen-specific antibody titers [297]. NOD2-signaling during rLA vaccination allows for a transient increase in inflammation through the adjuvant activity of MDP from the Gram positive rLA, ultimately leading to activation of the NF-κB pathway [294]. Since *L. acidophilus* is not detected in the intestines after three days of administration, this inflammatory response is short-lived and unlikely to cause the lasting responses associated with inflammatory bowel disease (IBD)[284]. Recently, NOD2 has been the target for enhancement of several vaccines. Specifically, the novel antigen Inarigivir was added to the Bacille Calmette-Guérin (BCG) vaccine to increase its immunogenicity in mice [298]. Confirming the critical role of NOD2 signaling in CD11c+ cells during rLA immunization will allow for similar optimization of rLA.

Additionally, there is a strong correlation between NOD2 deficiency and IBD, including Crohn's disease, colorectal cancer, and early-onset sarcoidosis [299–303]. Although these inflammatory diseases are likely multifactorial with influences from environment, early antibiotic exposure, mutations in NOD2, and the individuals' mucosal immune response all contributing to the development of disease, the composition of the gut microbiome has proven to be a significant factor [300, 301, 304]. Several studies have compared the microbiome of *Nod2-/-* and *Nod2+/+* mice with conflicting results on the direct role of NOD2 regarding dysbiosis [305–308], likely due to different marker-gene sequencing methods, microbiome analysis, and institutional differences in vivarium management (location and housing of mice) [309]. Ongoing improvements in microbiome protocols and standards might help to address these discrepancies. Furthermore, how specific NOD2-expressing cell types influence the microbiome under various conditions of health and disease is only partially understood.

Previously, we investigated the roles of TLR2, NOD2, and capsase-1 in macrophage phagocytosis and activation in response to co-culture with rLA *in vitro* and found NOD2 is required for a proinflammatory response against rLA. *In vivo* studies indicated that NOD2 is also critical for antigen-specific mucosal IgA and systemic IgG responses against rLA, but the specific NOD2-expressing cell type(s) responsible were not determined [218]. Here, we utilized Cre-Lox recombination to selectively disrupt NOD2 signaling in CD11c-expressing cells to investigate the role of NOD2 in DCs, upon vaccination with rLaOVA, a construct expressing the major histocompatibility complex (MHC) class II epitope from chicken egg ovalbumin (peptide 323-339) [310]. We show that NOD2 signaling in CD11c+ DCs is essential for rLA immunogenicity in both mucosal tissues and systemically. In addition, we determined the influence of CD11c-NOD2 signaling by *L. acidophilus* on the composition of the intestinal microbiome and identified several associated key taxa. These results will inform the rationale design of rLA vaccine constructs and provide insight into the mechanism and application of *L. acidophilus* as a probiotic.

3.2: Materials and Method

3.2.1: Ethics Statement and Study Design

This study was carried out under strict accordance with recommendations in the Guide for the Care and Use of Laboratory Animals of the National Institutes of Health and ARRIVE guidelines (https://arriveguidelines.org). Protocol 17-7495A was approved by the Colorado State University Institutional Animal Care and Use Committee (IACUC). Animal welfare and health was monitored daily, and in instances where medical intervention was not effective, animals were humanely euthanized, and every effort was made to minimize animal suffering. Four to eight mice were assigned to experimental groups (described in Table 3.1), depending on the availability of mice with the correct genotype for each group during breeding for a total of 45 mice. Experimental groups with respective genotype and vaccine treatment are shown in Table 3.1. Throughout analysis, the dosing buffer groups were used as the negative

control to compare the GAD19 and NCK1895 results, and randomization strategy for library preparation is described in microbiome methods below.

3.2.2: Bacterial Culture Conditions

Lactobacillus acidophilus strain NCK1895 and recombinant strains LaOVA and NCK1909 were grown in MRS broth (BD Diagnostics, Sparks, MD) with 5 μg/ml of erythromycin (Em) [214]. *Lactobacillus* cultures were incubated overnight at 37°C under static conditions. *Escherichia coli* strains were grown aerobically with shaking in LB medium (BD Diagnostics) with or without 200 μg/ml of Em and 40 μg/ml of kanamycin (Km) at 37°C.

3.2.3: Construction of rLA-OVA and Verification of OVA Expression

Recombinant *L. acidophilus* expressing the peptide $OVA_{323-339}$ (LaOVA) on the surface layer protein A (slpA) was generated using methods similar to those previously described [214, 217]. Briefly, the chicken egg Ovalbumin peptide 323-339 was used as a model peptide because it is a known epitope for the I-A(d) major histocompatibility complex class II (MHC-class II) protein, with the sequence ISQAVHAAHAEINEAGR. Plasmid pGAD18 was created using pTRK935 with modified slpA inserted with $OVA_{323-339}$, using published methods [214, 311]. The resulting plasmid was transformed into *L. acidophilus* strain NCK1909. $OVA_{323-339}$ was introduced into the genome via homologous double cross over with the pGAD18. The chromosomal insertion of $OVA_{323-339}$ into *L. acidophilus* was confirmed with both flow cytometry and Sanger sequencing (Genewiz LLC.) for external expression and detection of any mutations, with results shown in Figure 3.1. For flow cytometry, bacterial cells were grown overnight, washed three times with PBS, and incubated with rabbit anti-chicken $OVA_{323-339}$ IgG (Alpha Diagnostic Intl. Inc., OVA3231-A) at 10 μg/ml in 1% BSA PBS buffer. Cells were washed and incubated with donkey anti-rabbit IgG conjugated with FITC at 5 μg/ml (Biolegend, San Diego, CA, 406403). Cell population data were collected with the Beckman Coulter Gallios Flow Cytometer and analyzed with FlowJo software.

Cells were gated on forward scatter (FSC) and side scatter (SSC) to eliminate debris, and then FL1 was used to identify FITC positive events to indicate OVA-positive expressing cells.

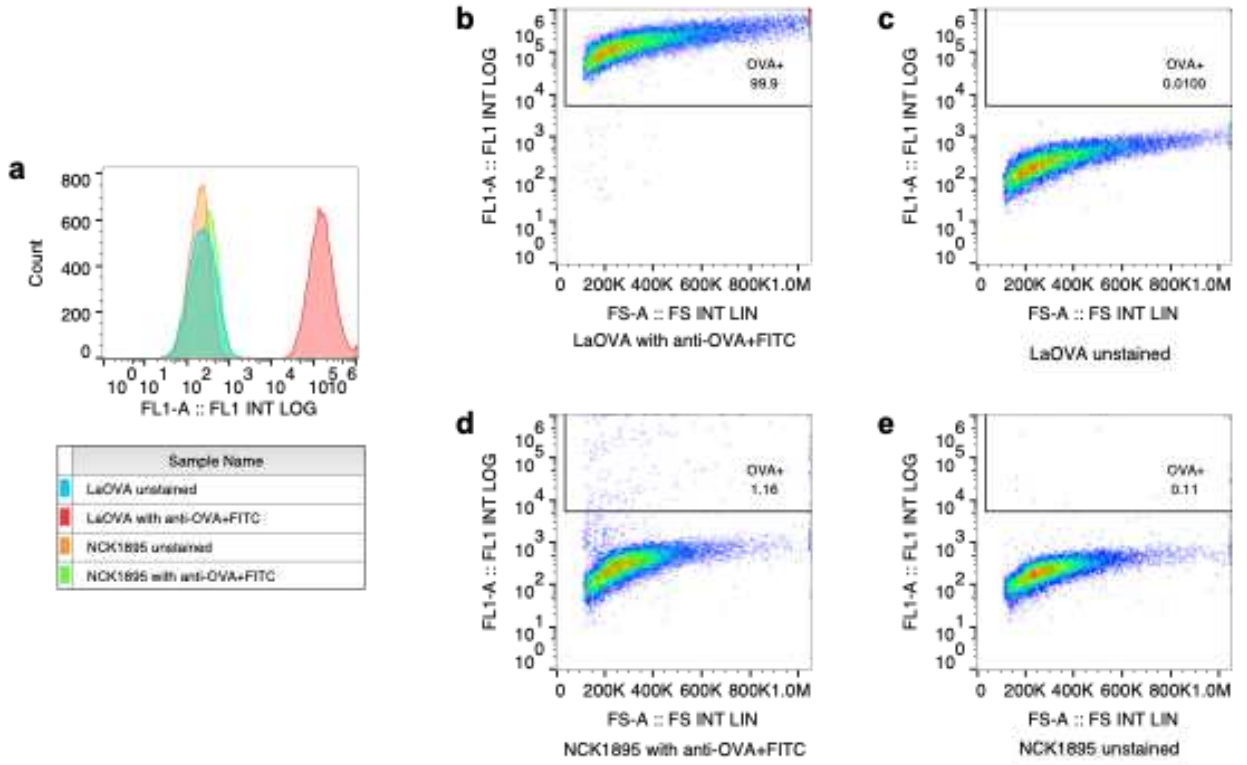

Figure 3.1. Expression of $OVA_{323-339}$ by LaOVA. Histograms (a) and dot plots (b-e) show the expression of $OVA_{323-339}$ by LaOVA, but not NCK1895. LaOVA plots are shown in (b) with an anti-OVA antibody and secondary antibody conjugated with FITC, and (c) as unstained. NCK1895 plots are similarly shown in (d) with anti-OVA and FITC-secondary antibodies, and (e) as unstained.

3.2.4: Tissue-Specific NOD2 Knockout Mice

NOD2-floxed ($NOD2^{fl/fl}$) mice and CD11c-Cre mice were bred to generate mice with a tissue specific knockout of NOD2 used in this study. $NOD2^{fl/fl}$ mice on the C57BL/6 background were provided by Dr. David Prescott at the University of Toronto [294, 312]. $NOD2^{fl/fl}$ have a proximal loxP site within intron 1 of the *Nod2* gene and the distal loxP site within intron 3. Mice expressing the Cd11c-Cre transgene (Itgax-Cre) on the C57BL/6 background were obtained from the Jackson Laboratory (Bar Harbor, Maine). These two strains of mice were bred to generate $NOD2^{fl/fl}$-$CD11c^{cre}$ mice (referenced as $NOD2^{\Delta DC}$ here). Expression of Cre-recombinase in these $NOD2^{fl/fl}$-$CD11c^{cre}$ mice results in the deletion of the genomic

region between the two loxP sites, which includes exon 2 and the cryptic start codon of exon 3, leaving NOD2 non-functional in CD11c+ cells. Genetic controls used in this study included mice heterozygous for the NOD2 loxP sites and expressing Cre-recombinase ($NOD2^{fl}$-$CD11c^{cre}$), homozygous for NOD2 loxP sites without Cre-recombinase ($NOD2^{fl/fl}$), and mice expressing Cre-recombinase without loxP sites ($CD11c^{cre}$). The genotypes of mice were confirmed using PCR to amplify NOD2-lox sites, Cre-recombinase, and an internal Cre control. Primers for NOD2 included F: 5'-CGGTTGGTGGGATTTCCTGTGC-3' and reverse: 5'-CAGCCAGGGGTGATGATAACAGG-3', which produced a 379-bp band for loxP-negative alleles, and a 499-bp band for alleles harboring the loxP sites. To identify the presence of Cre-recombinase, the following primers were used: Cre transgene F: 5'-CCATCTGCCACCAGCCAG-3', R: 5'-TCGCCATCTTCCAGCAGG-3'; internal Cre control F: 5'-ACTGGGATCTTCGAACTCTTTGGAC-3', R: 5'-GATGTTGGGGCACTGCTCATTCACC-3'. These primers produce a 281-bp band if Cre-recombinase is present and no band if it is absent. The internal Cre controls primers serve as a positive control and produces a 420-bp band.

One concern with any animal study using DNA nickases for gene-editing is the potential for non-specific side effects on the normal immune response. Mice expressing Cre ($CD11c^{cre}$) were used to compare with $NOD2^{\Delta DC}$ groups so that any genotoxic effects induced by Cre were similar between all mice. Extra genotype controls were also designed to ensure loxP sites were not interfering with NOD2 function. Therefore, we are confident results presented here are due to the critical role of NOD2 and not off-target effects of Cre recombinase. All mice were kept under specific pathogen free conditions and had ad libitum water and standard chow at CSU's Lab Animal Resources (LAR) throughout the duration of the study.

Table 3.1. Genotype and treatment of mouse groups used in this study.

Group	NOD2-Flx	Cd11c-Cre	Purpose	Treatment	N
$CD11c^{cre}$ + NCK1895	-/-	+	Cre control	NCK1895	5
$CD11c^{cre}$ + LaOVA	-/-	+	Cre control	LaOVA	6
$CD11c^{cre}$ + Buffer	-/-	+	Cre control	Buffer	6
$NOD2^{\Delta DC}$ + NCK1895	+/+	+	$NOD2^{DC}$-Kockout	NCK1895	5
$NOD2^{\Delta DC}$ + LaOVA	+/+	+	$NOD2^{DC}$-Kockout	LaOVA	6
$NOD2^{\Delta DC}$ + Buffer	+/+	+	$NOD2^{DC}$-Kockout	Buffer	4
$NOD2^{fl}$-$CD11c^{cre}$ + LaOVA	+/-	+	Single NOD2-KO	LaOVA	5
$NOD2^{fl/fl}$ + LaOVA	+/+	-	NOD2-loxP control	LaOVA	8

3.2.5: Mouse Immunization, Housing, and Sample Collection

Female mice breeding strategies described above were used when they reached 6-8 weeks of age. Live-bacterial vaccines were prepared using freshly grown overnight bacterial cultures. NCK1895 and LaOVA bacterial cells were washed twice in PBS (Corning, Corning, NY) and resuspended in a dosing buffer containing soybean trypsin inhibitor (STI, Sigma) and sodium bicarbonate ($NaHCO_3$). Mice were given $2x10^9$ CFU of either NCK1895 or LaOVA in 200ul of dosing buffer, or 200 ul of the dosing buffer alone (negative control). Vaccines were delivered intragastrically three days in a row during weeks 0, 2, 4, 6, 8, and 10, with an additional dose 18 hours before sacrifice at week 12 for stimulation of cytokine production. Mice were housed in groups of two to four. Groups with respective genetic background and vaccine treatment are shown in Table 3.1, and vaccine timeline is shown in Figure 3.2. Two weeks after the last dosing timepoint, mice were euthanized, and tissues were processed to obtain single-cell suspensions, as described below.

Blood, fecal, and vaginal samples were collected from each animal prior to administration of vaccination for investigation of antibody titers. Fecal samples used for antibody detection were collected and homogenized with PBS supplemented with ProteaseArrest at a 10x weight to volume ratio. Homogenates were spun at 9,390 RCF for 10 minutes to pellet particulates and bacteria. Clear supernatants

were aliquoted and stored at -80°C for long term storage. Fecal samples for microbiome analysis were collected directly from the anus of the animal into a sterile PCR tube and placed immediately on ice and transferred to -80°C freezer for long term storage. Serum samples were collected via tail bleeds. Blood was collected with a microvette (Sarstedt, Nümbrecht, Germany) and processed according to manufacturer's protocols for serum isolation. Serum was aliquoted and stored at -80°C. Vaginal lavage samples were collected by gently washing the vagina of mice with 100ul of PBS. The collected fluid sample was immediately put on ice. Samples were then spun at 9,390 RCF and supernatants were aliquoted and stored at -80°C.

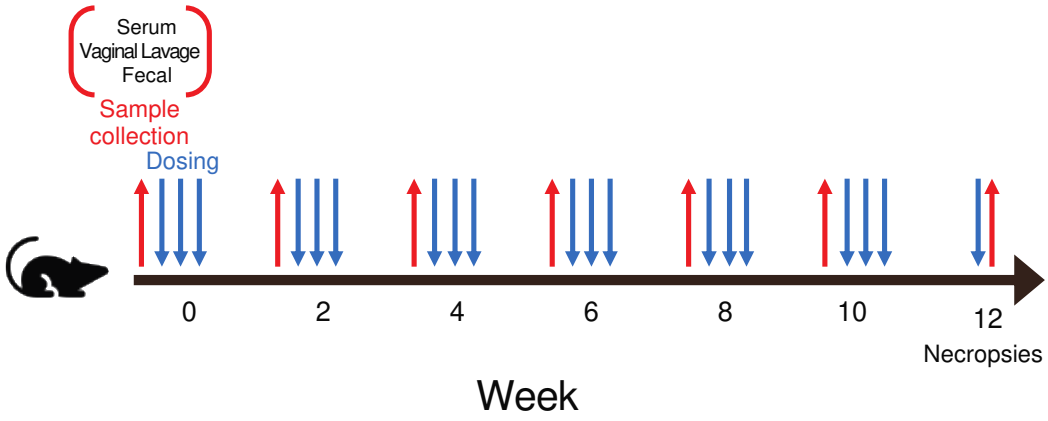

Figure 3.2. Experimental design and vaccination schedule. Samples were collected from mice every two weeks, with vaccination beginning immediately after collection. Mice were immunized with either buffer only, NCK1895, or LaOVA for once every three days at each boost.

3.2.6: Preparation of Single Cell Suspensions

Two weeks after the last immunization, mice were euthanized via carbon dioxide inhalation and thoracotomy. Tissues collected included the spleen (Sp), mesenteric lymph nodes (MLN), Peyer's patches (PP), large intestine (LI), and female reproductive tract (FRT), as previously described [218, 241]. Briefly, Sp and PP were prepared using a GentleMACS dissociator and filtered through cell strainers to obtain single cell suspensions. The MLNs were isolated and mashed through a cell strainer, washed, and filtered for a

single cell suspension. Mucus and epithelium were removed from LI and FRT and placed in digestion media with agitation for 30 minutes at 37°C. Lymphocytes were isolated using a Percol (GE Healthcare) underlay step, then washed and filtered once more to obtained single cells. Viability and concentration of cells were determined using the Cellometer Auto 2000 Cell Viability Counter (Nexcelom Biosciences). Purity of B cells was determined using flow cytometry. Cells were stained with anti-mouse CD45-FITC, CD19-Pacific Blue, and 7-ADD, and gated based on single cells, live cells, CD45+, and CD19+ to obtain antibody-secreting cell (ASC) populations.

3.2.7: Colorimetric ELISA and ELISpot Assay

An enzyme-linked immunosorbent assay (ELISA) was developed for the detection of OVA-specific murine antibodies from serum, fecal, and vaginal samples. Plates (Maxisorp; Nunc, Rochester, NY) were coated with $OVA_{323-339}$ peptide (AnaSpec, Inc., Fremont, CA) at 1 μg/ml in PBS and incubated overnight at 4°C. Plates were washed five times with PBS containing 0.05% Tween-20 (PBST) and blocked with 1% bovine serum albumin (BSA) in PBS for one hour at room temperature (RT). Plates were washed five times again with PBST. Samples were serially diluted in 1% BSA, 0.1% Kathon in PBS and incubated for 2 hours at RT. Plates were washed five times with PBST and incubated with either anti-mouse IgG (Cell Signaling Technology, 20ng/mL) for serum samples, or IgA (Bethyl Laboratories, 40ng/mL) for vaginal wash and fecal samples. Both anti-mouse IgG and IgA antibodies were conjugated with horseradish peroxidase (HRP) and incubated for 1 hour at RT. Plates were washed four times with PBST and three times with PBS. 3,3',5,5'-Tetramethylbenzidine (TMB) peroxidase (SeraCar, Milford, MA) was filtered with a 40uM syringe-filter and acclimated to RT before adding to each well. The reaction was stopped with an equal volume of 1N sulfuric acid. The absorbance was read with a plate reader (BioTek, Winooski, VT), with both 450nm and 570nm recorded (to remove any background noise with 570nm reading).

IgA secreting cells and OVA-specific IgA secreting cells were quantified using the enzyme-linked immunosorbent spot (ELISpot) assay, similar to what has been described previously [217]. Ninety-six-well

MultiScreenHTS IP filter plates (Millipore Sigma) were treated with 35% ethanol and washed with sterile distilled water. Plates were coated with 15 μg/ml anti-mouse IgA (Mabtech) in PBS and incubated overnight at 4°C. Plates were washed five times with PBS and blocked with CTL medium for 1 hour at 37°C. Cells from single cell suspensions were added in triplicate at a concentration of 2 X 10^5 for OVA-specific detection and 1 X 10^4 for total IgA. Plates were incubated for 20 hours at 37°C. Plates were then washed with PBST six times to remove cells. For total IgA, 1 μg/ml of biotinylated polyclonal goat anti-mouse IgA (Mabtech) in PBS with 1% FBS was added to each well. For OVA-specific IgA, 1 μg/ml of biotinylated $OVA_{323-339}$ peptide (AnaSpec) was used in the same buffer. Plates were incubated for 2 hours at RT and washed six times. Streptavidin conjugated with horseradish peroxidase (HRP) was added to wells in PBS with 1% FBS and incubated for 1 hour at RT. Plates were washed three times with PBST, and three times with PBS. TMB was filtered with 0.44μM filter and added to wells for either two minutes for total IgA or 10 minutes for OVA-specific IgA. Plates were washed with distilled water ten times and air dried. Spots were counted with an ImmunoSpot analyzer (Cellular Technology Limited).

3.2.8: RT-qPCR Cytokine Analysis

Cells collected from MLN and PP at the end of the study were used to analyze mRNA expression of several cytokine targets. Cells were washed with PBS, and the pellet was frozen at -80C until RNA could be extracted. The Quick-RNA Miniprep Kit from Zymo was used to extract RNA according to manufacturer's protocol. RNase Inhibitor (New England Biolabs) was added to extracted RNA for further preservation. RNA was measured via Qubit with reagents for broad-range RNA detection (Thermo Fisher Scientific), and RNA quality was assessed via Tape Station. RNA was then diluted to 5ng/μL and aliquoted. Six genes (aldh1a1, aldh1a2, Tnfsf13 (BAFF), TGF-β, IL-21, and IL-6) and two house-keeping genes (B2M and HPRT) were used in the multiplexed RT-qPCR assay. The SPUD assay was also included to measure any inhibition in samples or between plates [313]. Primer pairs and probes used for each cytokine are reported in Table 3.2. A pooled control was created to ensure consistent results between each PCR plate.

Results were normalized to the B2M and HPRT reference genes for each sample. The $2^{-\Delta\Delta CT}$ Method [314] was used for analysis of relative changes in expression. Control groups included NOD2$^{\Delta DC}$+Buffer and *CD11c*^{cre}+Buffer to avoid bias due to differences in gene expression based on genotype.

Table 3.2. Primer and Probe pair sequences for cytokines used in RT-qPCR.

Gene	Primer Sequences	Probe Sequence
HPRT Exon: 6-7	5'-AAC AAA GTC TGG CCT GTA TCC-3' 5'-CCC CAA AAT GGT TAA GGT TGC-3'	5'-/56-FAM/CTT GCT GGT/ZEN/GAA AAG GAC CTC TCG GAA/3IABkFQ/-3'
B2m Exon: 1-2	5'-GGG TGG AAC TGT GTT ACG TAG-3' 5'-TGG TCT TTC TGG TGC TTG TC-3'	5'-/56-FAM/CCG GAG AAT/ZEN/GGG AAG CCG AAC ATA C/3IABkFQ/-3'
Aldh1a1 Exon: 11-13	5'-ACC CAG TTC TCT TCC ATT TCC-3' 5'-CAT CAC TGT GTC ATC TGC TCT-3'	5'-/56-FAM/ACA CTG CCC/ZEN/AAC AAT TCC TGC TAC T/3IABkFQ/-3'
Aldh1a2 Exon: 8-9	5'-CAC TGG CCT TGG TTG AAG A-3' 5'-GAA GTA ACC TGA AGA GAG TGA CC-3'	5'-/5HEX/AGA TGC TGA/ZEN/CTT GGA CTA CGC TGT G/3IABkFQ/-3'
Tnfsf13b (BAFF) Exon: 6-7	5'-TCA TCT CCT TCT TCC AGC CT-3' 5'-GAC CCT GTT CCG ATG TAT TCA G-3'	5'-/56-FAM/ACA CTG CCC/ZEN/AAC AAT TCC TGC TAC T/3IABkFQ/-3'
IL21 Exon: 1-3	5'-GGT TTG ATG GCT TGA GTT TGG-3' 5'-TGA CTT GGA TCC TGA ACT TCT ATC-3'	5'-/5HEX/TGC TCA CAG/ZEN/TGC CCC TTT ACA TCT T/3IABkFQ/-3'
IL6 Exon: 4-5	5'-TCC TTA GCC ACT CCT TCT GT-3' 5'-AGC CAG AGT CCT TCA GAG A-3'	5'-/56-FAM/AGT TAA CCC/ZEN/ACA CCA CCC CAG C/3IABkFQ/-3'
TGFb1 Exon: 1-2	5'-CCG AAT GTC TGA CGT ATT GAA GA-3' 5'-GCG GAC TAC TAT GCT AAA GAG G-3'	5'-/5HEX/ATA GAT GGCZEN/GTT GTT GCG GTC CA/3IABkFQ/-3'

3.2.9: Statistical Analysis of Immunological Data

ELISA, ELISpot, and cytokine data were analyzed using R version 3.6.1. Since these data were not normally distributed, a Kruskal-Wallis test of analysis of variance was used. Dunn's multiple comparison test was preformed post-hoc, with Benjamini-Hochberg adjustment applied for correction of multiple comparisons. Statistical significance was set to $P < 0.05$ for all data, with adjusted p-values being used. Adjusted P-values for pairwise comparisons from ELISA, ELISpot, and Cytokine data are shown in S3.1, S3.2, S3.3, respectively.

3.2.10: Microbiome Library Preparation

Murine fecal pellets collected from animals were stored at -80C until all samples could be processed. Randomization was used to minimize any batch-bias. Samples were organized into a 96-well plate format, where temporal samples from each animal were all processed on the same plate, and animals from each group were randomized between the four plates. This method of randomization reduces within mouse variability by removing plate-to-plate bias that may contaminate temporal analysis. Each plate received a set of controls, which included no-template controls (NTC) from extractions and PCR to track any possible introduction of contamination. Several microbial community standards (mock communities) from ZymoBIOMICS were used as positive controls to assess DNA extraction efficiency and PCR errors from different microbial taxa. Both the ZymoBIOMICS Gut Microbiome Standard (D6331) and ZYMOBIOMICS Microbial Community standard (D6300) were used as positive controls for DNA extraction, and the ZymoBIOMICS Microbial Community DNA Standard (D6305) was used as a positive control for PCR reactions. DNA was extracted from all samples using the ZymoBIOMICS 96 DNA Kit, utilizing lysis tubes to prevent sample-to-sample contamination during the lysis of cells. Extracted DNA was used to create Illumina library molecules from the hyper variable region 4 (V4) of the 16S rDNA gene as described previously [287]. Dual indexed libraries were purified using magnetic Mag-Bind TotalPure NGS beads (Omega Bio-Tek), and purified libraries were estimated using the AccuBlue dsDNA Quantitation Kit (Biotim). An equimolar amount of each sample combined into one pool and sequenced on an Illumina MiSeq with the v2 500-cycle kit at Colorado State University's Next Generation Sequencing Core Facility (Fort Collins, CO).

3.2.11: Microbiome Data Processing

We used the software fastqc [315] to identify quality of fastq reads from the MiSeq, totaling 28,983,350 demultiplexed reads. The software trimmomatic (version 0.39) was used to filter and trim data. Parameters included a sliding window of four and a cutoff quality of PHRED 20, and a cutoff of 150 base-pairs or longer in order to select for high quality reads for downstream analysis. Filtered data were processed

using mothur [245] (version 1.44.2) with the developers' standard operating procedure (SOP). 9,326,492 reads were used in contig assembly, and further screening lead to 7,947,996 reads with 279,391 being unique. The SILVA database (version 132) was used for alignment and classification, resulting in the discovery of 1351 OTUs. A cutoff for all samples was set to 5000 reads, and the cutoff for individual OTUs was set to ten. OTU0078 (taxonomy) was removed from analysis due to contamination being traced back to the ZymoBIOMICS Gut Microbiome Standard (D6331). Rarefaction curves were generated with the package vegan [248] in R to ensure the depth of coverage for each sample allowed for full discovery of OTUs (Fig. 3.3). Raw reads are available on the National Center for Biotechnology Information's (NCBI) Sequence Read Archive (SRA) under BioProject PRJNA751895.

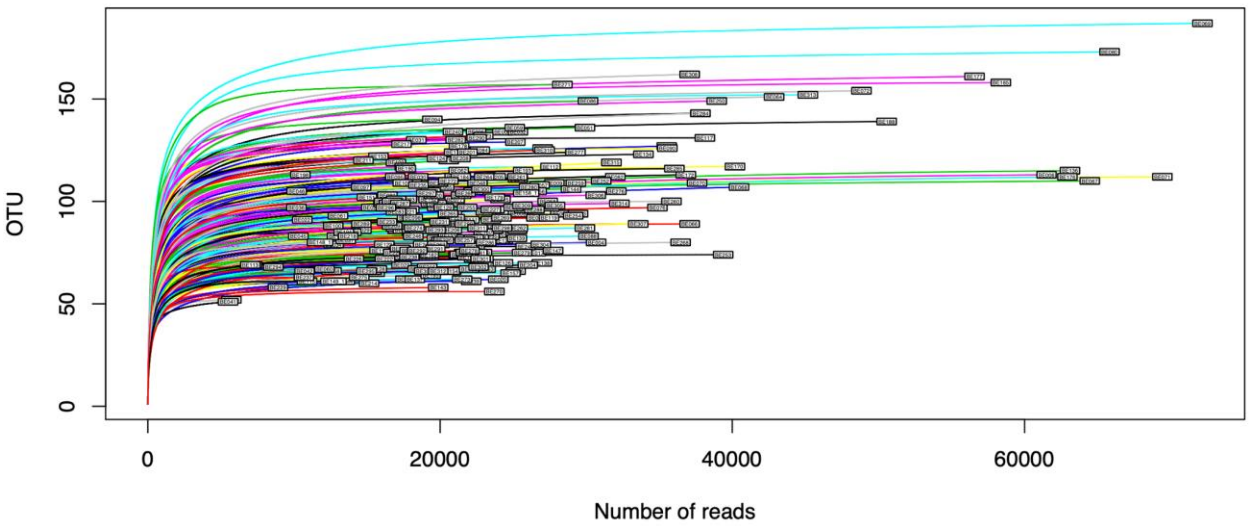

Figure 3.3. Rarefaction curve of OTUs. Samples are each represented by colored lines, with OTU counts per sample on the X-axis and number of reads per sample on the y-axis. Plateauing of lines indicate a lower chance for OTU discovery based on the number of reads.

3.2.12: Alpha Diversity, Beta Diversity, and Random Forest Analysis

Alpha diversity was analyzed using rarified richness and the Shannon diversity index. Briefly, richness was calculated from rarified data with the package vegan [248], and Shannon diversity was estimated using the phyloseq [247] package in R. A linear mixed effects model was used to predict values of richness and Shannon to account for random effects from sampling the same mice over time by using

individual mice as subject-specific random effects and experimental group as the fixed variable. Predicted values were plotted to show the mean and standard error.

Beta diversity was investigated by creating Nonmetric Multidimensional Scaling (NMDS) plots. Data from the OTU level was normalized using Cumulative Sum Scaling [249]. Ordination was performed using the Bray-Curtis dissimilarity from the vegan package and had a stress of 0.129 using 3 dimensions. Plots are shown using 95% confidence ellipsoids for each timepoint or experimental group.

Random Forests [250] was used to find the most influential taxa for separating the microbiome of each experimental group, and the R package randomForest was used [251]. The optimal number of features was determined by iteration with the tuneRF function. The ntreeTry value was set to 200, and the best mtry value was found to be 25. All OTUs, sample timepoint, and processing plate number were included in classification. The features from this analysis were represented by the mean decreasing Gini [252] of the top 10 features, but full classification and Gini coefficient for all features are provided in Supplementary Table S3.1. A homology search was conducted using NCBI's BLAST [316] with the representative fastq sequence of each selected OTU identified from RF.

3.3: Results

3.3.1: NOD2 signaling in CD11c+ cells is required for an OVA-specific humoral response

To investigate the role of NOD2 expression by CD11c+ dendritic cells for the antigen-specific humoral immune responses against LaOVA, longitudinal mucosal and systemic antibody responses against OVA were measured by ELISA. Fecal, serum, and vaginal lavage samples were collected from mice that were gavaged with LaOVA, control *L. acidophilus* strain NCK1895, or dosing buffer alone. These mice either had functional NOD2 ($CD11c^{cre}$) or NOD2 was knocked out in CD11c-expressing cells ($NOD2^{\Delta DC}$). Additional mouse groups included two genotype controls, $NOD2^{fl}$-$CD11c^{cre}$ and $NOD2^{fl/f}$ (Table 1). IgA and IgG OVA-specific antibody responses from each experimental group are shown in Figure 3.4. Optical density readings from week 0 were used to determine the cutoff dilutions for endpoint titers. An early OVA-

specific IgA humoral immune response was seen in fecal samples for all mice harboring functional NOD2 in DCs and vaccinated LaOVA (CD11c^{cre}+LaOVA, NOD2^{fl}-CD11c^{cre}+LaOVA, and NOD2$^{fl/fl}$+LaOVA, Fig. 3.4A). Anti-OVA endpoint titers in these groups were all significantly higher compared to NOD2$^{\Delta DC}$ groups by week 6 (Fig. 3.4A). Additionally, significant levels of fecal anti-OVA IgA were detected in NOD2$^{fl/fl}$+LaOVA mice at week 2 and 4, and CD11c^{cre}+LaOVA had significant levels at week 4 compared to NCK1895 and Buffer groups. Significant production of fecal anti-OVA IgA continued in these three groups throughout the end of the study.

Similarly, serum anti-OVA IgG endpoint titers in the CD11c^{cre}+LaOVA and two genotypic controls receiving LaOVA (NOD2^{fl}-CD11c^{cre}+LaOVA, and NOD2$^{fl/fl}$+LaOVA) all had significant antibody levels starting at week 8 when compared to buffer groups (Fig. 3.4B) and continued through the end of the study. Genotype control group NOD2$^{fl/fl}$+LaOVA also had significantly higher levels of anti-OVA serum IgG after just one dosing series (week 2). Groups CD11c^{cre}+LaOVA and NOD2^{fl}-CD11c^{cre}+LaOVA both showed significantly higher levels of vaginal anti-OVA IgA starting at week 6 (Fig. 3.4C) compared to all other groups. However, group NOD2$^{fl/fl}$+LaOVA did not show significant levels of vaginal anti-OVA IgA and were similar to titers found in the NOD2$^{\Delta DC}$+LaOVA mice (Fig. 3.4C). Conversely, NOD2$^{fl/fl}$+LaOVA had significant levels of anti-OVA antibodies in fecal and serum samples after the first vaccination series compared to buffer groups (Figs 3.4A and 3.4B, week 2). These results show the strong immunogenicity of the LaOVA vaccine construct, and the essential role of NOD2 in mounting an antigen-specific immune response for both IgA and IgG.

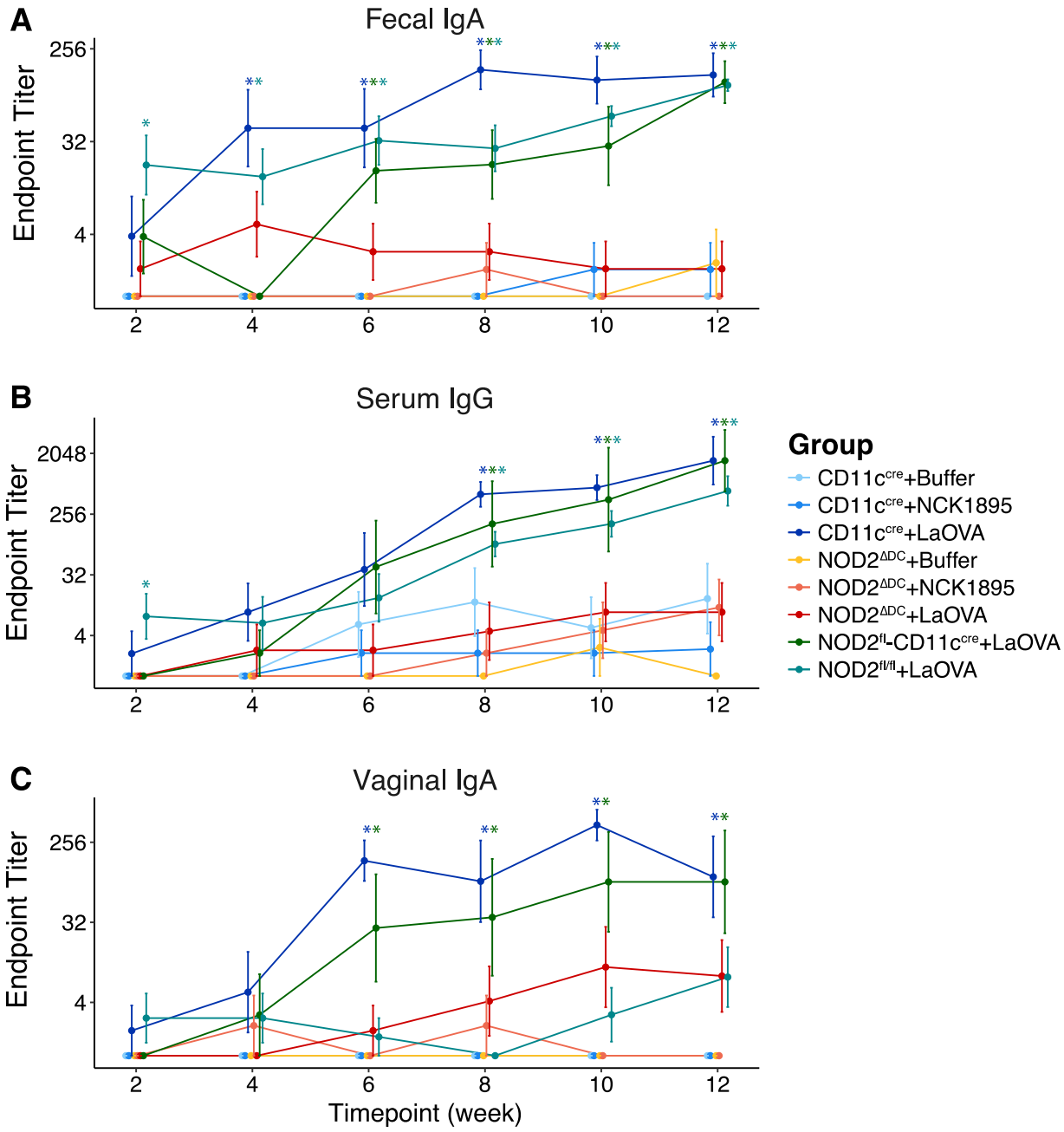

Figure 3.4. OVA-specific IgA and IgG is dependent on NOD2 signaling in CD11c+ cells. $CD11c^{cre}$ and $NOD2^{\Delta DC}$ mice were administered buffer only, NCK1895, or LaOVA, and genotype controls were administered LaOVA. Fecal IgA (A), serum IgG (B), and vaginal IgA (C) were all measured via ELISA with $OVA_{323-339}$ peptide. Data are reported as endpoint titer where cutoff was determined as described in the methods and represented by mean and standard error. P-values for all pairwise comparisons are shown in Supplementary Table S3.2 and adjusted for multiple testing via Benjamini-Hochberg adjustment. For all data asterisk (*) indicates significance ($P < 0.05$) compared to buffer groups, and N = 4-8 mice per group.

Total IgA and OVA-specific antibody secreting cells (ASCs) were determined via ELISpot. Lymphocytes were collected from the female reproductive tract (FRT), large intestine (LI), mesenteric lymph nodes (MLN), Peyer's patches (PP), and spleen (Sp) at sacrifice for both flow cytometry and ELISpot (Fig. 3.5). Flow cytometry gates were used to obtain live B-cell population percentages ($7AAD^{-}$ $CD45^{+}CD19^{+}$), which were used in the calculation of spot forming units (SFU) for total IgA and OVA-specific IgA producing cells. Each tissue that was assessed had a significant higher number of OVA-specific SFU from at least one of the LaOVA dosed groups with functional DC-NOD2 (Fig. 3.5A). Low numbers of OVA-specific SFU were detected in the spleen and FRT tissues of $NOD2^{\Delta DC}$+LaOVA mice but were not significant compared to buffer and NCK1895 groups. (Fig. 3.5A). Levels of total IgA-ASCs were similar between all the groups, with the exception of $NOD2^{fl}$-$CD11c^{cre}$+LaOVA, where both the LI and MLN had significantly higher counts compared to at least one other group (Fig. 3.5B). P-values, adjusted for multiple testing, for each pairwise comparison for both ELISA and ELISpot analyses are shown in Supplementary Tables S3.2 and S3.3. Together, these results highlight the critical role that NOD2 plays specifically in CD11c+ dendritic cells in mounting both mucosal and systemic humoral immune responses against LaOVA.

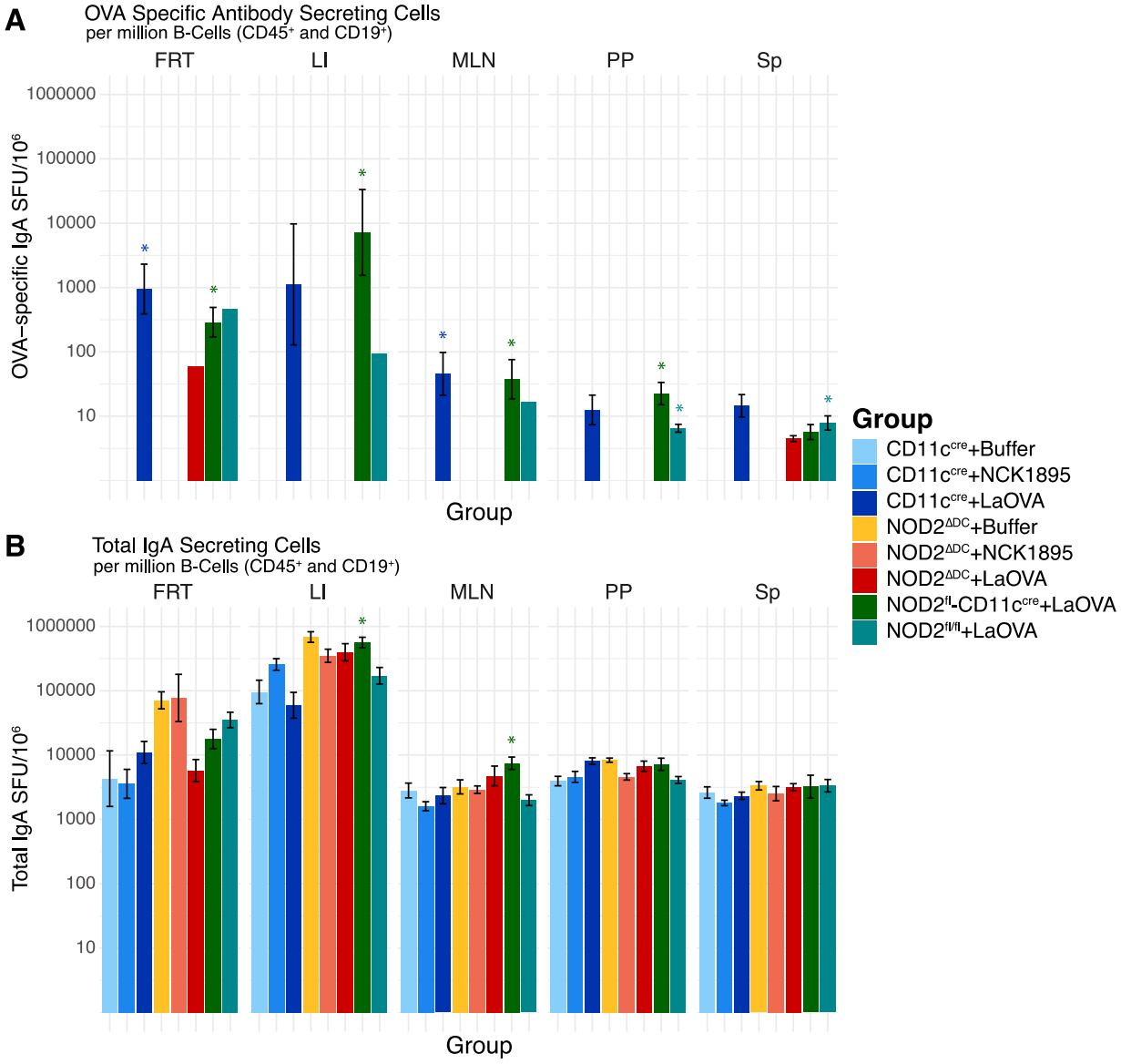

Figure 3.5. NOD2 signaling in CD11c+ cells is required for OVA-specific IgA secreting cells. At sacrifice, lymphocytes from the female reproductive tract (FRT), large intestine (LI), mesenteric lymph nodes (MLN), Peyer's patches (PP), and spleen (Sp) were isolated. Cells from each tissue were applied to OVA-specific (A) and total IgA (B) ELISpots. Data represented as sport forming units (SFU) per million antibody secreting cells (defined as $CD45^+CD19^+7\text{-}AAD^-$) for each group. Data was plotted at mean with standard error, and P-values from pairwise comparisons using Benjamini-Hochberg adjustment for multiple testing are listed in Supplementary Table S3.3. For all data asterisk (*) indicates significance ($P < 0.05$) compared to buffer groups, and N = 4-8 mice per group.

3.3.2: NOD2 Signaling and LaOVA Vaccination Impacts Cytokine Production

Cytokines with importance for IgA class switch and secretion were analyzed from both MLN and PP tissues via RT-qPCR. These cytokines included retinaldehyde dehydrogenase 1 (*aladh1a1*), retinaldehyde dehydrogenase 2 (*aladh1a2*), B-cell-activating factor (*BAFF*, also known as tumor necrosis factor ligand superfamily member 13B (*Tnsf13b*)), *IL-6, IL-21*, and transforming growth factor beta (*TGF-β*). To measure the effects from vaccination, cytokines were measured 18 hours after the final vaccination during week 12. Levels are reported as log change compared with the buffer group from the respective genotype. Significant differences were found between both retinaldehyde dehydrogenase-1 and *TGF-β* in both tissues, as well as *BAFF* in Peyer's patches (Fig. 3.6), indicating these cytokines are impacted by the NOD2 signaling pathway.

Notably, MLN tissues showed significant differences in retinaldehyde dehydrogenase-1 and TGF-β in all groups except between groups with similar genotypes (Fig. 3.6A). Retinaldehyde dehydrogenase-1 levels were elevated in the $NOD2^{\Delta DC}$+LaOVA and slightly in $NOD2^{\Delta DC}$+NCK1895, while levels were significantly decreased in $CD11C^{cre}$+LaOVA and $CD11C^{cre}$+NCK1895 mice. Conversely, levels of *TGF-β* were increased in $CD11C^{cre}$ groups and decreased in $NOD2^{\Delta DC}$ groups in MLN tissues. Similar patterns between the genotypes of mice were seen in *BAFF* and *IL-21* levels but were not significant. PP tissues showed more significant differences based on vaccination strain, but only within the $CD11C^{cre}$ groups (Fig. 3.6B). Levels of retinaldehyde dehydrogenase-1 (*aldh1a1*) were increased in the $CD11C^{cre}$+NCK1895 group and significantly decreased in the $CD11C^{cre}$+LaOVA group relative to each other. Similarly, *TGF-β* levels were significantly increased in the $CD11C^{cre}$+NCK1895 group compared with the decreased levels found in $CD11C^{cre}$+LaOVA and $NOD2^{\Delta DC}$+LaOVA. Significant differences in *BAFF* levels appeared between $CD11C^{cre}$+LaOVA and the increased levels of $NOD2^{\Delta DC}$+LaOVA and $CD11C^{cre}$+NCK1895. $NOD2^{\Delta DC}$+LaOVA and $CD11C^{cre}$+NCK1895 also had significantly different levels of BAFF between each other. The cytokine IL-6 was elevated in both $CD11C^{cre}$+NCK1895 and $CD11C^{cre}$+LaOVA, with levels in $CD11C^{cre}$+NCK1895 being significantly higher than the $NOD2^{\Delta DC}$ groups. Collectively, these results show

the multiple impacts of both inhibition of NOD2-signaling and administration of *L. acidophilus* have on these cytokines with known importance to IgA production.

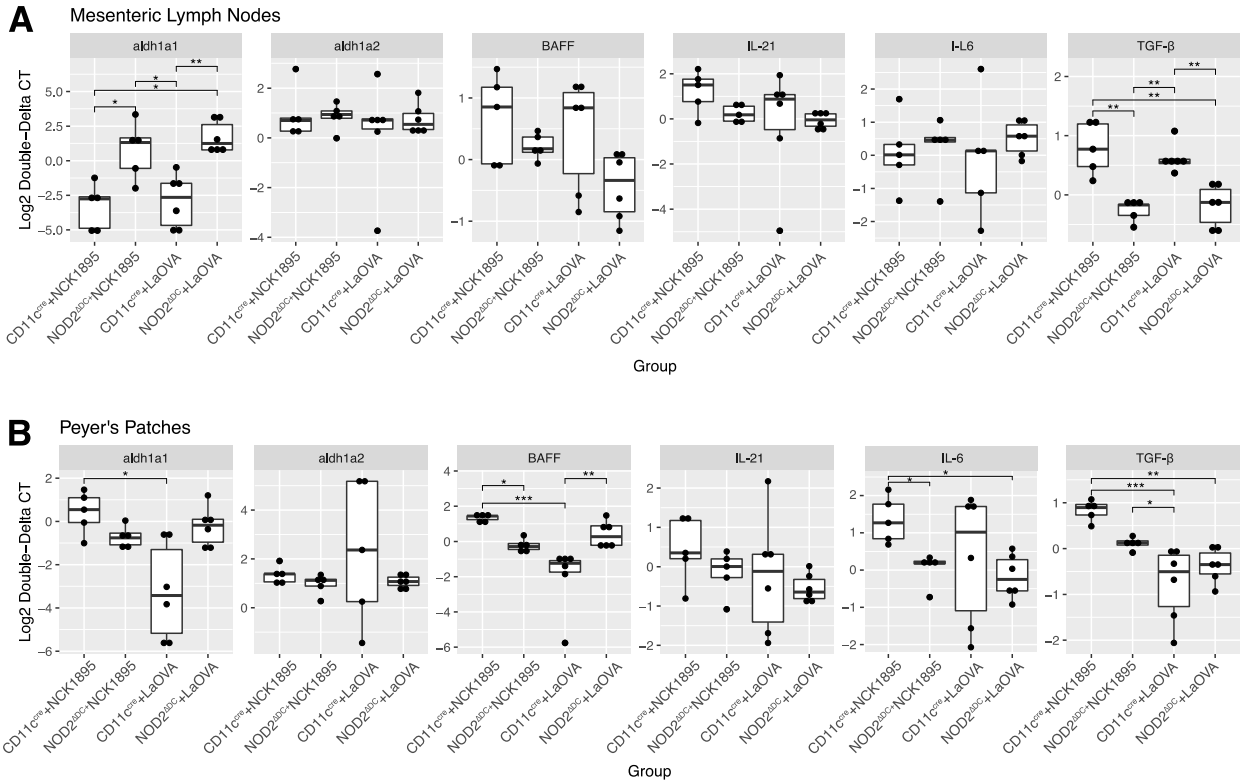

Figure 3.6. Cytokine production following oral vaccination. 18 hours after vaccination, mice were sacrificed and cells from mesenteric lymph nodes (A) and Peyer's patches (B) were saved for analysis of cytokine expression using RT-qPCR. Relative changes in expression were determined using the $2^{-\Delta\Delta CT}$ Method with the buffer group from the respective genotype ($CD11c^{cre}$ or $NOD2^{\Delta DC}$) being used for baseline expression levels. Significance is represented by (*) for ($P < 0.05$), (**) for ($P < 0.01$), and (***) for ($P < 0.001$), as determined by the Kruskal-Wallis test of analysis of variance with Dunn's multiple comparison test and Benjamini-Hochberg adjustment (Supplementary Table S3.4).

3.3.3: NOD2 Signaling Alters Bacterial Microbial Diversity and Composition

Several NOD2 polymorphisms have been directly associated with Crohn's disease [317], and mice with NOD2-deficincies often have an altered microbiota resulting from the lack of maintenance provided by NOD2 [289, 308]. However, the role of NOD2 specifically in dendritic cells in relation to disturbances to the microbiome has yet to be shown. 16S rRNA sequencing of the fecal microbiome was used to better understand this unknown relationship. Predicted values of alpha diversity, as shown by both Shannon index

and richness, appear to be influenced by both NOD2 function and vaccination (Fig. 3.7). Figure 3.7A shows the initial pre-vaccination differences in predicted values of richness at week 0 between the different genotypes. These differences expanded after mice were vaccinated. This was especially apparent at week six, where $NOD2^{\Delta DC}$+LaOVA mice had the highest predicted value of richness and was significantly higher than $NOD2^{\Delta DC}$+Buffer, $CD11C^{cre}$+Buffer, and $CD11C^{cre}$+LaOVA. While $NOD2^{\Delta DC}$ mice generally had higher alpha-diversity, the $NOD2^{\Delta DC}$+Buffer group had the lowest value at week four. A similar trend was observed in Shannon diversity (Fig 3.7B) with values for $NOD2^{\Delta DC}$+Buffer being significantly lower than both $NOD2^{\Delta DC}$+LaOVA and $CD11C^{cre}$+Buffer. Additionally, both predicted richness and Shannon diversity for $NOD2^{\Delta DC}$+LaOVA were significantly higher than $CD11C^{cre}$+LaOVA values after just one round of vaccination (week 2, Fig 3.7A and 3.7B). Notably, the predicted values of both richness and Shannon diversity are very similar for weeks 8-12 with no significant differences between groups, indicating the initial disruption caused by administration of L. acidophilus was resolved by week eight. These results provide initial evidence that innate NOD2 signaling in CD11c+ DCs impacts the alpha-diversity of the bacterial microbiome, but differences due to both NOD2 and repeated administration of L. acidophilus are temporary and were not found past the 6^{th} week.

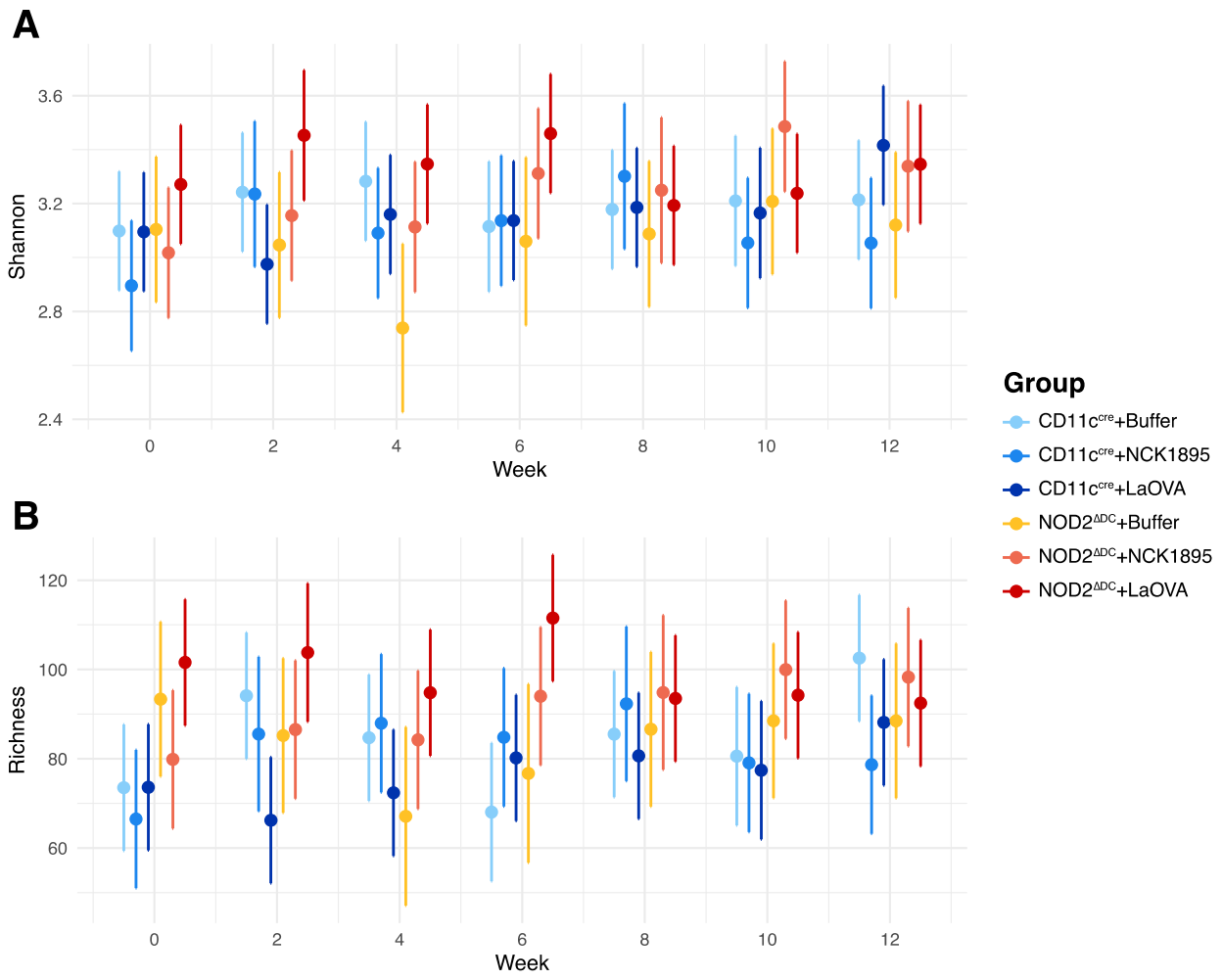

Figure 3.7. Alpha Diversity minimally influenced by vaccination and genotype. Predicted values of Shannon diversity (a) and richness (b) at each timepoint (weeks -2, 0, 2, 4, 6, 8, 10, 12) are represented by the 95% credibility intervals. Linear mixed effects models were used to determine predicted values for each diversity index (Shannon and observed richness).

Figure 3.8 highlights the differences in beta-diversity of the microbiome based on both vaccination and NOD2-genotype. The figure indicates differences in the microbiome between the wild type CD11C^{cre} and the NOD2$^{\Delta DC}$ mice in general, where there is no overlap between the ellipsoids associated with these genotypes at any treatment level (Fig. 3.8A). Response to perturbation due to treatment within the NOD2$^{\Delta DC}$ genotype was different compared to the CD11C^{cre} genotype. The CD11C^{cre} groups separate based on administration of *L. acidophilus*; CD11C^{cre}+LaOVA and CD11C^{cre}+NCK1895 groups are not significantly different from each other but are both significantly different compared to the negative control Buffer group

(Fig. 3.8A). Alternatively, the NOD2$^{\Delta DC}$+LaOVA group is significantly different than both NCK1895 and Buffer NOD2$^{\Delta DC}$ groups. The combined effect of CD11c-NOD2 signaling and LaOVA vaccination on the microbiome is further shown by the 2D NMDS projections (Fig 3.8B and 3.8C). These results highlight the increased susceptibility to disturbances to the microbiome in mice with NOD2$^{\Delta DC}$ from LaOVA vaccination compared to the wild-type CD11C^{cre} mice.

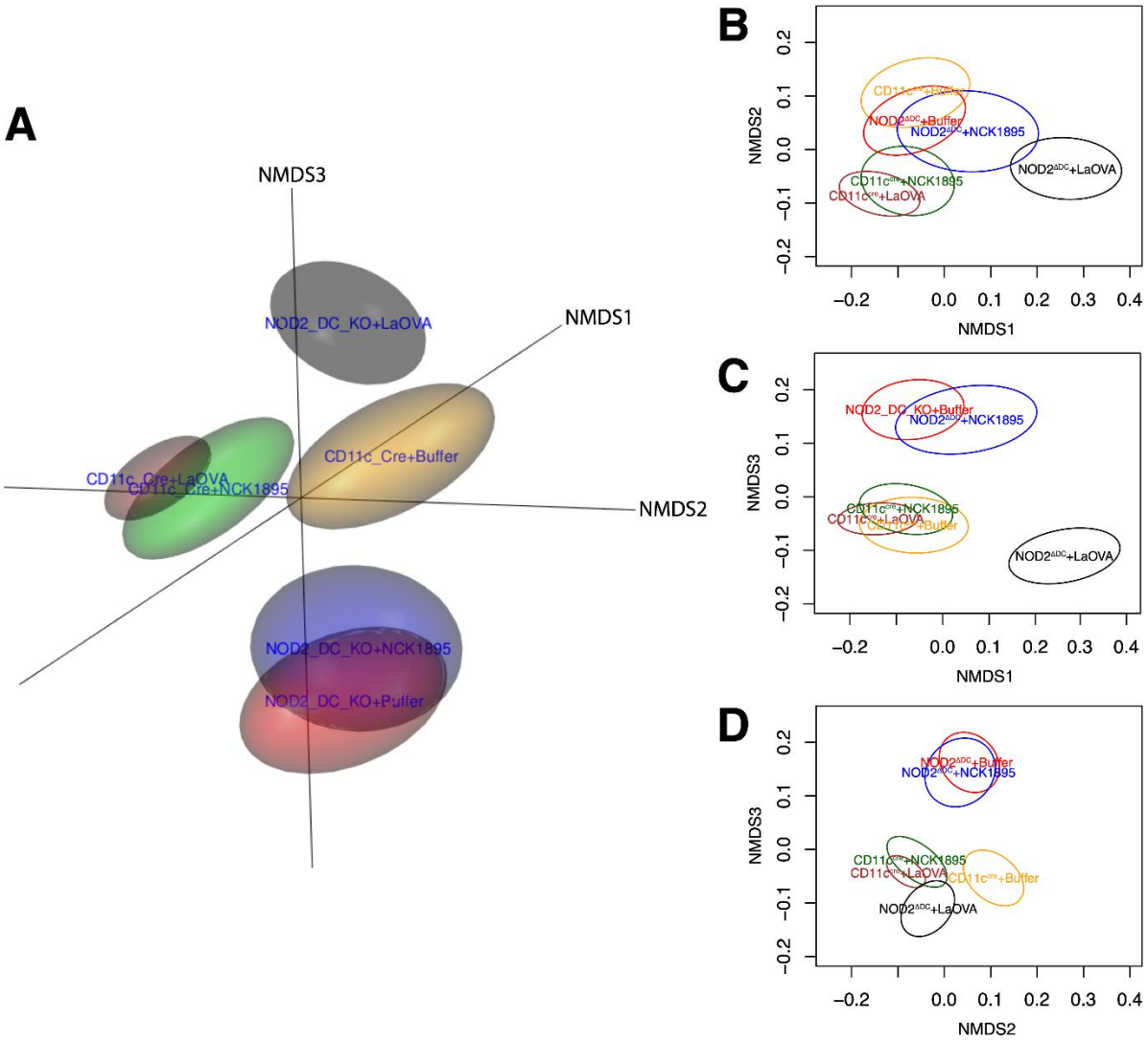

Figure 3.8. Changes to beta-diversity from genotype and *L. acidophilus* administration. Nonmetric multidimensional scaling (NMDS) plots show alterations to the microbiome community structure between groups. (A) The three-dimensional plot represents the three NMDS axis. The two-dimensional projections NMDS1 and NMDS2 are shown in (B), NMDS1 and NMDS3 are shown in (C), and NMDS2 and NMDS3 are shown in (D). Data is represented by the 95% confidence ellipsoids and includes all samples from all timepoint from each experimental group, where non-overlapping groups denotes significance.

To understand the temporal changes in the microbiome after repeated oral boosters of *L. acidophilus*, NMDS plots were generated to show the microbial composition of each group at each timepoint (Fig. 3.9). The 2D projections of the 3D ordination are shown in each column, with NMDS1 and NMDS2 in column 1, NMDS1 and NMDS3 in column 2, and NMDS2 and NMDS3 in column 3. The pre-vaccination microbiome is shown in the first plots (week 0) indicating an overlap between all ellipsoids as expected prior to *L. acidophilus* administration. An immediate alteration after one round of dosing with LaOVA is seen in the week 2 plot by the separation between the $NOD2^{\Delta DC}$+LaOVA and $NOD2^{\Delta DC}$+NCK1895. Differences in microbiome composition were greatest at week 6 with the least amount of overlap between groups occurring at this time point. Separation between the $CD11C^{cre}$ groups and the $NOD2^{\Delta DC}$+Buffer and $NOD2^{\Delta DC}$+NCK1895 animals was most prominent at week 8 and also week 10 for $NOD2^{\Delta DC}$+Buffer mice. The expanded ellipsoids for both the $NOD2^{\Delta DC}$+NCK1895 and $NOD2^{\Delta DC}$+LaOVA groups during week 10 also signifies a greater variance between $NOD2^{\Delta DC}$ animals administered *L. acidophilus*, alluding to NOD2's role in stabilizing the microbiome during vaccination.

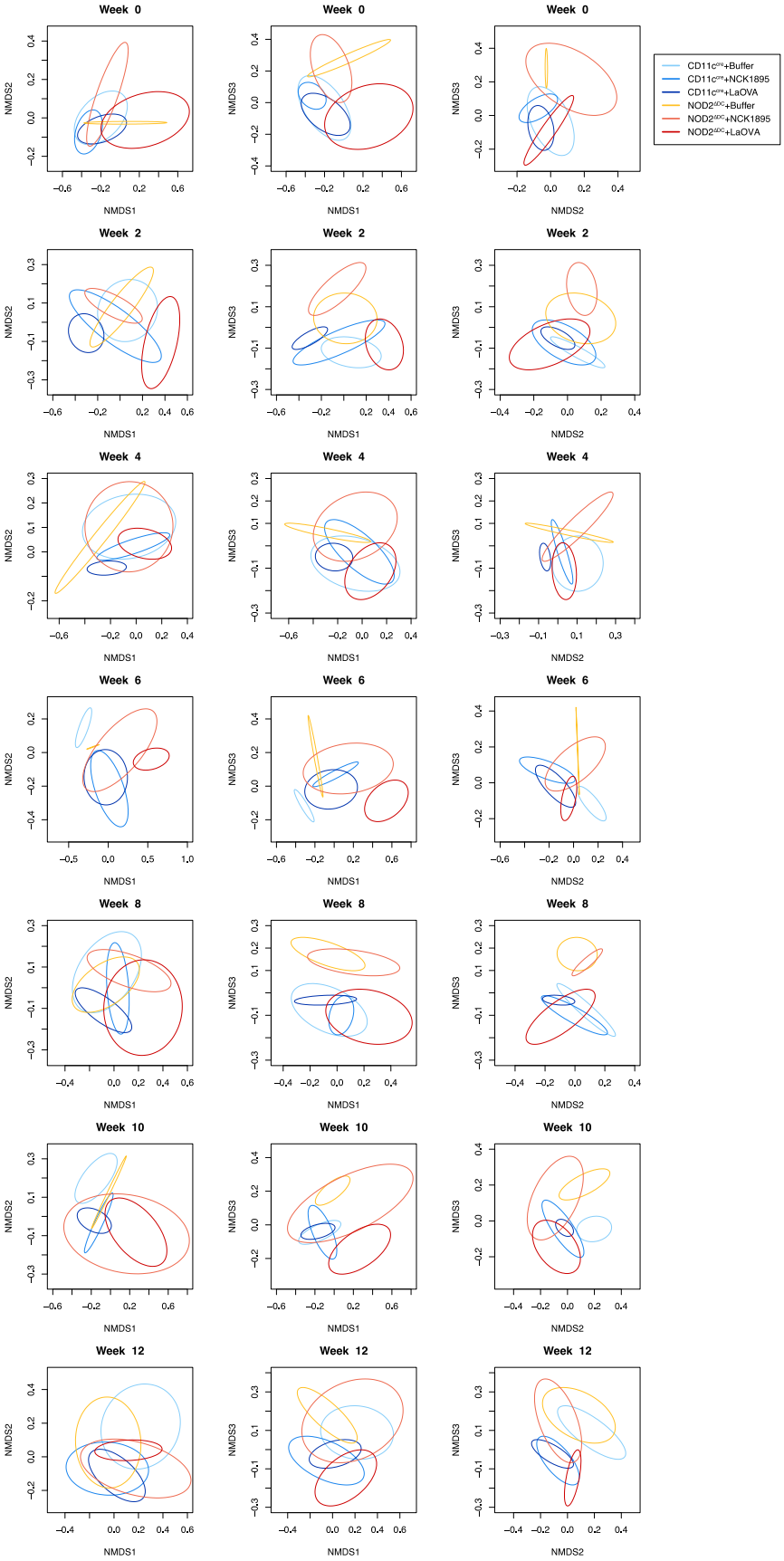
Week 0
Week 0
Week 0
Week 2
Week 2
Week 2
Week 4
Week 4
Week 4
Week 6
Week 6
Week 6
Week 8
Week 8
Week 8
Week 10
Week 10
Week 10
Week 12
Week 12
Week 12
NMDS1
NMDS2
NMDS3
CD11c^cre+Buffer
CD11c^cre+NCK1895
CD11c^cre+LaOVA
NOD2^40C+Buffer
NOD2^40C+NCK1895
NOD2^40C+LaOVA

Figure 3.9. Temporal changes in beta-diversity. NMDS ordinations with data separated into plots for each timepoint (week). The three columns show the projections of NMDS1, NMDS2, and NMDS3, with NMDS1 and NMDS2 in column 1, NMDS1 and NMDS3 in column 2, and NMDS2 and NMDS3 in column 3. Ellipsoids represent the 95% confidence intervals for each group at each timepoint.

Temporal changes within each group can also be seen in Figure 3.10, where NMDS plots show the similarities of the microbiome within each experimental group throughout the study with no indication of a major shift in the microbiome state from the starting point. Week 6 (represented by grey ellipses in each group) again shows the most differences, especially within the $NOD2^{\Delta DC}$+LaOVA and $CD11C^{cre}$+Buffer plots. Between the two genotypes, the microbiome of the $NOD2^{\Delta DC}$ groups appear to be less stable compared to the $CD11C^{cre}$ animals (Fig. 3.10), as indicated by the greater shifts between the centroids of each ellipsoid. Together, these results provide evidence for the critical role of NOD2 signaling on the composition of the intestinal microbiome when a live probiotic is administered.

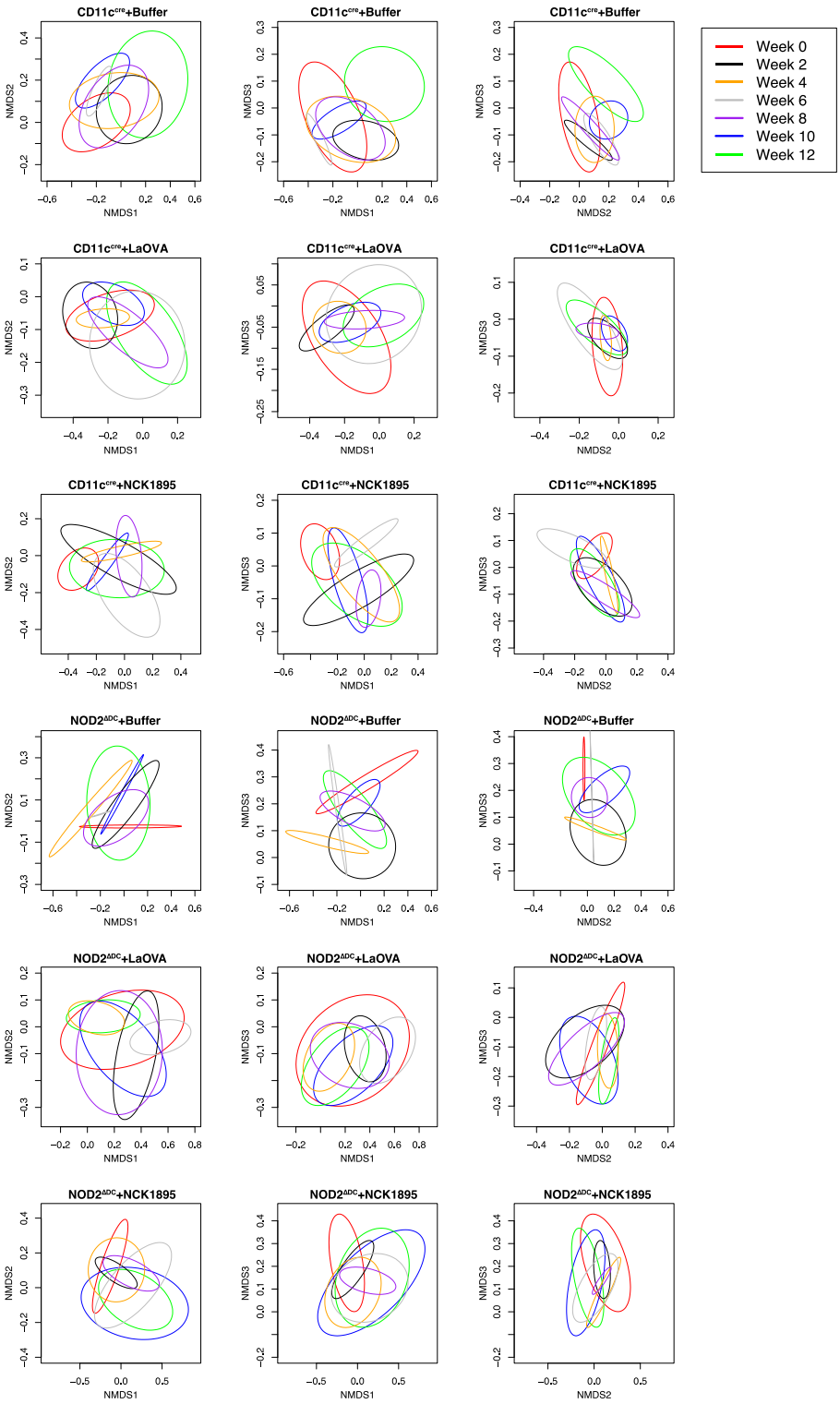

Figure 3.10. Changes in beta-diversity within groups over time. NMDS ordinations with data separated by experimental groups with ellipsoids representing the 95% confidence intervals for each timepoint (week) within that group. The three columns show the projections of NMDS1, NMDS2, and NMDS3, with NMDS1 and NMDS2 in column 1, NMDS1 and NMDS3 in column 2, and NMDS2 and NMDS3 in column 3.

3.3.4: Random Forests Reveals Important Taxa for Classification

To identify taxa that were important for separation of experimental groups (treatment and genotype), the Random Forests [251] (RF) machine learning approach was used. The RF model used the experimental group (Table 3.1) as the target of classification and identified OTU drivers of classification. The confusion matrix shows the respective error rate and classification for each group (Table 3.3). Overall, the RF model had 13.49% out-of-bag (OOB) classification error rate with overall range between 4.88% and 24.24%. The highest per-group error rate belonging to the CD11c^{cre}+NCK1895 group (24.24%) where out of the 33 CD11c^{cre}+ NCK1895 samples, 25 were correctly assigned and 7 were erroneously classified as CD11c^{cre}+ LaOVA, again indicating these two groups had similar microbiomes. This pattern was not observed in the NOD2$^{\Delta DC}$ groups, with misclassification error rates ranging between 4.88% to 15.38%. For all classifications, error rates were minimized by selecting the optimal number of features to use when creating the regression trees for the RF model. The lowest median OOB error was 25 and is shown in Figure 3.11.

Table 3.3. Confusion Matrix from RF model.

Type of Random Forest: classification
Number of trees: 1000
Number of variables tried a teach split: 25
OOB estimate of error rate: 13.49%

	CD11c^{cre}+ Buffer	**CD11c^{cre}+ NCK1895**	**CD11c^{cre}+ LaOVA**	**NOD2$^{\Delta DC}$+ Buffer**	**NOD2$^{\Delta DC}$+ NCK1895**	**NOD2$^{\Delta DC}$+ LaOVA**	**Class error**
CD11c^{cre}+ Buffer	35	0	3	0	1	1	0.125000
CD11c^{cre}+ NCK1895	0	25	7	0	1	0	0.242424
CD11c^{cre}+ LaOVA	2	2	36	0	0	1	0.121951
NOD2$^{\Delta DC}$+ Buffer	0	2	1	22	1	0	0.153846
NOD2$^{\Delta DC}$+ NCK1895	3	1	0	0	29	1	0.147058
NOD2$^{\Delta DC}$+ LaOVA	0	0	2	0	0	39	0.048780

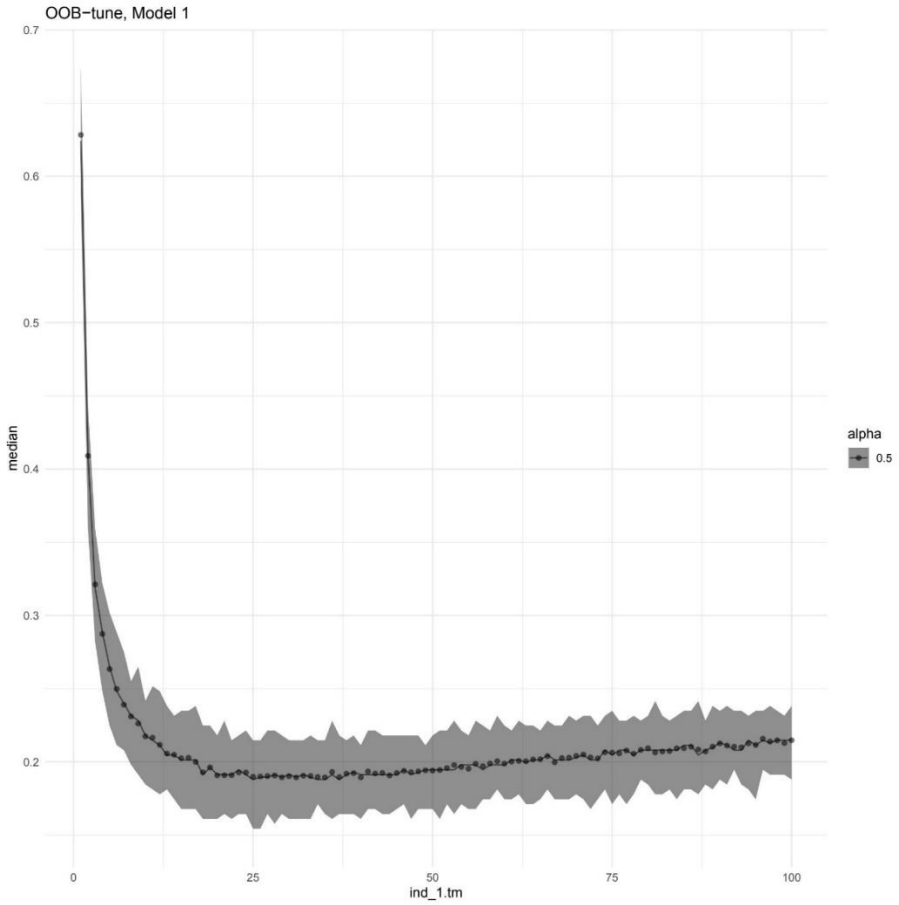

Figure 3.11. Median OOB errors of Random Forests. Out-of-bag (OOB) tuning model shows the error rates (y-axis) while iterating over 100 features (x-axis). The respective feature number with the lowest median error rate was chosen for used in the Random Forest model.

Figure 3.12 identifies the taxa that were classified as most important, represented by the Mean Decreasing Gini (MDG) coefficient. The genus *Muribaculaceae_ge* was recognized as the most important driver, and three additional OTUs in the same genus were amongst the top 10 important taxa. *Odoribacter* was identified as the third most important OTU for classification (Fig. 3.12). The other Bacteroidetes OTU that was identified was OTU0147 and is a member of the *Parabacteroides* genus. Other OTUs identified with the highest MDG include members of the Firmicutes phylum, including *Lachnospiraceae_unclassified*, an uncultured genus in the Lachnospiraceae family, *Ruminococcaceae_ge*,

and *Dubosiella*. The complete list of OTUs with associated MDG coefficient are shown in Supplementary Table S3.1.

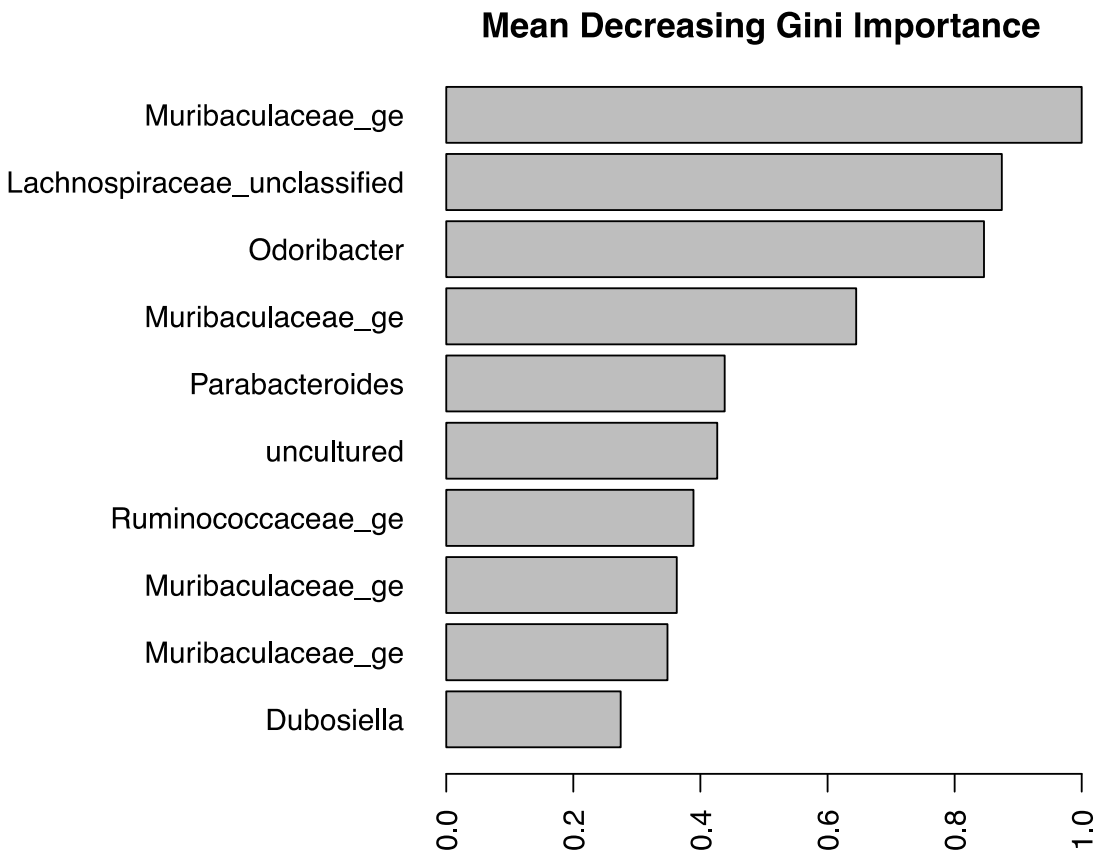

Figure 3.12. Mean Decreasing Gini (MDG) coefficients plot for important OTUs. The top 10 important OTUs, as identified from the Random Forest classification for experimental groups, are displayed by the associated genus and in order of MDG coefficient.

To further understand why these OTUs were highlighted as important in the RF model, the abundances of each OTU were plotted. Figure 3.13 displays the relative abundances within each experimental group for the top 10 OTUs that were identified by the RF model in order of MDG. The phylum and genus of each OTU are displayed above the individual plots. Two Firmicute members, OTU0104 (*Ruminococcaceae_ge*) and OTU0072 (uncultured genus in the Lachnospiraceae family) had higher abundances within the NOD2$^{\Delta DC}$ groups. Each of the four OTUs identified within the *Muribaculaceae_ge*

genus were all highly abundant in the NOD2$^{\Delta DC}$+LaOVA group. The only Bacteroidetes shown that was not highly abundant within the NOD2$^{\Delta DC}$+LaOVA group was OTU0147, which belonged to the *Parabacteroides* genus. A NCBI BLASTN search using consensus fastq files from these OTUs was conducted to obtain further taxonomic classifications. OTU0063 aligned with the *Culturomica* sp., a bacterium that has recently been isolated from the human gut. The strain of *Culturomica massiliensis* was 91% similar to *Odoribacter laneus*, allowing its new genus classification. OTU0147, originally classified in the Parabacteroides genus, was further identified as a *P. goldsteinii* species. Collectively, these RF results show that the composition of the microbiome was highly influenced by both the genotype and treatment, as indicated by the low error rates between all experimental groups. Additionally, the *Muribaculaceae* genus was responsible for many of the correct classifications, due to many OTUs with a high MDG coefficient (Supplementary Table S3.1).

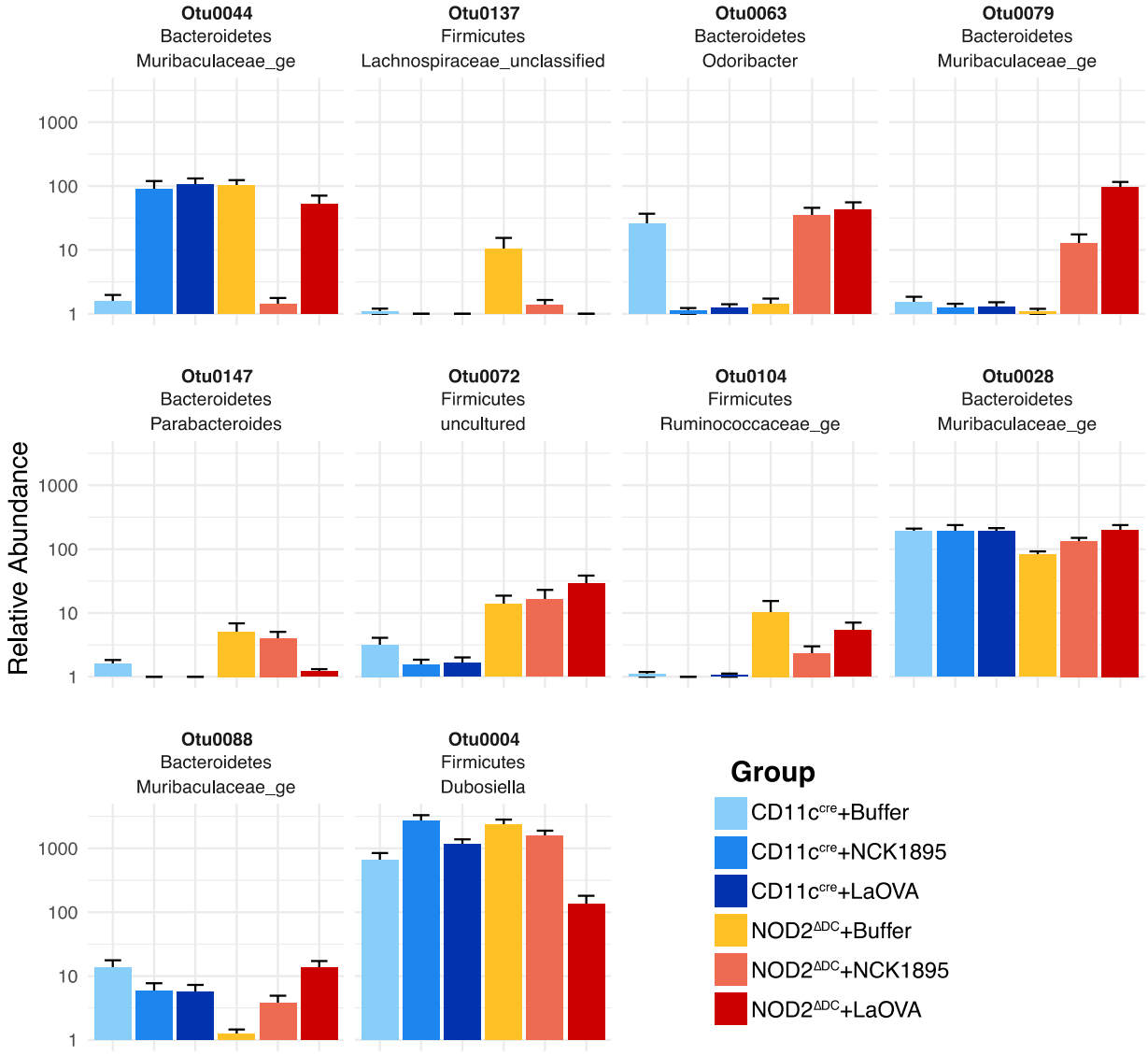

Figure 3.13. Relative abundance of important taxa. The relative abundances of the top ten important taxa identified in the Random Forest classification are shown. The phylum and genus classification for each OTU is also displayed.

3.4: Discussion

NOD2-signalling, specifically in CD11c+ cells, was assessed to understand NOD2's role in mounting an antigen-specific humoral immune response against our recombinant *Lactobacillus acidophilus* vaccine platform. Using mice with a CD11c-specific NOD2 knockout, we demonstrated that NOD2 signaling in CD11c+ phagocytic cells is required for the stimulation of the OVA-specific humoral immune

response both in the mucosa and systemically, based on antibody responses from mucosal sites and serum and OVA-specific IgA secreting cells (Fig. 3.4 and Fig. 3.5). Cytokine profiles provided additional support for the role of NOD2 in the humoral response to rLA, as several important cytokines for IgA-class switching were not upregulated in CD11c-NOD2 deficient mice ($NOD2^{\Delta DC}$ groups, Fig. 3.5). The results presented here also indicated that NOD2 plays an important role in the maintenance of the microbiome in response to administration of a live probiotic. All experimental groups were identified with relatively high accuracy with RF, indicating that genotype and *L. acidophilus* administration both influence the microbiome composition. Importantly, the microbiome composition was primary separated based on genotype, and secondarily based on administration of either LaOVA or NCK1895 (Fig. 3.8).

Signaling from innate pattern recognition receptors is critical for mounting an adaptive immune response and NOD2 has long been exploited by Freud's adjuvant containing MDP from Mycobacterium [318]. More recently, novel adjuvants and muramyl peptide derivatives targeting NOD2 have shown great potential at further increasing the immunogenicity of current vaccine constructs including BCG, the nanoparticulate HIV-1 p24 vaccine, and the influenza subunit vaccine, among others [298, 319, 320]. Since it is also known that the structure of MDP can result in varying stimulation of NOD2 based on its acylation, we previously demonstrated that *L. acidophilus* was capable of activating NOD2 *in vitro* [218]. That study also recognized NOD2 as a key factor in the humoral immune response against rLA *in vivo*, but specific cell types remained unidentified. Here, we provided evidence that NOD2 signaling specifically in CD11c+ phagocytic cells, such as dendritic cells, is critical for the humoral immune response against LaOVA.

NOD2 played a role in both the mucosal immune response and trafficking to the systemic immune system throughout vaccination with LaOVA (Fig. 3.4 and 3.5). Furthermore, cytokine responses corroborated the absence of a humoral immune response in $NOD2^{\Delta DC}$ groups (Fig. 3.6). TGF-β plays a dual role in regulating the survival and proliferation of B-cells by inducing apoptosis and growth arrest, and promoting the production of IgA through IgA class switching [321]. The increase of this cytokine in the MLN of $CD11C^{cre}$ mice administered strains of *L. acidophilus* (LaOVA and NCK1895), in results presented

here, indicates the humoral immune response is coordinated through TGF-β signaling while promoting the production of OVA-specific IgA. The low levels of *TGF-β* in both the MLN and PP of NOD2$^{\Delta DC}$ animals further confirms that deficient NOD2 signaling in CD11c+ DCs inhibits the humoral immune response that would be controlled by TGF-β signaling. However, results from the Peyer's patches were less definitive, with the exception of IL-6. This cytokine has previously been shown to be an important regulator of IgA production in response to the LAB *Pediococcus acidilactici* K15 [322], and data shown here indicate *L. acidophilus* is also a potent inducer of IL-6 in PPs. The lack of *IL-6* production in NOD2$^{\Delta DC}$ groups also provides insight into the downstream effects of NOD2 signaling in CD11c+ DCs in response to the commensal microbiota.

NOD2 is of particular interest in relation to inflammatory bowel diseases, especially Crohn's disease (CD). Although the specific etiology of CD is still unknown and likely multifactorial, meta analyses of CD-cohorts have revealed that specific mutations in *NOD2* are strongly associated with CD onset, with the majority being ileal CD, as well as other inflammatory bowel diseases [300, 301, 323–325]. One characteristic of CD is a shift in the composition of the microbiome, usually with an increase in pro-inflammatory *Proteobacteria* species [326]. The resulting dysbiosis connected to NOD2 was thought to be related to a decrease in antimicrobial peptide production from Paneth cells, and thus assumed to be a result of NOD2 mutations in nonhematopoietic cells [327]. However, results presented here demonstrate that NOD2 signaling in antigen presenting cells of hematopoietic origin (CD11c+) also play a critical role in maintaining the composition of the baseline microbiome, specifically shown by the separation of the microbiome composition between NOD2$^{\Delta DC}$ and CD11c^{cre} mice belonging to the same treatment group (Fig. 3.8). Furthermore, the vast separation of NOD2$^{\Delta DC}$+LaOVA compared to NOD2$^{\Delta DC}$+NCK1895 and NOD2$^{\Delta DC}$+Buffer in Figure 3.8 indicates that NOD2 signaling in CD11c+ is required to prevent a shift in community structure during an innate immune response associated with LaOVA. The lack of anti-OVA antibodies in NOD2$^{\Delta DC}$ suggests only an innate response was initiated during vaccination, and LaOVA vaccination was enough to alter the microbiome without regulation from NOD2-signaling. Conversely, the

similarities between the CD11c^{cre} mice administered LaOVA or NCK1895 suggests the impact on the microbiome by these strains were comparably regulated by NOD2 signaling. Figure 3.9 showed that these two groups had similar microbiome compositions throughout the study with the exception of week 4.

Results from Random Forest indicated several taxa were instrumental in classifying experimental groups correctly, with many taxa belonging to the *Muribaculaceae* genus. In addition to *Muribaculaceae,* other Bacteroidetes genera with high MDG coefficients included *Odoribacter* and *Parabacteroides*. All of these genera are common commensals of the mammalian gut microbiome, with decreased abundances of *Odoribacter* specifically being linked to inflammatory bowel disease (IBD) [328]. Recent results have shown that *Muribaculaceae* is negatively correlated with inflammation within the colitis mouse model [329]. Although this genus was often abundant in the NOD2$^{\Delta DC}$ groups, the species and strain differences within this and many other genera should be considered. For this reason, an NCBI BLAST search was conducted to further classify important OTUs to either the species or strain level. OTU147 was aligned with *Parabacteroides goldsteinii*, which has been shown to reduce obesity in mice fed a high-fat diet [330]. Additionally, OTU063 aligned to *Culturomica* sp, a newly isolated bacterium from the human gut [331] and is phylogenetically close to *Odoribacter* (which OTU063 was classified as based on our alignment). However, the function of this species remains unknown.

3.5: Conclusion

Taken together, results presented here show that humoral immune induction by the rLA platform is restricted to the NOD2 pathway with no evidence of redundancy through other innate immune pathways. This is in contrast to bacterial pathogens such as Salmonella, where a robust immune response was achieved with both MYD88/TRIF and Caspase-1/-11 deficient mice [332]. Further studies are needed to identify compartments of the microbiome that may be disproportionately affected by a disfunction in NOD2 along the gastrointestinal tract, especially within the smaller intestine where NOD2 is thought to be most active [300, 308]. Additional experiments utilizing germ-free mice with NOD2 deficiencies would aid in the

understanding of NOD2's reciprocal influence on inflammation within the gut and how *L. acidophilus* and rLA may serve to reduce this inflammation associated with IBD caused by NOD2 mutations [333]. Future mucosal vaccine development will require targeting critical immune pathways in conjunction with nutritional priming of the gastrointestinal tract to achieve high efficacy globally.

CHAPTER 4: Summary and Future Directions

4.1: Concluding Remarks

The mucosal immune system has developed a dynamic and unique relationship with the microbes that inhabit nearly every cavity of the body. Details of this relationship are still being uncovered, but the mounting body of literature supports a crucial role of the microbiota in health and disease. Therefore, any vaccine that may be widely distributed must be thoroughly examined for any immediate and long-lasting impacts that may disturb the microbiome. In this dissertation, we provided evidence that utilizing recombinant *Lactobacillus acidophilus* (rLA) as vaccine platform does not lead to lasting off-target effects on the microbiome while inducing humoral immunity.

In Chapter 2, we evaluated effects of repeated administration of rLA and the rice bran diet on the microbiome. We found diet had a primary impact on shifts in the bacterial community structure. Utilizing IgA-seq, we were able to distinguish how diet impacted the IgA-bound and unbound fractions of the microbiome. We showed that the 10% rice bran diet mainly altered the IgA-bound bacterial community and not the IgA-negative fraction. Second to diet, administration of *L. acidophilus* also led to changes in beta-diversity of the fecal microbiome. Importantly, our vaccine construct (LA expressing MPER and secreting murine IL-1β) had similar intermediate effects on the microbiome when compared to the wild-type strain. Diets that include probiotics, either through supplements or fermented foods, are known to cause beneficial alterations in the intestinal microbiome, so expression of exogenous antigens by rLA does not seem to cause any additional changes.

Further analysis provided by Random Forests classifications and Spearman's correlation revealed that the *Lachnospiraceae* family may by highly important for immune induction. Although findings are often strain dependent, many members of the *Lachnospiraceae* family and the *Erysipelatoclostridium* genus have been associated with intestinal inflammation, obesity, and diabetes. We hypothesize that these taxa may be providing additional adjuvant activity during rLA vaccination. However, Spearman's correlation noted both positive and negative correlations between *Lachnospiraceae* abundance and MPER-specific IgA

production. Therefore, over-inflammation of the mucosal immune system by certain commensal adjuvants may contribute to a suppressed immune response towards rLA.

In this study, we also evaluated how the inclusion of prebiotic rice bran may impact the kinetics of the humoral mucosal immune response during rLA vaccination. Previous studies have provided evidence for rice bran's unique ability to increase levels of *Lactobacillus* and total IgA in fecal fractions [238]. Our results showed that a 10% rice bran diet leads to an accelerated induction of antigen-specific antibodies in fecal and serum samples. Collectively, these results justify continued investigations into rice bran's ability to increase vaccine efficacy in models of enteric inflammation.

In Chapter 3, we aimed to better understand how NOD2 signaling contributes to the adaptive immune response to rLA. Previously, NOD2 signaling was identified as a critical innate immune pathway for an adaptive immune response against rLA, but the specific cell type involved in NOD2 signaling was unknown [218]. In this dissertation, we showed that CD11c+ cells are critical for NOD2 signaling in response to LaOVA vaccination. Mice deficient in NOD2 signaling only in CD11c+ cells ($NOD2^{\Delta DC}$) did not mount a humoral immune response to LaOVA, as shown by the lack of OVA-specific IgA and IgG from fecal, serum, and vaginal samples, and OVA-specific antibody secreting cells from tissues.

Longitudinal changes in microbiome profiles from $NOD2^{\Delta DC}$ and control mice also revealed that NOD2 has a notable impact on the composition of the microbiome. Beta-diversity analysis revealed experimental groups primarily separated based on genotype, and secondly by administration of *L. acidophilus*. Furthermore, the greater separation of bacterial communities between $NOD2^{\Delta DC}$ mice administered LaOVA, *L. acidophilus*, and an empty buffer control compared to control mice with the same treatments suggests that expression of NOD2 in antigen presenting cells plays primary role in responding to perturbations from *Lactobacillus* administration.

Collectively, these results demonstrate that rLA is capable of eliciting a humoral immune response within mucosal and systemic systems, thus protecting against proliferation and damage at mucosal tissues, and against systemic spread. In addition to induction of the immune system, rLA provides inherent benefits

common to probiotics. This dual function of rLA could be critical in eliciting protective immunity in individuals with an inflammatory state within the mucosa. Logistically, rLA is safer (needleless) and easier to distribute to rural populations, making its use in pandemic situations highly desirable. These results also suggested there are no major perturbations to the microbiome by rLA, but further studies are needed to identify possible transcriptional changes to the microbiome during rLA vaccination.

4.2: Future Directions

Future studies using rLA or other LAB as vaccine platforms should continue to investigate reciprocal impacts on the gastrointestinal microbiome. Here, we have evaluated influences to the fecal microbiome during the course of vaccination, but administration of wild-type *L. acidophilus,* or other LAB with similar epitopes, several weeks or months following rLA vaccination, have not been assessed for possible pro-inflammatory responses. Additionally, studies presented here were performed using healthy mice without any known prior exposure to *L. acidophilus*. Therefore, it would be important to confirm rLA's immunogenicity following wild-type *L. acidophilus* administration to ensure this would not induce tolerance to rLA.

The use of healthy mice in the above studies also limited our understanding of rLA's immunogenicity and impact on the microbiome. The use of animals with altered microbiota and mucosal environments that represent the proinflammatory conditions found in individuals with environmental enteric dysfunction (EED) would provide valuable insight into rLAs "real-world" application. This EED model would also reveal the full potential of rLA and rice bran to enhance vaccine efficacy in low-income countries. Subsequent challenge studies in animals susceptible to infection by the pathogen target of rLA are also critically needed to gauge the biological protection offered by rLA.

Finally, an in-depth look into the anatomical changes, i.e. within the large and small intestine, to the microbiome and metatranscriptome following rLA vaccination are also needed. Here, we showed that the IgA-coated and whole fecal microbiome were able to return to a pre-vaccination state within the 12-week study period. However, immediate changes to the transcriptional profiles of the commensal

microbiota with close proximity to sites of immune induction are lacking. From a safety perspective, a wholistic understanding the rLA vaccine platform on the microbiome and other metrics of immune induction are needed before it can be used clinically.

REFERENCES

1. Turnbaugh PJ, Ley RE, Hamady M, Fraser-Liggett CM, Knight R, Gordon JI. The Human Microbiome Project. Nature. 2007;449:804–10.

2. Martinez FD. The human microbiome. Early life determinant of health outcomes. Ann Am Thorac Soc. 2014;11 Suppl 1:S7-12.

3. The Integrative HMP (iHMP) Research Network Consortium. The Integrative Human Microbiome Project. Nature. 2019;569:641–8.

4. Yang I, Edwards S, Dunlop A, Hertzberg VS. The Microbiome in Health and Disease. In: Systems Medicine. Elsevier; 2021. p. 232–46. doi:10.1016/B978-0-12-801238-3.11462-X.

5. Arumugam M, Raes J, Pelletier E, Le Paslier D, Yamada T, Mende DR, et al. Enterotypes of the human gut microbiome. Nature. 2011;473:174–80.

6. Shao X, Ding X, Wang B, Li L, An X, Yao Q, et al. Antibiotic Exposure in Early Life Increases Risk of Childhood Obesity: A Systematic Review and Meta-Analysis. Front Endocrinol. 2017;8:170.

7. Tanaka M, Nakayama J. Development of the gut microbiota in infancy and its impact on health in later life. Allergol Int. 2017;66:515–22.

8. Fox GE, Magrum LJ, Balch WE, Wolfe RS, Woese CR. Classification of methanogenic bacteria by 16S ribosomal RNA characterization. Proc Natl Acad Sci. 1977;74:4537–41.

9. Rappé MS, Giovannoni SJ. The Uncultured Microbial Majority. Annu Rev Microbiol. 2003;57:369–94.

10. Sims D, Sudbery I, Ilott NE, Heger A, Ponting CP. Sequencing depth and coverage: key considerations in genomic analyses. Nat Rev Genet. 2014;15:121–32.

11. Gotschlich EC, Colbert RA, Gill T. Methods in microbiome research: Past, present, and future. Best Pract Res Clin Rheumatol. 2019;33:101498.

12. Youssef N, Sheik CS, Krumholz LR, Najar FZ, Roe BA, Elshahed MS. Comparison of Species Richness Estimates Obtained Using Nearly Complete Fragments and Simulated Pyrosequencing-Generated Fragments in 16S rRNA Gene-Based Environmental Surveys. Appl Environ Microbiol. 2009;75:5227–36.

13. Aird D, Ross MG, Chen W-S, Danielsson M, Fennell T, Russ C, et al. Analyzing and minimizing PCR amplification bias in Illumina sequencing libraries. Genome Biol. 2011;12:R18.

14. Sinclair L, Osman OA, Bertilsson S, Eiler A. Microbial Community Composition and Diversity via 16S rRNA Gene Amplicons: Evaluating the Illumina Platform. PLOS ONE. 2015;10:e0116955.

15. Kim M, Morrison M, Yu Z. Evaluation of different partial 16S rRNA gene sequence regions for phylogenetic analysis of microbiomes. J Microbiol Methods. 2011;84:81–7.

16. Tanca A, Palomba A, Fraumene C, Pagnozzi D, Manghina V, Deligios M, et al. The impact of sequence database choice on metaproteomic results in gut microbiota studies. Microbiome. 2016;4:51.

17. Poretsky R, Rodriguez-R LM, Luo C, Tsementzi D, Konstantinidis KT. Strengths and Limitations of 16S rRNA Gene Amplicon Sequencing in Revealing Temporal Microbial Community Dynamics. PLoS ONE. 2014;9:e93827.

18. Petersen LM, Martin IW, Moschetti WE, Kershaw CM, Tsongalis GJ. Third-Generation Sequencing in the Clinical Laboratory: Exploring the Advantages and Challenges of Nanopore Sequencing. J Clin Microbiol. 2019;58. doi:10.1128/JCM.01315-19.

19. Chiu CY, Miller SA. Clinical metagenomics. Nat Rev Genet. 2019;20:341–55.

20. Ciuffreda L, Rodríguez-Pérez H, Flores C. Nanopore sequencing and its application to the study of microbial communities. Comput Struct Biotechnol J. 2021;19:1497–511.

21. Singh RK, Chang H-W, Yan D, Lee KM, Ucmak D, Wong K, et al. Influence of diet on the gut microbiome and implications for human health. J Transl Med. 2017;15:73.

22. Ramirez J, Guarner F, Bustos Fernandez L, Maruy A, Sdepanian VL, Cohen H. Antibiotics as Major Disruptors of Gut Microbiota. Front Cell Infect Microbiol. 2020;10:572912.

23. Alkanani AK, Hara N, Gottlieb PA, Ir D, Robertson CE, Wagner BD, et al. Alterations in Intestinal Microbiota Correlate With Susceptibility to Type 1 Diabetes. Diabetes. 2015;64:3510–20.

24. Berer K, Mues M, Koutrolos M, Rasbi ZA, Boziki M, Johner C, et al. Commensal microbiota and myelin autoantigen cooperate to trigger autoimmune demyelination. Nature. 2011;479:538–41.

25. Kostic AD, Xavier RJ, Gevers D. The Microbiome in Inflammatory Bowel Disease: Current Status and the Future Ahead. Gastroenterology. 2014;146:1489–99.

26. Petersen C, Round JL. Defining dysbiosis and its influence on host immunity and disease. Cell Microbiol. 2014;16:1024–33.

27. Benakis C, Brea D, Caballero S, Faraco G, Moore J, Murphy M, et al. Commensal microbiota affects ischemic stroke outcome by regulating intestinal γδ T cells. Nat Med. 2016;22:516–23.

28. DeGruttola AK, Low D, Mizoguchi A, Mizoguchi E. Current Understanding of Dysbiosis in Disease in Human and Animal Models: Inflamm Bowel Dis. 2016;22:1137–50.

29. Schulz MD, Atay Ç, Heringer J, Romrig FK, Schwitalla S, Aydin B, et al. High-fat-diet-mediated dysbiosis promotes intestinal carcinogenesis independently of obesity. Nature. 2014;514:508–12.

30. Zhang X, Li L, Butcher J, Stintzi A, Figeys D. Advancing functional and translational microbiome research using meta-omics approaches. Microbiome. 2019;7:154.

31. Pérez-Cobas AE, Gosalbes MJ, Friedrichs A, Knecht H, Artacho A, Eismann K, et al. Gut microbiota disturbance during antibiotic therapy: a multi-omic approach. Gut. 2013;62:1591–601.

32. Dudek-Wicher RK, Junka A, Bartoszewicz M. The influence of antibiotics and dietary components on gut microbiota. Gastroenterol Rev. 2018;13:85–92.

33. Bokulich NA, Chung J, Battaglia T, Henderson N, Jay M, Li H, et al. Antibiotics, birth mode, and diet shape microbiome maturation during early life. Sci Transl Med. 2016;8:343ra82-343ra82.

34. Guo X, Li J, Tang R, Zhang G, Zeng H, Wood RJ, et al. High Fat Diet Alters Gut Microbiota and the Expression of Paneth Cell-Antimicrobial Peptides Preceding Changes of Circulating Inflammatory Cytokines. Mediators Inflamm. 2017;2017:1–9.

35. Turnbaugh PJ, Ridaura VK, Faith JJ, Rey FE, Knight R, Gordon JI. The Effect of Diet on the Human Gut Microbiome: A Metagenomic Analysis in Humanized Gnotobiotic Mice. Sci Transl Med. 2009;1:6ra14-6ra14.

36. Araújo JR, Tomas J, Brenner C, Sansonetti PJ. Impact of high-fat diet on the intestinal microbiota and small intestinal physiology before and after the onset of obesity. Biochimie. 2017;141:97–106.

37. Wang B, Kong Q, Li X, Zhao J, Zhang H, Chen W, et al. A High-Fat Diet Increases Gut Microbiota Biodiversity and Energy Expenditure Due to Nutrient Difference. Nutrients. 2020;12:3197.

38. Turnbaugh PJ, Ley RE, Mahowald MA, Magrini V, Mardis ER, Gordon JI. An obesity-associated gut microbiome with increased capacity for energy harvest. Nature. 2006;444:1027–31.

39. Tan J, McKenzie C, Potamitis M, Thorburn AN, Mackay CR, Macia L. The Role of Short-Chain Fatty Acids in Health and Disease. In: Advances in Immunology. Elsevier; 2014. p. 91–119. doi:10.1016/B978-0-12-800100-4.00003-9.

40. den Besten G, van Eunen K, Groen AK, Venema K, Reijngoud D-J, Bakker BM. The role of short-chain fatty acids in the interplay between diet, gut microbiota, and host energy metabolism. J Lipid Res. 2013;54:2325–40.

41. Martinez-Medina M, Denizot J, Dreux N, Robin F, Billard E, Bonnet R, et al. Western diet induces dysbiosis with increased *E coli* in CEABAC10 mice , alters host barrier function favouring AIEC colonisation. Gut. 2014;63:116–24.

42. Brown JM, Hazen SL. The Gut Microbial Endocrine Organ: Bacterially Derived Signals Driving Cardiometabolic Diseases. Annu Rev Med. 2015;66:343–59.

43. Carvalho BM, Guadagnini D, Tsukumo DML, Schenka AA, Latuf-Filho P, Vassallo J, et al. Modulation of gut microbiota by antibiotics improves insulin signalling in high-fat fed mice. Diabetologia. 2012;55:2823–34.

44. Rastelli M, Knauf C, Cani PD. Gut Microbes and Health: A Focus on the Mechanisms Linking Microbes, Obesity, and Related Disorders: Mechanisms Linking Microbes and Obesity. Obesity. 2018;26:792–800.

45. Deopurkar R, Ghanim H, Friedman J, Abuaysheh S, Sia CL, Mohanty P, et al. Differential Effects of Cream, Glucose, and Orange Juice on Inflammation, Endotoxin, and the Expression of Toll-Like Receptor-4 and Suppressor of Cytokine Signaling-3. Diabetes Care. 2010;33:991–7.

46. Do M, Lee E, Oh M-J, Kim Y, Park H-Y. High-Glucose or -Fructose Diet Cause Changes of the Gut Microbiota and Metabolic Disorders in Mice without Body Weight Change. Nutrients. 2018;10:761.

47. Zoetendal EG, Raes J, van den Bogert B, Arumugam M, Booijink CC, Troost FJ, et al. The human small intestinal microbiota is driven by rapid uptake and conversion of simple carbohydrates. ISME J. 2012;6:1415–26.

48. Ramne S, Brunkwall L, Ericson U, Gray N, Kuhnle GGC, Nilsson PM, et al. Gut microbiota composition in relation to intake of added sugar, sugar-sweetened beverages and artificially sweetened beverages in the Malmö Offspring Study. Eur J Nutr. 2021;60:2087–97.

49. Jones RB, Alderete TL, Kim JS, Millstein J, Gilliland FD, Goran MI. High intake of dietary fructose in overweight/obese teenagers associated with depletion of *Eubacterium* and *Streptococcus* in gut microbiome. Gut Microbes. 2019;10:712–9.

50. Ruiz-Ojeda FJ, Plaza-Díaz J, Sáez-Lara MJ, Gil A. Effects of Sweeteners on the Gut Microbiota: A Review of Experimental Studies and Clinical Trials. Adv Nutr. 2019;10 suppl_1:S31–48.

51. Shan K, Qu H, Zhou K, Wang L, Zhu C, Chen H, et al. Distinct Gut Microbiota Induced by Different Fat-to-Sugar-Ratio High-Energy Diets Share Similar Pro-obesity Genetic and Metabolite Profiles in Prediabetic Mice. mSystems. 2019;4. doi:10.1128/mSystems.00219-19.

52. Faith JJ, McNulty NP, Rey FE, Gordon JI. Predicting a Human Gut Microbiota's Response to Diet in Gnotobiotic Mice. Science. 2011;333:101–4.

53. Russell WR, Gratz SW, Duncan SH, Holtrop G, Ince J, Scobbie L, et al. High-protein, reduced-carbohydrate weight-loss diets promote metabolite profiles likely to be detrimental to colonic health. Am J Clin Nutr. 2011;93:1062–72.

54. Wu GD, Chen J, Hoffmann C, Bittinger K, Chen Y-Y, Keilbaugh SA, et al. Linking Long-Term Dietary Patterns with Gut Microbial Enterotypes. Science. 2011;334:105–8.

55. Ley RE, Turnbaugh PJ, Klein S, Gordon JI. Human gut microbes associated with obesity. Nature. 2006;444:1022–3.

56. David LA, Maurice CF, Carmody RN, Gootenberg DB, Button JE, Wolfe BE, et al. Diet rapidly and reproducibly alters the human gut microbiome. Nature. 2014;505:559–63.

57. O'Keefe SJD, Li JV, Lahti L, Ou J, Carbonero F, Mohammed K, et al. Fat, fibre and cancer risk in African Americans and rural Africans. Nat Commun. 2015;6:6342.

58. de Menezes EW, Giuntini EB, Dan MCT, Sardá FAH, Lajolo FM. Codex dietary fibre definition – Justification for inclusion of carbohydrates from 3 to 9 degrees of polymerisation. Food Chem. 2013;140:581–5.

59. Dhingra D, Michael M, Rajput H, Patil RT. Dietary fibre in foods: a review. J Food Sci Technol. 2012;49:255–66.

60. De Filippo C, Cavalieri D, Di Paola M, Ramazzotti M, Poullet JB, Massart S, et al. Impact of diet in shaping gut microbiota revealed by a comparative study in children from Europe and rural Africa. Proc Natl Acad Sci. 2010;107:14691–6.

61. De Filippo C, Di Paola M, Ramazzotti M, Albanese D, Pieraccini G, Banci E, et al. Diet, Environments, and Gut Microbiota. A Preliminary Investigation in Children Living in Rural and Urban Burkina Faso and Italy. Front Microbiol. 2017;8:1979.

62. Schnorr SL, Candela M, Rampelli S, Centanni M, Consolandi C, Basaglia G, et al. Gut microbiome of the Hadza hunter-gatherers. Nat Commun. 2014;5:3654.

63. Makki K, Deehan EC, Walter J, Bäckhed F. The Impact of Dietary Fiber on Gut Microbiota in Host Health and Disease. Cell Host Microbe. 2018;23:705–15.

64. Menni C. Gut microbiome diversity and high-fibre intake are related to lower long-term weight gain. Int J Obes. 2017;41:7.

65. Jain A, Li XH, Chen WN. Similarities and differences in gut microbiome composition correlate with dietary patterns of Indian and Chinese adults. AMB Express. 2018;8:104.

66. De Filippis F, Pasolli E, Tett A, Tarallo S, Naccarati A, De Angelis M, et al. Distinct Genetic and Functional Traits of Human Intestinal Prevotella copri Strains Are Associated with Different Habitual Diets. Cell Host Microbe. 2019;25:444-453.e3.

67. Vitaglione P, Mennella I, Ferracane R, Rivellese AA, Giacco R, Ercolini D, et al. Whole-grain wheat consumption reduces inflammation in a randomized controlled trial on overweight and obese subjects with unhealthy dietary and lifestyle behaviors: role of polyphenols bound to cereal dietary fiber. Am J Clin Nutr. 2015;101:251–61.

68. De Angelis M, Montemurno E, Vannini L, Cosola C, Cavallo N, Gozzi G, et al. Effect of Whole-Grain Barley on the Human Fecal Microbiota and Metabolome. Appl Environ Microbiol. 2015;81:7945–56.

69. Kovatcheva-Datchary P, Nilsson A, Akrami R, Lee YS, De Vadder F, Arora T, et al. Dietary Fiber-Induced Improvement in Glucose Metabolism Is Associated with Increased Abundance of Prevotella. Cell Metab. 2015;22:971–82.

70. Alpizar-Rodriguez D, Lesker TR, Gronow A, Gilbert B, Raemy E, Lamacchia C, et al. *Prevotella copri* in individuals at risk for rheumatoid arthritis. Ann Rheum Dis. 2019;78:590–3.

71. Larsen JM. The immune response to *Prevotella* bacteria in chronic inflammatory disease. Immunology. 2017;151:363–74.

72. Kellow NJ, Coughlan MT, Reid CM. Metabolic benefits of dietary prebiotics in human subjects: a systematic review of randomised controlled trials. Br J Nutr. 2014;111:1147–61.

73. de Cossío LF, Fourrier C, Sauvant J, Everard A, Capuron L, Cani PD, et al. Impact of prebiotics on metabolic and behavioral alterations in a mouse model of metabolic syndrome. Brain Behav Immun. 2017;64:33–49.

74. Gibson GR, Roberfroid MB. Dietary Modulation of the Human Colonic Microbiota: Introducing the Concept of Prebiotics. J Nutr. 1995;125:1401–12.

75. Gibson GR, Hutkins R, Sanders ME, Prescott SL, Reimer RA, Salminen SJ, et al. Expert consensus document: The International Scientific Association for Probiotics and Prebiotics (ISAPP) consensus statement on the definition and scope of prebiotics. Nat Rev Gastroenterol Hepatol. 2017;14:491–502.

76. Everard A, Lazarevic V, Gaïa N, Johansson M, Ståhlman M, Backhed F, et al. Microbiome of prebiotic-treated mice reveals novel targets involved in host response during obesity. ISME J. 2014;8:2116–30.

77. Enam F, Mansell TJ. Prebiotics: tools to manipulate the gut microbiome and metabolome. J Ind Microbiol Biotechnol. 2019;46:1445–59.

78. Respondek F, Gerard P, Bossis M, Boschat L, Bruneau A, Rabot S, et al. Short-Chain Fructo-Oligosaccharides Modulate Intestinal Microbiota and Metabolic Parameters of Humanized Gnotobiotic Diet Induced Obesity Mice. PLoS ONE. 2013;8:e71026.

79. McLoughlin RF, Berthon BS, Jensen ME, Baines KJ, Wood LG. Short-chain fatty acids, prebiotics, synbiotics, and systemic inflammation: a systematic review and meta-analysis. Am J Clin Nutr. 2017. doi:10.3945/ajcn.117.156265.

80. Campbell-Platt G. Fermented foods — a world perspective. Food Res Int. 1994;27:253–7.

81. Stiemsma LT, Nakamura RE, Nguyen JG, Michels KB. Does Consumption of Fermented Foods Modify the Human Gut Microbiota? J Nutr. 2020;150:1680–92.

82. Wastyk HC, Fragiadakis GK, Perelman D, Dahan D, Merrill BD, Yu FB, et al. Gut-microbiota-targeted diets modulate human immune status. Cell. 2021;184:4137-4153.e14.

83. Taylor BC, Lejzerowicz F, Poirel M, Shaffer JP, Jiang L, Aksenov A, et al. Consumption of Fermented Foods Is Associated with Systematic Differences in the Gut Microbiome and Metabolome. mSystems. 2020;5. doi:10.1128/mSystems.00901-19.

84. Freeman J. Antibiotics and Clostridium difficile. Microbes Infect. 1999;1:377–84.

85. Buffie CG, Jarchum I, Equinda M, Lipuma L, Gobourne A, Viale A, et al. Profound Alterations of Intestinal Microbiota following a Single Dose of Clindamycin Results in Sustained Susceptibility to Clostridium difficile-Induced Colitis. Infect Immun. 2012;80:62–73.

86. Bassis CM, Theriot CM, Young VB. Alteration of the Murine Gastrointestinal Microbiota by Tigecycline Leads to Increased Susceptibility to Clostridium difficile Infection. Antimicrob Agents Chemother. 2014;58:2767–74.

87. Kuppala VS, Meinzen-Derr J, Morrow AL, Schibler KR. Prolonged Initial Empirical Antibiotic Treatment is Associated with Adverse Outcomes in Premature Infants. J Pediatr. 2011;159:720–5.

88. Roubaud-Baudron C, Ruiz VE, Swan AM, Vallance BA, Ozkul C, Pei Z, et al. Long-Term Effects of Early-Life Antibiotic Exposure on Resistance to Subsequent Bacterial Infection. mBio. 2019;10. doi:10.1128/mBio.02820-19.

89. Volkova A, Ruggles K, Schulfer A, Gao Z, Ginsberg SD, Blaser MJ. Effects of early-life penicillin exposure on the gut microbiome and frontal cortex and amygdala gene expression. iScience. 2021;24:102797.

90. Patrick DM, Sbihi H, Dai DLY, Al Mamun A, Rasali D, Rose C, et al. Decreasing antibiotic use, the gut microbiota, and asthma incidence in children: evidence from population-based and prospective cohort studies. Lancet Respir Med. 2020;8:1094–105.

91. Aversa Z, Atkinson EJ, Schafer MJ, Theiler RN, Rocca WA, Blaser MJ, et al. Association of Infant Antibiotic Exposure With Childhood Health Outcomes. Mayo Clin Proc. 2021;96:66–77.

92. Kronman MP, Zaoutis TE, Haynes K, Feng R, Coffin SE. Antibiotic Exposure and IBD Development Among Children: A Population-Based Cohort Study. PEDIATRICS. 2012;130:e794–803.

93. Mikkelsen KH, Knop FK, Frost M, Hallas J, Pottegård A. Use of Antibiotics and Risk of Type 2 Diabetes: A Population-Based Case-Control Study. J Clin Endocrinol Metab. 2015;100:3633–40.

94. Angelakis E, Million M, Kankoe S, Lagier J-C, Armougom F, Giorgi R, et al. Abnormal Weight Gain and Gut Microbiota Modifications Are Side Effects of Long-Term Doxycycline and Hydroxychloroquine Treatment. Antimicrob Agents Chemother. 2014;58:3342–7.

95. Lane JA, Murray LJ, Harvey IM, Donovan JL, Nair P, Harvey RF. Randomised clinical trial: Helicobacter pylori eradication is associated with a significantly increased body mass index in a placebo-controlled study: Randomised clinical trial: the impact of H. pylori eradication on BMI and weight. Aliment Pharmacol Ther. 2011;33:922–9.

96. Zaura E, Brandt BW, Teixeira de Mattos MJ, Buijs MJ, Caspers MPM, Rashid M-U, et al. Same Exposure but Two Radically Different Responses to Antibiotics: Resilience of the Salivary Microbiome versus Long-Term Microbial Shifts in Feces. mBio. 2015;6. doi:10.1128/mBio.01693-15.

97. Jernberg C, Löfmark S, Edlund C, Jansson JK. Long-term ecological impacts of antibiotic administration on the human intestinal microbiota. ISME J. 2007;1:56–66.

98. Ng KM, Ferreyra JA, Higginbottom SK, Lynch JB, Kashyap PC, Gopinath S, et al. Microbiota-liberated host sugars facilitate post-antibiotic expansion of enteric pathogens. Nature. 2013;502:96–9.

99. Cabral DJ, Penumutchu S, Reinhart EM, Zhang C, Korry BJ, Wurster JI, et al. Microbial Metabolism Modulates Antibiotic Susceptibility within the Murine Gut Microbiome. Cell Metab. 2019;30:800-823.e7.

100. Suez J, Zmora N, Zilberman-Schapira G, Mor U, Dori-Bachash M, Bashiardes S, et al. Post-Antibiotic Gut Mucosal Microbiome Reconstitution Is Impaired by Probiotics and Improved by Autologous FMT. Cell. 2018;174:1406-1423.e16.

101. Silva-Sanchez A, Randall TD. Anatomical Uniqueness of the Mucosal Immune System (GALT, NALT, iBALT) for the Induction and Regulation of Mucosal Immunity and Tolerance. In: Mucosal Vaccines. Elsevier; 2020. p. 21–54. doi:10.1016/B978-0-12-811924-2.00002-X.

102. McDermott MR, Bienenstock J. Evidence for a Common Mucosal Immunologic System. J Immunol. 1979;122:1892.

103. Murphy K, Weaver C. Chapter 12: The Mucosal Immune System. In: Janeway's immunobiology. 9th edition. New York, NY: Garland Science/Taylor & Francis Group, LLC; 2016.

104. Bunker JJ, Bendelac A. IgA Responses to Microbiota. Immunity. 2018;49:211–24.

105. Kunisawa J, Kurashima Y, Kiyono H. Gut-associated lymphoid tissues for the development of oral vaccines. Adv Drug Deliv Rev. 2012;64:523–30.

106. Grasset EK, Chorny A, Casas-Recasens S, Gutzeit C, Bongers G, Thomsen I, et al. Gut T cell–independent IgA responses to commensal bacteria require engagement of the TACI receptor on B cells. Sci Immunol. 2020;5:eaat7117.

107. Houston SA, Cerovic V, Thomson C, Brewer J, Mowat AM, Milling S. The lymph nodes draining the small intestine and colon are anatomically separate and immunologically distinct. Mucosal Immunol. 2016;9:468–78.

108. Mora JR, von Andrian UH. Role of retinoic acid in the imprinting of gut-homing IgA-secreting cells. Semin Immunol. 2009;21:28–35.

109. Wagner N, Löhler J, Kunkel EJ, Ley K, Leung E, Krissansen G, et al. Critical role for β7 integrins in formation of the gut-associated lymphoid tissue. Nature. 1996;382:366–70.

110. Kunkel EJ, Kim CH, Lazarus NH, Vierra MA, Soler D, Bowman EP, et al. CCR10 expression is a common feature of circulating and mucosal epithelial tissue IgA Ab-secreting cells. J Clin Invest. 2003;111:1001–10.

111. Pabst O, Ohl L, Wendland M, Wurbel M-A, Kremmer E, Malissen B, et al. Chemokine Receptor CCR9 Contributes to the Localization of Plasma Cells to the Small Intestine. J Exp Med. 2004;199:411–6.

112. Mora JR, Iwata M, Eksteen B, Song S-Y, Junt T, Senman B, et al. Generation of Gut-Homing IgA-Secreting B Cells by Intestinal Dendritic Cells. Science. 2006;314:1157–60.

113. Ross AC, Chen Q, Ma Y. Vitamin A and Retinoic Acid in the Regulation of B-Cell Development and Antibody Production. In: Vitamins & Hormones. Elsevier; 2011. p. 103–26. doi:10.1016/B978-0-12-386960-9.00005-8.

114. Liang Y, Hasturk H, Elliot J, Noronha A, Liu X, Wetzler LM, et al. Toll-like receptor 2 induces mucosal homing receptor expression and IgA production by human B cells. Clin Immunol. 2011;138:33–40.

115. Kaetzel CS, Mestecky J, Johansen F-E. Two Cells, One Antibody: The Discovery of the Cellular Origins and Transport of Secretory IgA. J Immunol. 2017;198:1765–7.

116. Kerr MA. The structure and function of human IgA. Biochem J. 1990;271:285–96.

117. Wolf HM, Fischer MB, Pühringer H, Samstag A, Vogel E, Eibl MM. Human serum IgA downregulates the release of inflammatory cytokines (tumor necrosis factor-alpha, interleukin-6) in human monocytes. Blood. 1994;83:1278–88.

118. Bunker JJ, Erickson SA, Flynn TM, Henry C, Koval JC, Meisel M, et al. Natural polyreactive IgA antibodies coat the intestinal microbiota. Science. 2017;358. doi:10.1126/science.aan6619.

119. Woof JM, Kerr MA. The function of immunoglobulin A in immunity. J Pathol. 2006;208:270–82.

120. Boehm MK, Woof JM, Kerr MA, Perkins SJ. The fab and fc fragments of IgA1 exhibit a different arrangement from that in IgG: a study by X-ray and neutron solution scattering and homology modelling 1 1Edited by R. Huber. J Mol Biol. 1999;286:1421–47.

121. Steffen U, Koeleman CA, Sokolova MV, Bang H, Kleyer A, Rech J, et al. IgA subclasses have different effector functions associated with distinct glycosylation profiles. Nat Commun. 2020;11:120.

122. Monteiro RC. Role of IgA and IgA Fc Receptors in Inflammation. J Clin Immunol. 2010;30:1–9.

123. Van Epps DE, Williams RC. Suppression of leukocyte chemotaxis by human IgA myeloma components. J Exp Med. 1976;144:1227–42.

124. Nikolova EB, Russell MW. Dual function of human IgA antibodies: inhibition of phagocytosis in circulating neutrophils and enhancement of responses in IL-8-stimulated cells. J Leukoc Biol. 1995;57:875–82.

125. Breedveld A, van Egmond M. IgA and FcαRI: Pathological Roles and Therapeutic Opportunities. Front Immunol. 2019;10:553.

126. Carayannopoulos L, Hexham JM, Capra JD. Localization of the binding site for the monocyte immunoglobulin (Ig) A-Fc receptor (CD89) to the domain boundary between Calpha2 and Calpha3 in human IgA1. J Exp Med. 1996;183:1579–86.

127. Woof JM, Russell MW. Structure and function relationships in IgA. Mucosal Immunol. 2011;4:590–7.

128. Posgai MT, Tonddast-Navaei S, Jayasinghe M, Ibrahim GM, Stan G, Herr AB. FcαRI binding at the IgA1 C_H2–C_H3 interface induces long-range conformational changes that are transmitted to the hinge region. Proc Natl Acad Sci. 2018;115:E8882–91.

129. Reboldi A, Cyster JG. Peyer's patches: organizing B-cell responses at the intestinal frontier. Immunol Rev. 2016;271:230–45.

130. Huus KE, Petersen C, Finlay BB. Diversity and dynamism of IgA−microbiota interactions. Nat Rev Immunol. 2021;21:514–25.

131. Hoces D, Arnoldini M, Diard M, Loverdo C, Slack E. Growing, evolving and sticking in a flowing environment: understanding IgA interactions with bacteria in the gut. Immunology. 2020;159:52–62.

132. Lycke N, Erlandsson L, Ekman L, Schön K, Leanderson T. Lack of J Chain Inhibits the Transport of Gut IgA and Abrogates the Development of Intestinal Antitoxic Protection. J Immunol. 1999;163:913.

133. Mantis NJ, Rol N, Corthésy B. Secretory IgA's complex roles in immunity and mucosal homeostasis in the gut. Mucosal Immunol. 2011;4:603–11.

134. Fagarasan S. Critical Roles of Activation-Induced Cytidine Deaminase in the Homeostasis of Gut Flora. Science. 2002;298:1424–7.

135. Cunningham-Rundles C. Physiology of IgA and IgA deficiency. J Clin Immunol. 2001;21:303–9.

136. Donaldson GP, Ladinsky MS, Yu KB, Sanders JG, Yoo BB, Chou W-C, et al. Gut microbiota utilize immunoglobulin A for mucosal colonization. Science. 2018;360:795–800.

137. Phalipon A, Kaufmann M, Michetti P, Cavaillon JM, Huerre M, Sansonetti P, et al. Monoclonal immunoglobulin A antibody directed against serotype-specific epitope of Shigella flexneri lipopolysaccharide protects against murine experimental shigellosis. J Exp Med. 1995;182:769–78.

138. Forbes SJ, Bumpus T, McCarthy EA, Corthésy B, Mantis NJ. Transient Suppression of Shigella flexneri Type 3 Secretion by a Protective O-Antigen-Specific Monoclonal IgA. mBio. 2011;2. doi:10.1128/mBio.00042-11.

139. Cullender TC, Chassaing B, Janzon A, Kumar K, Muller CE, Werner JJ, et al. Innate and Adaptive Immunity Interact to Quench Microbiome Flagellar Motility in the Gut. Cell Host Microbe. 2013;14:571–81.

140. Mantis NJ, Forbes SJ. Secretory IgA: Arresting Microbial Pathogens at Epithelial Borders. Immunol Invest. 2010;39:383–406.

141. Peterson DA, McNulty NP, Guruge JL, Gordon JI. IgA Response to Symbiotic Bacteria as a Mediator of Gut Homeostasis. Cell Host Microbe. 2007;2:328–39.

142. Skwarczynski M, Toth I. Non-invasive mucosal vaccine delivery: advantages, challenges and the future. Expert Opin Drug Deliv. 2020;17:435–7.

143. Lavelle EC, Ward RW. Mucosal vaccines — fortifying the frontiers. Nat Rev Immunol. 2021. doi:10.1038/s41577-021-00583-2.

144. Miquel-Clopés A, Bentley EG, Stewart JP, Carding SR. Mucosal vaccines and technology. Clin Exp Immunol. 2019;:cei.13285.

145. Neutra MR, Kozlowski PA. Mucosal vaccines: the promise and the challenge. Nat Rev Immunol. 2006;6:148–58.

146. Kim S-H, Jang Y-S. The development of mucosal vaccines for both mucosal and systemic immune induction and the roles played by adjuvants. Clin Exp Vaccine Res. 2017;6:15.

147. Ball JM, Hardy ME, Atmar RL, Conner ME, Estes MK. Oral Immunization with Recombinant Norwalk Virus-Like Particles Induces a Systemic and Mucosal Immune Response in Mice. J Virol. 1998;72:1345–53.

148. Bermúdez-Humarán LG, Cortes-Perez NG, Lefèvre F, Guimarães V, Rabot S, Alcocer-Gonzalez JM, et al. A Novel Mucosal Vaccine Based on Live Lactococci Expressing E7 Antigen and IL-12 Induces Systemic and Mucosal Immune Responses and Protects Mice against Human Papillomavirus Type 16-Induced Tumors. J Immunol. 2005;175:7297–302.

149. Kajikawa A, Zhang L, LaVoy A, Bumgardner S, Klaenhammer TR, Dean GA. Mucosal Immunogenicity of Genetically Modified Lactobacillus acidophilus Expressing an HIV-1 Epitope within the Surface Layer Protein. PLOS ONE. 2015;10:15.

150. Belyakov IM, Ahlers JD. What Role Does the Route of Immunization Play in the Generation of Protective Immunity against Mucosal Pathogens? J Immunol. 2009;183:6883–92.

151. Azegami T, Yuki Y, Kiyono H. Challenges in mucosal vaccines for the control of infectious diseases. Int Immunol. 2014;26:517–28.

152. Musich T, Thovarai V, Venzon DJ, Mohanram V, Tuero I, Miller-Novak LK, et al. A Prime/Boost Vaccine Regimen Alters the Rectal Microbiome and Impacts Immune Responses and Viremia Control Post-Simian Immunodeficiency Virus Infection in Male and Female Rhesus Macaques. J Virol. 2020;94:26.

153. Vitetta L, Saltzman E, Thomsen M, Nikov T, Hall S. Adjuvant Probiotics and the Intestinal Microbiome: Enhancing Vaccines and Immunotherapy Outcomes. Vaccines. 2017;5:50.

154. Boyaka PN. Inducing Mucosal IgA: A Challenge for Vaccine Adjuvants and Delivery Systems. J Immunol. 2017;199:9–16.

155. Dupont A, Heinbockel L, Brandenburg K, Hornef MW. Antimicrobial peptides and the enteric mucus layer act in concert to protect the intestinal mucosa. Gut Microbes. 2014;5:761–5.

156. Renukuntla J, Vadlapudi AD, Patel A, Boddu SHS, Mitra AK. Approaches for enhancing oral bioavailability of peptides and proteins. Int J Pharm. 2013;447:75–93.

157. Tordesillas L, Berin MC. Mechanisms of Oral Tolerance. Clin Rev Allergy Immunol. 2018;55:107–17.

158. Coombes JL, Siddiqui KRR, Arancibia-Cárcamo CV, Hall J, Sun C-M, Belkaid Y, et al. A functionally specialized population of mucosal CD103+ DCs induces Foxp3+ regulatory T cells via a TGF-β– and retinoic acid–dependent mechanism. J Exp Med. 2007;204:1757–64.

159. Garg S, Bal V, Rath S, George A. Effect of Multiple Antigenic Exposures in the Gut on Oral Tolerance and Induction of Antibacterial Systemic Immunity. Infect Immun. 1999;67:5917–24.

160. Elson CO, Ealding W. Cholera toxin feeding did not induce oral tolerance in mice and abrogated oral tolerance to an unrelated protein antigen. J Immunol Baltim Md 1950. 1984;133:2892–7.

161. Liu L, Johnson HL, Cousens S, Perin J, Scott S, Lawn JE, et al. Global, regional, and national causes of child mortality: an updated systematic analysis for 2010 with time trends since 2000. The Lancet. 2012;379:2151–61.

162. Desselberger U. Differences of Rotavirus Vaccine Effectiveness by Country: Likely Causes and Contributing Factors. Pathogens. 2017;6:65.

163. Patriarca PA, Wright PF, John TJ. Factors Affecting the Immunogenicity of Oral Poliovirus Vaccine in Developing Countries: Review. Clin Infect Dis. 1991;13:926–39.

164. Parker EP, Ramani S, Lopman BA, Church JA, Iturriza-Gómara M, Prendergast AJ, et al. Causes of impaired oral vaccine efficacy in developing countries. Future Microbiol. 2018;13:97–118.

165. Zhang Y, Li M, Du G, Chen X, Sun X. Advanced oral vaccine delivery strategies for improving the immunity. Adv Drug Deliv Rev. 2021;177:113928.

166. Foged C. Subunit vaccines of the future: the need for safe, customized and optimized particulate delivery systems. Ther Deliv. 2011;2:1057–77.

167. Guthrie T, Hobbs CGL, Davenport V, Horton RE, Heyderman RS, Williams NA. Parenteral Influenza Vaccination Influences Mucosal and Systemic T Cell–Mediated Immunity in Healthy Adults. J Infect Dis. 2004;190:1927–35.

168. Renegar KB, Small PA, Boykins LG, Wright PF. Role of IgA versus IgG in the Control of Influenza Viral Infection in the Murine Respiratory Tract. J Immunol. 2004;173:1978–86.

169. Leigh SA, Evans JD, Collier SD, Branton SL. The impact of vaccination route on Mycoplasma gallisepticum vaccine efficacy. Poult Sci. 2018;97:3072–5.

170. Ackerman ME, Das J, Pittala S, Broge T, Linde C, Suscovich TJ, et al. Route of immunization defines multiple mechanisms of vaccine-mediated protection against SIV. Nat Med. 2018;24:1590–8.

171. Benn JS, Chaki SP, Xu Y, Ficht TA, Rice-Ficht AC, Cook WE. Protective antibody response following oral vaccination with microencapsulated Bacillus Anthracis Sterne strain 34F2 spores. Npj Vaccines. 2020;5:59.

172. Wang Y-Y, Lai SK, Suk JS, Pace A, Cone R, Hanes J. Addressing the PEG Mucoadhesivity Paradox to Engineer Nanoparticles that "Slip" through the Human Mucus Barrier. Angew Chem Int Ed. 2008;47:9726–9.

173. Nakamura M, Awaad, Ishimura. Histochemical and biochemical analysis of the size-dependent nanoimmunoresponse in mouse Peyer's patches using fluorescent organosilica particles. Int J Nanomedicine. 2012;:1423.

174. Szatraj K, Szczepankowska AK, Chmielewska-Jeznach M. Lactic acid bacteria - promising vaccine vectors: possibilities, limitations, doubts. J Appl Microbiol. 2017;123:325–39.

175. Wyszyńska A, Kobierecka P, Bardowski J, Jagusztyn-Krynicka EK. Lactic acid bacteria—20 years exploring their potential as live vectors for mucosal vaccination. Appl Microbiol Biotechnol. 2015;99:2967–77.

176. Vilander AC, Dean GA. Adjuvant Strategies for Lactic Acid Bacterial Mucosal Vaccines. Vaccines. 2019;7:150.

177. Christensen HR, Frøkiær H, Pestka JJ. Lactobacilli Differentially Modulate Expression of Cytokines and Maturation Surface Markers in Murine Dendritic Cells. J Immunol. 2002;168:171–8.

178. Jiang B, Li Z, Ou B, Duan Q, Zhu G. Targeting ideal oral vaccine vectors based on probiotics: a systematical view. Appl Microbiol Biotechnol. 2019;103:3941–53.

179. Tseng Y-H, Hsieh C-C, Kuo T-Y, Liu J-R, Hsu T-Y, Hsieh S-C. Construction of a Lactobacillus plantarum Strain Expressing the Capsid Protein of Porcine Circovirus Type 2d (PCV2d) as an Oral Vaccine. Indian J Microbiol. 2019;59:490–9.

180. Cavin JF, Barthelmebs L, Diviès C. Molecular characterization of an inducible p-coumaric acid decarboxylase from Lactobacillus plantarum: gene cloning, transcriptional analysis, overexpression in Escherichia coli, purification, and characterization. Appl Environ Microbiol. 1997;63:1939–44.

181. Tregoning JS, Russell RF, Kinnear E. Adjuvanted influenza vaccines. Hum Vaccines Immunother. 2018;14:550–64.

182. Li R, Chowdhury MYE, Kim J-H, Kim T-H, Pathinayake P, Koo W-S, et al. Mucosally administered Lactobacillus surface-displayed influenza antigens (sM2 and HA2) with cholera toxin subunit A1 (CTA1) Induce broadly protective immune responses against divergent influenza subtypes. Vet Microbiol. 2015;179:250–63.

183. Kajikawa A, Masuda K, Katoh M, Igimi S. Adjuvant Effects for Oral Immunization Provided by Recombinant Lactobacillus casei Secreting Biologically Active Murine Interleukin-1β. Clin Vaccine Immunol. 2010;17:43–8.

184. Lynn DJ, Benson SC, Lynn MA, Pulendran B. Modulation of immune responses to vaccination by the microbiota: implications and potential mechanisms. Nat Rev Immunol. 2021. doi:10.1038/s41577-021-00554-7.

185. Oh JZ, Ravindran R, Chassaing B, Carvalho FA, Maddur MS, Bower M, et al. TLR5-Mediated Sensing of Gut Microbiota Is Necessary for Antibody Responses to Seasonal Influenza Vaccination. Immunity. 2014;41:478–92.

186. Lamousé-Smith ES, Tzeng A, Starnbach MN. The Intestinal Flora Is Required to Support Antibody Responses to Systemic Immunization in Infant and Germ Free Mice. PLoS ONE. 2011;6:e27662.

187. Lynn MA, Tumes DJ, Choo JM, Sribnaia A, Blake SJ, Leong LEX, et al. Early-Life Antibiotic-Driven Dysbiosis Leads to Dysregulated Vaccine Immune Responses in Mice. Cell Host Microbe. 2018;23:653-660.e5.

188. Harris VC, Armah G, Fuentes S, Korpela KE, Parashar U, Victor JC, et al. Significant Correlation Between the Infant Gut Microbiome and Rotavirus Vaccine Response in Rural Ghana. J Infect Dis. 2017;215:34–41.

189. Harris V, Ali A, Fuentes S, Korpela K, Kazi M, Tate J, et al. Rotavirus vaccine response correlates with the infant gut microbiota composition in Pakistan. Gut Microbes. 2018;9:93–101.

190. Zhao T, Li J, Fu Y, Ye H, Liu X, Li G, et al. Influence of gut microbiota on mucosal IgA antibody response to the polio vaccine. Npj Vaccines. 2020;5:47.

191. Harris VC, Haak BW, Handley SA, Jiang B, Velasquez DE, Hykes BL, et al. Effect of Antibiotic-Mediated Microbiome Modulation on Rotavirus Vaccine Immunogenicity: A Human, Randomized-Control Proof-of-Concept Trial. Cell Host Microbe. 2018;24:197-207.e4.

192. Hagan T, Cortese M, Rouphael N, Boudreau C, Linde C, Maddur MS, et al. Antibiotics-Driven Gut Microbiome Perturbation Alters Immunity to Vaccines in Humans. Cell. 2019;178:1313-1328.e13.

193. Miyazaki A, Kandasamy S, Michael H, Langel SN, Paim FC, Chepngeno J, et al. Protein deficiency reduces efficacy of oral attenuated human rotavirus vaccine in a human infant fecal microbiota transplanted gnotobiotic pig model. Vaccine. 2018;36:6270–81.

194. Kumar A, Vlasova AN, Deblais L, Huang H-C, Wijeratne A, Kandasamy S, et al. Impact of nutrition and rotavirus infection on the infant gut microbiota in a humanized pig model. BMC Gastroenterol. 2018;18:93.

195. Benyacoub J, Rochat F, Saudan K-Y, Rochat I, Antille N, Cherbut C, et al. Feeding a Diet Containing a Fructooligosaccharide Mix Can Enhance Salmonella Vaccine Efficacy in Mice. J Nutr. 2008;138:123–9.

196. Leite FLL, Singer RS, Ward T, Gebhart CJ, Isaacson RE. Vaccination Against Lawsonia intracellularis Decreases Shedding of Salmonella enterica serovar Typhimurium in Co-Infected Pigs and Alters the Gut Microbiome. Sci Rep. 2018;8:2857.

197. Leite FL, Winfield B, Miller EA, Weber BP, Johnson TJ, Sylvia F, et al. Oral Vaccination Reduces the Effects of Lawsonia intracellularis Challenge on the Swine Small and Large Intestine Microbiome. Front Vet Sci. 2021;8:692521.

198. Eloe-Fadrosh EA, McArthur MA, Seekatz AM, Drabek EF, Rasko DA, Sztein MB, et al. Impact of Oral Typhoid Vaccination on the Human Gut Microbiota and Correlations with S. Typhi-Specific Immunological Responses. PLoS ONE. 2013;8:e62026.

199. Salgado VR, Fukutani KF, Fukutani E, Lima JV, Rossi EA, Barral A, et al. Effects of 10-valent pneumococcal conjugate (PCV10) vaccination on the nasopharyngeal microbiome. Vaccine. 2020;38:1436–43.

200. Aldovini A. Mucosal Vaccination for Prevention of HIV Infection and AIDS. Curr HIV Res. 2016;14:247–59.

201. Abdo Z, LeCureux J, LaVoy A, Eklund B, Ryan EP, Dean GA. Impact of oral probiotic Lactobacillus acidophilus vaccine strains on the immune response and gut microbiome of mice. PLOS ONE. 2019;14:23.

202. Redweik GAJ, Daniels K, Severin AJ, Lyte M, Mellata M. Oral Treatments With Probiotics and Live Salmonella Vaccine Induce Unique Changes in Gut Neurochemicals and Microbiome in Chickens. Front Microbiol. 2020;10:3064.

203. Becattini S, Sorbara MT, Kim SG, Littmann EL, Dong Q, Walsh G, et al. Rapid transcriptional and metabolic adaptation of intestinal microbes to host immune activation. Cell Host Microbe. 2021;29:378-393.e5.

204. Kang S, Hong S, Lee Y-K, Cho S. Oral Vaccine Delivery for Intestinal Immunity—Biological Basis, Barriers, Delivery System, and M Cell Targeting. Polymers. 2018;10:948.

205. Sperandio B, Fischer N, Sansonetti PJ. Mucosal physical and chemical innate barriers: Lessons from microbial evasion strategies. Semin Immunol. 2015;27:111–8.

206. Thakur A, Foged C. Nanoparticles for mucosal vaccine delivery. In: Nanoengineered Biomaterials for Advanced Drug Delivery. Elsevier; 2020. p. 603–46. doi:10.1016/B978-0-08-102985-5.00025-5.

207. Rhee JH. Current and New Approaches for Mucosal Vaccine Delivery. In: Mucosal Vaccines. Elsevier; 2020. p. 325–56. doi:10.1016/B978-0-12-811924-2.00019-5.

208. Wells JM. Immunomodulatory mechanisms of lactobacilli. Microb Cell Factories. 2011;10 Suppl 1:S17.

209. Malamud M, Carasi P, Assandri MH, Freire T, Lepenies B, Serradell M de los Á. S-Layer Glycoprotein From Lactobacillus kefiri Exerts Its Immunostimulatory Activity Through Glycan Recognition by Mincle. Front Immunol. 2019;10:1422.

210. Zeuthen LH, Fink LN, Frøkiaer H. Toll-like receptor 2 and nucleotide-binding oligomerization domain-2 play divergent roles in the recognition of gut-derived lactobacilli and bifidobacteria in dendritic cells. Immunology. 2008;124:489–502.

211. Matsuguchi T, Takagi A, Matsuzaki T, Nagaoka M, Ishikawa K, Yokokura T, et al. Lipoteichoic Acids from Lactobacillus Strains Elicit Strong Tumor Necrosis Factor Alpha-Inducing Activities in Macrophages through Toll-Like Receptor 2. Clin Diagn Lab Immunol. 2003;10:259–66.

212. Girardin SE, Boneca IG, Viala J, Chamaillard M, Labigne A, Thomas G, et al. Nod2 Is a General Sensor of Peptidoglycan through Muramyl Dipeptide (MDP) Detection. J Biol Chem. 2003;278:8869–72.

213. Pan X, Chen F, Wu T, Tang H, Zhao Z. The acid, bile tolerance and antimicrobial property of Lactobacillus acidophilus NIT. Food Control. 2009;20:598–602.

214. Kajikawa A, Zhang L, LaVoy A, Bumgardner S, Klaenhammer TR, Dean GA. Mucosal Immunogenicity of Genetically Modified Lactobacillus acidophilus Expressing an HIV-1 Epitope within the Surface Layer Protein. PLOS ONE. 2015;10:e0141713.

215. Shakya AK, Chowdhury MYE, Tao W, Gill HS. Mucosal vaccine delivery: Current state and a pediatric perspective. J Controlled Release. 2016;240:394–413.

216. Raya Tonetti F, Arce L, Salva S, Alvarez S, Takahashi H, Kitazawa H, et al. Immunomodulatory Properties of Bacterium-Like Particles Obtained From Immunobiotic Lactobacilli: Prospects for Their Use as Mucosal Adjuvants. Front Immunol. 2020;11:15.

217. Kajikawa A, Zhang L, Long J, Nordone S, Stoeker L, LaVoy A, et al. Construction and Immunological Evaluation of Dual Cell Surface Display of HIV-1 Gag and Salmonella enterica Serovar Typhimurium FliC in Lactobacillus acidophilus for Vaccine Delivery. Clin Vaccine Immunol. 2012;19:1374–81.

218. Bumgardner SA, Zhang L, LaVoy AS, Andre B, Frank CB, Kajikawa A, et al. Nod2 is required for antigen-specific humoral responses against antigens orally delivered using a recombinant Lactobacillus vaccine platform. PLOS ONE. 2018;13:e0196950.

219. Garrett WS, Gordon JI, Glimcher LH. Homeostasis and Inflammation in the Intestine. Cell. 2010;140:859–70.

220. Sun M, He C, Cong Y, Liu Z. Regulatory immune cells in regulation of intestinal inflammatory response to microbiota. Mucosal Immunol. 2015;8:969–78.

221. Brown EM, Sadarangani M, Finlay BB. The role of the immune system in governing host-microbe interactions in the intestine. Nat Immunol. 2013;14:660–7.

222. Kubinak JL, Round JL. Do antibodies select a healthy microbiota? Nat Rev Immunol. 2016;16:767–74.

223. Sterlin D, Fadlallah J, Slack E, Gorochov G. The antibody/microbiota interface in health and disease. Mucosal Immunol. 2020;13:3–11.

224. Sterlin D, Fadlallah J, Adams O, Fieschi C, Parizot C, Dorgham K, et al. Human IgA binds a diverse array of commensal bacteria. J Exp Med. 2020;217:e20181635.

225. Nakajima A, Vogelzang A, Maruya M, Miyajima M, Murata M, Son A, et al. IgA regulates the composition and metabolic function of gut microbiota by promoting symbiosis between bacteria. J Exp Med. 2018;215:2019–34.

226. Okai S, Usui F, Yokota S, Hori-i Y, Hasegawa M, Nakamura T, et al. High-affinity monoclonal IgA regulates gut microbiota and prevents colitis in mice. Nat Microbiol. 2016;1:16103.

227. de Jong SE, Olin A, Pulendran B. The Impact of the Microbiome on Immunity to Vaccination in Humans. Cell Host Microbe. 2020;28:169–79.

228. Pabst O, Hornef M. Gut Microbiota: A Natural Adjuvant for Vaccination. Immunity. 2014;41:349–51.

229. Sui Y. Influence of gut microbiome on mucosal immune activation and SHIV viral transmission in naive macaques. Mucosal Immunol. 2018;:11.

230. Kim M, Qie Y, Park J, Kim CH. Gut Microbial Metabolites Fuel Host Antibody Responses. Cell Host Microbe. 2016;20:202–14.

231. Zhang Y, Wu Q, Zhou M, Luo Z, Lv L, Pei J, et al. Composition of the murine gut microbiome impacts humoral immunity induced by rabies vaccines. Clin Transl Med. 2020;10. doi:10.1002/ctm2.161.

232. Littman DR. Do the Microbiota Influence Vaccines and Protective Immunity to Pathogens?: If So, Is There Potential for Efficacious Microbiota-Based Vaccines? Cold Spring Harb Perspect Biol. 2018;10:a029355.

233. Ang L, Arboleya S, Lihua G, Chuihui Y, Nan Q, Suarez M, et al. The establishment of the infant intestinal microbiome is not affected by rotavirus vaccination. Sci Rep. 2014;4.

234. Kau AL, Planer JD, Liu J, Rao S, Yatsunenko T, Trehan I, et al. Functional characterization of IgA-targeted bacterial taxa from undernourished Malawian children that produce diet-dependent enteropathy. Sci Transl Med. 2015;7:276ra24.

235. Leeming ER, Johnson AJ, Spector TD, Roy CIL. Effect of Diet on the Gut Microbiota: Rethinking Intervention Duration. Nutrients. 2019;11:28.

236. Lang P, Hasselwander S, Li H, Xia N. Effects of different diets used in diet-induced obesity models on insulin resistance and vascular dysfunction in C57BL/6 mice. Sci Rep. 2019;9:19556.

237. Yatsunenko T, Rey FE, Manary MJ, Trehan I, Dominguez-Bello MG, Contreras M, et al. Human gut microbiome viewed across age and geography. Nature. 2012;486:222–7.

238. Henderson AJ, Kumar A, Barnett B, Dow SW, Ryan EP. Consumption of Rice Bran Increases Mucosal Immunoglobulin A Concentrations and Numbers of Intestinal Lactobacillus spp. J Med Food. 2012;15:469–75.

239. Vandenplas Y, Greef ED, Veereman G. Prebiotics in infant formula. Gut Microbes. 5:7.

240. Duong T, Miller MJ, Barrangou R, Azcarate-Peril MA, Klaenhammer TR. Construction of vectors for inducible and constitutive gene expression in Lactobacillus. Microb Biotechnol. 2011;4:357–67.

241. Stoeker L, Nordone S, Gunderson S, Zhang L, Kajikawa A, LaVoy A, et al. Assessment of Lactobacillus gasseri as a candidate oral vaccine vector. Clin Vaccine Immunol CVI. 2011;18:1834–44.

242. Frey A, Di Canzio J, Zurakowski D. A statistically defined endpoint titer determination method for immunoassays. J Immunol Methods. 1998;221:35–41.

243. Andrews S, Krueger F, Segonds-Pichon A, Biggins L, Krueger C, Wingett S. FastQC: a quality control tool for high throughput sequence data. 2012. https://qubeshub.org/resources/fastqc.

244. Bolger AM, Lohse M, Usadel B. Trimmomatic: a flexible trimmer for Illumina sequence data. Bioinformatics. 2014;30:2114–20.

245. Schloss PD, Westcott SL, Ryabin T, Hall JR, Hartmann M, Hollister EB, et al. Introducing mothur: Open-Source, Platform-Independent, Community-Supported Software for Describing and Comparing Microbial Communities. Appl Environ Microbiol. 2009;75:7537–41.

246. Quast C, Pruesse E, Yilmaz P, Gerken J, Schweer T, Yarza P, et al. The SILVA ribosomal RNA gene database project: improved data processing and web-based tools. Nucleic Acids Res. 2012;41:D590–6.

247. McMurdie PJ, Holmes S. phyloseq: An R Package for Reproducible Interactive Analysis and Graphics of Microbiome Census Data. PLOS ONE. 2013;8:e61217.

248. Oksanen J. vegan: Community Ecology Package. 2014. https://cran.r-project.org, https://github.com/vegandevs/vegan.

249. Paulson JN, Stine OC, Bravo HC, Pop M. Differential abundance analysis for microbial marker-gene surveys. Nat Methods. 2013;10:1200–2.

250. Breiman L. Random Forests. Mach Learn. 2001;45:5–32.

251. Breiman L, Cutler A. Breiman and Cutler's Random Forests for Classification and Regression: Package 'randomForest.' 2018.

252. Hastie T, Friedman JH, Tibshirani R. The Elements of Statistical Learning: Data Mining, Inference, and Prediction; Second Edition. 2009.

253. D'Auria G, Peris-Bondia F, Džunková M, Mira A, Collado MC, Latorre A, et al. Active and secreted IgA-coated bacterial fractions from the human gut reveal an under-represented microbiota core. Sci Rep. 2013;3:3515.

254. Jalanka-Tuovinen J, Salonen A, Nikkilä J, Immonen O, Kekkonen R, Lahti L, et al. Intestinal Microbiota in Healthy Adults: Temporal Analysis Reveals Individual and Common Core and Relation to Intestinal Symptoms. PLOS ONE. 2011;6:e23035.

255. Kirkpatrick BD, McKenzie R, O'Neill JP, Larsson CJ, Bourgeois AL, Shimko J, et al. Evaluation of Salmonella enterica serovar Typhi (Ty2 aroC-ssaV-) M01ZH09, with a defined mutation in the Salmonella pathogenicity island 2, as a live, oral typhoid vaccine in human volunteers. Vaccine. 2006;24:116–23.

256. Zhao X, Zhang M, Li Z, Frankel FR. Vaginal Protection and Immunity after Oral Immunization of Mice with a Novel Vaccine Strain of Listeria monocytogenes Expressing Human Immunodeficiency Virus Type 1 gag. J Virol. 2006;80:8880–90.

257. Molinos-Albert LM, Clotet B, Blanco J, Carrillo J. Immunologic Insights on the Membrane Proximal External Region: A Major Human Immunode ciency Virus Type-1 Vaccine Target. Front Immunol. 2017;8:12.

258. Lapuente D, Storcksdieck genannt Bonsmann M, Maaske A, Stab V, Heinecke V, Watzstedt K, et al. IL-1β as mucosal vaccine adjuvant: the specific induction of tissue-resident memory T cells improves the heterosubtypic immunity against influenza A viruses. Mucosal Immunol. 2018;11:1265–78.

259. Staats HF, Ennis FA. IL-1 is an effective adjuvant for mucosal and systemic immune responses when coadministered with protein immunogens. J Immunol. 1999;162:6141–7.

260. Mestecky J, Russell MW, Elson CO. Perspectives on Mucosal Vaccines: Is Mucosal Tolerance a Barrier? J Immunol. 2007;179:5633–8.

261. Sutmuller RPM, den Brok MHMGM, Kramer M, Bennink EJ, Toonen LWJ, Kullberg B-J, et al. Toll-like receptor 2 controls expansion and function of regulatory T cells. J Clin Invest. 2006;116:485–94.

262. Scholtens PAMJ, Alliet P, Raes M, Alles MS, Kroes H, Boehm G, et al. Fecal Secretory Immunoglobulin A Is Increased in Healthy Infants Who Receive a Formula with Short-Chain Galacto-Oligosaccharides and Long-Chain Fructo-Oligosaccharides. J Nutr. 2008;138:1141–7.

263. Korpe PS, Petri WA. Environmental enteropathy: critical implications of a poorly understood condition. Trends Mol Med. 2012;18:328–36.

264. Uddin MI, Islam S, Nishat NS, Hossain M, Rafique TA, Rashu R, et al. Biomarkers of Environmental Enteropathy are Positively Associated with Immune Responses to an Oral Cholera Vaccine in Bangladeshi Children. PLoS Negl Trop Dis. 2016;10:e0005039.

265. Pabst O, Slack E. IgA and the intestinal microbiota: the importance of being specific. Mucosal Immunol. 2020;13:12–21.

266. Yang Y, Palm NW. Immunoglobulin A and the microbiome. Curr Opin Microbiol. 2020;56:89–96.

267. Shade A, Jones SE, Caporaso JG, Handelsman J, Knight R, Fierer N, et al. Conditionally Rare Taxa Disproportionately Contribute to Temporal Changes in Microbial Diversity. mBio. 2014;5:e01371-14, mBio.01371-14.

268. Rizzatti G, Lopetuso LR, Gibiino G, Binda C, Gasbarrini A. Proteobacteria: A Common Factor in Human Diseases. BioMed Res Int. 2017;2017:1–7.

269. Jousset A, Bienhold C, Chatzinotas A, Gallien L, Gobet A, Kurm V, et al. Where less may be more: how the rare biosphere pulls ecosystems strings. ISME J. 2017;11:853–62.

270. Rosen CE, Palm NW. Functional Classification of the Gut Microbiota: The Key to Cracking the Microbiota Composition Code: Functional classifications of the gut microbiota reveal previously hidden contributions of indigenous gut bacteria to human health and disease. BioEssays. 2017;39:1700032.

271. van der Gast CJ, Walker AW, Stressmann FA, Rogers GB, Scott P, Daniels TW, et al. Partitioning core and satellite taxa from within cystic fibrosis lung bacterial communities. ISME J. 2011;5:780–91.

272. Rogers AWL, Tsolis RM, Bäumler AJ. Salmonella versus the Microbiome. Microbiol Mol Biol Rev. 2021;85:e00027-19.

273. Li H, Li T, Beasley DE, Heděnec P, Xiao Z, Zhang S, et al. Diet Diversity Is Associated with Beta but not Alpha Diversity of Pika Gut Microbiota. Front Microbiol. 2016;7. doi:10.3389/fmicb.2016.01169.

274. Grazul H, Kanda LL, Gondek D. Impact of probiotic supplements on microbiome diversity following antibiotic treatment of mice. Gut Microbes. 2016;7:101–14.

275. Derrien M, van Hylckama Vlieg JET. Fate, activity, and impact of ingested bacteria within the human gut microbiota. Trends Microbiol. 2015;23:354–66.

276. Gerritsen J, Smidt H, Rijkers GT, de Vos WM. Intestinal microbiota in human health and disease: the impact of probiotics. Genes Nutr. 2011;6:209–40.

277. Dassi E, Ferretti P, Covello G, Bertorelli R, Denti MA, De Sanctis V, et al. The short-term impact of probiotic consumption on the oral cavity microbiome. Sci Rep. 2018;8:10476.

278. Vacca M, Celano G, Calabrese FM, Portincasa P, Gobbetti M, De Angelis M. The Controversial Role of Human Gut Lachnospiraceae. Microorganisms. 2020;8:573.

279. Smith-Brown P, Morrison M, Krause L, Davies PSW. Dairy and plant based food intakes are associated with altered faecal microbiota in 2 to 3 year old Australian children. Sci Rep. 2016;6:32385.

280. Wu M-R, Chou T-S, Huang C-Y, Hsiao J-K. A potential probiotic- Lachnospiraceae NK4A136 group: Evidence from the restoration of the dietary pattern from a high-fat diet. 2020. doi:10.21203/rs.3.rs-48913/v1.

281. Wang C, Huang Z, Yu K, Ding R, Ye K, Dai C, et al. High-Salt Diet Has a Certain Impact on Protein Digestion and Gut Microbiota: A Sequencing and Proteome Combined Study. Front Microbiol. 2017;8:1838.

282. Byerley LO, Samuelson D, Blanchard E, Luo M, Lorenzen BN, Banks S, et al. Changes in the gut microbial communities following addition of walnuts to the diet. J Nutr Biochem. 2017;48:94–102.

283. Matsuyama M, Morrison M, Cao K-AL, Pruilh S, Davies PSW, Wall C, et al. Dietary intake influences gut microbiota development of healthy Australian children from the age of one to two years. Sci Rep. 2019;9:12476.

284. Amdekar S, Dwivedi D, Roy P, Kushwah S, Singh V. Probiotics: multifarious oral vaccine against infectious traumas. FEMS Immunol Med Microbiol. 2010;58:299–306.

285. LeCureux JS, Dean GA. *Lactobacillus* Mucosal Vaccine Vectors: Immune Responses against Bacterial and Viral Antigens. mSphere. 2018;3. doi:10.1128/mSphere.00061-18.

286. Wells J. Mucosal Vaccination and Therapy with Genetically Modified Lactic Acid Bacteria. Annu Rev Food Sci Technol. 2011;2:423–45.

287. Abdo Z, LeCureux J, LaVoy A, Eklund B, Ryan EP, Dean GA. Impact of oral probiotic Lactobacillus acidophilus vaccine strains on the immune response and gut microbiome of mice. PLOS ONE. 2019;14:e0225842.

288. Philpott DJ, Sorbara MT, Robertson SJ, Croitoru K, Girardin SE. NOD proteins: regulators of inflammation in health and disease. Nat Rev Immunol. 2014;14:9–23.

289. Al Nabhani Z, Dietrich G, Hugot J-P, Barreau F. Nod2: The intestinal gate keeper. PLOS Pathog. 2017;13:e1006177.

290. Geddes K, Rubino SJ, Magalhaes JG, Streutker C, Le Bourhis L, Cho JH, et al. Identification of an innate T helper type 17 response to intestinal bacterial pathogens. Nat Med. 2011;17:837–44.

291. Biswas A, Liu Y-J, Hao L, Mizoguchi A, Salzman NH, Bevins CL, et al. Induction and rescue of Nod2-dependent Th1-driven granulomatous inflammation of the ileum. Proc Natl Acad Sci. 2010;107:14739–44.

292. Caruso R, Warner N, Inohara N, Núñez G. NOD1 and NOD2: Signaling, Host Defense, and Inflammatory Disease. Immunity. 2014;41:898–908.

293. Wiese KM, Coates BM, Ridge KM. The Role of Nucleotide-Binding Oligomerization Domain–Like Receptors in Pulmonary Infection. Am J Respir Cell Mol Biol. 2017;57:151–61.

294. Kim D, Kim Y-G, Seo S-U, Kim D-J, Kamada N, Prescott D, et al. Nod2-mediated recognition of the microbiota is critical for mucosal adjuvant activity of cholera toxin. Nat Med. 2016;22:524–30.

295. Loving CL, Osorio M, Kim Y-G, Nuñez G, Hughes MA, Merkel TJ. Nod1/Nod2-Mediated Recognition Plays a Critical Role in Induction of Adaptive Immunity to Anthrax after Aerosol Exposure. Infect Immun. 2009;77:4529–37.

296. Kim D, Kim Y, Kim W, Park J, Núñez G, Seo S. Recognition of the microbiota by Nod2 contributes to the oral adjuvant activity of cholera toxin through the induction of interleukin-1 β. Immunology. 2019;158:219–29.

297. Maisonneuve C, Bertholet S, Philpott DJ, De Gregorio E. Unleashing the potential of NOD- and Toll-like agonists as vaccine adjuvants. Proc Natl Acad Sci. 2014;111:12294–9.

298. Khan A, Singh VK, Mishra A, Soudani E, Bakhru P, Singh CR, et al. NOD2/RIG-I Activating Inarigivir Adjuvant Enhances the Efficacy of BCG Vaccine Against Tuberculosis in Mice. Front Immunol. 2020;11:592333.

299. Couturier-Maillard A, Secher T, Rehman A, Normand S, De Arcangelis A, Haesler R, et al. NOD2-mediated dysbiosis predisposes mice to transmissible colitis and colorectal cancer. J Clin Invest. 2013;:JCI62236.

300. Sidiq T, Yoshihama S, Downs I, Kobayashi KS. Nod2: A Critical Regulator of Ileal Microbiota and Crohn's Disease. Front Immunol. 2016;7. doi:10.3389/fimmu.2016.00367.

301. Kennedy NA, Lamb CA, Berry SH, Walker AW, Mansfield J, Parkes M, et al. The Impact of NOD2 Variants on Fecal Microbiota in Crohn's Disease and Controls Without Gastrointestinal Disease. Inflamm Bowel Dis. 2018;24:583–92.

302. Tikka C, Manthari RK, Ommati MM, Niu R, Sun Z, Zhang J, et al. Immune disruption occurs through altered gut microbiome and NOD2 in arsenic induced mice: Correlation with colon cancer markers. Chemosphere. 2020;246:125791.

303. Negroni A, Pierdomenico M, Cucchiara S, Stronati L. NOD2 and inflammation: current insights. J Inflamm Res. 2018;Volume 11:49–60.

304. Goethel A, Croitoru K, Philpott DJ. The interplay between microbes and the immune response in inflammatory bowel disease: Interplay between NOD2, microbiota and immune response in IBD. J Physiol. 2018;596:3869–82.

305. Robertson SJ, Geddes K, Maisonneuve C, Streutker CJ, Philpott DJ. Resilience of the intestinal microbiota following pathogenic bacterial infection is independent of innate immunity mediated by NOD1 or NOD2. Microbes Infect. 2016;18:460–71.

306. Robertson SJ, Zhou JY, Geddes K, Rubino SJ, Cho JH, Girardin SE, et al. Nod1 and Nod2 signaling does not alter the composition of intestinal bacterial communities at homeostasis. Gut Microbes. 2013;4:222–31.

307. Rehman A, Sina C, Gavrilova O, Hasler R, Ott S, Baines JF, et al. Nod2 is essential for temporal development of intestinal microbial communities. Gut. 2011;60:1354–62.

308. Petnicki-Ocwieja T, Hrncir T, Liu Y-J, Biswas A, Hudcovic T, Tlaskalova-Hogenova H, et al. Nod2 is required for the regulation of commensal microbiota in the intestine. Proc Natl Acad Sci. 2009;106:15813–8.

309. Cullen CM, Aneja KK, Beyhan S, Cho CE, Woloszynek S, Convertino M, et al. Emerging Priorities for Microbiome Research. Front Microbiol. 2020;11:136.

310. Robertson JM, Jensen PE, Evavold BD. DO11.10 and OT-II T Cells Recognize a C-Terminal Ovalbumin 323–339 Epitope. J Immunol. 2000;164:4706–12.

311. Goh YJ, Azcï¿½rate-Peril MA, O'Flaherty S, Durmaz E, Valence F, Jardin J, et al. Development and Application of a upp-Based Counterselective Gene Replacement System for the Study of the S-Layer Protein SlpX of Lactobacillus acidophilus NCFM. Appl Environ Microbiol. 2009;75:3093–105.

312. Zanello G, Goethel A, Rouquier S, Prescott D, Robertson SJ, Maisonneuve C, et al. The Cytosolic Microbial Receptor Nod2 Regulates Small Intestinal Crypt Damage and Epithelial Regeneration following T Cell-Induced Enteropathy. J Immunol Baltim Md 1950. 2016;197:345–55.

313. Nolan T, Hands RE, Ogunkolade W, Bustin SA. SPUD: A quantitative PCR assay for the detection of inhibitors in nucleic acid preparations. Anal Biochem. 2006;351:308–10.

314. Livak KJ, Schmittgen TD. Analysis of Relative Gene Expression Data Using Real-Time Quantitative PCR and the 2−ΔΔCT Method. Methods. 2001;25:402–8.

315. FastQC. 2015. https://qubeshub.org/resources/fastqc.

316. Altschul S, Madden TL, Schaffer AA, Zhang J, Zhange Z, Miller W, et al. Gapped BLAST and PSI-BLAST: a new generation of protein database search programs. Nucleic Acids Res. 1997;25:3389–402.

317. Biswas A, Petnicki-Ocwieja T, Kobayashi KS. Nod2: a key regulator linking microbiota to intestinal mucosal immunity. J Mol Med. 2012;90:15–24.

318. Adam A, Ciorbaru R, Ellouz F, Petit J-F, Lederer E. Adjuvant activity of monomeric bacterial cell wall peptidoglycans. Biochem Biophys Res Commun. 1974;56:561–7.

319. Gutjahr A, Papagno L, Vernejoul F, Lioux T, Jospin F, Chanut B, et al. New chimeric TLR7/NOD2 agonist is a potent adjuvant to induce mucosal immune responses. EBioMedicine. 2020;58:102922.

320. Guryanova SV, Khaitov RM. Strategies for Using Muramyl Peptides - Modulators of Innate Immunity of Bacterial Origin - in Medicine. Front Immunol. 2021;12:607178.

321. Sanjabi S, Oh SA, Li MO. Regulation of the Immune Response by TGF-β: From Conception to Autoimmunity and Infection. Cold Spring Harb Perspect Biol. 2017;9:a022236.

322. Kawashima T, Ikari N, Kouchi T, Kowatari Y, Kubota Y, Shimojo N, et al. The molecular mechanism for activating IgA production by Pediococcus acidilactici K15 and the clinical impact in a randomized trial. Sci Rep. 2018;8:5065.

323. Turpin W, Bedrani L, Espin-Garcia O, Xu W, Silverberg MS, Smith MI, et al. Associations of NOD2 polymorphisms with Erysipelotrichaceae in stool of in healthy first degree relatives of Crohn's disease subjects. BMC Med Genet. 2020;21:204.

324. Horowitz JE, Warner N, Staples J, Crowley E, Gosalia N, Murchie R, et al. Mutation spectrum of NOD2 reveals recessive inheritance as a main driver of Early Onset Crohn's Disease. Sci Rep. 2021;11:5595.

325. Lesage S, Zouali H, Cézard J-P, Colombel J-F, Belaiche J, Almer S, et al. CARD15/NOD2 Mutational Analysis and Genotype-Phenotype Correlation in 612 Patients with Inflammatory Bowel Disease. Am J Hum Genet. 2002;70:845–57.

326. Lauro ML, Burch JM, Grimes CL. The effect of NOD2 on the microbiota in Crohn's disease. Curr Opin Biotechnol. 2016;40:97–102.

327. Alnabhani Z, Hugot J-P, Montcuquet N, Le Roux K, Dussaillant M, Roy M, et al. Respective Roles of Hematopoietic and Nonhematopoietic Nod2 on the Gut Microbiota and Mucosal Homeostasis. Inflamm Bowel Dis. 2016;22:763–73.

328. Hiippala K, Barreto G, Burrello C, Diaz-Basabe A, Suutarinen M, Kainulainen V, et al. Novel Odoribacter splanchnicus Strain and Its Outer Membrane Vesicles Exert Immunoregulatory Effects in vitro. Front Microbiol. 2020;11:575455.

329. Shang L, Liu H, Yu H, Chen M, Yang T, Zeng X, et al. Core Altered Microorganisms in Colitis Mouse Model: A Comprehensive Time-Point and Fecal Microbiota Transplantation Analysis. Antibiotics. 2021;10:643.

330. Wu T-R, Lin C-S, Chang C-J, Lin T-L, Martel J, Ko Y-F, et al. Gut commensal *Parabacteroides goldsteinii* plays a predominant role in the anti-obesity effects of polysaccharides isolated from *Hirsutella sinensis*. Gut. 2019;68:248–62.

331. Ndongo S, Lagier J-C, Fournier P-E, Raoult D, Khelaifia S. ' Culturomica massiliensis ', a new bacterium isolated from the human gut. New Microbes New Infect. 2016;13:60–1.

332. Pfister SP, Schären OP, Beldi L, Printz A, Notter MD, Mukherjee M, et al. Uncoupling of invasive bacterial mucosal immunogenicity from pathogenicity. Nat Commun. 2020;11:1978.

333. Park J-S, Choi JW, Jhun J, Kwon JY, Lee B-I, Yang CW, et al. *Lactobacillus acidophilus* Improves Intestinal Inflammation in an Acute Colitis Mouse Model by Regulation of Th17 and Treg Cell Balance and Fibrosis Development. J Med Food. 2018;21:215–24.

Chapter 2 Supplemental Tables and Figures

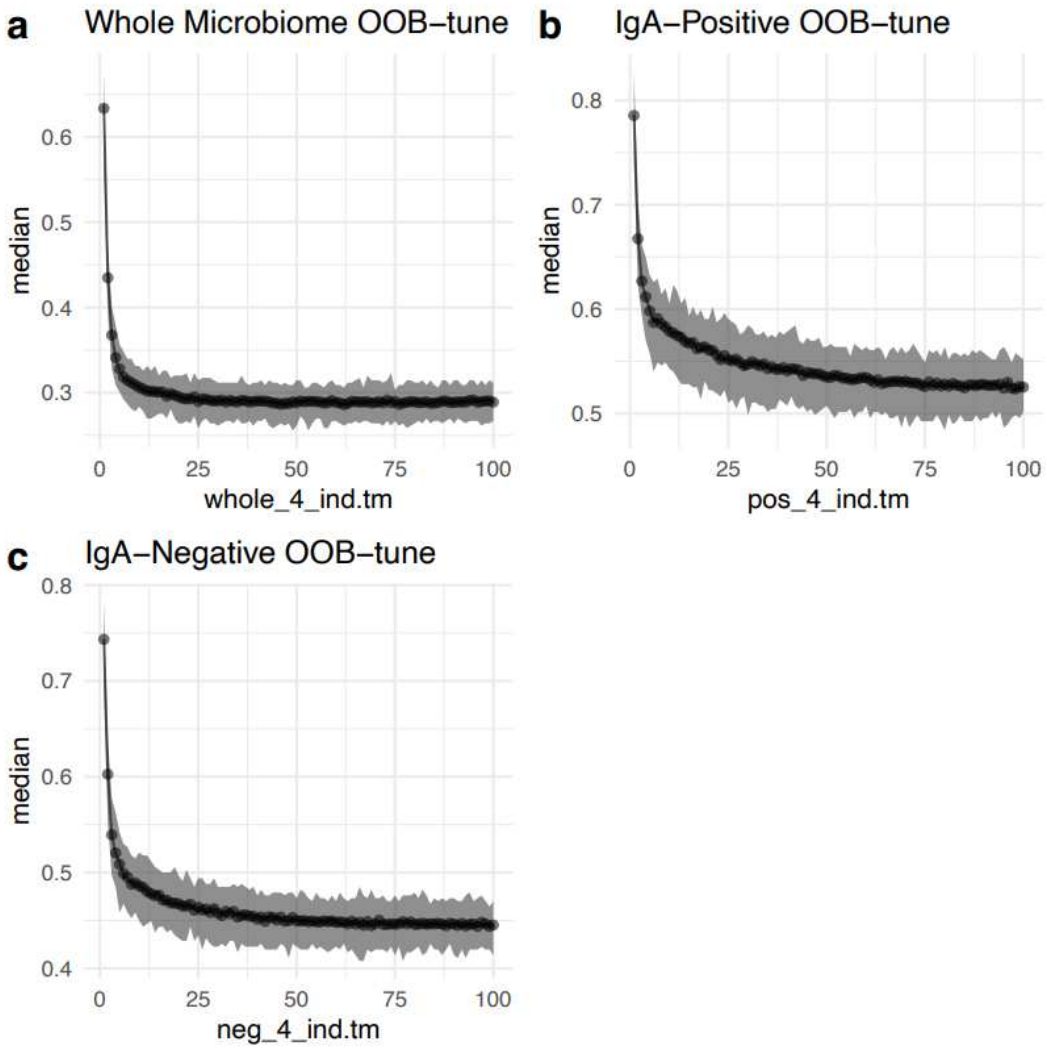

Supplementary Figure S2.1. Iteration of out-of-bag (OOB) error rates. OOB iterations for each microbiome fraction tuning model with (a) whole microbiome, (b) IgA-positive, and (c) IgA-negative fractions. The optimal number of features for each model (separated by microbiome fraction) was selected by iterating over 100 trees, with the median error rates displayed on the x-axis and number of features on the y-axis.

Supplementary Table S2.1. Confusion matrix for treatment RF model. Error rates for classification of treatment (Buffer, NCK1895, or GAD19). The confusion matrices are shown for each microbiome fraction (whole, IgA-positive, and IgA-negative, respectively).

```
Whole:
Call:
 randomForest(x = x_2_whole, y = y_2_whole, ntree = 1000, mtry = 77,      importance = TRUE)
               Type of random forest: classification
                     Number of trees: 1000
No. of variables tried at each split: 77

        OOB estimate of  error rate: 16.57%
Confusion matrix:
       Buffer Gad19 NCK1895 class.error
Buffer     96     3     8   0.1028037
Gad19       4   110    11   0.1200000
NCK1895    16    17    91   0.2661290



IgA_Positive
Call:
 randomForest(x = x_2_pos, y = y_2_pos, ntree = 1000, mtry = 80,      importance = TRUE)
               Type of random forest: classification
                     Number of trees: 1000
No. of variables tried at each split: 80

        OOB estimate of  error rate: 41.84%
Confusion matrix:
       Buffer Gad19 NCK1895 class.error
Buffer     66    23    13   0.3529412
Gad19      14    77    27   0.3474576
NCK1895    32    32    53   0.5470085



IgA_negative
Call:
 randomForest(x = x_2_neg, y = y_2_neg, ntree = 1000, mtry = 74,      importance = TRUE)
               Type of random forest: classification
                     Number of trees: 1000
No. of variables tried at each split: 74

        OOB estimate of  error rate: 38.1%
Confusion matrix:
       Buffer Gad19 NCK1895 class.error
Buffer     61    17    22   0.3900000
Gad19      11    90    18   0.2436975
NCK1895    26    34    57   0.5128205
```

Supplementary Table S2.2. Confusion matrix for diet RF model. Error rates for classification of diet (rice bran or standard chow). The confusion matrices are shown for each microbiome fraction (whole, IgA-positive, and IgA-negative, respectively).

```
Whole:
Call:
 randomForest(x = x_3_whole, y = y_3_whole, ntree = 1000, mtry = 5,      importance = TRUE)
               Type of random forest: classification
                     Number of trees: 1000
No. of variables tried at each split: 5

        OOB estimate of  error rate: 14.61%
Confusion matrix:
          Rice_bran Standard_chow  class.error
Rice_bran       144            36   0.20000000
Standard_chow    16           160   0.09090909




IgA_Positive
Call:
 randomForest(x = x_3_pos, y = y_3_pos, ntree = 1000, mtry = 66,      importance = TRUE)
               Type of random forest: classification
                     Number of trees: 1000
No. of variables tried at each split: 66

        OOB estimate of  error rate: 25.82%
Confusion matrix:
          Rice_bran Standard_chow  class.error
Rice_bran       125            46    0.2690058
Standard_chow    41           125    0.2469880




IgA_negative
Call:
 randomForest(x = x_3_neg, y = y_3_neg, ntree = 1000, mtry = 97,      importance = TRUE)
               Type of random forest: classification
                     Number of trees: 1000
No. of variables tried at each split: 97

        OOB estimate of  error rate: 24.11%
Confusion matrix:
          Rice_bran Standard_chow  class.error
Rice_bran       121            44    0.2666667
Standard_chow    37           134    0.2163743
```

Supplementary Table S2.3. Mean decreasing Gini coefficients for whole microbiome features. The top 150 features from the RF model are shown with their taxonomic classification. Extension of MDG coefficients shown in Figure 2.11. MDG: Mean decreasing Gini.

Feature	Kingdom	Phylum	Class	Order	Family	Genus	MDG
Otu0023	Bacteria	Firmicutes	Clostridia	Clostridiales	Lachnospiraceae	Lachnospiraceae_UCG-001	1
Otu0109	Bacteria	Firmicutes	Clostridia	Clostridiales	Lachnospiraceae	uncultured	0.986265
Otu0071	Bacteria	Firmicutes	Clostridia	Clostridiales	Ruminococcaceae	Ruminococcaceae_UCG-005	0.797841
Otu0073	Bacteria	Tenericutes	Mollicutes	Anaeroplasmatales	Anaeroplasmataceae	Anaeroplasma	0.77873
Otu0157	Bacteria	Firmicutes	Clostridia	Clostridiales	Ruminococcaceae	Oscillibacter	0.777496
Otu0061	Bacteria	Firmicutes	Clostridia	Clostridiales	Lachnospiraceae	Lachnospiraceae_NK4A136_group	0.715178
Otu0010	Bacteria	Firmicutes	Clostridia	Clostridiales	Lachnospiraceae	Lachnospiraceae_NK4A136_group	0.700986
Otu0089	Bacteria	Firmicutes	Clostridia	Clostridiales	Ruminococcaceae	Anaerotruncus	0.658964
Otu0070	Bacteria	Firmicutes	Erysipelotrichia	Erysipelotrichales	Erysipelotrichaceae	Erysipelatoclostridium	0.494404
Otu0068	Bacteria	Firmicutes	Clostridia	Clostridiales	Lachnospiraceae	Lachnospiraceae_unc	0.491523
Otu0100	Bacteria	Firmicutes	Clostridia	Clostridiales	Lachnospiraceae	uncultured	0.48781
Otu0104	Bacteria	Firmicutes	Clostridia	Clostridiales	Lachnospiraceae	Tyzzerella	0.475825
Otu0087	Bacteria	Firmicutes	Bacilli	Lactobacillales	Streptococcaceae	Lactococcus	0.463715
Otu0057	Bacteria	Firmicutes	Clostridia	Clostridiales	Lachnospiraceae	uncultured	0.431506
Otu0013	Bacteria	Firmicutes	Clostridia	Clostridiales	Lachnospiraceae	Lachnospiraceae_NK4A136_group	0.356777
Otu0037	Bacteria	Firmicutes	Clostridia	Clostridiales	Lachnospiraceae	Lachnospiraceae_unc	0.351467
Otu0024	Bacteria	Firmicutes	Clostridia	Clostridiales	Ruminococcaceae	Ruminococcaceae_ge	0.344948
Otu0048	Bacteria	Firmicutes	Clostridia	Clostridiales	Lachnospiraceae	Acetatifactor	0.336915
Otu0053	Bacteria	Firmicutes	Clostridia	Clostridiales	Lachnospiraceae	Lachnospiraceae_UCG-006	0.332727
Otu0040	Bacteria	Firmicutes	Clostridia	Clostridiales	Lachnospiraceae	Lachnospiraceae_NK4A136_group	0.301761
Otu0015	Bacteria	Firmicutes	Clostridia	Clostridiales	Lachnospiraceae	Roseburia	0.219227
Otu0026	Bacteria	Firmicutes	Clostridia	Clostridiales	Lachnospiraceae	Lachnospiraceae_unc	0.204112
Otu0051	Bacteria	Firmicutes	Clostridia	Clostridiales	Ruminococcaceae	Ruminococcaceae_UCG-014	0.199991
Otu0064	Bacteria	Firmicutes	Erysipelotrichia	Erysipelotrichales	Erysipelotrichaceae	Turicibacter	0.189668
Otu0047	Bacteria	Firmicutes	Clostridia	Clostridiales	Lachnospiraceae	Lachnospiraceae_unc	0.181059
Otu0081	Bacteria	Firmicutes	Clostridia	Clostridiales	Lachnospiraceae	Lachnoclostridium	0.181054
Otu0161	Bacteria	Firmicutes	Clostridia	Clostridiales	Clostridiales_vadinBB60_group	Clostridiales_vadinBB60_group_ge	0.164678
Otu0009	Bacteria	Firmicutes	Clostridia	Clostridiales	Clostridiaceae_1	Clostridium_sensu_stricto_1	0.163278
Otu0042	Bacteria	Firmicutes	Clostridia	Clostridiales	Lachnospiraceae	Lachnospiraceae_unc	0.149017
Otu0076	Bacteria	Firmicutes	Clostridia	Clostridiales	Lachnospiraceae	uncultured	0.146486
Otu0097	Bacteria	Firmicutes	Clostridia	Clostridiales	Lachnospiraceae	GCA-900066575	0.142831
Otu0096	Bacteria	Firmicutes	Clostridia	Clostridiales	Lachnospiraceae	uncultured	0.140324
Otu0151	Bacteria	Firmicutes	Clostridia	Clostridiales	Lachnospiraceae	Lachnospiraceae_unc	0.133589
Otu0139	Bacteria	Firmicutes	Clostridia	Clostridiales	Lachnospiraceae	Lachnospiraceae_NK4A136_group	0.130322
Otu0168	Bacteria	Firmicutes	Clostridia	Clostridiales	Clostridiales_vadinBB60_group	Clostridiales_vadinBB60_group_ge	0.121859
Otu0184	Bacteria	Firmicutes	Clostridia	Clostridiales	Lachnospiraceae	Lachnospiraceae_unc	0.108888
Otu0091	Bacteria	Firmicutes	Clostridia	Clostridiales	Lachnospiraceae	Lachnospiraceae_FCS020_group	0.104076
Otu0018	Bacteria	Firmicutes	Clostridia	Clostridiales	Ruminococcaceae	Ruminococcaceae_unc	0.10148
Otu0142	Bacteria	Firmicutes	Clostridia	Clostridiales	Lachnospiraceae	Lachnospiraceae_unc	0.098501
Otu0075	Bacteria	Firmicutes	Clostridia	Clostridiales	Lachnospiraceae	Lachnospiraceae_unc	0.093059
Otu0036	Bacteria	Firmicutes	Clostridia	Clostridiales	Lachnospiraceae	Lachnospiraceae_unc	0.091861
Otu0012	Bacteria	Firmicutes	Clostridia	Clostridiales	Lachnospiraceae	Lachnospiraceae_unc	0.087298
Otu0195	Bacteria	Firmicutes	Clostridia	Clostridiales	Clostridiales_unc	Clostridiales_unc	0.086837
Otu0088	Bacteria	Firmicutes	Clostridia	Clostridiales	Ruminococcaceae	Butyricicoccus	0.086435
Otu0006	Bacteria	Firmicutes	Clostridia	Clostridiales	Lachnospiraceae	Lachnospiraceae_unc	0.083263
Otu0111	Bacteria	Firmicutes	Clostridia	Clostridiales	Lachnospiraceae	Lachnospiraceae_unc	0.078221
Otu0190	Bacteria	Firmicutes	Clostridia	Clostridiales	Lachnospiraceae	Lachnospiraceae_unc	0.077403
Otu0162	Bacteria	Firmicutes	Clostridia	Clostridiales	Lachnospiraceae	Lachnospiraceae_unc	0.07721
Otu0153	Bacteria	Firmicutes	Clostridia	Clostridiales	Ruminococcaceae	Ruminococcaceae_unc	0.076318

Otu0106	Bacteria	Firmicutes	Clostridia	Clostridiales	Peptococcaceae	uncultured	0.069227
Otu0084	Bacteria	Firmicutes	Clostridia	Clostridiales	Ruminococcaceae	Ruminiclostridium_6	0.068597
Otu0028	Bacteria	Firmicutes	Clostridia	Clostridiales	Lachnospiraceae	Lachnospiraceae_unc	0.064591
Otu0016	Bacteria	Firmicutes	Clostridia	Clostridiales	Lachnospiraceae	Lachnospiraceae_unc	0.060983
Otu0159	Bacteria	Firmicutes	Clostridia	Clostridiales	Ruminococcaceae	Ruminococcaceae_UCG-009	0.058549
Otu0098	Bacteria	Firmicutes	Clostridia	Clostridiales	Ruminococcaceae	Ruminococcaceae_UCG-014	0.057557
Otu0020	Bacteria	Firmicutes	Clostridia	Clostridiales	Lachnospiraceae	Lachnospiraceae_NK4A136_group	0.054215
Otu0212	Bacteria	Firmicutes	Clostridia	Clostridiales	Ruminococcaceae	Ruminococcaceae_unc	0.050373
Otu0011	Bacteria	Firmicutes	Clostridia	Clostridiales	Lachnospiraceae	Lachnospiraceae_NK4A136_group	0.047623
Otu0027	Bacteria	Firmicutes	Clostridia	Clostridiales	Lachnospiraceae	Acetatifactor	0.044714
Otu0095	Bacteria	Firmicutes	Clostridia	Clostridiales	Lachnospiraceae	Lachnospiraceae_NK4A136_group	0.044558
Otu0115	Bacteria	Firmicutes	Clostridia	Clostridiales	Lachnospiraceae	Tyzzerella_3	0.044352
Otu0029	Bacteria	Firmicutes	Clostridia	Clostridiales	Lachnospiraceae	Lachnospiraceae_unc	0.043583
Otu0149	Bacteria	Firmicutes	Clostridia	Clostridiales	Ruminococcaceae	Ruminococcaceae_NK4A214_group	0.041736
Otu0017	Bacteria	Firmicutes	Bacilli	Lactobacillales	Lactobacillaceae	Lactobacillus	0.040728
Otu0164	Bacteria	Firmicutes	Clostridia	Clostridiales	Ruminococcaceae	Ruminococcaceae_UCG-014	0.039596
Otu0019	Bacteria	Firmicutes	Clostridia	Clostridiales	Ruminococcaceae	Ruminiclostridium_9	0.037651
Otu0155	Bacteria	Firmicutes	Clostridia	Clostridiales	Ruminococcaceae	Anaerotruncus	0.035314
Otu0178	Bacteria	Firmicutes	Clostridia	Clostridiales	Lachnospiraceae	Lachnospiraceae_unc	0.03289
Otu0171	Bacteria	Firmicutes	Clostridia	Clostridiales	Ruminococcaceae	Ruminococcaceae_UCG-010	0.032788
Otu0031	Bacteria	Firmicutes	Clostridia	Clostridiales	Lachnospiraceae	Marvinbryantia	0.031412
Otu0173	Bacteria	Firmicutes	Clostridia	Clostridiales	Ruminococcaceae	Ruminococcaceae_UCG-014	0.03091
Otu0083	Bacteria	Firmicutes	Clostridia	Clostridiales	Ruminococcaceae	Ruminococcaceae_UCG-014	0.028143
Otu0137	Bacteria	Firmicutes	Clostridia	Clostridiales	Lachnospiraceae	Lachnospiraceae_unc	0.027853
Otu0121	Bacteria	Firmicutes	Clostridia	Clostridiales	Lachnospiraceae	Lachnospiraceae_unc	0.026869
Otu0086	Bacteria	Firmicutes	Clostridia	Clostridiales	Lachnospiraceae	Lachnospiraceae_unc	0.026031
Otu0174	Bacteria	Firmicutes	Clostridia	Clostridiales	Lachnospiraceae	Lachnospiraceae_unc	0.025641
Otu0130	Bacteria	Firmicutes	Clostridia	Clostridiales	Ruminococcaceae	Oscillibacter	0.023628
Otu0055	Bacteria	Firmicutes	Clostridia	Clostridiales	Lachnospiraceae	A2	0.023394
Otu0035	Bacteria	Proteobacteria	Gammaproteobacteria	Enterobacteriales	Enterobacteriaceae	Enterobacteriaceae_unc	0.022122
Otu0146	Bacteria	Firmicutes	Clostridia	Clostridiales	Lachnospiraceae	Lachnospiraceae_unc	0.021789
Otu0144	Bacteria	Firmicutes	Clostridia	Clostridiales	Lachnospiraceae	Lachnospiraceae_unc	0.021667
Otu0110	Bacteria	Firmicutes	Clostridia	Clostridiales	Lachnospiraceae	Lachnospiraceae_unc	0.020556
Otu0078	Bacteria	Firmicutes	Clostridia	Clostridiales	Ruminococcaceae	Ruminococcaceae_UCG-014	0.019954
Otu0129	Bacteria	Firmicutes	Clostridia	Clostridiales	Ruminococcaceae	Ruminococcaceae_UCG-014	0.018902
Otu0189	Bacteria	Firmicutes	Clostridia	Clostridiales	Lachnospiraceae	Lachnospiraceae_unc	0.017437
Otu0193	Bacteria	Firmicutes	Clostridia	Clostridiales	Ruminococcaceae	Ruminiclostridium	0.017413
Otu0202	Bacteria	Firmicutes	Clostridia	Clostridiales	Clostridiales_vadinBB60_group	Clostridiales_vadinBB60_group_ge	0.016698
Otu0090	Bacteria	Firmicutes	Clostridia	Clostridiales	Ruminococcaceae	Ruminococcaceae_unc	0.016095
Otu0134	Bacteria	Firmicutes	Clostridia	Clostridiales	Lachnospiraceae	Lachnospiraceae_NK4B4_group	0.016033
Otu0141	Bacteria	Actinobacteria	Coriobacteriia	Coriobacteriales	Eggerthellaceae	Eggerthellaceae_unc	0.015963
Otu0003	Bacteria	Firmicutes	Clostridia	Clostridiales	Lachnospiraceae	Lachnospiraceae_NK4A136_group	0.015735
Otu0079	Bacteria	Firmicutes	Clostridia	Clostridiales	Lachnospiraceae	Lachnospiraceae_unc	0.015678
Otu0056	Bacteria	Firmicutes	Clostridia	Clostridiales	Lachnospiraceae	uncultured	0.015672
Otu0183	Bacteria	Firmicutes	Clostridia	Clostridiales	Ruminococcaceae	Ruminiclostridium_5	0.015511
Otu0001	Bacteria	Bacteroidetes	Bacteroidia	Bacteroidales	Muribaculaceae	Muribaculaceae_ge	0.015172
Otu0192	Bacteria	Firmicutes	Clostridia	Clostridiales	Lachnospiraceae	Lachnospiraceae_UCG-006	0.014953
Otu0116	Bacteria	Firmicutes	Clostridia	Clostridiales	Lachnospiraceae	Lachnospiraceae_unc	0.014708
Otu0166	Bacteria	Firmicutes	Clostridia	Clostridiales	Ruminococcaceae	Oscillibacter	0.013977
Otu0118	Bacteria	Firmicutes	Clostridia	Clostridiales	Clostridiales_vadinBB60_group	Clostridiales_vadinBB60_group_ge	0.013439
Otu0099	Bacteria	Actinobacteria	Coriobacteriia	Coriobacteriales	Eggerthellaceae	Adlercreutzia	0.013032
Otu0092	Bacteria	Firmicutes	Clostridia	Clostridiales	Lachnospiraceae	Lachnospiraceae_unc	0.012929
Otu0120	Bacteria	Firmicutes	Clostridia	Clostridiales	Ruminococcaceae	Ruminococcaceae_unc	0.012664
Otu0145	Bacteria	Firmicutes	Clostridia	Clostridiales	Lachnospiraceae	Lachnospiraceae_unc	0.012052

Otu0043	Bacteria	Firmicutes	Clostridia	Clostridiales	Ruminococcaceae	Ruminiclostridium	0.011127
Otu0147	Bacteria	Firmicutes	Clostridia	Clostridiales	Lachnospiraceae	Lachnospiraceae_unc	0.011042
Otu0108	Bacteria	Firmicutes	Clostridia	Clostridiales	Lachnospiraceae	Lachnospiraceae_unc	0.010955
Otu0117	Bacteria	Firmicutes	Clostridia	Clostridiales	Ruminococcaceae	Ruminiclostridium	0.010484
Otu0182	Bacteria	Firmicutes	Clostridia	Clostridiales	Lachnospiraceae	Lachnospiraceae_unc	0.010378
Otu0065	Bacteria	Firmicutes	Bacilli	Lactobacillales	Enterococcaceae	Enterococcus	0.010241
Otu0102	Bacteria	Firmicutes	Clostridia	Clostridiales	Ruminococcaceae	Ruminococcaceae_unc	0.010223
Otu0257	Bacteria	Firmicutes	Clostridia	Clostridiales	Ruminococcaceae	Ruminiclostridium_5	0.010125
Otu0112	Bacteria	Firmicutes	Clostridia	Clostridiales	Lachnospiraceae	Lachnospiraceae_unc	0.009337
Otu0158	Bacteria	Firmicutes	Clostridia	Clostridiales	Ruminococcaceae	Ruminococcaceae_unc	0.009294
Otu0255	Bacteria	Firmicutes	Clostridia	Clostridiales	Ruminococcaceae	Oscillibacter	0.009148
Otu0196	Bacteria	Firmicutes	Erysipelotrichia	Erysipelotrichales	Erysipelotrichaceae	Erysipelotrichaceae_unc	0.00901
Otu0234	Bacteria	Bacteroidetes	Bacteroidia	Bacteroidales	Muribaculaceae	Muribaculaceae_ge	0.00897
Otu0005	Bacteria	Bacteroidetes	Bacteroidia	Bacteroidales	Muribaculaceae	Muribaculaceae_ge	0.008925
Otu0030	Bacteria	Firmicutes	Clostridia	Clostridiales	Ruminococcaceae	Oscillibacter	0.008556
Otu0180	Bacteria	Firmicutes	Clostridia	Clostridiales	Ruminococcaceae	Oscillibacter	0.007668
Otu0025	Bacteria	Firmicutes	Clostridia	Clostridiales	Lachnospiraceae	Lachnospiraceae_unc	0.007207
Otu0179	Bacteria	Firmicutes	Clostridia	Clostridiales	Lachnospiraceae	Lachnospiraceae_unc	0.007047
Otu0216	Bacteria	Firmicutes	Clostridia	Clostridiales	Lachnospiraceae	Lachnospiraceae_unc	0.006945
Otu0069	Bacteria	Firmicutes	Clostridia	Clostridiales	Lachnospiraceae	uncultured	0.006728
Otu0235	Bacteria	Firmicutes	Clostridia	Clostridiales	Clostridiales_vadinBB60_group	Clostridiales_vadinBB60_group_ge	0.006388
Otu0058	Bacteria	Firmicutes	Clostridia	Clostridiales	Lachnospiraceae	uncultured	0.006387
Otu0222	Bacteria	Firmicutes	Erysipelotrichia	Erysipelotrichales	Erysipelotrichaceae	Candidatus_Stoquefichus	0.006121
Otu0114	Bacteria	Firmicutes	Clostridia	Clostridiales	Lachnospiraceae	Lachnospiraceae_unc	0.005893
Otu0077	Bacteria	Firmicutes	Clostridia	Clostridiales	Ruminococcaceae	Ruminiclostridium_9	0.005684
Otu0059	Bacteria	Firmicutes	Clostridia	Clostridiales	Lachnospiraceae	GCA-900066575	0.005679
Otu0259	Bacteria	Tenericutes	Mollicutes	Mollicutes_RF39	Mollicutes_RF39_fa	Mollicutes_RF39_ge	0.005605
Otu0186	Bacteria	Firmicutes	Clostridia	Clostridiales	Lachnospiraceae	Lachnospiraceae_unc	0.005267
Otu0004	Bacteria	Firmicutes	Bacilli	Lactobacillales	Lactobacillaceae	Lactobacillus	0.005225
Otu0243	Bacteria	Firmicutes	Clostridia	Clostridiales	Lachnospiraceae	Lachnospiraceae_unc	0.004757
Otu0245	Bacteria	Firmicutes	Clostridia	Clostridiales	Ruminococcaceae	Ruminococcaceae_unc	0.004607
Otu0150	Bacteria	Firmicutes	Clostridia	Clostridiales	Lachnospiraceae	Lachnospiraceae_unc	0.004483
Otu0066	Bacteria	Firmicutes	Clostridia	Clostridiales	Lachnospiraceae	Lachnospiraceae_unc	0.003853
Otu0185	Bacteria	Firmicutes	Clostridia	Clostridiales	Ruminococcaceae	Ruminococcaceae_unc	0.003768
Otu0229	Bacteria	Firmicutes	Clostridia	Clostridiales	Lachnospiraceae	Lachnospiraceae_NK4A136_group	0.003768
Otu0163	Bacteria	Firmicutes	Clostridia	Clostridiales	Lachnospiraceae	Lachnospiraceae_unc	0.003742
Otu0218	Bacteria	Firmicutes	Clostridia	Clostridiales	Ruminococcaceae	Ruminococcaceae_UCG-014	0.003643
Otu0107	Bacteria	Proteobacteria	Alphaproteobacteria	Rhizobiales	Rhizobiaceae	Brucella	0.00355
Otu0236	Bacteria	Firmicutes	Clostridia	Clostridiales	Ruminococcaceae	Ruminiclostridium_9	0.003345
Otu0228	Bacteria	Tenericutes	Mollicutes	Mollicutes_RF39	Mollicutes_RF39_fa	Mollicutes_RF39_ge	0.003245
Otu0230	Bacteria	Firmicutes	Clostridia	Clostridiales	Lachnospiraceae	Lachnospiraceae_unc	0.003181
Otu0062	Bacteria	Proteobacteria	Alphaproteobacteria	Rhizobiales	Rhizobiaceae	Rhizobiaceae_unc	0.003053
Otu0154	Bacteria	Firmicutes	Clostridia	Clostridiales	Lachnospiraceae	Lachnospiraceae_unc	0.002947
Otu0214	Bacteria	Firmicutes	Clostridia	Clostridiales	Lachnospiraceae	Lachnospiraceae_UCG-001	0.002856
Otu0022	Bacteria	Proteobacteria	Gammaproteobacteria	Enterobacteriales	Enterobacteriaceae	Escherichia-Shigella	0.002191
Otu0253	Bacteria	Firmicutes	Clostridia	Clostridiales	Clostridiales_vadinBB60_group	Clostridiales_vadinBB60_group_ge	0.002055

Supplementary Table S2.4. MDG coefficients from IgA-positive Random Forest model. The top 150 features are shown with assigned taxonomic classification.

Feature	Kingdom	Phylum	Class	Order	Family	Genus	MDG
Otu0071	Bacteria	Firmicutes	Clostridia	Clostridiales	Ruminococcaceae	Ruminococcaceae_UCG-005	1
Otu0023	Bacteria	Firmicutes	Clostridia	Clostridiales	Lachnospiraceae	Lachnospiraceae_UCG-001	0.67293
Otu0087	Bacteria	Firmicutes	Bacilli	Lactobacillales	Streptococcaceae	Lactococcus	0.467362
Otu0009	Bacteria	Firmicutes	Clostridia	Clostridiales	Clostridiaceae_1	Clostridium_sensu_stricto_1	0.436323
Otu0100	Bacteria	Firmicutes	Clostridia	Clostridiales	Lachnospiraceae	uncultured	0.322184
Otu0089	Bacteria	Firmicutes	Clostridia	Clostridiales	Ruminococcaceae	Anaerotruncus	0.289518
Otu0053	Bacteria	Firmicutes	Clostridia	Clostridiales	Lachnospiraceae	Lachnospiraceae_UCG-006	0.268312
Otu0076	Bacteria	Firmicutes	Clostridia	Clostridiales	Lachnospiraceae	uncultured	0.228268
Otu0048	Bacteria	Firmicutes	Clostridia	Clostridiales	Lachnospiraceae	Acetatifactor	0.2197
Otu0109	Bacteria	Firmicutes	Clostridia	Clostridiales	Lachnospiraceae	uncultured	0.217344
Otu0064	Bacteria	Firmicutes	Erysipelotrichia	Erysipelotrichales	Erysipelotrichaceae	Turicibacter	0.187751
Otu0026	Bacteria	Firmicutes	Clostridia	Clostridiales	Lachnospiraceae	Lachnospiraceae_unc	0.182919
Otu0010	Bacteria	Firmicutes	Clostridia	Clostridiales	Lachnospiraceae	Lachnospiraceae_NK4A136_group	0.178079
Otu0070	Bacteria	Firmicutes	Erysipelotrichia	Erysipelotrichales	Erysipelotrichaceae	Erysipelatoclostridium	0.177375
Otu0017	Bacteria	Firmicutes	Bacilli	Lactobacillales	Lactobacillaceae	Lactobacillus	0.176532
Otu0047	Bacteria	Firmicutes	Clostridia	Clostridiales	Lachnospiraceae	Lachnospiraceae_unc	0.170573
Otu0061	Bacteria	Firmicutes	Clostridia	Clostridiales	Lachnospiraceae	Lachnospiraceae_NK4A136_group	0.160885
Otu0051	Bacteria	Firmicutes	Clostridia	Clostridiales	Ruminococcaceae	Ruminococcaceae_UCG-014	0.135477
Otu0084	Bacteria	Firmicutes	Clostridia	Clostridiales	Ruminococcaceae	Ruminiclostridium_6	0.13113
Otu0057	Bacteria	Firmicutes	Clostridia	Clostridiales	Lachnospiraceae	uncultured	0.112944
Otu0111	Bacteria	Firmicutes	Clostridia	Clostridiales	Lachnospiraceae	Lachnospiraceae_unc	0.105924
Otu0075	Bacteria	Firmicutes	Clostridia	Clostridiales	Lachnospiraceae	Lachnospiraceae_unc	0.101105
Otu0184	Bacteria	Firmicutes	Clostridia	Clostridiales	Lachnospiraceae	Lachnospiraceae_unc	0.091289
Otu0024	Bacteria	Firmicutes	Clostridia	Clostridiales	Ruminococcaceae	Ruminococcaceae_ge	0.090989
Otu0096	Bacteria	Firmicutes	Clostridia	Clostridiales	Lachnospiraceae	uncultured	0.087982
Otu0142	Bacteria	Firmicutes	Clostridia	Clostridiales	Lachnospiraceae	Lachnospiraceae_unc	0.08151
Otu0068	Bacteria	Firmicutes	Clostridia	Clostridiales	Lachnospiraceae	Lachnospiraceae_unc	0.081454
Otu0040	Bacteria	Firmicutes	Clostridia	Clostridiales	Lachnospiraceae	Lachnospiraceae_NK4A136_group	0.080927
Otu0055	Bacteria	Firmicutes	Clostridia	Clostridiales	Lachnospiraceae	A2	0.062543
Otu0006	Bacteria	Firmicutes	Clostridia	Clostridiales	Lachnospiraceae	Lachnospiraceae_unc	0.060795
Otu0013	Bacteria	Firmicutes	Clostridia	Clostridiales	Lachnospiraceae	Lachnospiraceae_NK4A136_group	0.057608
Otu0157	Bacteria	Firmicutes	Clostridia	Clostridiales	Ruminococcaceae	Oscillibacter	0.056628
Otu0015	Bacteria	Firmicutes	Clostridia	Clostridiales	Lachnospiraceae	Roseburia	0.056373
Otu0035	Bacteria	Proteobacteria	Gammaproteobacteria	Enterobacteriales	Enterobacteriaceae	Enterobacteriaceae_unc	0.053858
Otu0097	Bacteria	Firmicutes	Clostridia	Clostridiales	Lachnospiraceae	GCA-900066575	0.049912
Otu0139	Bacteria	Firmicutes	Clostridia	Clostridiales	Lachnospiraceae	Lachnospiraceae_NK4A136_group	0.048476
Otu0020	Bacteria	Firmicutes	Clostridia	Clostridiales	Lachnospiraceae	Lachnospiraceae_NK4A136_group	0.047895
Otu0014	Bacteria	Firmicutes	Clostridia	Clostridiales	Lachnospiraceae	Lachnospiraceae_NK4A136_group	0.044379
Otu0037	Bacteria	Firmicutes	Clostridia	Clostridiales	Lachnospiraceae	Lachnospiraceae_unc	0.039064
Otu0125	Bacteria	Firmicutes	Erysipelotrichia	Erysipelotrichales	Erysipelotrichaceae	uncultured	0.037786
Otu0059	Bacteria	Firmicutes	Clostridia	Clostridiales	Lachnospiraceae	GCA-900066575	0.037396
Otu0042	Bacteria	Firmicutes	Clostridia	Clostridiales	Lachnospiraceae	Lachnospiraceae_unc	0.037386
Otu0056	Bacteria	Firmicutes	Clostridia	Clostridiales	Lachnospiraceae	uncultured	0.035669
Otu0105	Bacteria	Firmicutes	Clostridia	Clostridiales	Lachnospiraceae	Lachnospiraceae_unc	0.035371
Otu0028	Bacteria	Firmicutes	Clostridia	Clostridiales	Lachnospiraceae	Lachnospiraceae_unc	0.033542
Otu0039	Bacteria	Firmicutes	Clostridia	Clostridiales	Lachnospiraceae	Lachnospiraceae_unc	0.031761
Otu0145	Bacteria	Firmicutes	Clostridia	Clostridiales	Lachnospiraceae	Lachnospiraceae_unc	0.030187
Otu0038	Bacteria	Firmicutes	Clostridia	Clostridiales	Lachnospiraceae	Lachnospiraceae_unc	0.028933
Otu0162	Bacteria	Firmicutes	Clostridia	Clostridiales	Lachnospiraceae	Lachnospiraceae_unc	0.026729
Otu0063	Bacteria	Firmicutes	Clostridia	Clostridiales	Lachnospiraceae	Lachnospiraceae_unc	0.026472
Otu0090	Bacteria	Firmicutes	Clostridia	Clostridiales	Ruminococcaceae	Ruminococcaceae_unc	0.02641

Otu0083	Bacteria	Firmicutes	Clostridia	Clostridiales	Ruminococcaceae	Ruminococcaceae_UCG-014	0.025417
Otu0116	Bacteria	Firmicutes	Clostridia	Clostridiales	Lachnospiraceae	Lachnospiraceae_unc	0.025203
Otu0022	Bacteria	Proteobacteria	Gammaproteobacteria	Enterobacteriales	Enterobacteriaceae	Escherichia-Shigella	0.023676
Otu0110	Bacteria	Firmicutes	Clostridia	Clostridiales	Lachnospiraceae	Lachnospiraceae_unc	0.023516
Otu0058	Bacteria	Firmicutes	Clostridia	Clostridiales	Lachnospiraceae	uncultured	0.023402
Otu0081	Bacteria	Firmicutes	Clostridia	Clostridiales	Lachnospiraceae	Lachnoclostridium	0.022538
Otu0016	Bacteria	Firmicutes	Clostridia	Clostridiales	Lachnospiraceae	Lachnospiraceae_unc	0.022307
Otu0092	Bacteria	Firmicutes	Clostridia	Clostridiales	Lachnospiraceae	Lachnospiraceae_unc	0.021656
Otu0117	Bacteria	Firmicutes	Clostridia	Clostridiales	Ruminococcaceae	Ruminiclostridium	0.021538
Otu0036	Bacteria	Firmicutes	Clostridia	Clostridiales	Lachnospiraceae	Lachnospiraceae_unc	0.020795
Otu0132	Bacteria	Actinobacteria	Actinobacteria	Micrococcales	Micrococcaceae	Micrococcaceae_unc	0.02076
Otu0101	Bacteria	Firmicutes	Clostridia	Clostridiales	Lachnospiraceae	ASF356	0.020525
Otu0074	Bacteria	Firmicutes	Clostridia	Clostridiales	Lachnospiraceae	Lachnospiraceae_unc	0.020472
Otu0149	Bacteria	Firmicutes	Clostridia	Clostridiales	Ruminococcaceae	Ruminococcaceae_NK4A214_group	0.020008
Otu0073	Bacteria	Tenericutes	Mollicutes	Anaeroplasmatales	Anaeroplasmataceae	Anaeroplasma	0.019977
Otu0112	Bacteria	Firmicutes	Clostridia	Clostridiales	Lachnospiraceae	Lachnospiraceae_unc	0.019632
Otu0128	Bacteria	Firmicutes	Clostridia	Clostridiales	Family_XIII	Family_XIII_ge	0.01953
Otu0119	Bacteria	Firmicutes	Clostridia	Clostridiales	Ruminococcaceae	Ruminiclostridium	0.018497
Otu0050	Bacteria	Firmicutes	Clostridia	Clostridiales	Ruminococcaceae	Oscillibacter	0.018439
Otu0088	Bacteria	Firmicutes	Clostridia	Clostridiales	Ruminococcaceae	Butyricicoccus	0.018246
Otu0153	Bacteria	Firmicutes	Clostridia	Clostridiales	Ruminococcaceae	Ruminococcaceae_unc	0.017896
Otu0174	Bacteria	Firmicutes	Clostridia	Clostridiales	Lachnospiraceae	Lachnospiraceae_unc	0.017813
Otu0135	Bacteria	Firmicutes	Clostridia	Clostridiales	Lachnospiraceae	Lachnospiraceae_unc	0.01753
Otu0032	Bacteria	Firmicutes	Clostridia	Clostridiales	Ruminococcaceae	Ruminiclostridium_5	0.016388
Otu0130	Bacteria	Firmicutes	Clostridia	Clostridiales	Ruminococcaceae	Oscillibacter	0.015375
Otu0243	Bacteria	Firmicutes	Clostridia	Clostridiales	Lachnospiraceae	Lachnospiraceae_unc	0.014265
Otu0159	Bacteria	Firmicutes	Clostridia	Clostridiales	Ruminococcaceae	Ruminococcaceae_UCG-009	0.014246
Otu0018	Bacteria	Firmicutes	Clostridia	Clostridiales	Ruminococcaceae	Ruminococcaceae_unc	0.014062
Otu0046	Bacteria	Firmicutes	Clostridia	Clostridiales	Lachnospiraceae	Lachnospiraceae_unc	0.012762
Otu0069	Bacteria	Firmicutes	Clostridia	Clostridiales	Lachnospiraceae	uncultured	0.011927
Otu0190	Bacteria	Firmicutes	Clostridia	Clostridiales	Lachnospiraceae	Lachnospiraceae_unc	0.011772
Otu0060	Bacteria	Firmicutes	Clostridia	Clostridiales	Peptostreptococcaceae	Romboutsia	0.011691
Otu0134	Bacteria	Firmicutes	Clostridia	Clostridiales	Lachnospiraceae	Lachnospiraceae_NK4B4_group	0.011353
Otu0175	Bacteria	Firmicutes	Clostridia	Clostridiales	Ruminococcaceae	Ruminococcaceae_unc	0.011061
Otu0144	Bacteria	Firmicutes	Clostridia	Clostridiales	Lachnospiraceae	Lachnospiraceae_unc	0.010898
Otu0183	Bacteria	Firmicutes	Clostridia	Clostridiales	Ruminococcaceae	Ruminiclostridium_5	0.010134
Otu0201	Bacteria	Firmicutes	Clostridia	Clostridiales	Ruminococcaceae	Anaerotruncus	0.010066
Otu0065	Bacteria	Firmicutes	Bacilli	Lactobacillales	Enterococcaceae	Enterococcus	0.009992
Otu0129	Bacteria	Firmicutes	Clostridia	Clostridiales	Ruminococcaceae	Ruminococcaceae_UCG-014	0.009315
Otu0045	Bacteria	Firmicutes	Bacilli	Bacillales	Staphylococcaceae	Staphylococcus	0.009112
Otu0182	Bacteria	Firmicutes	Clostridia	Clostridiales	Lachnospiraceae	Lachnospiraceae_unc	0.009076
Otu0099	Bacteria	Actinobacteria	Coriobacteriia	Coriobacteriales	Eggerthellaceae	Adlercreutzia	0.008542
Otu0077	Bacteria	Firmicutes	Clostridia	Clostridiales	Ruminococcaceae	Ruminiclostridium_9	0.008197
Otu0141	Bacteria	Actinobacteria	Coriobacteriia	Coriobacteriales	Eggerthellaceae	Eggerthellaceae_unc	0.008035
Otu0093	Bacteria	Firmicutes	Clostridia	Clostridiales	Ruminococcaceae	Ruminiclostridium_5	0.007376
Otu0126	Bacteria	Firmicutes	Clostridia	Clostridiales	Lachnospiraceae	Lachnospiraceae_unc	0.0073
Otu0106	Bacteria	Firmicutes	Clostridia	Clostridiales	Peptococcaceae	uncultured	0.007274
Otu0027	Bacteria	Firmicutes	Clostridia	Clostridiales	Lachnospiraceae	Acetatifactor	0.007117
Otu0168	Bacteria	Firmicutes	Clostridia	Clostridiales	Clostridiales_vadinBB60_group	Clostridiales_vadinBB60_group_ge	0.00703
Otu0131	Bacteria	Proteobacteria	Alphaproteobacteria	Caulobacterales	Caulobacteraceae	Brevundimonas	0.006729
Otu0103	Bacteria	Firmicutes	Clostridia	Clostridiales	Lachnospiraceae	Lachnoclostridium	0.006605
Otu0167	Bacteria	Firmicutes	Clostridia	Clostridiales	Ruminococcaceae	Ruminiclostridium_9	0.006599

Otu0080	Bacteria	Firmicutes	Clostridia	Clostridiales	Lachnospiraceae	uncultured	0.006323
Otu0191	Bacteria	Firmicutes	Clostridia	Clostridiales	Clostridiales_vadinBB60_group	Clostridiales_vadinBB60_group_ge	0.006183
Otu0008	Bacteria	Firmicutes	Clostridia	Clostridiales	Lachnospiraceae	uncultured	0.005948
Otu0012	Bacteria	Firmicutes	Clostridia	Clostridiales	Lachnospiraceae	Lachnospiraceae_unc	0.005945
Otu0062	Bacteria	Proteobacteria	Alphaproteobacteria	Rhizobiales	Rhizobiaceae	Rhizobiaceae_unc	0.005922
Otu0161	Bacteria	Firmicutes	Clostridia	Clostridiales	Clostridiales_vadinBB60_group	Clostridiales_vadinBB60_group_ge	0.005904
Otu0001	Bacteria	Bacteroidetes	Bacteroidia	Bacteroidales	Muribaculaceae	Muribaculaceae_ge	0.005817
Otu0085	Bacteria	Firmicutes	Clostridia	Clostridiales	Lachnospiraceae	Lachnospiraceae_unc	0.005722
Otu0170	Bacteria	Firmicutes	Clostridia	Clostridiales	Lachnospiraceae	GCA-900066575	0.005454
Otu0034	Bacteria	Firmicutes	Clostridia	Clostridiales	Lachnospiraceae	Acetatifactor	0.005432
Otu0003	Bacteria	Firmicutes	Clostridia	Clostridiales	Lachnospiraceae	Lachnospiraceae_NK4A136_group	0.005409
Otu0151	Bacteria	Firmicutes	Clostridia	Clostridiales	Lachnospiraceae	Lachnospiraceae_unc	0.004726
Otu0177	Bacteria	Firmicutes	Clostridia	Clostridiales	Lachnospiraceae	Lachnospiraceae_unc	0.004692
Otu0136	Bacteria	Actinobacteria	Actinobacteria	Corynebacteriales	Nocardiaceae	Rhodococcus	0.004663
Otu0021	Bacteria	Firmicutes	Clostridia	Clostridiales	Lachnospiraceae	Lachnospiraceae_unc	0.004607
Otu0160	Bacteria	Firmicutes	Clostridia	Clostridiales	Ruminococcaceae	Ruminococcaceae_UCG-014	0.004508
Otu0205	Bacteria	Firmicutes	Clostridia	Clostridiales	Ruminococcaceae	Ruminococcaceae_UCG-005	0.004508
Otu0207	Bacteria	Firmicutes	Clostridia	Clostridiales	Lachnospiraceae	Lachnospiraceae_NK4A136_group	0.004285
Otu0152	Bacteria	Tenericutes	Mollicutes	Mollicutes_RF39	Mollicutes_RF39_fa	Mollicutes_RF39_ge	0.004181
Otu0044	Bacteria	Firmicutes	Bacilli	Bacillales	Listeriaceae	Listeria	0.003851
Otu0140	Bacteria	Firmicutes	Clostridia	Clostridiales	Lachnospiraceae	Lachnospiraceae_unc	0.003731
Otu0163	Bacteria	Firmicutes	Clostridia	Clostridiales	Lachnospiraceae	Lachnospiraceae_unc	0.003685
Otu0002	Bacteria	Bacteroidetes	Bacteroidia	Bacteroidales	Muribaculaceae	Muribaculaceae_ge	0.003667
Otu0150	Bacteria	Firmicutes	Clostridia	Clostridiales	Lachnospiraceae	Lachnospiraceae_unc	0.003638
Otu0072	Bacteria	Proteobacteria	Gammaproteobacteria	Pseudomonadales	Pseudomonadaceae	Pseudomonas	0.003618
Otu0193	Bacteria	Firmicutes	Clostridia	Clostridiales	Ruminococcaceae	Ruminiclostridium	0.003367
Otu0054	Bacteria	Firmicutes	Clostridia	Clostridiales	Lachnospiraceae	Lachnospiraceae_unc	0.003048
Otu0166	Bacteria	Firmicutes	Clostridia	Clostridiales	Ruminococcaceae	Oscillibacter	0.002816
Otu0214	Bacteria	Firmicutes	Clostridia	Clostridiales	Lachnospiraceae	Lachnospiraceae_UCG-001	0.002811
Otu0232	Bacteria	Firmicutes	Clostridia	Clostridiales	Ruminococcaceae	Ruminococcaceae_unc	0.002792
Otu0079	Bacteria	Firmicutes	Clostridia	Clostridiales	Lachnospiraceae	Lachnospiraceae_unc	0.002661
Otu0187	Bacteria	Firmicutes	Clostridia	Clostridiales	Lachnospiraceae	Acetatifactor	0.002626
Otu0198	Bacteria	Firmicutes	Clostridia	Clostridiales	Clostridiales_vadinBB60_group	Clostridiales_vadinBB60_group_ge	0.002454
Otu0121	Bacteria	Firmicutes	Clostridia	Clostridiales	Lachnospiraceae	Lachnospiraceae_unc	0.002145
Otu0231	Bacteria	Firmicutes	Clostridia	Clostridiales	Lachnospiraceae	Lachnospiraceae_unc	0.00199
Otu0192	Bacteria	Firmicutes	Clostridia	Clostridiales	Lachnospiraceae	Lachnospiraceae_UCG-006	0.001975
Otu0172	Bacteria	Firmicutes	Clostridia	Clostridiales	Lachnospiraceae	Lachnospiraceae_UCG-001	0.001875
Otu0218	Bacteria	Firmicutes	Clostridia	Clostridiales	Ruminococcaceae	Ruminococcaceae_UCG-014	0.001769
Otu0242	Bacteria	Proteobacteria	Gammaproteobacteria	Betaproteobacteriales	Burkholderiaceae	Ralstonia	0.001745
Otu0228	Bacteria	Tenericutes	Mollicutes	Mollicutes_RF39	Mollicutes_RF39_fa	Mollicutes_RF39_ge	0.00156
Otu0229	Bacteria	Firmicutes	Clostridia	Clostridiales	Lachnospiraceae	Lachnospiraceae_NK4A136_group	0.00156
Otu0292	Bacteria	Firmicutes	Clostridia	Clostridiales	Lachnospiraceae	Lachnospiraceae_unc	0.001396
Otu0230	Bacteria	Firmicutes	Clostridia	Clostridiales	Lachnospiraceae	Lachnospiraceae_unc	0.001263
Otu0238	Bacteria	Proteobacteria	Alphaproteobacteria	Rhizobiales	Xanthobacteraceae	Bradyrhizobium	0.001263
Otu0221	Bacteria	Firmicutes	Clostridia	Clostridiales	Ruminococcaceae	GCA-900066225	0.001206
Otu0235	Bacteria	Firmicutes	Clostridia	Clostridiales	Clostridiales_vadinBB60_group	Clostridiales_vadinBB60_group_ge	0.001153

Supplementary Table S2.5. MDG coefficients from IgA-Negative Random Forest model. The top 150 features are shown with assigned taxonomic classification.

Feature	Kingdom	Phylum	Class	Order	Family	Genus	MDG
Otu0023	Bacteria	Firmicutes	Clostridia	Clostridiales	Lachnospiraceae	Lachnospiraceae_UCG-001	1
Otu0109	Bacteria	Firmicutes	Clostridia	Clostridiales	Lachnospiraceae	uncultured	0.854053
Otu0048	Bacteria	Firmicutes	Clostridia	Clostridiales	Lachnospiraceae	Acetatifactor	0.539027
Otu0064	Bacteria	Firmicutes	Erysipelotrichia	Erysipelotrichales	Erysipelotrichaceae	Turicibacter	0.512364
Otu0058	Bacteria	Firmicutes	Clostridia	Clostridiales	Lachnospiraceae	uncultured	0.359442
Otu0089	Bacteria	Firmicutes	Clostridia	Clostridiales	Ruminococcaceae	Anaerotruncus	0.309309
Otu0040	Bacteria	Firmicutes	Clostridia	Clostridiales	Lachnospiraceae	Lachnospiraceae_NK4A136_group	0.240638
Otu0111	Bacteria	Firmicutes	Clostridia	Clostridiales	Lachnospiraceae	Lachnospiraceae_unc	0.233953
Otu0057	Bacteria	Firmicutes	Clostridia	Clostridiales	Lachnospiraceae	uncultured	0.202801
Otu0009	Bacteria	Firmicutes	Clostridia	Clostridiales	Clostridiaceae_1	Clostridium_sensu_stricto_1	0.196545
Otu0013	Bacteria	Firmicutes	Clostridia	Clostridiales	Lachnospiraceae	Lachnospiraceae_NK4A136_group	0.190137
Otu0015	Bacteria	Firmicutes	Clostridia	Clostridiales	Lachnospiraceae	Roseburia	0.187285
Otu0061	Bacteria	Firmicutes	Clostridia	Clostridiales	Lachnospiraceae	Lachnospiraceae_NK4A136_group	0.185688
Otu0037	Bacteria	Firmicutes	Clostridia	Clostridiales	Lachnospiraceae	Lachnospiraceae_unc	0.178223
Otu0076	Bacteria	Firmicutes	Clostridia	Clostridiales	Lachnospiraceae	uncultured	0.147698
Otu0010	Bacteria	Firmicutes	Clostridia	Clostridiales	Lachnospiraceae	Lachnospiraceae_NK4A136_group	0.131539
Otu0047	Bacteria	Firmicutes	Clostridia	Clostridiales	Lachnospiraceae	Lachnospiraceae_unc	0.127867
Otu0157	Bacteria	Firmicutes	Clostridia	Clostridiales	Ruminococcaceae	Oscillibacter	0.127195
Otu0087	Bacteria	Firmicutes	Bacilli	Lactobacillales	Streptococcaceae	Lactococcus	0.120524
Otu0097	Bacteria	Firmicutes	Clostridia	Clostridiales	Lachnospiraceae	GCA-900066575	0.119339
Otu0026	Bacteria	Firmicutes	Clostridia	Clostridiales	Lachnospiraceae	Lachnospiraceae_unc	0.094823
Otu0153	Bacteria	Firmicutes	Clostridia	Clostridiales	Ruminococcaceae	Ruminococcaceae_unc	0.09016
Otu0096	Bacteria	Firmicutes	Clostridia	Clostridiales	Lachnospiraceae	uncultured	0.089982
Otu0042	Bacteria	Firmicutes	Clostridia	Clostridiales	Lachnospiraceae	Lachnospiraceae_unc	0.08808
Otu0071	Bacteria	Firmicutes	Clostridia	Clostridiales	Ruminococcaceae	Ruminococcaceae_UCG-005	0.079808
Otu0075	Bacteria	Firmicutes	Clostridia	Clostridiales	Lachnospiraceae	Lachnospiraceae_unc	0.078068
Otu0038	Bacteria	Firmicutes	Clostridia	Clostridiales	Lachnospiraceae	Lachnospiraceae_unc	0.072773
Otu0100	Bacteria	Firmicutes	Clostridia	Clostridiales	Lachnospiraceae	uncultured	0.068615
Otu0011	Bacteria	Firmicutes	Clostridia	Clostridiales	Lachnospiraceae	Lachnospiraceae_NK4A136_group	0.066798
Otu0091	Bacteria	Firmicutes	Clostridia	Clostridiales	Lachnospiraceae	Lachnospiraceae_FCS020_group	0.066765
Otu0022	Bacteria	Proteobacteria	Gammaproteobacteria	Enterobacteriales	Enterobacteriaceae	Escherichia-Shigella	0.06638
Otu0051	Bacteria	Firmicutes	Clostridia	Clostridiales	Ruminococcaceae	Ruminococcaceae_UCG-014	0.066014
Otu0068	Bacteria	Firmicutes	Clostridia	Clostridiales	Lachnospiraceae	Lachnospiraceae_unc	0.064522
Otu0012	Bacteria	Firmicutes	Clostridia	Clostridiales	Lachnospiraceae	Lachnospiraceae_unc	0.055872
Otu0139	Bacteria	Firmicutes	Clostridia	Clostridiales	Lachnospiraceae	Lachnospiraceae_NK4A136_group	0.052349
Otu0020	Bacteria	Firmicutes	Clostridia	Clostridiales	Lachnospiraceae	Lachnospiraceae_NK4A136_group	0.051168
Otu0016	Bacteria	Firmicutes	Clostridia	Clostridiales	Lachnospiraceae	Lachnospiraceae_unc	0.050137
Otu0053	Bacteria	Firmicutes	Clostridia	Clostridiales	Lachnospiraceae	Lachnospiraceae_UCG-006	0.049899
Otu0060	Bacteria	Firmicutes	Clostridia	Clostridiales	Peptostreptococcaceae	Romboutsia	0.049764
Otu0155	Bacteria	Firmicutes	Clostridia	Clostridiales	Ruminococcaceae	Anaerotruncus	0.046435
Otu0117	Bacteria	Firmicutes	Clostridia	Clostridiales	Ruminococcaceae	Ruminiclostridium	0.045463
Otu0184	Bacteria	Firmicutes	Clostridia	Clostridiales	Lachnospiraceae	Lachnospiraceae_unc	0.044633
Otu0025	Bacteria	Firmicutes	Clostridia	Clostridiales	Lachnospiraceae	Lachnospiraceae_unc	0.040837
Otu0088	Bacteria	Firmicutes	Clostridia	Clostridiales	Ruminococcaceae	Butyricicoccus	0.04024
Otu0154	Bacteria	Firmicutes	Clostridia	Clostridiales	Lachnospiraceae	Lachnospiraceae_unc	0.039949
Otu0024	Bacteria	Firmicutes	Clostridia	Clostridiales	Ruminococcaceae	Ruminococcaceae_ge	0.03955
Otu0006	Bacteria	Firmicutes	Clostridia	Clostridiales	Lachnospiraceae	Lachnospiraceae_unc	0.03675
Otu0101	Bacteria	Firmicutes	Clostridia	Clostridiales	Lachnospiraceae	ASF356	0.036317
Otu0183	Bacteria	Firmicutes	Clostridia	Clostridiales	Ruminococcaceae	Ruminiclostridium_5	0.036217
Otu0033	Bacteria	Firmicutes	Clostridia	Clostridiales	Lachnospiraceae	A2	0.034219
Otu0086	Bacteria	Firmicutes	Clostridia	Clostridiales	Lachnospiraceae	Lachnospiraceae_unc	0.033504

Otu0216	Bacteria	Firmicutes	Clostridia	Clostridiales	Lachnospiraceae	Lachnospiraceae_unc	0.033114
Otu0003	Bacteria	Firmicutes	Clostridia	Clostridiales	Lachnospiraceae	Lachnospiraceae_NK4A136_group	0.033084
Otu0148	Bacteria	Firmicutes	Clostridia	Clostridiales	Lachnospiraceae	Lachnospiraceae_unc	0.031887
Otu0081	Bacteria	Firmicutes	Clostridia	Clostridiales	Lachnospiraceae	Lachnoclostridium	0.029982
Otu0027	Bacteria	Firmicutes	Clostridia	Clostridiales	Lachnospiraceae	Acetatifactor	0.0289
Otu0128	Bacteria	Firmicutes	Clostridia	Clostridiales	Family_XIII	Family_XIII_ge	0.028485
Otu0052	Bacteria	Firmicutes	Clostridia	Clostridiales	Lachnospiraceae	Lachnospiraceae_unc	0.027192
Otu0055	Bacteria	Firmicutes	Clostridia	Clostridiales	Lachnospiraceae	A2	0.027132
Otu0049	Bacteria	Firmicutes	Bacilli	Bacillales	Bacillaceae	Bacillus	0.026374
Otu0121	Bacteria	Firmicutes	Clostridia	Clostridiales	Lachnospiraceae	Lachnospiraceae_unc	0.025713
Otu0074	Bacteria	Firmicutes	Clostridia	Clostridiales	Lachnospiraceae	Lachnospiraceae_unc	0.024904
Otu0028	Bacteria	Firmicutes	Clostridia	Clostridiales	Lachnospiraceae	Lachnospiraceae_unc	0.024221
Otu0095	Bacteria	Firmicutes	Clostridia	Clostridiales	Lachnospiraceae	Lachnospiraceae_NK4A136_group	0.024135
Otu0140	Bacteria	Firmicutes	Clostridia	Clostridiales	Lachnospiraceae	Lachnospiraceae_unc	0.021971
Otu0014	Bacteria	Firmicutes	Clostridia	Clostridiales	Lachnospiraceae	Lachnospiraceae_NK4A136_group	0.021512
Otu0135	Bacteria	Firmicutes	Clostridia	Clostridiales	Lachnospiraceae	Lachnospiraceae_unc	0.021181
Otu0142	Bacteria	Firmicutes	Clostridia	Clostridiales	Lachnospiraceae	Lachnospiraceae_unc	0.02114
Otu0001	Bacteria	Bacteroidetes	Bacteroidia	Bacteroidales	Muribaculaceae	Muribaculaceae_ge	0.020931
Otu0114	Bacteria	Firmicutes	Clostridia	Clostridiales	Lachnospiraceae	Lachnospiraceae_unc	0.020096
Otu0178	Bacteria	Firmicutes	Clostridia	Clostridiales	Lachnospiraceae	Lachnospiraceae_unc	0.019409
Otu0041	Bacteria	Firmicutes	Clostridia	Clostridiales	Lachnospiraceae	Lachnoclostridium	0.01886
Otu0066	Bacteria	Firmicutes	Clostridia	Clostridiales	Lachnospiraceae	Lachnospiraceae_unc	0.018802
Otu0173	Bacteria	Firmicutes	Clostridia	Clostridiales	Ruminococcaceae	Ruminococcaceae_UCG-014	0.017874
Otu0034	Bacteria	Firmicutes	Clostridia	Clostridiales	Lachnospiraceae	Acetatifactor	0.016435
Otu0032	Bacteria	Firmicutes	Clostridia	Clostridiales	Ruminococcaceae	Ruminiclostridium_5	0.016376
Otu0070	Bacteria	Firmicutes	Erysipelotrichia	Erysipelotrichales	Erysipelotrichaceae	Erysipelatoclostridium	0.015416
Otu0146	Bacteria	Firmicutes	Clostridia	Clostridiales	Lachnospiraceae	Lachnospiraceae_unc	0.013952
Otu0077	Bacteria	Firmicutes	Clostridia	Clostridiales	Ruminococcaceae	Ruminiclostridium_9	0.01349
Otu0039	Bacteria	Firmicutes	Clostridia	Clostridiales	Lachnospiraceae	Lachnospiraceae_unc	0.013063
Otu0031	Bacteria	Firmicutes	Clostridia	Clostridiales	Lachnospiraceae	Marvinbryantia	0.012507
Otu0122	Bacteria	Firmicutes	Clostridia	Clostridiales	Ruminococcaceae	Ruminiclostridium_9	0.012463
Otu0062	Bacteria	Proteobacteria	Alphaproteobacteria	Rhizobiales	Rhizobiaceae	Rhizobiaceae_unc	0.012456
Otu0050	Bacteria	Firmicutes	Clostridia	Clostridiales	Ruminococcaceae	Oscillibacter	0.012282
Otu0090	Bacteria	Firmicutes	Clostridia	Clostridiales	Ruminococcaceae	Ruminococcaceae_unc	0.012055
Otu0134	Bacteria	Firmicutes	Clostridia	Clostridiales	Lachnospiraceae	Lachnospiraceae_NK4B4_group	0.011866
Otu0166	Bacteria	Firmicutes	Clostridia	Clostridiales	Ruminococcaceae	Oscillibacter	0.011693
Otu0078	Bacteria	Firmicutes	Clostridia	Clostridiales	Ruminococcaceae	Ruminococcaceae_UCG-014	0.011239
Otu0099	Bacteria	Actinobacteria	Coriobacteriia	Coriobacteriales	Eggerthellaceae	Adlercreutzia	0.011224
Otu0019	Bacteria	Firmicutes	Clostridia	Clostridiales	Ruminococcaceae	Ruminiclostridium_9	0.011141
Otu0193	Bacteria	Firmicutes	Clostridia	Clostridiales	Ruminococcaceae	Ruminiclostridium	0.010921
Otu0054	Bacteria	Firmicutes	Clostridia	Clostridiales	Lachnospiraceae	Lachnospiraceae_unc	0.010178
Otu0107	Bacteria	Proteobacteria	Alphaproteobacteria	Rhizobiales	Rhizobiaceae	Brucella	0.009612
Otu0174	Bacteria	Firmicutes	Clostridia	Clostridiales	Lachnospiraceae	Lachnospiraceae_unc	0.009497
Otu0147	Bacteria	Firmicutes	Clostridia	Clostridiales	Lachnospiraceae	Lachnospiraceae_unc	0.008697
Otu0190	Bacteria	Firmicutes	Clostridia	Clostridiales	Lachnospiraceae	Lachnospiraceae_unc	0.008621
Otu0131	Bacteria	Proteobacteria	Alphaproteobacteria	Caulobacterales	Caulobacteraceae	Brevundimonas	0.008094
Otu0182	Bacteria	Firmicutes	Clostridia	Clostridiales	Lachnospiraceae	Lachnospiraceae_unc	0.007964
Otu0056	Bacteria	Firmicutes	Clostridia	Clostridiales	Lachnospiraceae	uncultured	0.007864
Otu0045	Bacteria	Firmicutes	Bacilli	Bacillales	Staphylococcaceae	Staphylococcus	0.007826
Otu0227	Bacteria	Firmicutes	Clostridia	Clostridiales	Ruminococcaceae	Ruminococcaceae_unc	0.007397
Otu0207	Bacteria	Firmicutes	Clostridia	Clostridiales	Lachnospiraceae	Lachnospiraceae_NK4A136_group	0.007026
Otu0069	Bacteria	Firmicutes	Clostridia	Clostridiales	Lachnospiraceae	uncultured	0.006931
Otu0163	Bacteria	Firmicutes	Clostridia	Clostridiales	Lachnospiraceae	Lachnospiraceae_unc	0.006724
Otu0126	Bacteria	Firmicutes	Clostridia	Clostridiales	Lachnospiraceae	Lachnospiraceae_unc	0.006385

Otu0079	Bacteria	Firmicutes	Clostridia	Clostridiales	Lachnospiraceae	Lachnospiraceae_unc	0.006147
Otu0002	Bacteria	Bacteroidetes	Bacteroidia	Bacteroidales	Muribaculaceae	Muribaculaceae_ge	0.006057
Otu0145	Bacteria	Firmicutes	Clostridia	Clostridiales	Lachnospiraceae	Lachnospiraceae_unc	0.006055
Otu0104	Bacteria	Firmicutes	Clostridia	Clostridiales	Lachnospiraceae	Tyzzerella	0.006034
Otu0168	Bacteria	Firmicutes	Clostridia	Clostridiales	Clostridiales_vadinBB60_group	Clostridiales_vadinBB60_group_ge	0.005993
Otu0098	Bacteria	Firmicutes	Clostridia	Clostridiales	Ruminococcaceae	Ruminococcaceae_UCG-014	0.005969
Otu0004	Bacteria	Firmicutes	Bacilli	Lactobacillales	Lactobacillaceae	Lactobacillus	0.005937
Otu0029	Bacteria	Firmicutes	Clostridia	Clostridiales	Lachnospiraceae	Lachnospiraceae_unc	0.00569
Otu0225	Bacteria	Firmicutes	Clostridia	Clostridiales	Family_XIII	Family_XIII_ge	0.00548
Otu0123	Bacteria	Firmicutes	Clostridia	Clostridiales	Lachnospiraceae	Lachnospiraceae_NK4A136_group	0.004995
Otu0083	Bacteria	Firmicutes	Clostridia	Clostridiales	Ruminococcaceae	Ruminococcaceae_UCG-014	0.00481
Otu0085	Bacteria	Firmicutes	Clostridia	Clostridiales	Lachnospiraceae	Lachnospiraceae_unc	0.004773
Otu0214	Bacteria	Firmicutes	Clostridia	Clostridiales	Lachnospiraceae	Lachnospiraceae_UCG-001	0.004762
Otu0133	Bacteria	Firmicutes	Clostridia	Clostridiales	Ruminococcaceae	Ruminococcaceae_unc	0.004689
Otu0209	Bacteria	Firmicutes	Clostridia	Clostridiales	Peptococcaceae	uncultured	0.004573
Otu0162	Bacteria	Firmicutes	Clostridia	Clostridiales	Lachnospiraceae	Lachnospiraceae_unc	0.004482
Otu0248	Bacteria	Firmicutes	Clostridia	Clostridiales	Ruminococcaceae	Ruminococcaceae_unc	0.004286
Otu0189	Bacteria	Firmicutes	Clostridia	Clostridiales	Lachnospiraceae	Lachnospiraceae_unc	0.00397
Otu0018	Bacteria	Firmicutes	Clostridia	Clostridiales	Ruminococcaceae	Ruminococcaceae_unc	0.003894
Otu0205	Bacteria	Firmicutes	Clostridia	Clostridiales	Ruminococcaceae	Ruminococcaceae_UCG-005	0.003879
Otu0035	Bacteria	Proteobacteria	Gammaproteobacteria	Enterobacteriales	Enterobacteriaceae	Enterobacteriaceae_unc	0.003805
Otu0233	Bacteria	Firmicutes	Clostridia	Clostridiales	Lachnospiraceae	Lachnospiraceae_unc	0.003531
Otu0202	Bacteria	Firmicutes	Clostridia	Clostridiales	Clostridiales_vadinBB60_group	Clostridiales_vadinBB60_group_ge	0.003491
Otu0165	Bacteria	Firmicutes	Bacilli	Bacillales	Bacillaceae	Bacillus	0.003284
Otu0243	Bacteria	Firmicutes	Clostridia	Clostridiales	Lachnospiraceae	Lachnospiraceae_unc	0.003273
Otu0172	Bacteria	Firmicutes	Clostridia	Clostridiales	Lachnospiraceae	Lachnospiraceae_UCG-001	0.003265
Otu0229	Bacteria	Firmicutes	Clostridia	Clostridiales	Lachnospiraceae	Lachnospiraceae_NK4A136_group	0.003182
Otu0149	Bacteria	Firmicutes	Clostridia	Clostridiales	Ruminococcaceae	Ruminococcaceae_NK4A214_group	0.003015
Otu0270	Bacteria	Firmicutes	Clostridia	Clostridiales	Lachnospiraceae	Lachnospiraceae_NK4A136_group	0.002782
Otu0137	Bacteria	Firmicutes	Clostridia	Clostridiales	Lachnospiraceae	Lachnospiraceae_unc	0.002709
Otu0118	Bacteria	Firmicutes	Clostridia	Clostridiales	Clostridiales_vadinBB60_group	Clostridiales_vadinBB60_group_ge	0.002533
Otu0138	Bacteria	Firmicutes	Clostridia	Clostridiales	Ruminococcaceae	Ruminococcaceae_unc	0.00233
Otu0224	Bacteria	Firmicutes	Clostridia	Clostridiales	Lachnospiraceae	Lachnospiraceae_unc	0.002021
Otu0152	Bacteria	Tenericutes	Mollicutes	Mollicutes_RF39	Mollicutes_RF39_fa	Mollicutes_RF39_ge	0.001973
Otu0161	Bacteria	Firmicutes	Clostridia	Clostridiales	Clostridiales_vadinBB60_group	Clostridiales_vadinBB60_group_ge	0.001796
Otu0120	Bacteria	Firmicutes	Clostridia	Clostridiales	Ruminococcaceae	Ruminococcaceae_unc	0.001723
Otu0186	Bacteria	Firmicutes	Clostridia	Clostridiales	Lachnospiraceae	Lachnospiraceae_unc	0.001637
Otu0171	Bacteria	Firmicutes	Clostridia	Clostridiales	Ruminococcaceae	Ruminococcaceae_UCG-010	0.001594
Otu0221	Bacteria	Firmicutes	Clostridia	Clostridiales	Ruminococcaceae	GCA-900066225	0.001546
Otu0272	Bacteria	Firmicutes	Clostridia	Clostridiales	Ruminococcaceae	Ruminococcaceae_UCG-013	0.001546
Otu0228	Bacteria	Tenericutes	Mollicutes	Mollicutes_RF39	Mollicutes_RF39_fa	Mollicutes_RF39_ge	0.001464
Otu0232	Bacteria	Firmicutes	Clostridia	Clostridiales	Ruminococcaceae	Ruminococcaceae_unc	0.001464
Otu0292	Bacteria	Firmicutes	Clostridia	Clostridiales	Lachnospiraceae	Lachnospiraceae_unc	0.001464
Otu0115	Bacteria	Firmicutes	Clostridia	Clostridiales	Lachnospiraceae	Tyzzerella_3	0.00146

Chapter 3 Supplemental Tables

Supplementary Table S3.1. Mean decreasing Gini coefficients for whole microbiome features. The features with Mean Decreasing Gini coefficient greater than 0.

Feature	Kingdom	Phylum	Class	Order	Family	Genus	MDG
Otu0044	Bacteria	Bacteroidetes	Bacteroidia	Bacteroidales	Muribaculaceae	Muribaculaceae_ge	1
Otu0045	Bacteria	Bacteroidetes	Bacteroidia	Bacteroidales	Marinifilaceae	Odoribacter	0.607574
Otu0089	Bacteria	Firmicutes	Clostridia	Clostridiales	Lachnospiraceae	Marvinbryantia	0.348745
Otu0063	Bacteria	Bacteroidetes	Bacteroidia	Bacteroidales	Marinifilaceae	Odoribacter	0.2393
Otu0022	Bacteria	Bacteroidetes	Bacteroidia	Bacteroidales	Muribaculaceae	Muribaculaceae_ge	0.232579
Otu0079	Bacteria	Bacteroidetes	Bacteroidia	Bacteroidales	Muribaculaceae	Muribaculaceae_ge	0.229033
Otu0104	Bacteria	Firmicutes	Clostridia	Clostridiales	Ruminococcaceae	Ruminococcaceae_ge	0.180286
Otu0020	Bacteria	Firmicutes	Erysipelotrichia	Erysipelotrichales	Erysipelotrichaceae	Turicibacter	0.142087
Otu0134	Bacteria	Firmicutes	Clostridia	Clostridiales	Lachnospiraceae	Lachnospiraceae_unclassified	0.11957
Otu0049	Bacteria	Bacteroidetes	Bacteroidia	Bacteroidales	Bacteroidaceae	Bacteroides	0.119285
Otu0017	Bacteria	Bacteroidetes	Bacteroidia	Bacteroidales	Muribaculaceae	Muribaculaceae_ge	0.08551
Otu0029	Bacteria	Firmicutes	Clostridia	Clostridiales	Peptostreptococcaceae	Romboutsia	0.073177
Otu0205	Bacteria	Firmicutes	Clostridia	Clostridiales	Lachnospiraceae	Lachnospiraceae_unclassified	0.047286
Otu0072	Bacteria	Firmicutes	Clostridia	Clostridiales	Lachnospiraceae	uncultured	0.0415
Otu0069	Bacteria	Bacteroidetes	Bacteroidia	Bacteroidales	Rikenellaceae	Alistipes	0.039755
Otu0099	Bacteria	Firmicutes	Clostridia	Clostridiales	Lachnospiraceae	Lachnospiraceae_unclassified	0.034015
Otu0012	Bacteria	Bacteroidetes	Bacteroidia	Bacteroidales	Muribaculaceae	Muribaculaceae_ge	0.032235
Otu0005	Bacteria	Verrucomicrobia	Verrucomicrobiae	Verrucomicrobiales	Akkermansiaceae	Akkermansia	0.032094
Otu0073	Bacteria	Firmicutes	Clostridia	Clostridiales	Lachnospiraceae	Lachnospiraceae_unclassified	0.028594
Otu0024	Bacteria	Firmicutes	Bacilli	Lactobacillales	Lactobacillaceae	Lactobacillus	0.028453
Otu0088	Bacteria	Bacteroidetes	Bacteroidia	Bacteroidales	Muribaculaceae	Muribaculaceae_ge	0.028371
Otu0160	Bacteria	Firmicutes	Clostridia	Clostridiales	Lachnospiraceae	Lachnospiraceae_NK4A136_group	0.028077
Otu0014	Bacteria	Bacteroidetes	Bacteroidia	Bacteroidales	Muribaculaceae	Muribaculaceae_ge	0.027737
Otu0004	Bacteria	Firmicutes	Erysipelotrichia	Erysipelotrichales	Erysipelotrichaceae	Dubosiella	0.027208
Otu0142	Bacteria	Firmicutes	Clostridia	Clostridiales	Lachnospiraceae	uncultured	0.025559
Otu0032	Bacteria	Bacteroidetes	Bacteroidia	Bacteroidales	Muribaculaceae	Muribaculaceae_ge	0.025483
Otu0034	Bacteria	Bacteroidetes	Bacteroidia	Bacteroidales	Muribaculaceae	Muribaculaceae_ge	0.024999
Otu0111	Bacteria	Firmicutes	Clostridia	Clostridiales	Ruminococcaceae	Ruminiclostridium_5	0.023786
Otu0021	Bacteria	Bacteroidetes	Bacteroidia	Bacteroidales	Muribaculaceae	Muribaculaceae_ge	0.023604
Otu0082	Bacteria	Firmicutes	Clostridia	Clostridiales	Lachnospiraceae	Lachnospiraceae_unclassified	0.020673
Otu0062	Bacteria	Firmicutes	Clostridia	Clostridiales	Lachnospiraceae	Lachnospiraceae_NK4A136_group	0.020022
Otu0161	Bacteria	Firmicutes	Clostridia	Clostridiales	Lachnospiraceae	Roseburia	0.018697
Otu0131	Bacteria	Firmicutes	Clostridia	Clostridiales	Lachnospiraceae	Lachnospiraceae_unclassified	0.018152
Otu0103	Bacteria	Bacteroidetes	Bacteroidia	Bacteroidales	Muribaculaceae	Muribaculaceae_ge	0.018104
Otu0019	Bacteria	Bacteroidetes	Bacteroidia	Bacteroidales	Muribaculaceae	Muribaculaceae_ge	0.017887
Otu0011	Bacteria	Bacteroidetes	Bacteroidia	Bacteroidales	Muribaculaceae	Muribaculaceae_ge	0.017326
Otu0010	Bacteria	Actinobacteria	Actinobacteria	Bifidobacteriales	Bifidobacteriaceae	Bifidobacterium	0.017235
Otu0054	Bacteria	Firmicutes	Clostridia	Clostridiales	Lachnospiraceae	Lachnospiraceae_unclassified	0.016676
Otu0051	Bacteria	Firmicutes	Clostridia	Clostridiales	Lachnospiraceae	Lachnospiraceae_unclassified	0.016343
Otu0070	Bacteria	Tenericutes	Mollicutes	Anaeroplasmatales	Anaeroplasmataceae	Anaeroplasma	0.016125
Otu0149	Bacteria	Bacteroidetes	Bacteroidia	Bacteroidales	Rikenellaceae	Millionella	0.01608
Otu0068	Bacteria	Firmicutes	Clostridia	Clostridiales	Lachnospiraceae	Lachnospiraceae_unclassified	0.015345
Otu0150	Bacteria	Firmicutes	Clostridia	Clostridiales	Ruminococcaceae	Ruminococcaceae_UCG-014	0.014561
Otu0016	Bacteria	Bacteroidetes	Bacteroidia	Bacteroidales	Muribaculaceae	Muribaculaceae_ge	0.014534
Otu0154	Bacteria	Firmicutes	Clostridia	Clostridiales	Ruminococcaceae	Ruminiclostridium	0.014315
Otu0057	Bacteria	Bacteroidetes	Bacteroidia	Bacteroidales	Bacteroidales_unclassified	Bacteroidales_unclassified	0.014133
Otu0037	Bacteria	Firmicutes	Clostridia	Clostridiales	Lachnospiraceae	Lachnoclostridium	0.013606

Otu0130	Bacteria	Firmicutes	Clostridia	Clostridiales	Lachnospiraceae	Lachnospiraceae_NK4A136_group	0.012981
Otu0124	Bacteria	Bacteroidetes	Bacteroidia	Bacteroidales	Muribaculaceae	Muribaculaceae_ge	0.012803
Otu0023	Bacteria	Firmicutes	Clostridia	Clostridiales	Lachnospiraceae	Lachnospiraceae_UCG-006	0.012635
Otu0106	Bacteria	Firmicutes	Clostridia	Clostridiales	Lachnospiraceae	GCA-900066575	0.012296
Otu0001	Bacteria	Bacteroidetes	Bacteroidia	Bacteroidales	Muribaculaceae	Muribaculaceae_ge	0.012274
Otu0083	Bacteria	Firmicutes	Clostridia	Clostridiales	Ruminococcaceae	Ruminococcaceae_unclassified	0.012008
Otu0137	Bacteria	Firmicutes	Clostridia	Clostridiales	Lachnospiraceae	Lachnospiraceae_unclassified	0.011392
Otu0076	Bacteria	Firmicutes	Clostridia	Clostridiales	Lachnospiraceae	Lachnospiraceae_unclassified	0.011257
Otu0067	Bacteria	Firmicutes	Clostridia	Clostridiales	Ruminococcaceae	Ruminiclostridium_9	0.01114
Otu0006	Bacteria	Firmicutes	Bacilli	Lactobacillales	Lactobacillaceae	Lactobacillus	0.011106
Otu0093	Bacteria	Bacteroidetes	Bacteroidia	Bacteroidales	Rikenellaceae	Alistipes	0.010839
Otu0113	Bacteria	Bacteroidetes	Bacteroidia	Bacteroidales	Muribaculaceae	Muribaculaceae_ge	0.01059
Otu0119	Bacteria	Firmicutes	Clostridia	Clostridiales	Lachnospiraceae	Lachnospiraceae_UCG-001	0.010228
Otu0060	Bacteria	Firmicutes	Clostridia	Clostridiales	Lachnospiraceae	Lachnospiraceae_unclassified	0.010204
Otu0092	Bacteria	Firmicutes	Clostridia	Clostridiales	Lachnospiraceae	uncultured	0.010088
Otu0025	Bacteria	Bacteroidetes	Bacteroidia	Bacteroidales	Muribaculaceae	Muribaculaceae_ge	0.009174
Otu0177	Bacteria	Firmicutes	Clostridia	Clostridiales	Lachnospiraceae	Lachnospiraceae_UCG-001	0.009049
Otu0196	Bacteria	Firmicutes	Erysipelotrichia	Erysipelotrichales	Erysipelotrichaceae	Erysipelatoclostridium	0.007891
Otu0040	Bacteria	Firmicutes	Clostridia	Clostridiales	Ruminococcaceae	Ruminococcaceae_UCG-014	0.00783
Otu0086	Bacteria	Firmicutes	Clostridia	Clostridiales	Lachnospiraceae	Lachnospiraceae_unclassified	0.00772
Otu0115	Bacteria	Proteobacteria	Gammaproteobacteria	Betaproteobacteriales	Burkholderiaceae	Parasutterella	0.007591
Otu0122	Bacteria	Firmicutes	Clostridia	Clostridiales	Ruminococcaceae	Intestinimonas	0.007537
time	NA	NA	NA	NA	NA	NA	0.007483
Otu0129	Bacteria	Bacteroidetes	Bacteroidia	Bacteroidales	Rikenellaceae	Alistipes	0.007479
Otu0031	Bacteria	Bacteroidetes	Bacteroidia	Bacteroidales	Muribaculaceae	Muribaculum	0.007387
Otu0018	Bacteria	Firmicutes	Clostridia	Clostridiales	Lachnospiraceae	Lachnospiraceae_NK4A136_group	0.007199
Otu0117	Bacteria	Tenericutes	Mollicutes	Mollicutes_RF39	Mollicutes_RF39_fa	Mollicutes_RF39_ge	0.00698
Otu0144	Bacteria	Firmicutes	Bacilli	Lactobacillales	Streptococcaceae	Streptococcus	0.006703
Otu0053	Bacteria	Bacteroidetes	Bacteroidia	Bacteroidales	Muribaculaceae	Muribaculaceae_ge	0.006664
Otu0064	Bacteria	Firmicutes	Clostridia	Clostridiales	Lachnospiraceae	Lachnospiraceae_unclassified	0.006636
Otu0095	Bacteria	Firmicutes	Clostridia	Clostridiales	Lachnospiraceae	uncultured	0.006371
Otu0008	Bacteria	Bacteroidetes	Bacteroidia	Bacteroidales	Prevotellaceae	Prevotellaceae_UCG-001	0.006368
Otu0003	Bacteria	Bacteroidetes	Bacteroidia	Bacteroidales	Muribaculaceae	Muribaculaceae_ge	0.006021
Otu0148	Bacteria	Firmicutes	Clostridia	Clostridiales	Ruminococcaceae	Ruminococcaceae_UCG-014	0.005974
Otu0075	Bacteria	Firmicutes	Clostridia	Clostridiales	Lachnospiraceae	uncultured	0.005957
Otu0105	Bacteria	Firmicutes	Clostridia	Clostridiales	Lachnospiraceae	Lachnospiraceae_unclassified	0.005664
Otu0112	Bacteria	Firmicutes	Clostridia	Clostridiales	Ruminococcaceae	Butyricicoccus	0.005572
Otu0046	Bacteria	Bacteroidetes	Bacteroidia	Bacteroidales	Muribaculaceae	Muribaculaceae_ge	0.005463
Otu0007	Bacteria	Firmicutes	Clostridia	Clostridiales	Clostridiaceae_1	Clostridium_sensu_stricto_1	0.005337
Otu0176	Bacteria	Firmicutes	Clostridia	Clostridiales	Clostridiales_unclassified	Clostridiales_unclassified	0.005238
Otu0169	Bacteria	Proteobacteria	Alphaproteobacteria	Rhodospirillales	uncultured	uncultured_ge	0.0052
Otu0074	Bacteria	Bacteroidetes	Bacteroidia	Bacteroidales	Muribaculaceae	Muribaculaceae_ge	0.005005
Otu0047	Bacteria	Epsilonbacteraeota	Campylobacteria	Campylobacterales	Helicobacteraceae	Helicobacter	0.004983
Otu0128	Bacteria	Cyanobacteria	Melainabacteria	Gastranaerophilales	Gastranaerophilales_fa	Gastranaerophilales_ge	0.004932
Otu0071	Bacteria	Firmicutes	Clostridia	Clostridiales	Peptococcaceae	uncultured	0.004849
Otu0052	Bacteria	Firmicutes	Clostridia	Clostridiales	Lachnospiraceae	GCA-900066575	0.004847
Otu0123	Bacteria	Firmicutes	Clostridia	Clostridiales	Lachnospiraceae	Lachnospiraceae_unclassified	0.004833
Otu0094	Bacteria	Bacteroidetes	Bacteroidia	Bacteroidales	Muribaculaceae	Muribaculaceae_ge	0.004724
Otu0114	Bacteria	Firmicutes	Clostridia	Clostridiales	Lachnospiraceae	Lachnospiraceae_unclassified	0.004608
Otu0162	Bacteria	Firmicutes	Clostridia	Clostridiales	Clostridiaceae_1	Candidatus_Arthromitus	0.004467
Otu0133	Bacteria	Firmicutes	Clostridia	Clostridiales	Lachnospiraceae	Lachnospiraceae_unclassified	0.004389

Otu0097	Bacteria	Firmicutes	Clostridia	Clostridiales	Lachnospiraceae	Lachnospiraceae_unclassified	0.004361
Otu0085	Bacteria	Firmicutes	Erysipelotrichia	Erysipelotrichales	Erysipelotrichaceae	Faecalibaculum	0.00413
Otu0193	Bacteria	Firmicutes	Clostridia	Clostridiales	Lachnospiraceae	uncultured	0.004013
Otu0110	Bacteria	Firmicutes	Clostridia	Clostridiales	Lachnospiraceae	Acetatifactor	0.003993
Otu0058	Bacteria	Bacteroidetes	Bacteroidia	Bacteroidales	Muribaculaceae	Muribaculaceae_ge	0.003965
Otu0209	Bacteria	Firmicutes	Clostridia	Clostridiales	Ruminococcaceae	Ruminococcaceae_UCG-014	0.003779
Otu0041	Bacteria	Bacteroidetes	Bacteroidia	Bacteroidales	Muribaculaceae	Muribaculaceae_ge	0.003748
Otu0100	Bacteria	Firmicutes	Clostridia	Clostridiales	Ruminococcaceae	Ruminococcaceae_unclassified	0.003634
Otu0132	Bacteria	Firmicutes	Clostridia	Clostridiales	Ruminococcaceae	Ruminococcaceae_UCG-010	0.003619
Otu0035	Bacteria	Proteobacteria	Deltaproteobacteria	Desulfovibrionales	Desulfovibrionaceae	Desulfovibrio	0.003391
Otu0102	Bacteria	Actinobacteria	Coriobacteriia	Coriobacteriales	Eggerthellaceae	Eggerthellaceae_unclassified	0.003158
Otu0038	Bacteria	Proteobacteria	Gammaproteobacteria	Enterobacteriales	Enterobacteriaceae	Escherichia-Shigella	0.003044
Otu0109	Bacteria	Firmicutes	Clostridia	Clostridiales	Lachnospiraceae	Lachnospiraceae_NK4A136_group	0.003012
Otu0087	Bacteria	Actinobacteria	Coriobacteriia	Coriobacteriales	Eggerthellaceae	Enterorhabdus	0.002872
Otu0028	Bacteria	Bacteroidetes	Bacteroidia	Bacteroidales	Muribaculaceae	Muribaculaceae_ge	0.002797
Otu0098	Bacteria	Actinobacteria	Coriobacteriia	Coriobacteriales	Eggerthellaceae	DNF00809	0.002774
Otu0059	Bacteria	Bacteroidetes	Bacteroidia	Bacteroidales	Muribaculaceae	Muribaculaceae_ge	0.002591
Otu0027	Bacteria	Bacteroidetes	Bacteroidia	Bacteroidales	Muribaculaceae	Muribaculaceae_ge	0.002407
Otu0151	Bacteria	Firmicutes	Clostridia	Clostridiales	Lachnospiraceae	Lachnospiraceae_unclassified	0.002332
Otu0212	Bacteria	Firmicutes	Clostridia	Clostridiales	Ruminococcaceae	Ruminococcaceae_unclassified	0.002216
Otu0091	Bacteria	Firmicutes	Clostridia	Clostridiales	Ruminococcaceae	Ruminiclostridium	0.002164
Otu0281	Bacteria	Firmicutes	Clostridia	Clostridiales	Lachnospiraceae	Lachnospiraceae_unclassified	0.001938
Otu0015	Bacteria	Firmicutes	Clostridia	Clostridiales	Lachnospiraceae	Lachnospiraceae_NK4A136_group	0.001901
Otu0195	Bacteria	Firmicutes	Clostridia	Clostridiales	Ruminococcaceae	Ruminiclostridium_6	0.001782
Otu0120	Bacteria	Firmicutes	Clostridia	Clostridiales	Lachnospiraceae	Lachnospiraceae_unclassified	0.001726
Otu0002	Bacteria	Firmicutes	Bacilli	Lactobacillales	Lactobacillaceae	Lactobacillus	0.001713
Otu0013	Bacteria	Bacteroidetes	Bacteroidia	Bacteroidales	Muribaculaceae	Muribaculaceae_ge	0.001711
Otu0033	Bacteria	Firmicutes	Bacilli	Bacillales	Bacillaceae	Bacillus	0.001677
Otu0140	Bacteria	Firmicutes	Clostridia	Clostridiales	Ruminococcaceae	Intestinimonas	0.00164
Otu0188	Bacteria	Firmicutes	Clostridia	Clostridiales	Lachnospiraceae	uncultured	0.001431
Otu0182	Bacteria	Bacteroidetes	Bacteroidia	Bacteroidales	Rikenellaceae	Rikenella	0.001418
Otu0241	Bacteria	Firmicutes	Clostridia	Clostridiales	Lachnospiraceae	Lachnospiraceae_NK4A136_group	0.001359
Otu0080	Bacteria	Firmicutes	Clostridia	Clostridiales	Ruminococcaceae	Ruminiclostridium_9	0.001353
Otu0185	Bacteria	Firmicutes	Clostridia	Clostridiales	Ruminococcaceae	Ruminococcaceae_unclassified	0.00135
Otu0186	Bacteria	Firmicutes	Clostridia	Clostridiales	Lachnospiraceae	Lachnospiraceae_unclassified	0.001111
Otu0194	Bacteria	Proteobacteria	Alphaproteobacteria	Rhodospirillales	uncultured	uncultured_ge	0.000972
Otu0155	Bacteria	Firmicutes	Clostridia	Clostridiales	Lachnospiraceae	Lachnospiraceae_NK4A136_group	0.000895
Otu0191	Bacteria	Firmicutes	Clostridia	Clostridiales	Clostridiales_unclassified	Clostridiales_unclassified	0.000864
Otu0201	Bacteria	Firmicutes	Clostridia	Clostridiales	Lachnospiraceae	Lachnospiraceae_unclassified	0.000841
Otu0203	Bacteria	Firmicutes	Clostridia	Clostridiales	Family_XIII	Family_XIII_ge	0.000598
Otu0127	Bacteria	Firmicutes	Clostridia	Clostridiales	Lachnospiraceae	Acetatifactor	0.000555
Otu0214	Bacteria	Firmicutes	Clostridia	Clostridiales	Ruminococcaceae	Oscillibacter	0.000555
Otu0247	Bacteria	Firmicutes	Clostridia	Clostridiales	Lachnospiraceae	Lachnospiraceae_unclassified	0.000555
Otu0158	Bacteria	Firmicutes	Clostridia	Clostridiales	Ruminococcaceae	Ruminococcaceae_UCG-014	0.000527
Otu0164	Bacteria	Firmicutes	Clostridia	Clostridiales	Lachnospiraceae	Roseburia	0.000518
Otu0206	Bacteria	Firmicutes	Clostridia	Clostridiales	Ruminococcaceae	Ruminococcaceae_UCG-014	0.000486
Otu0157	Bacteria	Firmicutes	Clostridia	Clostridiales	Lachnospiraceae	Lachnospiraceae_UCG-006	0.000457
Otu0145	Bacteria	Firmicutes	Clostridia	Clostridiales	Lachnospiraceae	Lachnospiraceae_unclassified	0.000445
Otu0048	Bacteria	Bacteroidetes	Bacteroidia	Bacteroidales	Muribaculaceae	Muribaculaceae_ge	0.000441

Otu0174	Bacteria	Firmicutes	Clostridia	Clostridiales	Lachnospiraceae	Lachnospiraceae_unclassified	0.000432
Otu0036	Bacteria	Firmicutes	Bacilli	Bacillales	Staphylococcaceae	Staphylococcus	0.000425
Otu0268	Bacteria	Firmicutes	Clostridia	Clostridiales	Ruminococcaceae	Ruminococcaceae_unclassified	0.000409
Otu0141	Bacteria	Cyanobacteria	Melainabacteria	Gastranaerophilales	Gastranaerophilales_fa	Gastranaerophilales_ge	0.00038
Otu0030	Bacteria	Bacteroidetes	Bacteroidia	Bacteroidales	Muribaculaceae	Muribaculaceae_ge	0.00034
NA.1	NA	NA	NA	NA	NA	NA	0.000323
Otu0165	Bacteria	Firmicutes	Clostridia	Clostridiales	Lachnospiraceae	Lachnospiraceae_unclassified	0.000315
Otu0179	Bacteria	Firmicutes	Clostridia	Clostridiales	Lachnospiraceae	Lachnospiraceae_unclassified	0.000278
Otu0125	Bacteria	Firmicutes	Clostridia	Clostridiales	Lachnospiraceae	Lachnospiraceae_unclassified	0.000233
Otu0168	Bacteria	Firmicutes	Clostridia	Clostridiales	Family_XIII	Family_XIII_UCG-001	9.80E-05
Otu0181	Bacteria	Bacteroidetes	Bacteroidia	Bacteroidales	Tannerellaceae	Parabacteroides	7.67E-05
Otu0090	Bacteria	Firmicutes	Clostridia	Clostridiales	Ruminococcaceae	Oscillibacter	5.68E-05

Supplementary Table S3.2. Adjusted P-values for ELISA comparisons. The P-values from pairwise comparison of ELISA endpoint titers between experimental groups for each timepoint in the study. The Kruskal-Wallis test of analysis of variance was followed by Dunn's multiple comparison post-hoc test since data was not normally distributed. The Benjamini-Hochberg method was used to adjust p-values for multiple testing.

OVA-specific Fecal IgA

Comparison_1	Comparison_2	Week 2	Week 4	Week 6	Week 8	Week 10	Week 12
CD11c_Cre+ Buffer	CD11c_Cre+ LaOVA	0.2794	0.0106	0.0119	0.0007	0.0029	0.0025
CD11c_Cre+ Buffer	CD11c_Cre+ NCK1895	0.5000	0.5000	0.5000	0.5000	0.4442	0.5337
CD11c_Cre+ LaOVA	CD11c_Cre+ NCK1895	0.2162	0.0046	0.0065	0.0008	0.0033	0.0040
CD11c_Cre+ Buffer	NOD2_DC_KO+ Buffer	0.5185	0.5185	0.5185	0.5185	0.5000	0.5942
CD11c_Cre+ LaOVA	NOD2_DC_KO+ Buffer	0.2147	0.0072	0.0088	0.0014	0.0032	0.0069
CD11c_Cre+ NCK1895	NOD2_DC_KO+ Buffer	0.5385	0.5385	0.5385	0.5385	0.4236	0.5245
CD11c_Cre+ Buffer	NOD2_DC_KO+ LaOVA	0.4052	0.1252	0.3723	0.3520	0.4755	0.5547
CD11c_Cre+ LaOVA	NOD2_DC_KO+ LaOVA	0.3985	0.1002	0.0269	0.0028	0.0033	0.0038
CD11c_Cre+ NCK1895	NOD2_DC_KO+ LaOVA	0.3784	0.1163	0.3479	0.3492	0.5373	0.5176
NOD2_DC_KO+ Buffer	NOD2_DC_KO+ LaOVA	0.3773	0.1310	0.3507	0.3512	0.4537	0.5439
CD11c_Cre+ Buffer	NOD2_DC_KO+ NCK1895	0.5600	0.5600	0.5600	0.4449	0.5185	0.5000
CD11c_Cre+ LaOVA	NOD2_DC_KO+ NCK1895	0.2342	0.0062	0.0078	0.0021	0.0029	0.0031
CD11c_Cre+ NCK1895	NOD2_DC_KO+ NCK1895	0.5833	0.5833	0.5833	0.4332	0.4324	0.4904
NOD2_DC_KO+ Buffer	NOD2_DC_KO+ NCK1895	0.6087	0.6087	0.6087	0.4249	0.5385	0.5687
NOD2_DC_KO+ LaOVA	NOD2_DC_KO+ NCK1895	0.3983	0.1247	0.3684	0.4337	0.4626	0.5082
CD11c_Cre+ Buffer	NOD2_fl_CD11c_Cre+ LaOVA	0.3088	0.6364	0.0248	0.0278	0.0149	0.0036
CD11c_Cre+ LaOVA	NOD2_fl_CD11c_Cre+ LaOVA	0.5997	0.0092	0.3586	0.1104	0.2728	0.4947
CD11c_Cre+ NCK1895	NOD2_fl_CD11c_Cre+ LaOVA	0.2489	0.6667	0.0272	0.0328	0.0383	0.0081
NOD2_DC_KO+ Buffer	NOD2_fl_CD11c_Cre+ LaOVA	0.2224	0.7000	0.0349	0.0383	0.0246	0.0145
NOD2_DC_KO+ LaOVA	NOD2_fl_CD11c_Cre+ LaOVA	0.4020	0.1342	0.1072	0.0997	0.0372	0.0065
NOD2_DC_KO+ NCK1895	NOD2_fl_CD11c_Cre+ LaOVA	0.2738	0.7368	0.0295	0.0690	0.0184	0.0039
CD11c_Cre+ Buffer	NOD2_fl/fl+ LaOVA	0.0161	0.0124	0.0138	0.0071	0.0036	0.0049
CD11c_Cre+ LaOVA	NOD2_fl/fl+ LaOVA	0.1616	0.3232	0.6060	0.1423	0.4506	0.4928
CD11c_Cre+ NCK1895	NOD2_fl/fl+ LaOVA	0.0097	0.0129	0.0063	0.0100	0.0078	0.0040
NOD2_DC_KO+ Buffer	NOD2_fl/fl+ LaOVA	0.0145	0.0196	0.0073	0.0157	0.0053	0.0071
NOD2_DC_KO+ LaOVA	NOD2_fl/fl+ LaOVA	0.0289	0.2361	0.0227	0.0359	0.0064	0.0034
NOD2_DC_KO+ NCK1895	NOD2_fl/fl+ LaOVA	0.0145	0.0145	0.0084	0.0292	0.0034	0.0025
NOD2_fl_CD11c_Cre+ LaOVA	NOD2_fl/fl+ LaOVA	0.2003	0.0166	0.3484	0.4311	0.4777	0.5075

OVA-specific Vaginal IgA

Comparison_1	Comparison_2	2	4	6	8	10	12
CD11c_Cre+ Buffer	CD11c_Cre+ LaOVA	0.4418	0.5398	0.0010	0.0062	0.0010	0.0188
CD11c_Cre+ Buffer	CD11c_Cre+ NCK1895	0.5000	0.5000	0.5000	0.5000	0.5000	0.5000
CD11c_Cre+ LaOVA	CD11c_Cre+ NCK1895	0.3503	0.4289	0.0005	0.0071	0.0007	0.0104
CD11c_Cre+ Buffer	NOD2_DC_KO+ Buffer	0.5185	0.5185	0.5185	0.5185	0.5185	0.5185
CD11c_Cre+ LaOVA	NOD2_DC_KO+ Buffer	0.3571	0.3985	0.0011	0.0103	0.0014	0.0115

CD11c_Cre+ NCK1895	NOD2_DC_KO+ Buffer	0.5385	0.5385	0.5385	0.5385	0.5385	0.5385
CD11c_Cre+ Buffer	NOD2_DC_KO+ LaOVA	0.5600	0.5600	0.5794	0.2435	0.1420	0.1350
CD11c_Cre+ LaOVA	NOD2_DC_KO+ LaOVA	0.5050	1.0000	0.0015	0.0433	0.0221	0.1316
CD11c_Cre+ NCK1895	NOD2_DC_KO+ LaOVA	0.5833	0.5833	0.5225	0.2484	0.1401	0.1185
NOD2_DC_KO+ Buffer	NOD2_DC_KO+ LaOVA	0.6087	0.6087	0.5106	0.2597	0.1552	0.1193
CD11c_Cre+ Buffer	NOD2_DC_KO+ NCK1895	0.6364	0.3712	0.5600	0.3958	0.5600	0.5600
CD11c_Cre+ LaOVA	NOD2_DC_KO+ NCK1895	0.3853	0.3531	0.0007	0.0250	0.0011	0.0156
CD11c_Cre+ NCK1895	NOD2_DC_KO+ NCK1895	0.6667	0.3658	0.5833	0.3882	0.5833	0.5833
NOD2_DC_KO+ Buffer	NOD2_DC_KO+ NCK1895	0.7000	0.3671	0.6087	0.3850	0.6087	0.6087
NOD2_DC_KO+ LaOVA	NOD2_DC_KO+ NCK1895	0.7368	0.3998	0.5574	0.3950	0.1508	0.1259
CD11c_Cre+ Buffer	NOD2_fl_CD11c_Cre+ LaOVA	0.7778	0.4156	0.0283	0.0247	0.0134	0.0129
CD11c_Cre+ LaOVA	NOD2_fl_CD11c_Cre+ LaOVA	0.4281	0.4050	0.1978	0.4156	0.2552	0.5847
CD11c_Cre+ NCK1895	NOD2_fl_CD11c_Cre+ LaOVA	0.8235	0.4046	0.0293	0.0290	0.0144	0.0109
NOD2_DC_KO+ Buffer	NOD2_fl_CD11c_Cre+ LaOVA	0.8750	0.4041	0.0375	0.0372	0.0197	0.0154
NOD2_DC_KO+ LaOVA	NOD2_fl_CD11c_Cre+ LaOVA	0.9333	0.4618	0.0633	0.1919	0.1738	0.1162
NOD2_DC_KO+ NCK1895	NOD2_fl_CD11c_Cre+ LaOVA	1.0000	0.5910	0.0330	0.0905	0.0164	0.0127
CD11c_Cre+ Buffer	NOD2_fl/fl+ LaOVA	0.4655	0.4903	0.5108	0.5600	0.3355	0.1393
CD11c_Cre+ LaOVA	NOD2_fl/fl+ LaOVA	0.5823	0.3864	0.0010	0.0053	0.0014	0.1051
CD11c_Cre+ NCK1895	NOD2_fl/fl+ LaOVA	0.2300	0.4703	0.4716	0.5833	0.3196	0.1208
NOD2_DC_KO+ Buffer	NOD2_fl/fl+ LaOVA	0.2464	0.4709	0.4634	0.6087	0.3247	0.1164
NOD2_DC_KO+ LaOVA	NOD2_fl/fl+ LaOVA	0.9310	0.5884	0.5614	0.2288	0.2831	0.6171
NOD2_DC_KO+ NCK1895	NOD2_fl/fl+ LaOVA	0.2875	0.5686	0.4964	0.3983	0.3356	0.1294
NOD2_fl_CD11c_Cre+ LaOVA	NOD2_fl/fl+ LaOVA	0.3833	0.5962	0.0368	0.0220	0.0332	0.1365

OVA-specific Serum IgG

Comparison_1	Comparison_2	2	4	6	8	10	12
CD11c_Cre+ Buffer	CD11c_Cre+ LaOVA	0.5187	0.4475	0.2473	0.0293	0.0117	0.0137
CD11c_Cre+ Buffer	CD11c_Cre+ NCK1895	0.5000	0.5000	0.3980	0.2130	0.3856	0.3064
CD11c_Cre+ LaOVA	CD11c_Cre+ NCK1895	0.4158	0.1906	0.1662	0.0040	0.0097	0.0076
CD11c_Cre+ Buffer	NOD2_DC_KO+ Buffer	0.5185	0.5185	0.2425	0.1449	0.4209	0.2012
CD11c_Cre+ LaOVA	NOD2_DC_KO+ Buffer	0.4167	0.1927	0.1431	0.0068	0.0134	0.0085
CD11c_Cre+ NCK1895	NOD2_DC_KO+ Buffer	0.5385	0.5385	0.3650	0.3780	0.4695	0.4070
CD11c_Cre+ Buffer	NOD2_DC_KO+ LaOVA	0.5600	0.4409	0.3896	0.3291	0.4527	0.4067
CD11c_Cre+ LaOVA	NOD2_DC_KO+ LaOVA	0.5835	0.2907	0.1479	0.0096	0.0155	0.0070
CD11c_Cre+ NCK1895	NOD2_DC_KO+ LaOVA	0.5833	0.4028	0.4954	0.3549	0.3739	0.4399
NOD2_DC_KO+ Buffer	NOD2_DC_KO+ LaOVA	0.6087	0.3793	0.3648	0.2937	0.3931	0.3219
CD11c_Cre+ Buffer	NOD2_DC_KO+ NCK1895	0.6364	0.5600	0.2474	0.2256	0.4465	0.4271
CD11c_Cre+ LaOVA	NOD2_DC_KO+ NCK1895	0.4536	0.2860	0.2970	0.0060	0.0105	0.0078
CD11c_Cre+ NCK1895	NOD2_DC_KO+ NCK1895	0.6667	0.5833	0.3687	0.5000	0.4535	0.3987
NOD2_DC_KO+ Buffer	NOD2_DC_KO+ NCK1895	0.7000	0.6087	0.5000	0.3925	0.4406	0.3412
NOD2_DC_KO+ LaOVA	NOD2_DC_KO+ NCK1895	0.7368	0.4315	0.3837	0.3697	0.4342	0.4768
CD11c_Cre+ Buffer	NOD2_fl_CD11c_Cre+ LaOVA	0.7778	0.3939	0.2400	0.1302	0.0372	0.0265
CD11c_Cre+ LaOVA	NOD2_fl_CD11c_Cre+ LaOVA	0.4990	0.2759	0.5145	0.3120	0.4007	0.4424
CD11c_Cre+ NCK1895	NOD2_fl_CD11c_Cre+ LaOVA	0.8235	0.3461	0.1335	0.0251	0.0173	0.0073
NOD2_DC_KO+ Buffer	NOD2_fl_CD11c_Cre+ LaOVA	0.8750	0.3468	0.1342	0.0194	0.0288	0.0060
NOD2_DC_KO+ LaOVA	NOD2_fl_CD11c_Cre+ LaOVA	0.9333	0.6204	0.1264	0.0386	0.0462	0.0130
NOD2_DC_KO+ NCK1895	NOD2_fl_CD11c_Cre+ LaOVA	1.0000	0.3653	0.1963	0.0293	0.0300	0.0127
CD11c_Cre+ Buffer	NOD2_fl/fl+ LaOVA	0.0297	0.1793	0.3946	0.2160	0.0369	0.0271
CD11c_Cre+ LaOVA	NOD2_fl/fl+ LaOVA	0.1358	0.4395	0.3774	0.1349	0.2697	0.4130
CD11c_Cre+ NCK1895	NOD2_fl/fl+ LaOVA	0.0189	0.1587	0.2161	0.0394	0.0194	0.0066
NOD2_DC_KO+ Buffer	NOD2_fl/fl+ LaOVA	0.0272	0.1792	0.1336	0.0296	0.0274	0.0061
NOD2_DC_KO+ LaOVA	NOD2_fl/fl+ LaOVA	0.0594	0.4225	0.2116	0.0875	0.0482	0.0119
NOD2_DC_KO+ NCK1895	NOD2_fl/fl+ LaOVA	0.0236	0.1852	0.1594	0.0433	0.0289	0.0123
NOD2_fl_CD11c_Cre+ LaOVA	NOD2_fl/fl+ LaOVA	0.0315	0.3977	0.3615	0.3292	0.4574	0.4385

Supplementary Table S3.3. Adjusted P-values for ELISpot data. Spot forming units (SFU) from ELISpot results from each tissue type sampled were compared using the Kruskal-Wallis test of analysis of variance was followed by Dunn's multiple comparison post-hoc test, since data was also not normally distributed. The Benjamini-Hochberg method was used to adjust p-values for multiple testing.

OVA-specific SFU

Comparisons_1	Comparisons_2	FRT	LI	MLN	PP	Sp
CD11c_Cre+Buffer	CD11c_Cre+LaOVA	0.0201	0.1132	0.0025	0.1689	0.0961
CD11c_Cre+Buffer	CD11c_Cre+NCK1895	0.5000	0.5000	0.5000	0.5000	0.5000
CD11c_Cre+LaOVA	CD11c_Cre+NCK1895	0.0301	0.1258	0.0023	0.1653	0.0872
CD11c_Cre+Buffer	NOD2_DC_KO+Buffer	0.5185	0.5185	0.5185	0.5185	0.5185
CD11c_Cre+LaOVA	NOD2_DC_KO+Buffer	0.0373	0.1508	0.0033	0.1692	0.0908
CD11c_Cre+NCK1895	NOD2_DC_KO+Buffer	0.5385	0.5385	0.5385	0.5385	0.5385
CD11c_Cre+Buffer	NOD2_DC_KO+LaOVA	0.4117	0.5600	0.5600	0.5600	0.3002
CD11c_Cre+LaOVA	NOD2_DC_KO+LaOVA	0.0361	0.1415	0.0050	0.1830	0.2606
CD11c_Cre+NCK1895	NOD2_DC_KO+LaOVA	0.4346	0.5833	0.5833	0.5833	0.2681
NOD2_DC_KO+Buffer	NOD2_DC_KO+LaOVA	0.4006	0.6087	0.6087	0.6087	0.2766
CD11c_Cre+Buffer	NOD2_DC_KO+NCK1895	0.5600	0.6364	0.6364	0.6364	0.5600
CD11c_Cre+LaOVA	NOD2_DC_KO+NCK1895	0.0603	0.1618	0.0031	0.1771	0.1018
CD11c_Cre+NCK1895	NOD2_DC_KO+NCK1895	0.5833	0.6667	0.6667	0.6667	0.5833
NOD2_DC_KO+Buffer	NOD2_DC_KO+NCK1895	0.6087	0.7000	0.7000	0.7000	0.6087
NOD2_DC_KO+LaOVA	NOD2_DC_KO+NCK1895	0.4601	0.7368	0.7368	0.7368	0.2838
CD11c_Cre+Buffer	NOD2_fl_CD11c_Cre+LaOVA	0.0371	0.0095	0.0265	0.0034	0.1005
CD11c_Cre+LaOVA	NOD2_fl_CD11c_Cre+LaOVA	0.4075	0.2267	0.3550	0.0644	0.5768
CD11c_Cre+NCK1895	NOD2_fl_CD11c_Cre+LaOVA	0.0424	0.0127	0.0280	0.0029	0.0803
NOD2_DC_KO+Buffer	NOD2_fl_CD11c_Cre+LaOVA	0.0550	0.0205	0.0360	0.0045	0.0929
NOD2_DC_KO+LaOVA	NOD2_fl_CD11c_Cre+LaOVA	0.0997	0.0190	0.0302	0.0067	0.2970
NOD2_DC_KO+NCK1895	NOD2_fl_CD11c_Cre+LaOVA	0.0494	0.0381	0.0311	0.0039	0.0876
CD11c_Cre+Buffer	NOD2_fl/fl+LaOVA	0.4578	0.4638	0.5484	0.1976	0.0456
CD11c_Cre+LaOVA	NOD2_fl/fl+LaOVA	0.0508	0.2307	0.0030	0.7700	0.3310
CD11c_Cre+NCK1895	NOD2_fl/fl+LaOVA	0.4905	0.4928	0.5002	0.1887	0.0248
NOD2_DC_KO+Buffer	NOD2_fl/fl+LaOVA	0.4753	0.4746	0.4919	0.1561	0.0331
NOD2_DC_KO+LaOVA	NOD2_fl/fl+LaOVA	0.6037	0.5257	0.5876	0.2223	0.0836
NOD2_DC_KO+NCK1895	NOD2_fl/fl+LaOVA	0.5283	0.5632	0.5315	0.2076	0.0372
NOD2_fl_CD11c_Cre+LaOVA	NOD2_fl/fl+LaOVA	0.0968	0.0201	0.0452	0.0552	0.3093

Total_IgA SFU

Comparisons_1	Comparisons_2	FRT	LI	MLN	PP	Sp
CD11c_Cre+Buffer	CD11c_Cre+LaOVA	0.3502	0.3926	0.2792	0.0567	0.4521
CD11c_Cre+Buffer	CD11c_Cre+NCK1895	0.3839	0.2103	0.2009	0.4335	0.3598
CD11c_Cre+LaOVA	CD11c_Cre+NCK1895	0.2172	0.1389	0.3701	0.0612	0.3740
CD11c_Cre+Buffer	NOD2_DC_KO+Buffer	0.0599	0.0533	0.3935	0.0522	0.3665
CD11c_Cre+LaOVA	NOD2_DC_KO+Buffer	0.1544	0.0689	0.2482	0.5118	0.3526
CD11c_Cre+NCK1895	NOD2_DC_KO+Buffer	0.0688	0.1932	0.1534	0.0595	0.1838
CD11c_Cre+Buffer	NOD2_DC_KO+LaOVA	0.4312	0.1006	0.2823	0.0637	0.3322
CD11c_Cre+LaOVA	NOD2_DC_KO+LaOVA	0.2932	0.0659	0.1207	0.3335	0.3174
CD11c_Cre+NCK1895	NOD2_DC_KO+LaOVA	0.4083	0.3198	0.0565	0.1335	0.2231
NOD2_DC_KO+Buffer	NOD2_DC_KO+LaOVA	0.0646	0.2924	0.3584	0.3414	0.4658
CD11c_Cre+Buffer	NOD2_DC_KO+NCK1895	0.0653	0.1515	0.3622	0.4379	0.4967
CD11c_Cre+LaOVA	NOD2_DC_KO+NCK1895	0.1555	0.1135	0.3789	0.0621	0.4434
CD11c_Cre+NCK1895	NOD2_DC_KO+NCK1895	0.1108	0.4083	0.2753	0.4887	0.2910
NOD2_DC_KO+Buffer	NOD2_DC_KO+NCK1895	0.4337	0.2223	0.3058	0.0617	0.3549
NOD2_DC_KO+LaOVA	NOD2_DC_KO+NCK1895	0.0732	0.4007	0.1916	0.1340	0.3275
CD11c_Cre+Buffer	NOD2_fl_CD11c_Cre+LaOVA	0.2323	0.0272	0.0933	0.0666	0.4598
CD11c_Cre+LaOVA	NOD2_fl_CD11c_Cre+LaOVA	0.4002	0.0171	0.0208	0.3137	0.3683
CD11c_Cre+NCK1895	NOD2_fl_CD11c_Cre+LaOVA	0.1666	0.1317	0.0161	0.1419	0.2844
NOD2_DC_KO+Buffer	NOD2_fl_CD11c_Cre+LaOVA	0.2193	0.4384	0.1839	0.3170	0.4462
NOD2_DC_KO+LaOVA	NOD2_fl_CD11c_Cre+LaOVA	0.2253	0.2323	0.3011	0.4983	0.4419
NOD2_DC_KO+NCK1895	NOD2_fl_CD11c_Cre+LaOVA	0.2245	0.1842	0.0564	0.1422	0.4230

CD11c_Cre+Buffer	NOD2_fl/fl+LaOVA	0.0751	0.2803	0.2810	0.4956	0.4122
CD11c_Cre+LaOVA	NOD2_fl/fl+LaOVA	0.2099	0.2088	0.4416	0.0549	0.3416
CD11c_Cre+NCK1895	NOD2_fl/fl+LaOVA	0.0531	0.3499	0.3125	0.4470	0.1215
NOD2_DC_KO+Buffer	NOD2_fl/fl+LaOVA	0.3800	0.1057	0.2565	0.0567	0.4588
NOD2_DC_KO+LaOVA	NOD2_fl/fl+LaOVA	0.0718	0.2002	0.1066	0.0646	0.4356
NOD2_DC_KO+NCK1895	NOD2_fl/fl+LaOVA	0.4079	0.2596	0.3947	0.4492	0.3949
NOD2_fl_CD11c_Cre+LaOVA	NOD2_fl/fl+LaOVA	0.2856	0.0578	0.0277	0.0688	0.3451

Supplementary Table S3.4. Adjusted P-values for the pairwise comparison of RT-qPCR results. Data from each experimental group for each cytokine was compared using the Kruskal-Wallis test of analysis of variance was followed by Dunn's multiple comparison post-hoc test, and the Benjamini-Hochberg method was used to account for multiple testing.

Mesenteric Lymph Nodes

Comparisons_1	Comparisons_2	aladh1a1	aladh1a2	BAFF	IL21	IL6	TGFB
NOD2_DC_KO+ LaOVA	NOD2_DC_KO+ NCK1895	0.3801	0.5130	0.3898	0.1946	0.4594	0.4678
NOD2_DC_KO+ LaOVA	CD11c_Cre+LaOVA	0.0087	0.4738	0.0756	0.1972	0.8019	0.0057
NOD2_DC_KO+ NCK1895	CD11c_Cre+LaOVA	0.0100	0.4393	0.0958	0.0552	0.4739	0.0071
NOD2_DC_KO+ LaOVA	CD11c_Cre+NCK1895	0.0215	1.0000	0.4678	0.3451	0.4444	0.0048
NOD2_DC_KO+ NCK1895	CD11c_Cre+NCK1895	0.0170	0.5921	0.4441	0.2159	0.3806	0.0089
CD11c_Cre+LaOVA	CD11c_Cre+NCK1895	0.3956	0.7144	0.1128	0.2436	0.4537	0.3898

Peyer's Patches

Comparisons_1	Comparisons_2	aladh1a1	aladh1a2	BAFF	IL21	IL6	TGFB
NOD2_DC_KO+ LaOVA	NOD2_DC_KO+ NCK1895	0.2304	0.5155	0.1800	0.2323	0.4394	0.0953
NOD2_DC_KO+ LaOVA	CD11c_Cre+LaOVA	0.0550	0.3262	0.0076	0.2629	0.1998	0.2817
NOD2_DC_KO+ NCK1895	CD11c_Cre+LaOVA	0.1572	0.5384	0.0595	0.4899	0.2186	0.0378
NOD2_DC_KO+ LaOVA	CD11c_Cre+NCK1895	0.2240	0.3750	0.1116	0.1419	0.0381	0.0034
NOD2_DC_KO+ NCK1895	CD11c_Cre+NCK1895	0.1192	0.9242	0.0321	0.2840	0.0376	0.0864
CD11c_Cre+LaOVA	CD11c_Cre+NCK1895	0.0118	0.4594	0.0002	0.4112	0.1520	0.0009